Machine Learning in Computer Vision and String Processing

Supervisor:

Prof. PhD. Denis Enăchescu

Radu Tudor Ionescu

Department of Computer Science

Faculty of Mathematics and Computer Science

University of Bucharest

Bucharest, December 2013

I would like to dedicate this thesis to my loving parents and to my beautiful girlfriend, Andreea Lavinia.

Acknowledgements

Being a PhD student is an interesting and exciting journey. When you are on the verge of a new discovery, you realize how important and special this journey is. But, as every other journey in life, it has tough moments, when things don't always go as you expected. I only wonder how is it possible for me to reach the end of this beautiful journey? It is my belief that God was always there to guide me through my research and through my entire life. Thus, I would first like to thank God for helping me with my work. Of course, you always need some people to be close to you and help you during the tough moments, but also to share the joyful moments with you. Therefore, the time has come to thank all the people who were close to me during these years of my life and in many ways contributed directly or indirectly to this thesis.

I would like to acknowledge my PhD Supervisor Denis Enăchescu for helping me with this thesis and for attracting me towards the path of research in the field of machine learning. As a bachelor student, I was really attracted by the beautiful and interesting stories he told about artificial intelligence and neural networks during his lectures. I was mostly intrigued by the idea of building a machine that reaches human-level intelligence. This remains the ultimate goal of artificial intelligence, and it is an honor for me to join the community that tries to achieve this goal. Not only that professor Denis Enăchescu has introduced me to this field of study, but he has also continuously guided me during both the Masters and the PhD programs.

This is a good moment to thank all the committee members for their valuable comments regarding this thesis. I would also like to acknowl-

edge their interesting future work suggestions, that will enable me to take my research into new directions. Thanks to all.

I must admit that I started my research before the PhD program. My research started when Florentina Hristea decided that I am a good candidate to work on word sense disambiguation, under her guidance. She also introduced me to Marius Popescu, whom I consider to be one of the best researchers in natural language processing and machine learning. Thus, I must thank Florentina Hristea for giving me her trust and for helping me with my first steps on the path of research. I would also like to thank Marius Popescu for his guidance and for his continuous help with my research. I learned most of the important things I know today from many discussions with Marius Popescu, who has also become my friend. But, he is not the only new friend I made during my time as a PhD student. I would also like to acknowledge Liviu Dinu, another good friend, who helped me with my research from the early days. I must thank him for sharing his strong theoretical knowledge with me.

I would like to thank my loving parents for all their continuous effort in raising me as the person who I am today. I must thank them for giving me the best possible education and always encouraging me to follow my dreams. They were not too happy to hear that I was going to leave them after high school to study in Bucharest, but they understood this was the best choice for me. Thus, I would also like to thank them for supporting me during all these years away from home.

I must confess that there is a special person who supported me the most, while I was writing this thesis. She dedicated her time to take care of me and help me in all the possible ways that she could. I can only express my gratitude and deepest love for her, for my beautiful girlfriend, Andreea Lavinia.

This is the right moment to thank my uncle Cristi who has inspired me since I was a little boy. He was my role model as he inspired me to overcome my limits and to achieve great things by following my

dreams.

It is my greatest pleasure to thank Adrian, my dear friend whom I have met during my student years. We spent a lot of great moments together and we learned a lot from each other. He is not only a true friend, but also a young researcher as myself. I must thank him for continuing my work on using word sense disambiguation to improve information retrieval systems.

Last but not least, I would like to thank Silviu, Oana, Liviu, Dana, Cristina, Cosmin, Aluna, Roxana, Alin, Tiberiu, Vinicius, and all my other friends, colleagues, and family members.

List of Published Papers

1. Liviu P. Dinu and Radu Tudor Ionescu. A Genetic Approximation for Closest String via Rank Distance. *Proceedings of SYNASC*, pages 207–215, 2011.

2. Adrian-Gabriel Chifu and Radu Tudor Ionescu. Word Sense Disambiguation to Improve Precision for Ambiguous Queries. *Central European Journal of Computer Science*, 2(4):398–411, 2012.

3. Liviu P. Dinu and Radu Tudor Ionescu. An Efficient Rank Based Approach for Closest String and Closest Substring. *PLoS ONE*, 7(6): e37576, 06 2012.

4. Liviu P. Dinu and Radu Tudor Ionescu. A Rank-Based Approach of Cosine Similarity with Applications in Automatic Classiffication. *Proceedings of SYNASC*, pages 260–264, 2012.

5. Liviu P. Dinu and Radu Tudor Ionescu. Clustering Methods Based on Closest String via Rank Distance. *Proceedings of SYNASC*, pages 207–214, 2012.

6. Liviu P. Dinu and Radu Tudor Ionescu. Clustering Based on Rank Distance with Applications on DNA. *Proceedings of ICONIP*, 7667:722–729, 2012.

7. Liviu P. Dinu, Radu Tudor Ionescu, and Marius Popescu. Local Patch Dissimilarity for Images. *Proceedings of ICONIP*, 7663:117–126, 2012.

8. Liviu P. Dinu and Radu Tudor Ionescu. Clustering based on Median and Closest String via Rank Distance with Applications on DNA. *Neural Computing and Applications*, 24(1): 77–84, 2013.

9. Radu Tudor Ionescu. Unisort: An algorithm to sort uniformly distributed numbers in O(n) time. *International Journal on Information Technology (IREIT)*, 1(3): 1–10, 2013.

10. Radu Tudor Ionescu and Marius Popescu. Speeding Up Local Patch Dissimilarity. *Proceedings of ICIAP*, 8156:1–10, 2013.

11. Radu Tudor Ionescu and Marius Popescu. Kernels for Visual Words Histograms. *Proceedings of ICIAP*, 8156:81–90, 2013 – received Caianiello Best Young Paper Award.

12. Radu Tudor Ionescu, Marius Popescu, and Cristian Grozea. Local Learning to Improve Bag of Visual Words Model for Facial Expression Recognition. *Workshop on Challenges in Representation Learning, ICML*, 2013.

13. Marius Popescu and Radu Tudor Ionescu. The Story of the Characters, the DNA and the Native Language. *Proceedings of the Eighth Workshop on Innovative Use of NLP for Building Educational Applications*, pages 270–278, June 2013.

14. Radu Tudor Ionescu. Local Rank Distance. *Proceedings of SYNASC*, pages 221–228, 2013.

15. Andreea Lavinia Popescu, Dan Popescu, Radu Tudor Ionescu, Nicoleta Angelescu, and Romeo Cojocaru. Efficient Fractal Method for Texture Classification. *Proceedings of ICSCS*, IEEE Computer Society, August 2013.

16. Ian J. Goodfellow, Dumitru Erhan, Pierre Luc Carrier, Aaron Courville, Mehdi Mirza, Ben Hamner, Will Cukierski, Yichuan Tang, David Thaler, Dong-Hyun Lee, Yingbo Zhou, Chetan Ramaiah, Fangxiang Feng, Ruifan Li, Xiaojie Wang, Dimitris Athanasakis, John Shawe-Taylor, Maxim Milakov, John Park, Radu Tudor Ionescu, Marius Popescu, Cristian Grozea, James Bergstra, Jingjing Xie, Lukasz Romaszko, Bing Xu, Zhang Chuang, and Yoshua Bengio. Challenges in Representation Learning: A report on three machine learning contests. *Proceedings of ICONIP*, 8228:117–124, 2013.

17. Liviu P. Dinu and Radu Tudor Ionescu. An Efficient Algorithm for Rank Distance Consensus. *Proceedings of AI*IA*, 8249:505–516, 2013.

18. Andreea Lavinia Popescu, Radu Tudor Ionescu, and Dan Popescu. A Spatial Pyramid Approach for Texture Classification. *Proceedings of ISEEE*, IEEE Computer Society, October 2013.

19. Radu Tudor Ionescu, Andreea Lavinia Popescu, Dan Popescu, and Marius Popescu. Local Texton Dissimilarity with Applications on Biomass Classification. *Proceedings of VISAPP*, January 2014.

Abstract

Machine learning is currently a vast area of research with applications in a broad range of fields, such as computer vision, bioinformatics, information retrieval, natural language processing, audio processing, data mining, and many others. Among the variety of state of the art machine learning approaches for such applications, are the similarity-based learning methods. Learning based on similarity refers to the process of learning based on pairwise similarities between the training samples. The similarity-based learning process can be both supervised and unsupervised, and the pairwise relationship can be either a similarity, a dissimilarity, or a distance function.

This thesis studies several similarity-based learning approaches, such as Nearest Neighbor models, kernel methods and clustering algorithms. A Nearest Neighbor model based on a novel dissimilarity for images is presented in this thesis. It is used for handwritten digit recognition and achieves impressive results. Kernel methods are used in several tasks investigated in this thesis. First, a novel kernel for visual word histograms is presented. It achieves state of the art performance for object recognition in images. Several kernels based on a pyramid representation are presented next. They are used for facial expression recognition. An approach based on string kernels for native language identification is also presented in this work. The approach achieves state of the art performance levels, while being language independent and theory neutral. Several clustering algorithms are described in this thesis. The algorithms are evaluated on the phylogenetic analysis of mammals. One can easily observe that the machine learning tasks approached in this thesis can be divided into two different areas: computer vision and string processing.

Despite the fact that computer vision and string processing seem to be unrelated fields of study, image analysis and string processing are in some ways similar. As will be shown in this thesis, the concept of treating image and text in a similar fashion has proven to be very fertile for specific applications in computer vision. In fact, one of the state of the art methods for image categorization is inspired from the *bag of words* representation, which is very popular in information retrieval and natural language processing. Indeed, the *bag of visual words* model, which builds a vocabulary of visual words by clustering local image descriptors extracted from images, has demonstrated impressive levels of performance for image categorization and image retrieval. By adapting string processing techniques to image analysis or the other way around, knowledge from one domain can be transferred to the other. In fact, many breakthrough discoveries have been made by transferring knowledge between different domains. This thesis follows this line of research and presents novel approaches or improved methods that exploit this concept. First, a dissimilarity measure for images is presented. The dissimilarity measure is inspired from the rank distance measure for strings. The main concern is to extend rank distance from one-dimensional input (strings) to two-dimensional input (digital images). While rank distance is a highly accurate measure for strings, the empirical results presented in this thesis suggest that the proposed extension of rank distance to images is very accurate for handwritten digit recognition and texture analysis. Second, some improvements to the popular bag of visual words model are proposed in this thesis. As mentioned before, this model is inspired by the bag of words model from natural language processing and information retrieval. Third, a new distance measure for strings is introduced in this work. It is inspired from the image dissimilarity measure that is also described in this thesis. Designed to conform to more general principles and adapted to DNA strings, it comes to improve several state of the art methods for DNA sequence analysis. Furthermore, another application of this novel distance measure for

strings is discussed. More precisely, a kernel based on this distance measure is used for native language identification. To summarize, all the contributions presented in this thesis come to support the concept of treating image and text in a similar manner.

It is important to mention that the studied methods exhibit state of the art performance levels in the approached tasks. A few arguments come to support this claim. First of all, an improved bag of visual words model described in this work obtained the fourth place at the Facial Expression Recognition (FER) Challenge of the ICML 2013 Workshop in Challenges in Representation Learning (WREPL). Second of all, the system based on string kernels presented in this thesis ranked on third place in the closed Native Language Identification Shared Task of the BEA-8 Workshop of NAACL 2013. Third of all, the PQ kernel for visual word histograms described in this work received the Caianiello Best Young Paper Award at ICIAP 2013.

Contents

List of Figures

List of Tables

Chapter 1

Motivation and Overview

1.1 Introduction

Machine learning is a branch of artificial intelligence that studies computer systems that can learn from data. In this context, learning is about recognizing complex patterns and making intelligent decisions based on data. In the early years of artificial intelligence, the idea that human thinking could be rendered logically in a numerical computing machine emerged. But it was unclear if such a machine could model the complex human brain, until Alan Turing proposed a test to measure its performance in 1950. The Turing test states that a machine exhibits human-level intelligence if a human judge engages in a natural language conversation with the machine and cannot distinguish it from another human. Despite the fact that intelligent machines that can pass the Turing test have not been developed yet, many interesting systems that can learn from data have been proposed since then.

One of the first breakthrough intelligent system was developed in 1952 by Arthur Samuel from IBM. He developed a game-playing program, for checkers, to achieve sufficient skill to challenge a world champion. Its program was based on a search tree of the board positions reachable from the current state. Some of the early intelligent systems were based on decision rules. Such systems are best known as *expert systems*. The system that is often called the first expert system is ELIZA, which was developed between 1964 and 1966 by Joseph Weizenbaum

from MIT. ELIZA simulated a psychotherapist that could interact with a human patient. It was implemented using simple pattern matching techniques like string substitution and canned responses based on keywords. What is interesting to note is that when ELIZA originally appeared, some people actually mistook it for a human. At the same time with the development of expert systems, other approaches have been proposed. In 1957, Frank Rosenblatt invented the *perceptron* which is a mathematical model of the neuron. The perceptron is a very simple linear classifier, but it was shown that a powerful model can be created by combining perceptrons into a network. Despite the fact that neural network research went through many years of stagnation, the field was revived by the discovery of the *backpropagation* algorithm used for training multilayer perceptrons. In the early 90's the field of machine learning shifted to a more data-driven approach as compared to the more knowledge-driven expert systems, mainly due to the intersection of computer science and statistics. Many of the current machine learning approaches are based on the ideas developed at that time. A complete history of artificial intelligence is presented in [Nilsson, 2010].

Several learning paradigms have been proposed. The two most popular ones are supervised and unsupervised learning. *Supervised learning* refers to the task of building a classifier using labeled training data. The most studied approaches in machine learning are supervised and they include: Support Vector Machines [Cortes & Vapnik, 1995], Naive Bayes classifiers [Manning et al., 2008], neural networks [Bishop, 1995], Random Forests [Breiman, 2001] and many others [Caruana & Niculescu-Mizil, 2006]. *Unsupervised learning* refers to the task of finding hidden structure in unlabeled data. The best known form of unsupervised learning is *cluster analysis*, which aims at clustering objects into groups based on their similarity. Among the other learning paradigms are *semi-supervised learning*, which combines both labeled and unlabeled data, and *reinforcement learning*, which learns to take actions in an environment in order to maximize a long-term reward. Depending on the desired outcome of the machine learning algorithm or on the type of training input available for an application, a particular learning paradigm may be more suitable than the others.

Machine learning is currently a vast area of research with applications in a broad range of fields, such as computer vision [Fei-Fei & Perona, 2005; Forsyth

& Ponce, 2002; Zhang et al., 2007], bioinformatics [Dinu & Ionescu, 2013a; Inza et al., 2010; Leslie et al., 2002], information retrieval [Chifu & Ionescu, 2012; Manning et al., 2008], natural language processing [Lodhi et al., 2002; Popescu & Grozea, 2012], data mining [Enăchescu, 2004], and many others. Among the variety of state of the art machine learning approaches for such applications, are the similarity-based learning methods [Chen et al., 2009].

This thesis studies similarity-based learning approaches such as Nearest Neighbor models, kernel methods [Shawe-Taylor & Cristianini, 2004] and clustering analysis [Enăchescu, 2004]. The studied approaches exhibit state of the art performance levels in two different areas: computer vision and string processing. It is important to note that *string processing* refers to any task that needs to process string data such as text documents, DNA sequences, and so on. This work investigates string processing tasks ranging from phylogenetic analysis [Dinu & Ionescu, 2012a,c, 2013a; Ionescu, 2013a] and DNA comparison [Dinu & Ionescu, 2012b, 2013b] to native language identification [Popescu & Ionescu, 2013], from a machine learning perspective. On the other hand, a broad variety of computer vision tasks are also investigated in this thesis, such as object recognition [Ionescu & Popescu, 2013b], optical character recognition [Dinu et al., 2012; Ionescu & Popescu, 2013a], texture classification [Ionescu et al., 2014], and facial expression recognition [Ionescu et al., 2013].

1.2 Image and Text Processing: Common Concepts

In recent years, computer science specialists are faced with the challenge of processing massive amounts of data. The largest part of this data is actually unstructured and semi-structured data, available in the form of text documents, images, audio, video and so on. Researchers have developed methods and tools that extract relevant information and support efficient access to unstructured and semi-structured content. Such methods that aim at providing access to information are mainly studied by machine learning researchers. In fact, a tremendous amount of effort has been dedicated to this line of research [Agarwal & Roth,

2002; Lazebnik et al., 2005b, 2006; Leung & Malik, 2001; Manning et al., 2008]. In the context of machine learning, the aim is to obtain a good representation of the data that can later be used to build an efficient classifier. In computer vision, image representations are obtained by *feature detection* and *feature extraction*. Most of the feature extraction methods are handcrafted by researchers that have a good understanding of the application and a vast experience. This is the case of the bag of visual words model [Leung & Malik, 2001; Sivic et al., 2005] in computer vision. A different approach is *representation learning*, which aims at discovering a better representation of the data provided during training. This is the case of deep learning algorithms [Bengio, 2009; Montavon et al., 2012] that aim at discovering multiple levels of representation, or a hierarchy of features. Deep algorithms learn to transform one representation into another, by better disentangling the factors of variation that explain the observed data.

Whether the representation of the data is obtained through a handcrafted method or learned by a fully automatic process, common concepts of treating different kinds of unstructured and semi-structured data, such as image and text, naturally arise. Despite the fact that computer vision and string processing seem to be unrelated fields of study, the concept of treating image and text in a similar fashion has proven to be very fertile for several applications. Furthermore, by adapting string processing techniques to image analysis or the other way around, knowledge from one domain can be transferred to the other.

An example of similarity between text and image is discussed next. It refers to word sense disambiguation and object recognition in images. *Word sense disambiguation* (WSD) is a core research problem in computational linguistics and natural language processing, which was recognized since the beginning of the scientific interest in machine translation, and in artificial intelligence, in general. WSD is about determining the meaning of a word in a specific context. Actually all the WSD methods use the context to determine the meaning of an ambiguous word, because the entire information about the word sense is contained in the context [Agirre & Edmonds, 2006]. The basic concept is to extract features from the context that could help the WSD process. In a similar fashion, objects in images can be recognized using the entire image as a context. For example, a method that could detect the presence of the sun (as an object) in the image,

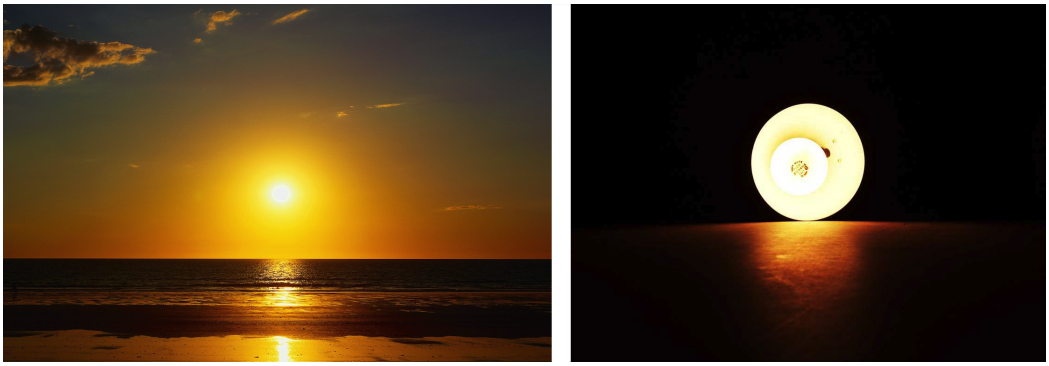

Figure 1.1: A picture of the sun in the left and a light bulb in the dark on the right. The light bulb can easily be mistaken for the sun if the rest of the image is disregarded. Copyrights of the two images are reserved to http://www.graphicshunt.com and http://hdwallpapers.lt, respectively.

would have to look for distinctive features such as the round shape of the sun, the color, and so on. However, there are other objects that have similar shape or color, such as spot lights or lamps. Thus, a better approach could be to look for other distinctive features in the image, such as the sky, the sun reflection in water, and so on. This approach will help avoid confusions such as recognizing a light bulb as the sun, which can be a quite common mistake as it can be observed in Figure 1.1.

Another example of treating image and text in a similar manner is a state of the art method for image categorization and image retrieval inspired from the *bag of words* representation, which is very popular in information retrieval and natural language processing. The bag of words model represents a text as an unordered collection of words, completely disregarding grammar, word order, and syntactic groups. The bag of words model has many applications from information retrieval [Manning et al., 2008] to natural language processing [Manning & Schütze, 1999] and word sense disambiguation [Agirre & Edmonds, 2006; Chifu & Ionescu, 2012]. In the context of image analysis, the concept of *word* needs to be defined somehow. Computer vision researchers have introduced the concept of *visual word*. Local image descriptors, such as SIFT [Lowe, 1999], are vector quantized to obtain a vocabulary of visual words. The vector quantization process can be done, for example, by k-means clustering [Leung & Malik, 2001] or by

probabilistic Latent Semantic Analysis [Sivic et al., 2005]. The frequency of each visual word is then recorded in a histogram which represents the final feature vector for the image. This histogram is the equivalent of the bag of words representation for text. The idea of representing images as *bag of visual words* has demonstrated impressive levels of performance for image categorization [Zhang et al., 2007] and image retrieval [Philbin et al., 2007].

One of the most important problems in computer vision is object recognition. Machine learning methods represent the state of the art approach for the object recognition problem. A common approach is to make some assumptions in order to treat object recognition as a classification problem. First, object categories are considered to be fixed and known. Second, each instance belongs to a single category. However, some researchers argue that these assumptions are obvious nonsense. The following example shows that these assumptions are indeed wrong. The object presented in Figure 1.2 can be described either as a plastic toy, a monkey, or both. It it clear that the object does not belong to a single category. Furthermore, the category of the object might be irrelevant for particular applications. Another drawback of this approach is that it misses out some of the subtle aspects of object recognition. For example, an object classification system does not understand the properties of an object and it cannot deal with unfamiliar objects. In other words, it fails to extract aspects of meaning. Thus, some computer vision researchers have proposed different approaches for the object recognition task. One alternative approach, proposed in [Duygulu et al., 2002], is to model object recognition as machine translation. The model is based on the observation that object recognition is a little like translation, in that a picture (or text in a source language) goes in, and a description (or text in a target language) comes out. In this model, object recognition becomes a process of annotating image regions with words. First, images are segmented into regions, which are then classified into region types. Next, a mapping between region types and keywords provided with the images is learned. This process is similar to learning a *lexicon* from data, a standard problem in machine translation literature [Jurafsky & Martin, 2000; Manning & Schütze, 1999]. This approach has proven fertile for this interpretation of object recognition. Research in this area has led to the development of other systems, such as the one described in [Farhadi et al., 2010]

Figure 1.2: An object that can be described by multiple categories such as plastic toy, monkey, or both. Image copyrights are reserved to http://www.allposters.com.

which generates sentences from images. The system computes a score linking an image to a sentence. This score can be used to attach a descriptive sentence to a given image, or to obtain images that illustrate a given sentence. To take this even further, the work of [Sadeghi & Farhadi, 2011] suggests that it is easier and more effective to generate descriptions of images in terms of chunks of meaning, such as "a person riding a horse", rather than individual components, such as "person" or "horse". In this approach, categories are replaced with visual phrases for recognition.

The examples described so far are successful cases of treating image as text. However, research that studies how to improve text processing techniques with knowledge from computer vision has also been conducted. A good example is the method introduced in [Barnard & Johnson, 2005], which proposes the use of images for WSD, either alone, or in conjunction with traditional text based methods. To integrate image information with text data, the authors exploit previous work on linking images and words [Barnard et al., 2003; Duygulu et al., 2002]. The empirical results strongly suggest that images can help disambiguate senses of words.

The concept of treating image and text in a similar manner is exploited in some way or another in the previous examples. The knowledge transfer from one domain to another has proven to be very fertile in the case of computer vision and natural language processing. This thesis follows this line of research and presents

novel approaches or improved methods that exploit this concept. First, a dissimilarity measure for images is presented in Chapter 4. The dissimilarity measure is inspired from the rank distance measure [Dinu, 2003]. The main concern is to extend rank distance from one-dimensional input (strings) to two-dimensional input (digital images). While rank distance is a highly accurate measure for strings, the experiments presented in Chapter 4 suggest that the proposed extension of rank distance to images is very accurate for handwritten digit recognition and texture analysis. Second, some improvements to the popular bag of visual words model are proposed in Chapter 5. As mentioned before, this model is inspired by the bag of words model from natural language processing and information retrieval. Third, a new distance measure for strings is introduced in Chapter 8. It is inspired from the image dissimilarity measure presented in Chapter 4. Designed to conform to more general principles and adapted to DNA strings, it comes to improve several state of the art methods for DNA sequence analysis. Furthermore, another application of this novel distance measure for strings is presented in Chapter 9. More precisely, a kernel based on this distance measure is used for native language identification. To summarize, all the contributions presented in this thesis come to support the concept of treating image and text in a similar manner.

1.3 Overview and Organization

The rest of this thesis is organized as follows. All the machine learning methods that are employed to obtain results for different applications of computer vision and string processing are described in Chapter 2. This chapter gives an overview of the main concepts of learning based on similarity. Specific machine learning methods that are based on these concepts are then presented. First, Nearest Neighbor models are discussed. A non-standard learning formulation based on the notions of similarity and nearest neighbors, known as *local learning*, is then presented. An overview of *kernel methods* is also given, since the state of the art methods consistently used in the supervised learning tasks presented throughout this thesis are kernel methods. This chapter ends with a discussion about cluster analysis. Several clustering techniques are proposed in this thesis and their utility

is shown on phylogenetic analysis.

The main content of this thesis is organized in two parts. Part I presents machine learning applications in computer vision. Part II presents machine learning applications in string processing, more precisely, in computational biology and natural language processing. Chapters 3, 4 and 5 belong to Part I, while Chapters 6, 7, 8 and 9 belong to Part II. Finally, the conclusions are drawn in Chapter 10.

The content of each chapter is briefly discussed next. Chapter 3 discusses the state of the art methods in computer vision for several tasks such as object recognition, texture analysis, and optical character recognition. Most of the state of the art approaches are based on patches or image descriptors, but other approaches, such as those based on deep learning, have shown impressive levels of performance. Image descriptors, which are another class of local image features besides patches, are also presented in this chapter. Since this thesis is focused on learning based on similarity, an entire section is dedicated to distance measures for image.

The first contribution of this thesis is discussed in Chapter 4. This chapter presents a novel dissimilarity measure for images, called Local Patch Dissimilarity (LPD), that was introduced in [Dinu et al., 2012]. This new distance measure is inspired from rank distance which is a distance measure for strings. Thus, it shows the concept of treating image and text in a similar way, in practice. An algorithm to compute LPD and theoretical properties of this dissimilarity are also given. This chapter describes several ways of improving LPD in terms of efficiency, such as using a hash table to store precomputed patch distances or skipping the comparison of overlapping patches. Another way to avoid the problem of the higher computational time on large sets of images is to turn to local learning methods. All these efficiency improvements were published in [Ionescu & Popescu, 2013a]. Several experiments are conducted on two data sets using both standard machine learning methods and local learning methods. The obtained results come to support the fact that LPD is a very good dissimilarity measure for images with applications in handwritten digit recognition and image classification. A variant of LPD introduced in [Ionescu et al., 2014], called Local Texton Dissimilarity (LTD), is also presented in this chapter. Local Texton Dis-

similarity aims at classifying texture images. It is based on textons, which are represented as a set of features extracted from image patches. One of the features is based on the development of an efficient box counting method for estimating fractal dimension, presented in [Popescu et al., 2013b]. Textons provide a lighter representation of patches, allowing for a faster computational time and a better accuracy when used for texture analysis. The performance level of the machine learning methods based on LTD is comparable to the state of the art methods for texture classification.

Chapter 5 presents some improvements of the bag of visual words model for two applications, namely object recognition and facial expression recognition. For the bag of visual words approach, images are represented as histograms of visual words from a codebook that is usually obtained with a simple clustering method. Next, kernel methods are used to compare such histograms. This chapter introduces a novel kernel for histograms of visual words, namely the PQ kernel. The PQ kernel was initially presented in [Ionescu & Popescu, 2013b]. It is worth mentioning that the paper of [Ionescu & Popescu, 2013b] received the Caianiello Best Young Paper Award. A proof that PQ is actually a kernel is also given in this chapter. The proof is based on building its feature map. Object recognition experiments are conducted to compare the PQ kernel with other state of the art kernels on two benchmark data sets. The PQ kernel has the best performance on both data sets. A novel formulation of the bag of visual words model is also proposed for classifying human facial expression from low resolution images. The modified bag of visual words model was presented in [Ionescu et al., 2013]. The proposed model participated at the Facial Expression Recognition (FER) Challenge of the ICML 2013 Workshop in Challenges in Representation Learning (WREPL), and ranked fourth with an accuracy of 67.484% on the final test. More details about the FER Challenge are provided in [Goodfellow et al., 2013]. The model extracts dense SIFT descriptors either from the whole image or from a spatial pyramid that divides the image into increasingly fine sub-regions. Then, it represents images as normalized (spatial) presence vectors of visual words. Linear kernels are built for several choices of spatial presence vectors, and combined into weighted sums for multiple kernel learning (MKL). Instead of building a global classifier for the machine learning task, local MKL was used to predict class labels

of test images. Empirical results indicate that the use of presence vectors, local learning and spatial information improve recognition performance.

Chapter 6 presents the state of the art methods for several problems that involve string processing. The problems studied by this work belong to two major scientific fields, namely computational biology and text mining. Consequently, this chapter is divided into two separate sections corresponding to the two fields of study. First, clustering methods used for phylogenetic analysis and other methods for sequencing and comparing DNA are discussed. An overview of state of the art natural language processing techniques is given next. The state of the art also includes recent advances in information retrieval showing that word sense disambiguation can improve the precision for difficult queries [Chifu & Ionescu, 2012].

Chapter 7 presents several clustering methods based on rank distance. The clustering algorithms were introduced in a series of recent papers [Dinu & Ionescu, 2012a,c, 2013a,b]. Two k-means algorithms are initially described. The k-means algorithm usually represents each cluster by a mean vector with respect to a distance measure. However, for the proposed k-means approaches, each cluster is represent either by the median string or by the closest string, which are computed with the genetic algorithms of [Dinu & Ionescu, 2011, 2012b]. In the genetic approaches for median or closest string, a novel algorithm for sorting uniformly distributed numbers in $O(n)$ time is used in the selection process of the next generation of chromosomes. The sorting algorithm was introduced in [Ionescu, 2013b]. This chapter also describes two hierarchical clustering techniques that use rank distance. Hierarchical clustering builds models based on distance connectivity. The proposed hierarchical methods join clusters based on the rank distance between their centroid strings. Again the cluster centroid is represented either by the median string or the closest string. This chapter also discusses the consensus string in the rank distance paradigm, which was initially investigated in [Dinu & Ionescu, 2013b]. Among the conditions that a string should satisfy in order to be accepted as consensus, are the median string and the closest string. Theoretical results indicate that it is not possible to identify a consensus string via rank distance for three or more strings. Thus, an efficient genetic algorithm is proposed to find the optimal consensus string, by adapting the approach proposed in [Dinu

& Ionescu, 2012b]. To show an application for the studied consensus problem, this chapter also discusses a hierarchical clustering algorithm based on consensus string. Experiments using mitochondrial DNA sequences extracted from several mammals are performed to compare the results of all the proposed clustering methods. Results demonstrate the clustering performance and the utility of the algorithms presented in this chapter.

In Chapter 8, a new distance measure, called Local Rank Distance (LRD), inspired from the image dissimilarity measure presented in Chapter 4, is introduced. LRD was initially presented in [Ionescu, 2013a]. Designed to conform to more general principles and adapted to DNA strings, LRD comes to improve several state of the art methods for DNA sequence analysis. This chapter shows two applications of LRD. The first application is the phylogenetic analysis of mammals. Experiments show that phylogenetic trees produced by LRD are better or at least similar to those reported in the literature. The second application is to find the closest string for a set of DNA strings, using a genetic algorithm based on LRD. The results obtained by LRD come to support the fact that concepts that make a good dissimilarity measure for images can be transferred with success in comparing and analyzing strings.

Chapter 9 presents an application of machine learning methods that work at the character level. More precisely, several string kernels and a kernel based on LRD are combined to obtain state of the art results for the native language identification task. This chapter is based on the work of [Popescu & Ionescu, 2013], which describes the approach based on string kernels for the closed Native Language Identification (NLI) Shared Task 2013. The method ranked on third place in this competition with an accuracy of 82.7%. The results are even more impressive, if one considers that the proposed approach is language independent and linguistic theory neutral. While string kernels have been used before in text analysis tasks, LRD is designed to work on DNA sequences. Thus, it is an interesting fact that LRD can be successfully applied in native language identification.

The conclusions presented in Chapter 10 point to the fact that the concept of treating image and text in a similar way is indeed fertile. Future work and new directions of exploiting this concept are also discussed in the final chapter.

Chapter 2

Learning Based on Similarity

Learning based on similarity refers to the process of learning based on pairwise similarities between the training samples. The similarity-based learning process can be both supervised and unsupervised, and the pairwise relationship can be either a similarity, a dissimilarity, or a distance function. Similarity functions may be asymmetric and even fail to satisfy other mathematical properties required for metrics or inner products, for example. When the learning process is supervised, the similarity-based method aims at estimating the class label of a test sample using both the pairwise similarities between the labeled training samples, and the similarities between the test sample and the set of training samples. When the learning process is unsupervised, the similarity-based method aims at finding hidden structure in unlabeled training samples, using the pairwise similarities between samples. An advantage of similarity-based learning is that it does not require direct access to the features, as long as the similarity function is well defined for any pair of samples. Thus, the feature space is not required to be an euclidean space.

Similarity-based learning methods have been widely used in several domains such as computer vision, natural language processing, computational biology, and information retrieval. Computer vision researchers proposed several methods based on computing similarity between images for object recognition and image retrieval. Such methods range from distance measures such as the Tangent distance [Simard et al., 1996], the Earth Mover's distance [Rubner et al., 2000], or the shape matching distance [Belongie et al., 2002], to kernel methods such

as the pyramid match kernel [Lazebnik et al., 2006] or the PQ kernel [Ionescu & Popescu, 2013b]. Most of the state of the art techniques in computational biology, such as those that obtain phylogenetic trees or those that compare DNA sequences, are based on distance measures for strings. Popular choices for recent techniques are the Hamming distance [Chimani et al., 2011; Vezzi et al., 2012], edit distance [Shapira & Storer, 2003], Kendall-tau distance [Popov, 2007] or rank distance [Dinu & Ionescu, 2012a,b]. Other popular similarity-based tools from computational biology are the FASTA algorithm [Lipman & Pearson, 1985] and the BLAST algorithm [Altschul et al., 1990]. These tools compute the similarity between different amino acid sequences for protein classification. The cosine similarity between term frequency-inverse document frequency (TF-IDF) vectors is widely used in information retrieval and text mining for document classification [Manning et al., 2008]. More recently, the string kernel [Shawe-Taylor & Cristianini, 2004], which computes the similarity between strings by counting common character n-grams, has demonstrated impressive levels of performance for text categorization (by topic) [Lodhi et al., 2002], authorship identification [Popescu & Dinu, 2007; Popescu & Grozea, 2012; Sanderson & Guenter, 2006], and native language identification [Popescu & Ionescu, 2013].

The similarity-based learning paradigm consists of a wide variety of algorithms and approaches. Among the variety of similarity-based learning methods, only four of them are extensively discussed in this thesis, namely the Nearest Neighbor model, the local learning methods, the kernel methods and the cluster analysis techniques. These four approaches are used in different applications presented in this work. Other similarity-based learning methods, such as treating similarities as features, or generative classifiers, are briefly discussed next. By treating the similarities between a sample and training samples as features, similarity-based classification problems can be regarded as standard classification problems [Chen et al., 2009; Graepel et al., 1999, 1998; Liao & Noble, 2003; Pekalska & Duin, 2002]. In other words, each sample is represented by a feature vector obtained by computing the similarity with a set of training samples. Generative classifiers provide a structured probabilistic model of the data. Training data is used for estimating the parameters of the generative model. Given the pairwise similarity of n samples, one approach to generative classification is using the similarities as

features. Then, the parameters of a standard generative model can be estimated from an n-dimensional feature space. Recently, another generative framework for similarity-based classification, termed similarity discriminant analysis, has been proposed in [Cazzanti et al., 2008]. It models the class-conditional distributions of similarity statistics. Other approaches designed to reduce bias are a local variant proposed in [Cazzanti & Gupta, 2007] and a mixture model variant discussed in [Chen et al., 2009].

The rest of this chapter is organized as follows. Nearest Neighbor models are discussed in Section 2.1. Section 2.2 presents local learning methods, which are based on the notions of similarity and nearest neighbors. An overview of kernel methods is given in Section 2.3. The chapter ends with Section 2.4, which gives an overview of clustering methods based on similarity.

2.1 Nearest Neighbor Model

Since the k-nearest neighbors algorithm (k-NN) was introduced in [Fix & Hodges, 1951], it has been studied by many researchers and it is still an active topic in machine learning. The k-nearest neighbors algorithm is one of the simplest of all the machine learning algorithms, proving that simple models are always attractive for researchers. The k-nearest neighbors classification rule works as follows: an object is assigned to the most common class of its k nearest neighbors, where k is a positive integer value. If $k = 1$, then the object is simply assigned to the class of its nearest neighbor. When $k > 1$, the decision is based on a majority vote. It is convenient to let k be odd, to avoid voting ties. However, if voting ties do occur, the object can be assigned to the class of its 1-nearest neighbor, or one of the tied classes can be randomly chosen to be the class assigned to the object.

The example about handwritten digit recognition presented in Figure 2.1 is supposed to give a more clear view of the k-NN model. In this example, digits are represented in a two-dimensional feature space. When a new sample x comes in, the algorithm selects the nearest 3 neighbors and assigns the majority class to x. In Figure 2.1, the majority label among the nearest 3 neighbors of x is 4. Thus, label 4 is assigned to x. This model can be referred to as a 3-NN model. To better understand how the decision of the k-NN model is taken in general, it

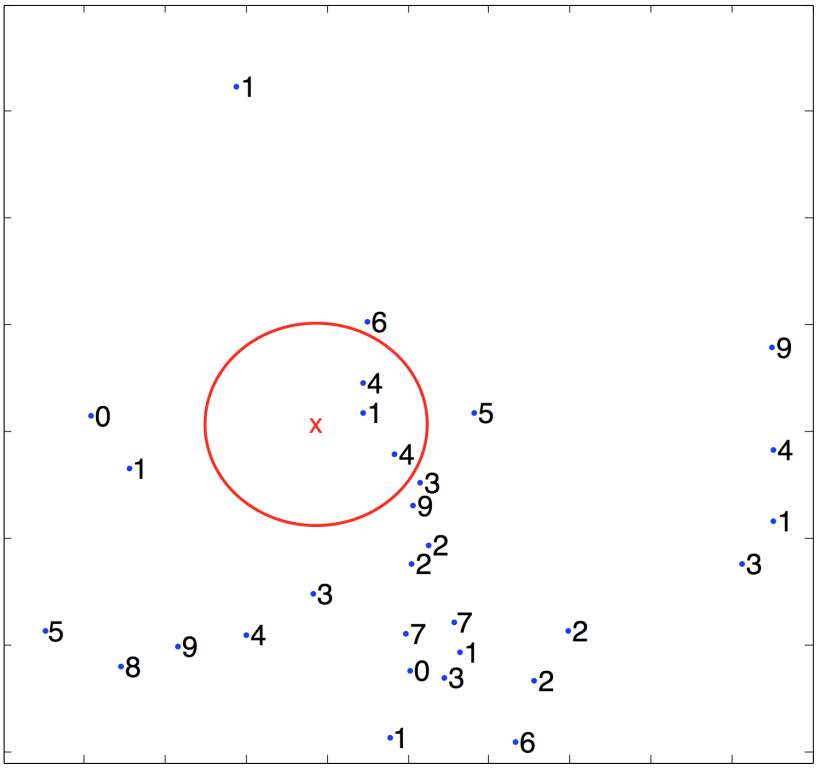

Figure 2.1: A 3-NN model for handwritten digit recognition. For visual interpretation, digits are represented in a two-dimensional feature space. The figure shows 30 digits sampled from the popular MNIST data set. When the new digit x needs to be recognized, the 3-NN model selects the nearest 3 neighbors and assigns label 4 based on a majority vote.

is worth considering a 1-NN model. For this model, the decision at every point is to assign the label of the closest data point. This process generates a Voronoi partition of the training samples, as seen in Figure 2.2. Each training data point corresponds to a Voronoi cell. When a new data point comes in, it is assigned to the class associated to the Voronoi cell that the respective data point falls in.

The k-NN algorithm is a non-parametric method for classification. Thus, no parameters have to be learned. In fact, the k-NN model does not require training at all. The decision of the classifier is only based on the nearest k neighbors of an object with respect to a similarity or distance function. The euclidean distance measure is a very common choice, but other similarity measures can also be used

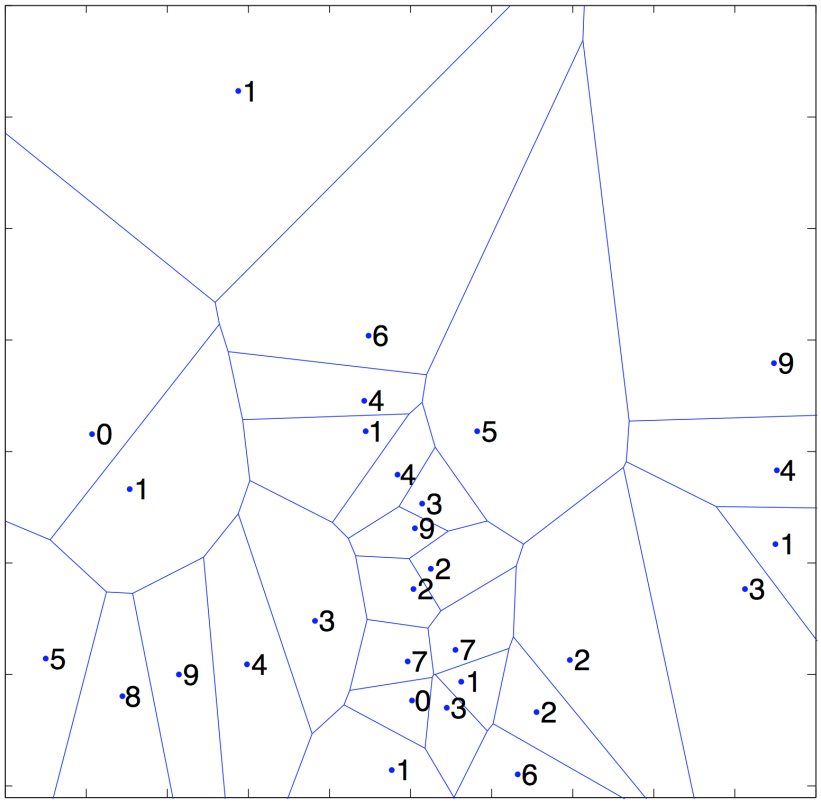

Figure 2.2: A 1-NN model for handwritten digit recognition. The figure shows 30 digits sampled from the popular MNIST data set. The decision boundary of the 1-NN model generates a Voronoi partition of the digits.

instead. Actually, the performance of the k-NN classifier depends on the strength and the discriminatory power of the distance measure used. It is worth mentioning that a good choice of the distance metric can help to achieve invariance with respect to a certain family of transformations. For example, a distance metric that is invariant to scale, rotation, luminosity and contrast changes is a suitable choice for computer vision tasks. Researchers continue to study and develop new similarity or dissimilarity measures for a broad variety of applications in different domains. But, when it comes to testing the similarity measure in machine learning tasks, the method of choice is the k-NN model, because it deeply reflects the strength of the similarity measure. Good examples of this fact are the Tangent distance [Simard et al., 1996] and the shape matching distance [Belongie et al.,

2002], which are both used for handwritten digit recognition. For the same reason, the k-NN model is used to assess the performance of the new dissimilarity measure for images presented in Chapter 4 of this work.

It is interesting to mention that the k-NN model is one of the first classifiers for which an upper bound of its error rate has been demonstrated. More precisely, a theoretical result demonstrated in [Cover & Hart, 1967] states that the nearest neighbor rule is asymptotically at most twice as bad as the Bayes rule. Furthermore, if k is allowed to grow with n such that $k/n \to 0$, the nearest neighbor rule is universally consistent. More consistency results and other theoretical aspects of the k-NN model are discussed in [Devroye et al., 1996].

The k-NN model defers all the computations to the test phase. This represents a great disadvantage when the computational time is taken into consideration. Searching for the k nearest neighbors among n training samples may take time proportional to $O(n \cdot k \cdot d)$ using a naive approach, where d represents the computational cost of the distance function. Different approaches based on multidimensional search trees that partition the space and guide the search have been proposed to reduce the time complexity [Dasarathy, 1991]. Other fast k-NN approaches are proposed in [Faragó et al., 1993] and [Zhang & Srihari, 2004].

2.2 Local Learning

The development of unconventional (or nonstandard) learning formulations and non-inductive types of inference was studied in [Vapnik, 2006]. The author argues in favor of introducing and developing unconventional learning methods, as an alternative to algorithmic improvements of existing learning methods. This view is consistent with the main principle of VC theory [Vapnik & Chervonenkis, 1971], suggesting that one should always use direct learning formulations for finite sample estimation problems, rather than more general settings (such as density estimation).

Local learning methods attempt to locally adjust the performance of the training system to the properties of the training set in each area of the input space. A simple local learning algorithm works as follows: for each test sample, select a few training samples located in the vicinity of the test sample, train a classifier

with only these few examples and apply the resulting classifier to predict the class label of the testing example. For example, the k-NN model and the Radial Basis Function (RBF) network are part of the family of local learning algorithms. Actually, the k-NN model is the simplest form of local learning, since the discriminant function is constant. But, almost any other classifier can be employed in the local learning paradigm. However, it is important to mention that besides the classifier, a similarity or distance measure is required to determine the neighbors located in the vicinity of a test sample. Local learning has a few advantages over standard learning methods. First, it divides a hard classification problem into more simple sub-problems. Second, it reduces the variety of samples in the training set, by selecting samples that are most similar to the test one. Third, it improves accuracy for data sets affected by labeling noise. Considering these advantages, the local learning paradigm is suitable for classification problems with large training data.

In [Bottou & Vapnik, 1992] the idea of local algorithms for pattern recognition was used. The approach is based on local linear rules instead of local constant rules, and VC bounds [Vapnik & Chervonenkis, 1971] instead of the distance to the k-th nearest neighbor. The local linear rules demonstrated an improvement in accuracy on the popular MNIST data set (from 4.1% to 3.2%).

For the regression estimation problem, a similar approach was used in the Nadaraya-Watson estimator [Nadaraya, 1964] with a slightly different concept of locality. Nadaraya and Watson suggested considering "soft locality" by using a kernel as a weighting function for estimating a value of interest.

In Chapter 4, a k-NN with filtering approach that is also a pure local learning algorithm is used. For the filter-based k-NN approach, the idea is to filter (or select) the nearest K neighbors (where K is larger than k) using a distance measure that is much faster and easy to compute. Instead of training a classifier, the next step is to select the nearest k neighbors from those filtered K examples using a distance measure that is able to capture much finer differences. This latter distance measure is allowed to consume more time in order to determine a better similarity (or dissimilarity) between training examples. This approach is appropriate when it is unreasonable, from the perspective of time, to compute the latter distance for all training examples. This two-step selection (or filtering)

process is much faster to compute than a standard k-NN based only on the computationally heavy distance measure.

In Chapter 5, the learning phase of the framework used for facial expression recognition is based on a local learning algorithm. The algorithm uses a kernel based on visual word occurrences to select nearest neighbors in the vicinity of a test image. Then, it trains a SVM classifier only on the selected neighbors to predict the class label of the test image.

2.3 Kernel Methods

In the similarity-based learning paradigm, a popular approach is to treat the pairwise similarities as inner products in some Hilbert space or to treat pairwise dissimilarities as distances in some euclidean space. This can be achieved in roughly two ways. One is to explicitly embed the samples in a euclidean space, according to the pairwise similarities (or dissimilarities) using multidimensional scaling [Borg & Groenen, 2005]. Another is to modify the similarities into kernels and apply kernel methods. This section is focused on the latter approach and it covers the following topics: an overview of kernel methods, methods of combining kernels, such as kernel alignment, multiple kernel learning (MKL), and state of the art kernel methods such as Support Vector Machines (SVM), Kernel Ridge Regression (KRR), Kernel Linear Discriminant Analysis (KDA), or Kernel Partial Least Squares Regression (KPLS). Special consideration is given to the topics that discuss kernel approaches used throughout the experiments presented in this thesis.

2.3.1 Mathematical Preliminaries and Properties of Kernels

This section follows the theoretical presentation given in [Shawe-Taylor & Cristianini, 2004]. Therefore, most of the definitions, propositions and theorems are reproduced from [Shawe-Taylor & Cristianini, 2004] for the sake of completeness of this chapter.

A definition of an inner product space is given next.

Definition 1 *A vector space X over the set of real numbers $\mathbb{R}$ is an inner product space, if there exists a real-valued symmetric bilinear (linear in each argument) map $\langle \cdot, \cdot \rangle$, that satisfies $\langle x, x \rangle \geq 0$, for all $x \in X$. The bilinear map is known as the inner product, dot product or scalar product.*

An inner product space is sometimes referred to as a Hilbert space, although most researchers agree that additional properties of completeness and separability are required. Formally, a *Hilbert space* can be defined as follows.

Definition 2 *A Hilbert Space $\mathcal{H}$ is an inner product space with the additional properties of completeness and separability. A space $\mathcal{H}$ is complete if every Cauchy sequence $\{h_n\}_{n \geq 1}$ of elements of $\mathcal{H}$ converges to a element $h \in \mathcal{H}$, where a Cauchy sequence is one that satisfies the property that*

$$\sup_{m>n} \|h_n - h_m\| \to 0, as\ n \to \infty.$$

A space $\mathcal{H}$ is separable if for any $\epsilon > 0$ there is a finite set of elements $\{h_1, ..., h_N\}$ of $\mathcal{H}$ such that for all $h \in \mathcal{H}$

$$\min_i \|h_i - h\| < \epsilon.$$

Note that $\mathbb{R}^n$ is a Hilbert space.

A kernel method performs a mapping into an embedding or feature space. An *embedding map* (or *feature map*) is a function

$$\phi : x \in \mathbb{R}^n \longmapsto \phi(x) \in F \subseteq \mathcal{H}.$$

A *kernel function* is defined as follows.

Definition 3 *A kernel is a function k that for all $x, z \in X$ satisfies*

$$k(x, z) = \langle \phi(x), \phi(z) \rangle,$$

where ϕ is a mapping from X to an inner product feature space F

$$\phi : x \longmapsto \phi(x) \in F.$$

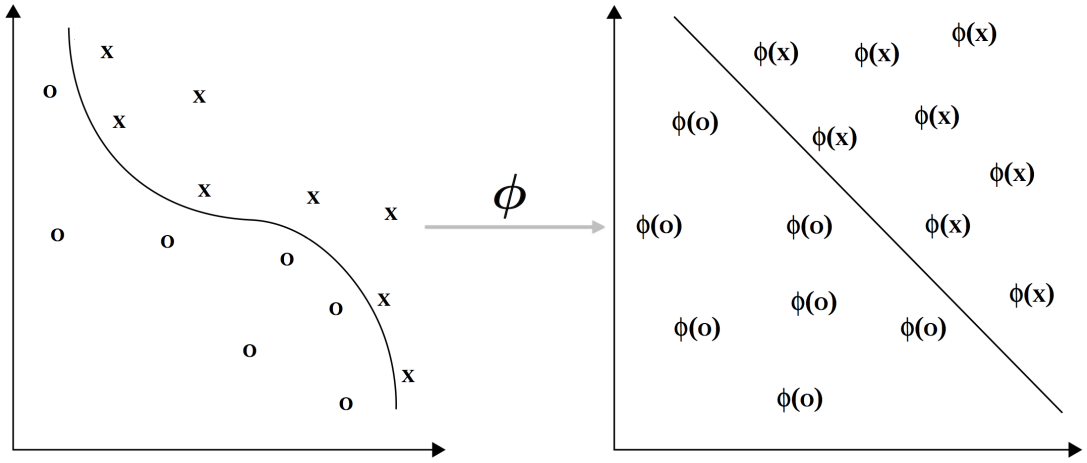

Figure 2.3: The function ϕ embeds the data into a feature space where the nonlinear relations now appear linear. Machine learning methods can easily detect such linear relations.

The choice of the map ϕ aims to convert the nonlinear relations from X into linear relations in the embedding space F. An example of feature embedding were nonlinear patterns are converted into linear ones is given in Figure 2.3.

Given a set of vectors in X, the pairwise kernels between these vectors generate a *kernel matrix*. The kernel matrix is defined next.

Definition 4 *Given a set of vectors $\{x_1, ..., x_l\}$ and a kernel function k employed to evaluate the inner products in a feature space with feature map ϕ. The kernel matrix is defined as the $l \times l$ matrix K with entries given by:*

$$K_{ij} = \langle \phi(x_i), \phi(x_j) \rangle = k(x_i, x_j).$$

Given a square matrix A, the real number λ and the non-zero vector x are an eigenvalue and corresponding eigenvector of A if $Ax = \lambda x$. A square matrix A is symmetric if $A' = A$, where A' represents the transpose of A. A symmetric matrix is positive semi-definite, if its eigenvalues are all non-negative.

Proposition 1 *Kernel matrices are positive semi-definite.*

Finitely positive semi-definite functions are defined next.

Definition 5 *A function $k : X \times X \longmapsto \mathbb{R}$ satisfies the finitely positive semi-definite property if it is a symmetric function for which the matrices formed by restriction to any finite subset of the space X are positive semi-definite.*

The following theorem gives the characterization of kernels.

Theorem 1 *A function $k : X \times X \longmapsto \mathbb{R}$ which is either continuous or has a finite domain, can be decomposed into a feature map ϕ into a Hilbert space F applied to both its arguments followed by the evaluation of the inner product in F as follows:*

$$k(x, z) = \langle \phi(x), \phi(z) \rangle,$$

if and only if it satisfies the finitely positive semi-definite property.

Given a function k that satisfies the finitely positive semi-definite property, its corresponding space F_k can be referred to as its *Reproducing Kernel Hilbert Space* (RKHS).

The following proposition shows the operations that can be used to build new kernels from existing kernels.

Proposition 2 *Let k_1 and k_2 be two kernels over $X \times X$, $X \subseteq \mathcal{H}$, $a \in \mathbb{R}^+$, $f(\cdot)$ a real-valued function on X, and B a symmetric positive semi-definite $n \times n$ matrix. Then the following functions are kernels:*

$$\begin{aligned}
(i)\ & k(x, z) = k_1(x, z) + k_2(x, z) \\
(ii)\ & k(x, z) = a k_1(x, z) \\
(iii)\ & k(x, z) = k_1(x, y) \cdot k_2(x, z) \\
(iv)\ & k(x, z) = f(x) \cdot f(z) \\
(v)\ & k(x, z) = x' B z
\end{aligned}$$

Since the concept of kernel method appeared, researchers have proposed several kernels. The most common kernel is the linear kernel that is obtained by computing the inner product of two vectors. The map function in this case is $\phi(x) = x$. Let $k_1(x, z)$ be a kernel over $X \times X$, where $x, z \in X$, and $p(x)$ is

a polynomial with positive coefficients. Then the following functions are also kernels. The *polynomial kernel* is defined by $k(x, y) = p(k_1(x, z))$. Another two kernels based on the exponential function are defined as $k(x, z) = \exp(k_1(x, z))$ and $k(x, z) = exp(-\|x - z\|^2/(2\sigma^2))$. The latter kernel is known as the *Gaussian kernel*. Such functions form the hidden units of RBF networks, and the Gaussian kernel is therefore also referred to as the *RBF kernel*. The *intersection kernel* is given by $k(x, z) = \sum_i \min\{x_i, z_i\}$. The definition of the *Hellinger's kernel* (also known as the *Bhattacharyya coefficient*) is $k(x, z) = \sum_i \sqrt{x_i \cdot z_i}$. Other examples of kernels from a broad variety of such functions are the χ^2 kernel, the Jensen-Shanon kernel, or the Matern kernel. A new kernel, termed the PQ kernel, is presented in Chapter 5 of this thesis.

2.3.2 Overview of Kernel Classifiers

Kernel-based learning algorithms work by embedding the data into a Hilbert space, and searching for linear relations in that space using a learning algorithm. The embedding is performed implicitly, that is by specifying the inner product between each pair of points rather than by giving their coordinates explicitly. The power of kernel methods lies in the implicit use of a RKHS induced by a positive semi-definite kernel function. Despite the fact that the mathematical meaning of a kernel is the inner product in a Hilbert space, another interpretation of a kernel is the pairwise similarity between samples.

The kernel function offers to the kernel methods the power to naturally handle input data that is not in the form of numerical vectors, such as strings, images, or even video and audio files. The kernel function captures the intuitive notion of similarity between objects in a specific domain and can be any function defined on the respective domain that is symmetric and positive definite. For strings, many such kernel functions exist with various applications in computational biology and computational linguistics [Shawe-Taylor & Cristianini, 2004]. For images, a state of the art approach is the pyramid match kernel [Lazebnik et al., 2006].

In the case of binary classification problems, kernel-based learning algorithms look for a discriminant function, a function that assigns $+1$ to examples belonging to one class and -1 to examples belonging to the other class. This function will

be a linear function in the space $\mathcal{F}$, that means it will have the form:

$$f(x) = \text{sign}(< w, \phi(x) > +b),$$

for some weight vector w. The kernel can be exploited whenever the weight vector can be expressed as a linear combination of the training points, $\sum_{i=1}^{n} \alpha_i \phi(x_i)$, implying that f can be expressed as follows:

$$f(x) = \text{sign}\left(\sum_{i=1}^{n} \alpha_i k(x_i, x) + b\right).$$

Various kernel methods differ by the way in which they find the vector w (or equivalently the vector α). Support Vector Machines [Cortes & Vapnik, 1995] try to find the vector w that defines the hyperplane that maximally separates the images in $\mathcal{F}$ of the training examples belonging to the two classes. Mathematically, the SVM classifier chooses the w and the b that satisfy the following optimization criterion:

$$\min_{w,b} \frac{1}{n} \sum_{i=1}^{n} [1 - y_i(< w, \phi(x_i) > +b)]_+ + \nu ||w||^2$$

where y_i is the label $(+1/-1)$ of the training example x_i, ν a regularization parameter and $[x]_+ = \max\{x, 0\}$.

Kernel Ridge Regression (KRR) selects the vector w that simultaneously has small empirical error and small norm in the RKHS generated by the kernel k. The resulting minimization problem is:

$$\min_{w} \frac{1}{n} \sum_{i=1}^{n} (y_i - < w, \phi(x_i) >)^2 + \lambda ||w||^2$$

where again y_i is the label $(+1/-1)$ of the training example x_i, and λ a regularization parameter.

The *Linear Discriminant Analysis* (LDA) method, also known as *Fisher Discriminant Analysis*, maximizes the ratio of between-class variance to the within-class variance in order to guarantee maximal separability for a particular set of samples. The work of [Fisher, 1936] derived the LDA approach for a two class

problem, under the assumptions that the classes have normal distributions and identical covariance matrices. The assumption of identical covariance matrices implies that the Bayes classifier is linear. Therefore, LDA provides a projection of the data points to a one-dimensional subspace where the Bayes classification error is smallest. The KDA method [Shawe-Taylor & Cristianini, 2004] is the kernel version of the LDA algorithm, which is somewhat similar to the KRR algorithm.

It appears that sometimes the covariance of the input vectors with the targets is more important than the variance of the vectors, for regression problems. The *partial least squares* (PLS) approach is based on the covariance to guide feature selection, before performing least-squares regression in the derived feature space. More precisely, PLS is used to find the fundamental relations between the input matrix X and response matrix Y. The kernel version of PLS is a powerful algorithm that can also be used for classification problems.

For a particular classification problem, some kernel methods may be more suitable than others. The accuracy level depends on many aspects such as class distribution, the number of classes, data noise, size of the training data, and so on. For example, the KRR classifier can be used with success for problems with well-balanced classes, while the kernel partial least squares (KPLS) classifier is more suitable for many class problems. In some particular cases, when the number of classes is greater than two, there is a serious problem with the regression methods. More precisely, some classes can be masked by others. The KDA classifier is able to improve accuracy by avoiding the masking problem [Hastie & Tibshirani, 2003]. More details about SVM, KRR, KDA and KPLS can be found in [Shawe-Taylor & Cristianini, 2004]. The important fact is that the optimization problems of these classifiers are solved in such a way that the coordinates of the embedded points are not needed, only their pairwise inner products which in turn are given by the kernel function k.

The SVM and KRR classifiers are used in Chapter 4 for handwritten character recognition and texture classification, and in Chapter 9 for native language identification. The SVM classifier is also used in Chapter 5 for object recognition and facial expression recognition. The KDA and KPLS methods are used in Chapter 4 for texture classification, along with the SVM and KRR methods.

The KDA classifier is also used in Chapter 9 for native language identification.

2.3.3 Kernel Normalization

An example of creating a new kernel from an existing one is provided by normalizing the existing kernel. Given a kernel $k(x, y)$ that corresponds to the feature mapping ϕ, the normalized kernel $\hat{k}(x, y)$ corresponds to the feature map given by:

$$x \longmapsto \phi(x) \longmapsto \frac{\phi(x)}{\|\phi(x)\|}.$$

Researchers have found that data normalization helps to improve machine learning performance for various applications. Since the range of values of raw data can have large variation, classifier objective functions will not work properly without normalization. Features are usually normalized through a process called *standardization*, which makes the values of each feature in the data have zero-mean and unit-variance. By normalization, each feature has an approximately equal contribution to the distance between two samples.

The kernel normalization can also be done directly on the kernel matrix. To obtain a normalized kernel matrix, each component is divided by the square root of the product of the two corresponding diagonal components:

$$\hat{K}_{ij} = \frac{K_{ij}}{\sqrt{K_{ii} \cdot K_{jj}}}. \tag{2.1}$$

This is equivalent to normalizing the kernel function as follows:

$$\hat{k}(x_i, x_j) = \frac{k(x_i, x_j)}{\sqrt{k(x_i, x_i) \cdot k(x_j, x_j)}} \tag{2.2}$$

An interesting study that gives a good insight into how different kernels should be normalized is [Vedaldi & Zisserman, 2010]. The authors state that γ-homogeneous kernels should be L_γ-normalized. For example, the linear kernel or the Jensen-Shannon kernel should be L_2-normalized, while the Hellinger's kernel should be L_1-normalized.

2.3.4 Combining Kernels

Different kernel representations can be obtained from the same data. The idea of combining all these kernels is natural when one wants to improve the performance of a classifier. When multiple kernels are combined, the features are actually embedded in a higher-dimensional space. As a consequence, the search space of linear patterns grows, which helps the classifier to select a better a discriminant function. The concept of learning using multiple kernels is known as *multiple kernel learning* (MKL).

The most natural way of combining two kernels is to sum them up. Summing up kernels or kernel matrices is equivalent to feature vector concatenation. But, the feature vectors are usually high-dimensional vectors, and the concatenation of such vectors is not a viable solution in terms of space and time. In this case, the kernel trick can be employed to obtain the kernel matrices that must be summed up. Another possibility to obtain a combination is to multiply the kernels. An interesting remark is that multiplying sparse kernel matrices (component-wise) will produce an even more sparse kernel matrix, which might not be desirable in some cases, since patterns simply disappear. These two methods of combining kernels are also given in Proposition 2.

Another option is to combine kernels by kernel alignment [Cristianini et al., 2001]. Instead of simply summing kernels, kernel alignment assigns weights for each of the two kernels based on how well they are aligned with the ideal kernel YY' obtained from labels. The work of [Cortes et al., 2013] presents a new algorithm for multi-class classification with multiple kernels, which is based on a natural notion of the multi-class margin of a kernel. The algorithm shows improvements over the performance of state of the art algorithms in binary and multi-class classification with multiple kernels. A review of MKL algorithms is presented in [Gonen & Alpaydin, 2011].

MKL based on kernel alignment and kernel sum is used in Chapter 5 to obtain spatial pyramids for facial expression recognition, and in Chapter 9 to combine string kernels for native language identification.

2.4 Clustering Analysis

A form of unsupervised learning used in data mining is clustering. Unlike supervised learning, it has the advantage that the training phase is not required and it has more general applications. Clustering has long played an important role in a wide variety of fields, such as biology, statistics, pattern recognition, information retrieval, machine learning, data mining, psychology and other social sciences.

Clustering is the task of assigning a set of objects into groups (termed clusters) so that the objects in the same cluster are more similar to each other than to those in other clusters. Objects are clustered based only on the information found in the data that describes the objects and their relationships. Pairwise relationships are usually described through a similarity or dissimilarity function. The goal of clustering is to maximize the similarity of objects within groups, and in the same time, to minimize the similarity of objects from different groups. The greater the similarity within a group and the greater the difference between groups, the better or more distinct the clustering. The clusters should capture the natural structure hidden in the data. An important remark is that the appropriate clustering algorithm and parameter settings, such as the distance function to use, the density threshold, or the number of expected clusters, all depend on individual data sets.

There are various clustering algorithms that differ significantly in their notion of what constitutes a cluster. Popular notions of clusters include groups with low distances among the cluster members, dense areas of the data space, intervals or particular statistical distributions. Clustering methods can be roughly divided into several categories, such as hierarchical clustering methods, centroid based methods, distribution based methods, grid based methods, and density based methods. This section discusses only the first two categories of clustering methods, which are also used in some of the experiments presented in this thesis. However, a complete reference of the major clustering methods is given in [Enăchescu, 2004]. It is important to mention that some of the recent approaches do not necessarily fall in one of these categories, such as the subspace clustering method of [Kailing et al., 2004], and some of them use mixed models [McCallum et al., 2000].

The k-means clustering technique is a simple method of cluster analysis which aims to partition a set of objects into K clusters in which each object belongs to the cluster with the nearest mean. The algorithm begins with choosing K initial centroids, where K is an *a priori* parameter, namely, the number of clusters desired. Each object is then assigned to the nearest centroid, and each group of objects assigned to a centroid is a cluster. The centroid of each cluster is then updated based on the objects assigned to that cluster. The assignment and update steps are repeated until no point changes clusters or until a maximum number of iterations is reached. The k-means algorithm aims at minimizing an objective function, given by

$$J = \sum_{j=1}^{K} \sum_{i=1}^{n} \|x_i^{(j)} - c_j\|^2$$

where $x_i^{(j)}$ is a vector in cluster j and c_j is the cluster centroid (or mean vector). The alternating optimization procedure that minimizes this objective function is given in [Enăchescu, 2004; Hastie & Tibshirani, 2003].

It is interesting to mention that the k-means algorithm generates a Voronoi partitioning of the data. Each cluster is a Voronoi cell determined by the cluster centroid. In Chapter 5, the k-means algorithm is used to obtain visual words from vector quantized image descriptors. Several k-means types for string objects are presented in Chapter 7.

Hierarchical clustering creates a hierarchical decomposition of a given set of data objects. Hierarchical methods can be divided into two main categories: *agglomerative* methods and *divisive* methods. Agglomerative methods start at the bottom and recursively join clusters two by two at each level, until a single cluster is obtained. On the other hand, divisive methods start at the top and recursively divide a cluster into two new clusters at each level, until objects are completely divided into separate clusters. Divisive methods are not generally available and have rarely been applied due to the difficulty of taking the right decision of dividing clusters at a high level. Thus, many hierarchical clustering techniques are variations of a single (agglomerative) algorithm: starting with individual objects as clusters, successively join the two nearest clusters until only

one cluster remains. These techniques connect objects to form clusters based on their distance. An important remark is that hierarchical algorithms do not provide a single partitioning of the data set, but an extensive hierarchy of clusters that merge with each other at certain distances. This structure can be represented using a *dendrogram*. Apart from the choice of a distance function, another decision is needed for the linkage criterion to be used. The most popular choices are the single-linkage, the complete-linkage, or the average-linkage. In the single-linkage method, the similarity between two clusters is measured by the similarity of the closest pair of data points from different clusters. The complete-linkage takes the similarity of the furthest pair of data points from different clusters. The average-linkage takes the average similarity between all the pairs of data points from different clusters. Several hierarchical clustering techniques are presented in Chapter 7, but instead of a linkage criterion they use a different approach, that is to determine a centroid string for each cluster and join clusters based on the rank distance between their centroid strings.

2.4.1 State of the Art

In recent years considerable effort has been made to improve the performance of the existing clustering algorithms. The work of [Huang, 1998] proposes an extension to the k-means algorithm for clustering large data sets with categorical values. A clustering method that aims to identify spatial structures that may be present in the data is proposed in [Ng & Han, 2002].

An unsupervised data mining algorithm used to perform hierarchical clustering over particularly large data-sets is presented in [Zhang et al., 1996]. The advantage of this algorithm is its ability to incrementally and dynamically cluster incoming, multi-dimensional metric data points in an attempt to produce the best quality clustering with a given set of resources.

With the recent need to process larger and larger data sets (also known as big data), the willingness to treat semantic meaning of the generated clusters for performance has been increasing. This led to the development of pre-clustering methods such as canopy clustering [McCallum et al., 2000], which can process huge data sets efficiently, but the resulting clusters are only a rough pre-partitioning

of the data set, to then analyze the partitions with existing slower methods such as k-means clustering.

The development of new clustering methods has led to the improvement or discovery of many classification methods. For example, in [Yin et al., 2013] a fast classification algorithm to address the multi-class problems with cooperative clustering is presented. The algorithm computes the cluster centers of all classes simultaneously. In computer vision, image features are vector quantized into visual words by k-means clustering [Leung & Malik, 2001], before training a classifier on the bag of visual words representation.

For high-dimensional data, many of the existing methods fail due to the curse of dimensionality, which renders particular distance functions problematic in high-dimensional spaces. This led to new clustering algorithms for high-dimensional data that focus on subspace clustering and correlation clustering [Kriegel et al., 2009]. An example of subspace clustering algorithm is SUBCLU [Kailing et al., 2004] which aims at automatically identifying subspaces of the feature space in which clusters exist. This algorithm is able to detect arbitrarily shaped and positioned clusters in subspaces. Another similar algorithm is CLIQUE [Agrawal et al., 1998] which identifies dense clusters in subspaces of maximum dimensionality. Ideas from density-based clustering methods have been adopted to subspace clustering [Achtert et al., 2006, 2007] and correlation clustering [Bohm et al., 2004].

Several different clustering systems based on mutual information have also been proposed. The author of [Meila, 2003] proposes an information theoretic criterion (called variation of information) for comparing two clusterings of the same data set. Also, message passing algorithms led to the creation of new types of clustering algorithms [Frey & Dueck, 2007].

Clustering is also used in natural language processing. For example, several unsupervised learning methods have been proposed for word sense disambiguation [Agirre & Edmonds, 2006]. Unsupervised WSD has a wide variety of applications, since annotated training data is not required. Recently, unsupervised WSD showed that it can improve the precision of an information retrieval (IR) system for difficult queries [Chifu & Ionescu, 2012].

Part I

Machine Learning in Computer Vision

Chapter 3

State of the Art

Computer vision is a field that studies methods for acquiring, processing, analyzing, and understanding images and video. Such methods attempt to solve different tasks including object recognition, scene reconstruction, event detection, video tracking, image retrieval, image segmentation, motion estimation, image restoration, and many others. One of the most important tasks in computer vision is object recognition. This task deals with building computer systems that attempt to identify objects represented in digitized images or video, thus enabling robots to see. Machine learning methods represent the state of the art approach for the object recognition problem. The mainstream approach is to treat object recognition as a classification task. Therefore, the problem is also referred to as *image classification* or *image categorization*.

Computer vision researchers have developed several learning methods for image categorization or related tasks. But, a preliminary task in order to obtain a state of the art image categorization method is feature detection and extraction. The goal is to obtain a better and more compact representation of the image. This is usually done by detecting interest points in the image using edge detectors or corner detectors, among others. The next step is to extract image descriptors from the nearby regions of interest points. For example, the *bag of visual words* model [Csurka et al., 2004; Fei-Fei & Perona, 2005; Leung & Malik, 2001; Sivic et al., 2005; Zhang et al., 2007] is one of the state of the art methods that employs interest point detection and feature extraction in a preliminary phase. It then builds a vocabulary of visual words by clustering local image descriptors

extracted from images. The bag of visual words model has demonstrated impressive levels of performance for image categorization [Zhang et al., 2007] and image retrieval [Philbin et al., 2007].

As discussed in Chapter 2, similarity-based learning methods are also used as state of the art methods in computer vision. Researchers have proposed several distance measures for images such as the Tangent distance [Simard et al., 1996], the Earth Mover's distance [Rubner et al., 2000], or the shape matching distance [Belongie et al., 2002].

A broad variety of methods are based on deep learning [Bengio, 2009; Montavon et al., 2012]. Deep learning is a way to transform one representation into another, by better disentangling the factors of variation that explain the observed data. Such algorithms aim at discovering multiple levels of representation, or a hierarchy of features. The main approach in this area is represented by the deep belief neural networks. Deep networks minimize a non-convex loss function, thus obtaining impressive levels of performance when very large training data is available. For example, the convolutional neural network of [Krizhevsky et al., 2012] won the ImageNet Large Scale Visual Recognition Challenge 2012. But, usually a lot of training data and time is needed to train such deep models. Indeed, the network of [Krizhevsky et al., 2012], consisting of $650,000$ neurons, 832 million synapses, and 60 million parameters, was trained with backpropagation on GPU for almost one week. Another motivation that supports the good results of deep networks is that handcrafted models are replaced by trainable models. Among all the applications of deep learning, that go far beyond computer vision, deep methods have also been used for 3D object classification in [Socher et al., 2012].

The chapter is organized as follows. State of the art image distance measures are presented in Section 3.1. An overview of image descriptors and interest point detectors is given in Section 3.3. Finally, Section 3.4 presents a state of the art and some variations of the bag of visual word model.

3.1 Image Distance Measures

Similarity measures of images can be categorized as follows: pixel-wise comparison of intensities, morphological measures that define the distance between images

by the distance between their level sets, and measures based on the gray value distributions of the image.

The similarity between vector representations of images is measured by usual practical distances: L_p-metrics, weighted editing metrics, Tanimoto distance, cosine distance, Mahalanobis distance and its extension, the Earth Mover distance. Among probability distances, the ones that are most used are Bhattacharyya 2, Hellinger, Kullback-Leibler, Jeffrey and for histograms χ^2, Kolmogorov-Smirnov, Kuiper distances [Deza & Deza, 1998]. Many distance measures are specific for a single type of images, such as color images, binary (black and white) images, gray-scale images, and so on.

3.1.1 Color Image Distances

The basic assumption of colorimetry, supported experimentally by [Indow, 1991], is that the perceptual color space admits a metric, the true color distance. This metric is expected to be locally euclidean. Another assumption is that there is a continuous mapping for the metric space of light stimuli to this metric space. However, a uniform color space, where equal distances in the color space correspond to equal differences in the color, was not obtained. Despite of this fact, several color distances have been proposed in different color spaces such as RGB, CIE $L^*u^*v^*$, CIE $L^*a^*b^*$, HSV or CMY. The main color image distances are the average color distance, the histogram intersection quasi-distance and the histogram quadratic distance.

For a given $3D$ color space and a list of n colors, let (c_{i1}, c_{i2}, c_{i3}) be a representation of the i-th color of the list in this space. For a color histogram $x = (x_1, ..., x_n)$, its average color is the vector $(\bar{x_1}, \bar{x_2}, \bar{x_3})$, where $\bar{x_j} = \sum_{i=1}^{n} x_i c_{ij}$ of the pixels in the image. For example, in the RGB color space, the average color vector contains the average red, green and blue values. The average color distance between two color histograms [Hafner et al., 1995] is the euclidean distance of their average colors.

Given two color histograms $x = (x_1, ..., x_n)$ and $y = (y_1, ..., y_n)$, where x_i and y_i represent number of pixels in the bin i, the Swain-Ballard's histogram

intersection quasi-distance between them is defined by

$$1 - \frac{\sum_{i=1}^{n} \min\{x_i, y_i\}}{\sum_{i=1}^{n} x_i}.$$

For L_1-normalized histograms the above quasi-distance becomes the usual L_1-metric

$$\sum_{i=1}^{n} |x_i - y_i|.$$

Given two color histograms $x = (x_1, ..., x_n)$ and $y = (y_1, ..., y_n)$ (where n is usually 256 or 64) representing the color percentages of two images, their histogram quadratic distance (used in IBM's Query by Image Content system) is the Mahalanobis distance, defined by

$$\sqrt{(x-y)'A(x-y)},$$

where $A = (a_{ij})$ is a symmetric positive-definite matrix, and weight a_{ij} is some (perceptually justified) similarity between colors i and j. One of the similarities used is given by

$$a_{ij} = 1 - \frac{d_{ij}}{\max\limits_{1 \leqslant p,q \leqslant n} d_{pq}},$$

where d_{ij} is the euclidean distance between vectors representing colors i and j in some 3D color space.

3.1.2 Gray-scale Image Distances

Let $f(x)$ and $g(x)$ denote the brightness values of two digital gray-scale images f and g at the pixel $x \in X$, where X is a raster of pixels. Any distance between point-weighted sets (X, f) and (X, g) (for example, the Earth Mover distance) can be applied for measuring distances between f and g. The most used distances,

which are sometimes called errors, between images f and g are the root mean-square error, the signal-to-noise ratio, and the normalized Hamming distance.

The root mean-square error is defined by

$$\left(\frac{1}{|X|}\sum_{x\in X}(f(x)-g(x))^2\right)^{\frac{1}{2}}.$$

Another variant is to use the L_1-norm $|f(x)-g(x)|$ instead of the L_2-norm.

The signal-to-noise ratio is defined by

$$\left(\frac{\sum_{x\in X} g(x)^2}{\sum_{x\in X}(f(x)-g(x))^2}\right)^{\frac{1}{2}}.$$

The normalized Hamming distance, also known as the the pixel misclassification error rate, is defined by

$$\frac{1}{|X|}|\{x\in X : f(x)\neq g(x)\}|.$$

3.1.3 Earth Mover's Distance

Given two distributions, the Earth Mover's distance [Rubner et al., 2000] is the least amount of work needed to transform earth or mass (which is properly spread in space) from one distribution to the other (a collection of holes in the same space). The Earth Mover's distance is a discrete form of the Monge-Kantorovich distance. Instead of histograms, the distance is based on *signatures*, which are variable-size descriptions of distributions. A signature is a set of the main clusters of a distribution. Each cluster is represented by its mean (or mode) and by the fraction of pixels that belong to that cluster.

3.1.4 Tangent Distance

Tangent distance [Simard et al., 1996] is a distance measure that is invariant with respect to specific transformation such as small distortions and translations of the image. If an image is considered as a point in a high dimensional pixel space, then an evolving distortion of the image traces out a curve in pixel space.

Taken together, all these distortions define a low-dimensional manifold in pixel space. For small distortions, this manifold can be approximated by a tangent plane. Tangent distance measures the closeness between the tangent planes of two images.

3.1.5 Shape Match Distance

The shape matching distance [Belongie et al., 2002] is based on an algorithm for finding correspondences between shapes. Shapes are represented by a set of points sampled from the output of an edge detector. To describe the coarse distribution of the entire of the shape with respect to a given point on the shape, the method introduces the *shape context* descriptor, which describes a point by its context. Finding correspondences between two shapes is then equivalent to finding a bipartite graph match between sample points on the two shapes that have the most similar shape context.

3.2 Patch-based Techniques

Image patches (or simply patches) denote squared subimages extracted from an image. The parameters that determine a patch uniquely are the horizontal and vertical location within the image, and its size. For a given location and size, the patch can be extracted by simply determining which image pixels are located within that particular square. Patches belong to the category of local features, which means that they describe properties of a certain region of an image. In contrast to that, global features provide information about an image as a whole.

For numerous computer vision applications, the image can be analyzed at the patch level rather than at the individual pixel level or global level. Patches contain contextual information and have advantages in terms of computation and generalization. For example, patch-based methods produce better results and are much faster than pixel-based methods for texture synthesis [Efros & Freeman, 2001]. However, patch-based techniques are still heavy to compute with current machines [Barnes et al., 2011].

A paper that describes a patch-based approach for rapid image correlation or

template matching is [Guo & Dyer, 2007]. By representing a template image with an ensemble of patches, the method is robust with respect to variations such as local appearance variation, partial occlusion, and scale changes. Rectangle filters are applied to each image patch for fast filtering based on the integral image representation.

An approach to object recognition was proposed by [Deselaers et al., 2005], where image patches are clustered using the EM algorithm for Gaussian mixture densities and images are represented as histograms of the patches over the (discrete) membership to the clusters. Patches are also regarded in [Paredes et al., 2001], where they are classified by a nearest neighbor based voting scheme.

The work of [Agarwal & Roth, 2002] describes a method where images are represented by binary feature vectors that encode which patches from a codebook appear in the images and which spatial relationship they have. The codebook is obtained by clustering patches from training images whose locations are determined by interest point detectors.

In [Passino & Izquierdo, 2007], an image classification system based on a Conditional Random Field model is proposed. The model is trained on simple features obtained from a small number of semantically representative image patches.

The patch transform, proposed in [Cho et al., 2010], represents an image as bag of overlapping patches sampled on a regular grid. This representation allows users to manipulate images in the patch domain, which then seeds the inverse patch transform to synthesize a modified image.

In [Barnes et al., 2011], a new randomized algorithm for quickly finding approximate nearest neighbor matches between image patches is introduced. This algorithm forms the basis for a variety of applications including image retargeting, completion, reshuffling, object detection, digital forgery detection, and video summarization.

3.3 Image Descriptors

Beside patches, another popular class of local image features are image descriptors. They describe elementary visual features of the contents of images, such as the shape, the color, the contrast and so on.

Image descriptors are usually extracted using interest point detectors. The most widely used detector is the Harris detector [Harris & Stephens, 1988]. Based on the concept of automatic scale selection [Lindeberg, 1998], the authors of [Mikolajczyk & Schmid, 2001] created robust and scale-invariant feature detectors, called Harris-Laplace and Hessian-Laplace. In [Lowe, 1999], the author approximated the Laplacian of Gaussian (LoG) by a Difference of Gaussians (DoG) filter. Among the other scale-invariant interest point detectors proposed in literature are the salient region detector proposed in [Kadir & Brady, 2001], and the edge-based region detector proposed in [Jurie & Schmid, 2004].

The most famous image descriptor is probably the Scale-invariant feature transform (SIFT) [Lowe, 1999]. The SIFT descriptor converts each extracted patch to a 128-dimensional vector containing a 3D histogram of gradient locations and orientations . Each image is then represented as a set of vectors of same dimension, where the order of different vectors is of no importance. The SIFT descriptor is invariant to image scaling, translation, rotation, illumination changes and affine or 3D projection. It has been used in a wide variety of applications, even for object matching in videos [Sivic & Zisserman, 2003].

Researchers have developed improved variants of the SIFT descriptor. The work of [Ke & Sukthankar, 2004] proposes the PCA-SIFT descriptor that uses the image gradient patch and applies PCA to reduce the size of the SIFT descriptor. In [Mikolajczyk & Schmid, 2005], another variant of the SIFT descriptor, termed GLOH, is proposed. The GLOH descriptor proved to be even more distinctive with the same number of dimensions. However, GLOH is computationally more expensive. The SURF descriptor [Bay et al., 2008] approximates or even outperforms previously proposed schemes, yet can be computed and compared much faster.

Shape context [Belongie et al., 2002] is similar to the SIFT descriptor, but is based on edges. Shape context is a 3D histogram of edge point locations and orientations. Edges are extracted by the Canny detector [Canny, 1986].

In [Dalal & Triggs, 2005], the use of grids of Histograms of Oriented Gradient (HOG) descriptors for human detection is proposed. The technique counts occurrences of gradient orientation in localized portions of an image. Using the appearance [Lowe, 1999] and shape [Dalal & Triggs, 2005] descriptors together

with the image spatial layout, the work of [Bosch et al., 2007] proposes two representations: a pyramid histogram of visual words (PHOW) descriptor for appearance and a pyramid HOG (PHOG) descriptor for shape. This method is similar to that of edge orientation histograms, SIFT descriptors, and shape contexts, but differs in that it is computed on a dense grid of uniformly spaced cells and uses overlapping local contrast normalization for improved accuracy.

Several other image descriptors have been proposed in literature. Examples, that are also evaluated in [Mikolajczyk & Schmid, 2005], are spin images, steerable filters, differential invariants, complex filters, moment invariants, and cross-correlation of sampled pixel values.

3.4 Bag of Visual Words

In computer vision, the *bag of words* (BOW) model can be applied to image classification and related tasks, by treating image descriptors as words. A bag of visual words is a sparse vector of occurrence counts of a vocabulary of local image features. This representation can also be described as a histogram of visual words. The vocabulary is usually obtained by vector quantizing image features into visual words. One of the most popular methods is to apply a k-means clustering on the image features [Leung & Malik, 2001]. Then, each cluster center becomes a visual word in the vocabulary. Recent papers have demonstrated the advantage of using a vocabulary tree [Nister & Stewenius, 2006] or a randomized forest of k-d trees [Philbin et al., 2007] to reduce search cost in the quantization stage.

Note that the classical BOW model ignores any spatial relationships between image features. Despite this fact, visual words showed a high discriminatory power and have been used for region or image level classification [Csurka et al., 2004; Fei-Fei & Perona, 2005; Zhang et al., 2007]. Although most approaches are based on sparse descriptors, others have used dense descriptors [Fei-Fei & Perona, 2005; Winn et al., 2005].

One of the early approaches of building a vocabulary of features is [Leung & Malik, 2001]. The main idea is to construct a vocabulary of prototype tiny surface patches, called 3D textons. Textons obtained by k-means clustering are used for texture classification. The work of [Sivic et al., 2005] also builds a

vocabulary of visual words using vector quantized SIFT descriptors. The vector quantization is done via a probabilistic Latent Semantic Analysis (pLSA). Others have used similar descriptors for object classification [Csurka et al., 2004], but in a supervised setting. There are many other successful approaches to obtain visual words from image data [Deselaers et al., 2005; Winn et al., 2005; Xie et al., 2010].

The method proposed in [Winn et al., 2005] classifies regions according to the proportions of different visual words. An optimally compact visual dictionary is learned by pair-wise merging of visual words from an initially large dictionary. The final visual words are described by Gaussian Mixture Models (GMM).

In [Xie et al., 2010], a novel texture classification method via patch-based sparse texton learning is proposed. The dictionary of textons is learned by applying sparse representation to image patches in the training data set.

Chapter 4

A New Dissimilarity for Images

The chapter aims to present two novel distance measures for images and textures, respectively. The first one is termed Local Patch Dissimilarity (LPD) and it was published in [Dinu et al., 2012]. This new distance measure is inspired from rank distance which is a distance measure for strings. Rank distance has been used with very good results in biology, computational linguistics and computer science. As many other computer vision techniques, LPD considers patches rather than pixels, in order to capture distinctive features such as edges, corners, shapes, and so on. Patches contain contextual information and have advantages in terms of generalization.

An algorithm that computes the Local Patch Dissimilarity between two images is presented in this chapter. Because patch-based techniques are known to be computational heavy, several ways of optimizing the LPD algorithm are presented, such as using a hash table to store precomputed patch distances or skipping the comparison of overlapping patches. Another way to avoid the problem of the higher computational time on large sets of images is to turn to local learning methods. All these ways of optimizing the LPD algorithm were also discussed in [Ionescu & Popescu, 2013a]. The theoretical properties of LPD are also discussed. LPD fits best in the definition of a semi-metric with a relaxed coincidence axiom. Several experiments are conducted on two data sets using both standard machine learning methods and local learning methods. All methods are based on LPD. The obtained results come to support the fact that LPD is a very good dissimilarity measure for images.

This chapter also presents a novel texture dissimilarity measure based on textons, namely the Local Texton Dissimilarity (LTD), inspired from LPD. Local Texton Dissimilarity was introduced in [Ionescu et al., 2014]. Instead of patches, LTD works with textons, which are represented as a set of features extracted from image patches. Similar textons are represented through similar features. Thus, image patches are implicitly quantized into textons. Textons provide a lighter representation of patches, allowing for a faster computational time and broader application to practical problems. One of the texton features is based on the development of an efficient box counting method for estimating fractal dimension, presented in [Popescu et al., 2013b]. Several experiments are conducted on three texture data sets. LTD shows its first application on biomass type identification, a direct application of texture classification. The other experiments are conducted on two popular texture classification data sets, namely Brodatz and UIUCTex. The proposed method benefits from a faster computational time compared to LPD and a better accuracy when used for texture classification. The performance level of the machine learning methods based on LTD is comparable to the state of the art methods.

The chapter is organized as follows. The concepts behind extending rank distance to images are presented in Section 4.1.1. An algorithm to compute LPD is described in Section 4.1.2. Section 4.1.3 presents several means of optimizing the LPD algorithm in terms of speed. Theoretical properties of LPD are discussed in Section 4.2. Experiments with both standard and local learning methods based on LPD are presented in Section 4.3. The Local Texton Dissimilarity is presented in Section 4.4. Related work about texton-based techniques is discussed in Section 4.4.1. An algorithm to compute LTD is described in Section 4.4.3. The algorithm is based on the texture features presented in Section 4.4.2. Experiments with machine learning methods based on LTD are presented in Section 4.5. Finally, a discussion about future work is given in Section 4.6.

4.1 Local Patch Dissimilarity

4.1.1 Extending Rank Distance to Images

Rank distance (RD) is a measure of similarity between strings proposed by [Dinu, 2003]. It has applications in many different fields such as computational biology [Dinu & Ionescu, 2012b, 2013a; Dinu & Sgarro, 2006], computational linguistics [Dinu & Dinu, 2005; Dinu & Popescu, 2009a] and computer science. In a recent study on DNA comparison [Dinu & Ionescu, 2012b], rank distance seems to achieve better results than other string distances such as Hamming distance or edit (Levenshtein) distance [Levenshtein, 1966]. Rank distance can be computed fast and benefits from some features of the edit distance.

The distance between two strings can be measured with rank distance by scanning (from left to right) both strings. First, characters need to be annotated with indexes in order to eliminate duplicates. For each annotated letter, rank distance measures the offset between its position in the first string and its position in the second string. Finally, all these offsets are summed up to obtain the rank distance. In other words, the rank distance measures the "gap" between the positions of a letter in the two given strings, and then sums up these values. Intuitively, the rank distance computes the total non-alignment score between two string.

There are a few aspects that need to be discussed and explained in order to extends rank distance (that works very good on text) to images. The first concern is that the rank distance, that works on one-dimensional input (strings), should be extended to make it work on two-dimensional input (digital images). A way of extending rank distance to images can be discovered by taking an example in order to better understand how rank distance works on text. For two strings s_1 and s_2, the characters must be annotated with indexes in order to eliminate duplicate characters. Then, the rank distance between s_1 and s_2 can easily be computed as in Example 1.

Example 1 *If* $s_1 = CCGAATTACG$ *and* $s_2 = AGACTCTGAC$*, the annotated strings are* $\bar{s_1} = C_1C_2G_1A_1A_2T_1T_2A_3C_3G_2$ *and* $\bar{s_2} = A_1G_1A_2C_1T_1C_2T_2G_2A_3C_3$.

The rank distance between s_1 and s_2 is

$$\Delta(s_1, s_2) = |1-4| + |2-6| + |3-2| + |4-1| + |5-3| + |6-5| + |7-7| \\ + |8-9| + |9-10| + |10-8| = 18.$$

In order to compute rank distance on strings, a global order is introduced by the annotation step. However, one may ask whether this global order is really necessary or whether it can be defined in another way. For example, should strings be annotated from right to left instead of left to right? Since text is unidimensional data, this question is easy to answer because there are not so many options. One can argue that strings can be annotated from left to right and from right to left, and the two distances obtained after annotation can be summed up. But, in order to define rank distance for images (two-dimensional data), answering such questions becomes difficult. One would have to ask which is the first pixel of the image, then which is the second one? There is a very large number of possibilities to define a global order on the pixels of an image. And one may ask if this global order is really necessary? All these questions have to be answered before extending rank distance to images.

If longer DNA strings, that contain only characters in the alphabet $\Sigma = \{A, C, G, T\}$, are considered, one can observe the local phenomenon without needing to introduce a global order, because the characters in DNA strings are almost randomly distributed and the frequency of the characters has a nearly uniform distribution. By considering two very long DNA strings and looking at some random aligned substrings (of the two strings):

$$...TTACGCTGAC...$$
$$...CATCTGACGA...$$

the local phenomenon, that appears disregarding the global order, is that a certain character (in the first string) should be paired with a similar character (in the second string) such that their positions are very close with respect to the size of the alphabet. In other words, rank distance can be computed (or rather approximated), without annotating the characters, just by pairing each character in one string with similar characters in the other string, that are nearby.

An interesting remark, that can be observed by looking at how rank distance actually works, is that the global order introduced by the standard definition of rank distance (for strings) is not really necessary. For images, introducing a global order is a problem in the first place, because there are too many ways of defining it. But this problem can be avoided by only replicating the local phenomenon and how rank distance works on strings.

Another observation that follows the concept of treating text and image in a similar fashion, is the difference between characters and pixels, which are the building blocks of text and image, respectively. To extract meaning from text, one should look at words, which are formed from a few characters. To extract meaning from image, one should look at certain features such as contour, contrast, shape, color, and so on. If rank distance measures the offset between characters in two strings, the extension of rank distance for images should measure the offset between features such as contrast, contour, shape, etc. It is clear that these features cannot be captured in single pixels, but rather in small, overlapping rectangles of fixed size (e.g., 4×4 pixels), called patches. It is reasonable to consider patches rather than pixels, since many researchers have developed state of the art methods for analyzing and editing digital images, that are patch-based [Barnes et al., 2011; Efros & Freeman, 2001; Guo & Dyer, 2007].

4.1.2 Local Patch Dissimilarity Algorithm

The algorithm to compute the extension of rank distance for gray-scale images, termed Local Patch Dissimilarity, is described next. To compute the dissimilarity between two images, the LPD algorithm sums up all the spatial offsets of similar patches between the two images. The LPD algorithm works as follows. For every patch in one image, the algorithm searches for a similar patch in the other image. First, it looks for similar patches in the same position in both images. If those patches are similar with respect to another distance that is computed between the two patches, then the algorithm sums up 0 since there is no offset (or gap) between the patches. If the patches are not similar, the algorithm starts looking in concentric squares around the initial patch position in the second image until it finds a patch similar to the one in the first image. In other words, this spatial

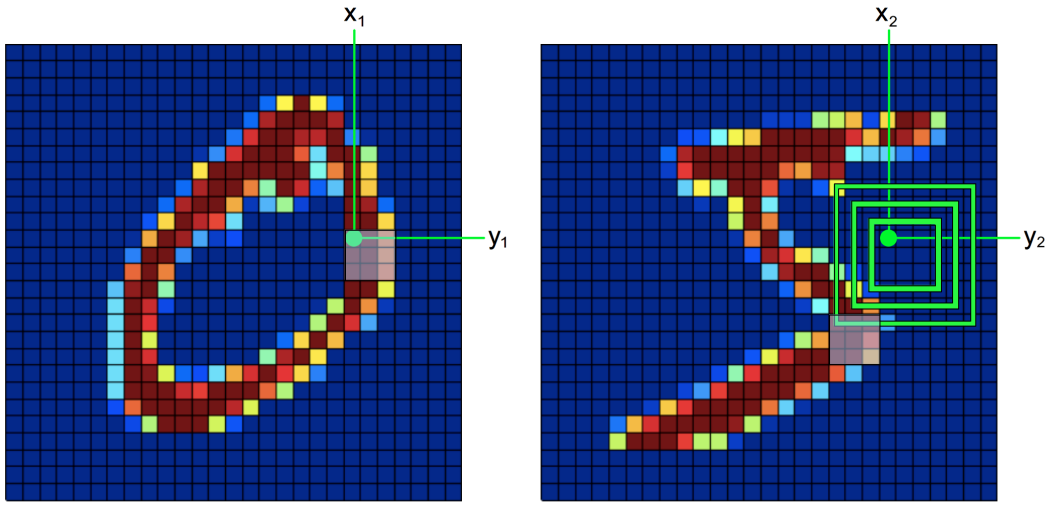

Figure 4.1: Two images that are compared with LPD. At a certain step, the patch at position (x_1, y_1) in the first image is matched with a patch at offset 3 from position (x_2, y_2) in the second image. No patches similar to the one at position (x_1, y_1) were found at offsets 0, 1 or 2.

search gradually explores the vicinity of the patch position from the first image in the second image. The spatial offset from the initial position is increased as the algorithm continues to search for a similar patch without success. If a similar patch is found during this process, the algorithm sums up the current offset which represents the minimum offset where a similar patch is found. The search goes on until the algorithm finds a similar patch or until the offset reaches the borders of the second image. In the latter case the algorithm sums up the latest offset, which should not be greater than the diagonal of the image. Figure 4.1 gives a visual hint of the steps involved in the computation of LPD.

Algorithm 1 computes the LPD between gray-scale images img_1 and img_2 using the underlying mean euclidean distance to compute the similarity between patches.

Algorithm 1 *Local Patch Dissimilarity*

Input:

img_1 – *a gray-scale image of* $h_1 \times w_1$ *pixels;*

img_2 – *another gray-scale image of* $h_2 \times w_2$ *pixels;*

p – *the square patch size (the patch has* $p \times p$ *pixels);*

th – *the patch similarity threshold.*

Initialization*:*

$dist = 0$

$h = \min\{h_1, h_2\} - p + 1$

$w = \min\{w_1, w_2\} - p + 1$

Computation*:*

for $x = 1$ *to* h

for $y = 1$ *to* w

get $patch^{left}$ *at position* (x, y) *in* img_1

$d = 0$

while did not find patch at offset d *similar to* $patch^{left}$

get $patch^{right}$ *at offset* d *from position* (x, y) *in* img_2

$$s_1 = \frac{1}{p^2} \sum_{i=1}^{p} \sum_{j=1}^{p} \left(patch_{ij}^{left} - patch_{ij}^{right} \right)^2$$

if $s_1 < th$

$dist = dist + d$

break

endif

if all patches at offset d *were tested*

$d = d + 1$

endif

endwhile

get $patch^{right}$ *at position* (x, y) *in* img_2

$d = 0$

while did not find patch at offset d *similar to* $patch^{right}$

get $patch^{left}$ *at offset* d *from position* (x, y) *in* img_1

$$s_2 = \frac{1}{p^2} \sum_{i=1}^{p} \sum_{j=1}^{p} \left(patch_{ij}^{right} - patch_{ij}^{left} \right)^2$$

if $s_2 < th$

$dist = dist + d$

break

endif

if all patches at offset d were tested

$d = d + 1$

endif

endwhile

endfor

endfor

***Output**:*

dist – the dissimilarity between img_1 and img_2.

In Algorithm 1, $patch_{ij}$ represents the pixel on row i and column j of the patch. The rank distance extension works with square patches of fixed size. The patches must not be greater than the image. Actually, the image-patch ratio should be somehow similar to the word-character ratio. In other words, the patch should be several times smaller than the image itself.

The time complexity of the LPD algorithm is $O(h^2 \times w^2)$, where h and w represent minimum height and width of the two compared images, respectively.

Algorithm 1 needs two input parameters besides the two images. The square patch size parameter is the height and width measured in pixels for the patches involved in the computation of LPD. The patch similarity threshold is a number in the $[0, 1]$ interval that determines when two patches are considered to be similar. These parameters need to be adjusted with respect to image width and height, type of information contained in the image, noise, etc.

It is important to mention that LPD is based on another distance between patches. Any image distance can be used to compute the similarity between patches, as long as a threshold, that determines what patches are similar and what patches are not, can be provided. Algorithm 1 determines patch similarity using the mean squared euclidean distance that corresponds to the L_2-norm. Another version of the LPD algorithm is also tested in the experiments, that determines patch similarity using the mean euclidean distance that corresponds to the L_1-norm. Both algorithms show good results.

4.1.3 LPD Algorithm Optimization

As stated in [Barnes et al., 2011], patch-based algorithms are heavy to compute with current computers because these algorithms must deal with millions of patches. Some means of improving the LPD algorithm in terms of speed are discussed here. It may not occur at first look, but LPD needs to compute the similarity between many pairs of patches and for some of them, even several times. Recomputation of patch similarities can be avoided by storing the precomputed values in a hash table. Some of the tests presented in Section 4.3 are performed using the hash table optimization which brings an $8 - 10\%$ speed improvement.

Another optimization is to stop the search for similar patches earlier. Recall that the search goes on until a similar patch is found or until a maximum offset is reached. It is very unlikely to find similar patches at high offset from each other. Even if two similar patches are found at a great distance from each other, it does not mean the images are similar. In fact, this phenomenon may bring noise into the computation of LPD. To avoid this extensive search that can potentially harm the dissimilarity measure, setting a maximum offset radius much lower than the image diagonal size is a good choice. This search limitation was included in all the experiments, which resulted in a great improvement in terms of speed and accuracy. However, one must be careful not to reduce the maximum offset by too much, which can badly alter the performance and strength of the dissimilarity measure. To stop the spatial search too early would mean to disregard some similar patches that bring important information in the dissimilarity computation. In the experiments, an offset radius of $25 - 50\%$ of the image diagonal size works very well. This also brings a speed improvement of $25 - 30\%$.

The last proposed algorithm optimization comes from the fact that LPD computes the similarity between many overlapping patches. A fast version of the LPD algorithm is to skip the comparison of overlapping patches. Basically, this means that LPD is computed on a dense grid over the image instead of the entire image. This can be achieved by increasing the offset by more than one unit, each time a similar patch is not found at the current offset. The results presented in Section 4.3.9 are obtained by increasing the offset with two units at every step, thus, skipping half of the comparisons between patches and speeding the LPD

algorithm by a factor of two. The proposed speed improvements do not affect the time complexity.

4.2 Properties of Local Patch Dissimilarity

LPD replicates only the local phenomenon and how rank distance works on strings. In order to do so, LPD is defined as a relaxed version of rank distance [Dinu, 2003]. Consequently, some of the distance properties are lost. Theoretical properties of LPD are studied next, as the concern of this section is to fit LPD into a standard definition. For this, the following definitions are needed.

Definition 6 *A metric on a set X is a function (called the distance function or simply distance) $d : X \times X \to \mathbb{R}$. For all $x, y, z \in X$, this function is required to satisfy the following conditions:*

$$
\begin{aligned}
&(i)\ d(x,y) \geqslant 0 \ \textit{(non-negativity, or separation axiom);}\\
&(ii)\ d(x,y) = 0 \ \textit{if and only if } x = y \ \textit{(coincidence axiom);}\\
&(iii)\ d(x,y) = d(y,x) \ \textit{(symmetry);}\\
&(iv)\ d(x,z) \leqslant d(x,y) + d(y,z) \ \textit{(triangle inequality).}
\end{aligned}
$$

Note that axioms (i) and (ii) from Definition 6 produce positive definiteness. One can also observe that the first condition is implied by the others.

Definition 7 *A pseudo-metric on X is a function $d : X \times X \to \mathbb{R}$ which satisfies the axioms for a metric, except that instead of the coincidence axiom only $d(x, x) = 0$ for all x is required.*

Definition 8 *A semi-metric on X is a function $d : X \times X \to \mathbb{R}$ that satisfies the first three axioms, but not necessarily the triangle inequality.*

In the LPD algorithm [Dinu et al., 2012], one can observe that the initial value of the distance to be computed is 0. The computation can only increase this distance by adding positive offsets of similar patches. This ensures the non-negativity condition in Definition 6. Note that the algorithm computes the distance by taking all the patches from the first image and by searching for similar

patches in the second image. In the same manner, it takes all the patches from the second image and searches for similar patches in the first one. Thus, the same output is obtained when images are swapped. This ensures the symmetry of LPD.

Because patches are allowed to be similar under a certain threshold, distinct (non-identical) images may have a LPD equal to 0. This is a plus if images with small differences in contrast or induced by noise must be considered similar. While this helps detect similar images even with noise, it also drops the coincidence axiom in the standard definition of a metric. However, the relaxed version in Definition 7 is still verified. The dissimilarity of two identical images computed with LPD is always 0, but allowing distinct images to also have a LPD equal to 0 drops the triangle inequality. Although the inequality is met in most cases (about 98.5%), LPD is not actually a distance. LPD fits best in the definition of a semi-metric with a relaxed coincidence axiom as in Definition 7. Note that adjusting the dissimilarity computation, so that conditions (ii) and (iv) in Definition 6 are met, may be possible and could be the subject of further work.

LPD measures the dissimilarity between two images. Knowing the maximum offset radius (used to stop similar patch searching), the maximum value of the dissimilarity between two images can be computed as the product between the maximum offset and the number of pairs of compared patches. Thus, LPD can be normalized to a value in the $[0, 1]$ interval. A value closer to 0 means that images are similar, and a value closer to 1 means that images are dissimilar.

4.3 Experiments and Results

4.3.1 Data Sets Description

Isolated handwritten character recognition has been extensively studied in the literature [Srihari, 1992; Suen et al., 1992], and was one of the early successful applications of neural networks [LeCun et al., 1989]. Comparative experiments on recognition of individual handwritten digits are reported in [LeCun et al., 1998]. While recognizing individual digits is one of many problems involved in designing a practical recognition system, it is an excellent benchmark for comparing shape

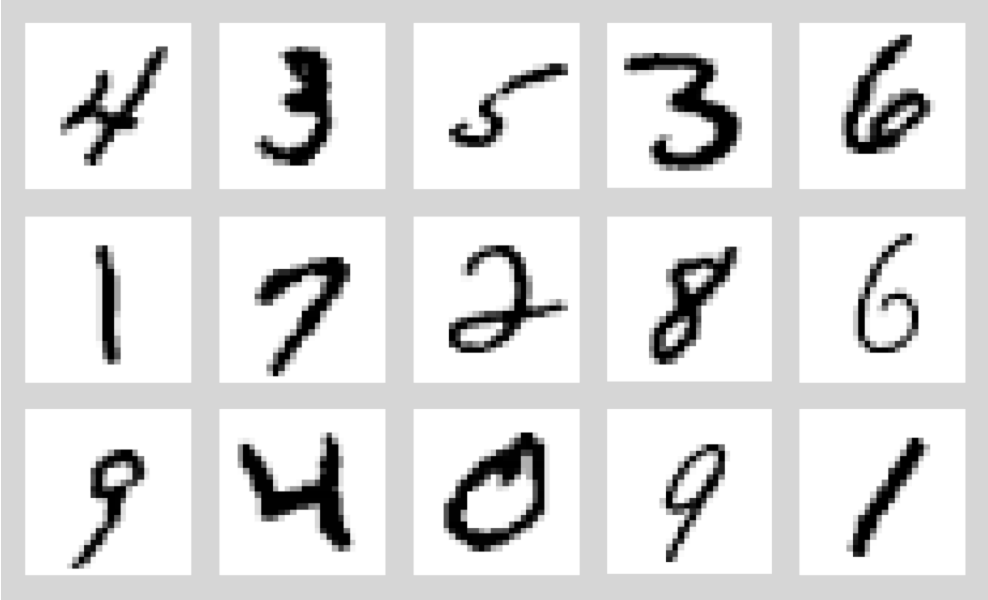

Figure 4.2: A random sample of 15 handwritten digits from the MNIST data set.

recognition methods.

The data set used for testing the dissimilarity presented in this paper is the MNIST set, which is described in detail in [LeCun et al., 1998]. The data set was constructed by mixing the handwritten digits collected among Census Bureau employees with the handwritten digits collected among high-school students. The regular MNIST database contains $60,000$ train samples and $10,000$ test samples, size-normalized to 20×20 pixels, and centered by center of mass in 28×28 fields. A random sample of 15 images from this data set is presented in Figure 4.2. The data set is available at `http://yann.lecun.com/exdb/mnist/`.

The second data set was collected from the Web by the authors of [Lazebnik et al., 2005a] and consists of 100 images each of six different classes of birds: egrets, mandarin ducks, snowy owls, puffins, toucans, and wood ducks. Because LPD is designed for gray-scale images, the images from the Birds data set are transformed to gray-scale. A random sample of 12 gray-scaled images from this data set is presented in Figure 4.3. The Birds data set is available at `http://www-cvr.ai.uiuc.edu/ponce_grp/data/`. The Birds data set is used in the last experiment presented in this section.

Figure 4.3: A random sample of 12 images from the Birds data set. There are two images per class. Images from the same class sit next to each other in this figure.

4.3.2 Learning Methods

The LPD measure is put into a learning context in order to evaluate its performance. Therefore, LPD is employed into several learning methods and used for classification. The first classifier, that is intensively used through all the experiments, is the k-nearest neighbors (k-NN). The k-NN classifier was chosen because it reflects the characteristics of the dissimilarity measure.

Most patch-based algorithms are heavy to compute with current computers [Barnes et al., 2011]. This is also the downside of LPD, because the time to compute k-NN based on LPD on the entire MNIST data set is too high to even consider (on an Intel Core Duo 2.26 GHz processor and 4 GB of RAM memory it would take almost one year). This time can be reduced by a factor of 15,

if the computation is done on GPU, but a faster learning algorithm is still of great interest. One way to improve the time efficiency is to use a k-NN with filtering algorithm, which is a pure local learning technique. For the k-NN with filtering approach, the idea is to filter the nearest K neighbors using the standard euclidean distance measure (that is much faster to compute). Then select the nearest k neighbors from those K images using LPD. The two-step selection process is much faster to compute on a large data set (such as MNIST data set) than a standard k-NN based only on LPD.

For the MNIST experiments, two state of the art kernel methods are used, namely the SVM [Cortes & Vapnik, 1995] and the Kernel Ridge Regression (KRR) [Shawe-Taylor & Cristianini, 2004]. In the Birds classification experiment, the KDA classifier is also used. As discussed in Chapter 2, kernel methods are based on similarity. LPD can be transformed into a similarity measure. The classical way to transform a dissimilarity measure into a similarity measure is to use the Gaussian-like kernel [Shawe-Taylor & Cristianini, 2004]:

$$k(img_1, img_2) = \exp\left(-\frac{LPD(img_1, img_2)}{2\sigma^2}\right),$$

where img_1 and img_2 are two gray-scale images. The parameter σ is usually chosen to match the number of features so that values of $k(img_1, img_2)$ are well scaled. The number of features in an image are actually the number of pixels contained in that image.

Several classification experiments are conducted using these machine learning methods based on LPD. The experiments are organized as follows. First, the LPD parameters are tuned using a 3-NN model in set of experiments described in Section 4.3.3. LPD is compared to a baseline 3-NN model based on the euclidean distance in Section 4.3.4. Kernel methods based on LPD are evaluated in Section 4.3.5. Machine learning methods based on LPD are also compared to the SVM+ model of [Vapnik & Vashist, 2009], in Section 4.3.6. The experiments mentioned so far are conducted on different subsets of the MNIST data set. The experiments described in Sections 4.3.7 and 4.3.8 are performed on the entire MNIST data set. Finally, an experiment on the Birds data set is presented in Section 4.3.9.

4.3.3 Parameter Tuning

A set of preliminary tests are performed to adjust the parameters of LPD, such as the patch size, the patch similarity threshold, or the maximum offset radius. Patch sizes ranging from 1×1 to 10×10 pixels were considered. The patch similarity threshold was adjusted with respect to the patch size, but this parameter was also tuned.

Experiments are conducted on the first 100 and 300 images extracted from the MNIST training set. Since the number of images in each set is relatively small, the tests were performed using the 10-fold cross-validation procedure. By repeating the 10-fold cross-validation procedure, variations in accuracy larger than 1% were observed. Thus, the reported accuracy rates represent an average of 10 runs of the 10-fold cross-validation procedure, in order to obtain a better approximation of the accuracy rate.

Figures 4.4, 4.5, 4.6, 4.7 and 4.8 show the results obtained by a 3-NN model based on LPD with several patch sizes and similarity thresholds. These results are obtained on the 100 images MNIST subset. For each patch size, a graph of the accuracy rates obtained by varying the patch similarity threshold is presented. The accuracy rates follow a Gaussian-like distribution, with the peak determined by a certain similarity threshold. To obtain the best accuracy rates, the patch similarity threshold must be increased as the patch size grows. It is interesting to mention that the accuracy rates obtained with pixel-sized patches presented in Figure 4.4(a) are relatively good. However, the empirical results obtained with patches greater than 2×2 pixels confirm that it is better to compare patches instead of pixels.

In the following experiment, conducted on the 300 images subset, patches of 1×1 pixels and 10×10 pixels are disregarded since they give lower accuracy rates. For each remaining patch size, the patch similarity threshold that gives the highest accuracy is selected. The accuracy rates averaged over 10 runs of the 10-fold cross-validation procedure using 300 images are presented in Table 4.1. A graph with these accuracy rates obtained by varying the patch size is presented in Figure 4.9. In this graph, a Gaussian-like distribution of the accuracy rates can be observed again. The patch size with the highest accuracy rate is selected

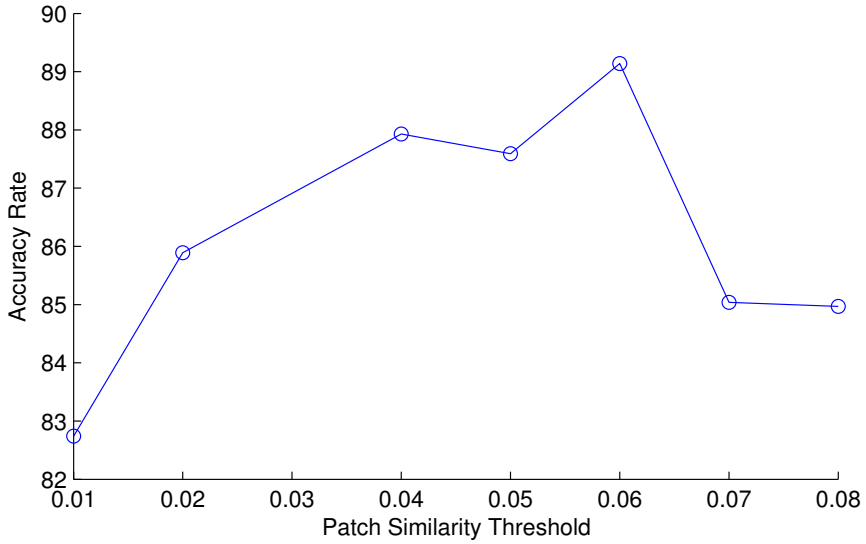

(a) Accuracy rates with patches of 1×1 pixels

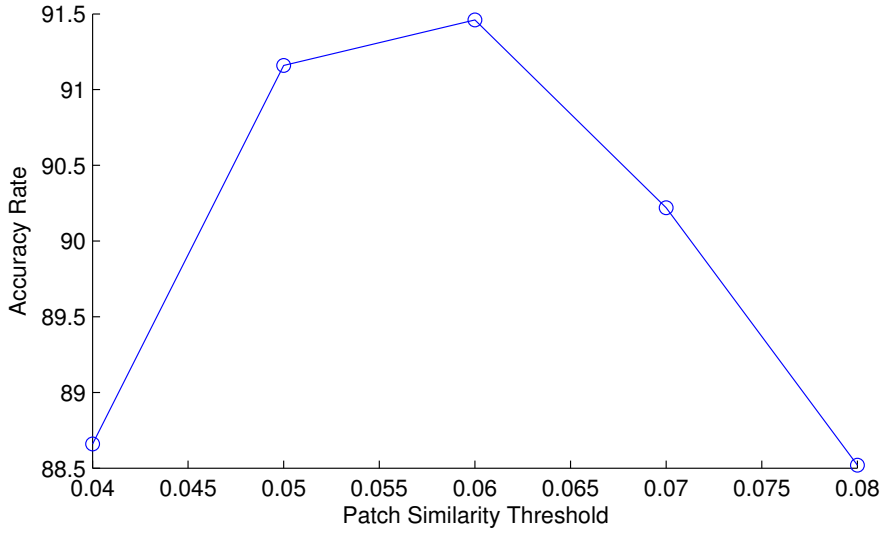

(b) Accuracy rates with patches of 2×2 pixels

Figure 4.4: Average accuracy rates of the 3-NN based on LPD model with patches of 1×1 pixels at the top and 2×2 pixels at the bottom. Experiment performed on the MNIST subset of 100 images.

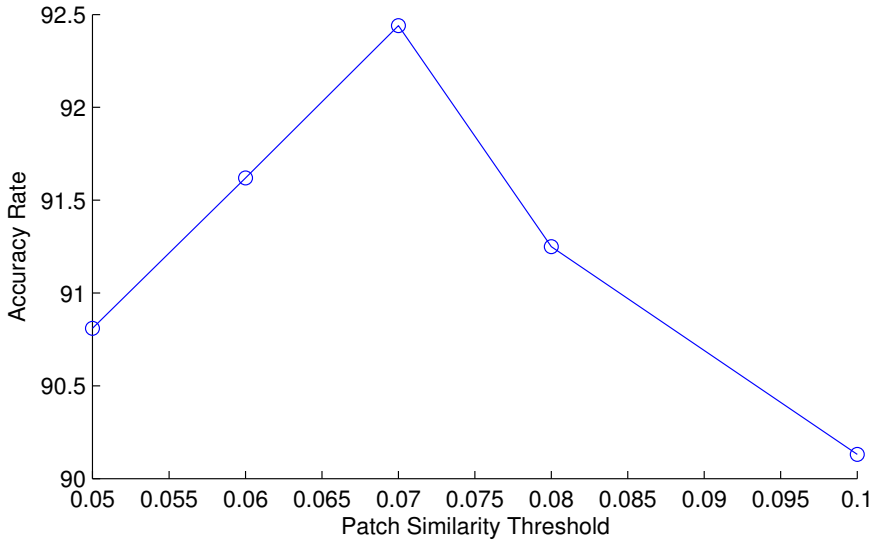

(a) Accuracy rates with patches of 3×3 pixels

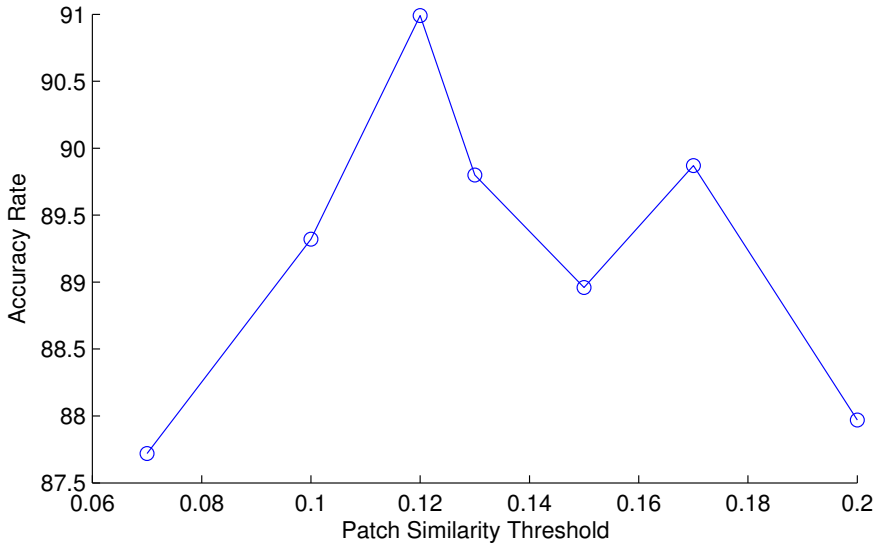

(b) Accuracy rates with patches of 4×4 pixels

Figure 4.5: Average accuracy rates of the 3-NN based on LPD model with patches of 3×3 pixels at the top and 4×4 pixels at the bottom. Experiment performed on the MNIST subset of 100 images.

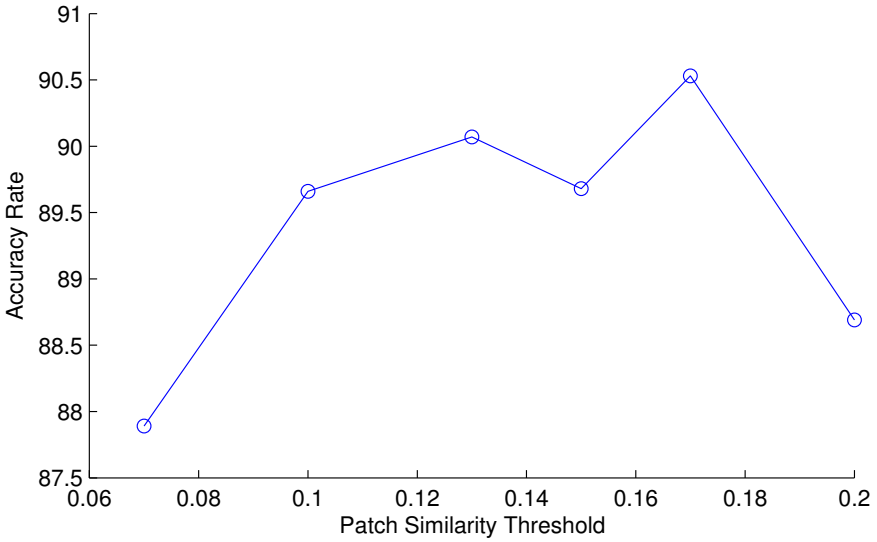

(a) Accuracy rates with patches of 5×5 pixels

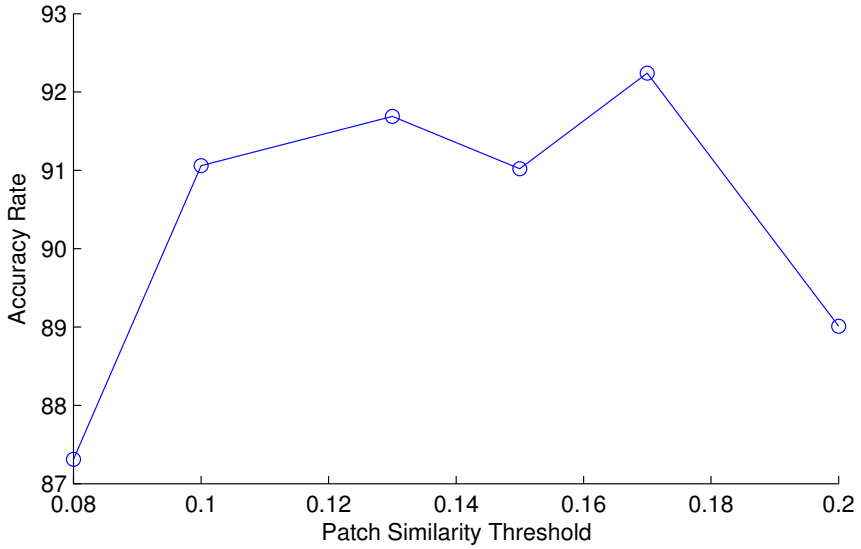

(b) Accuracy rates with patches of 6×6 pixels

Figure 4.6: Average accuracy rates of the 3-NN based on LPD model with patches of 5×5 pixels at the top and 6×6 pixels at the bottom. Experiment performed on the MNIST subset of 100 images.

(a) Accuracy rates with patches of 7×7 pixels

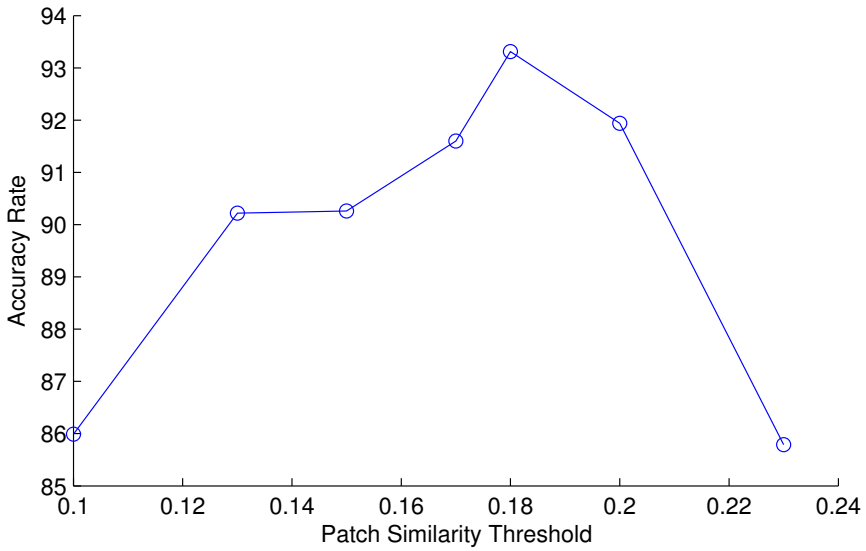

(b) Accuracy rates with patches of 8×8 pixels

Figure 4.7: Average accuracy rates of the 3-NN based on LPD model with patches of 7×7 pixels at the top and 8×8 pixels at the bottom. Experiment performed on the MNIST subset of 100 images.

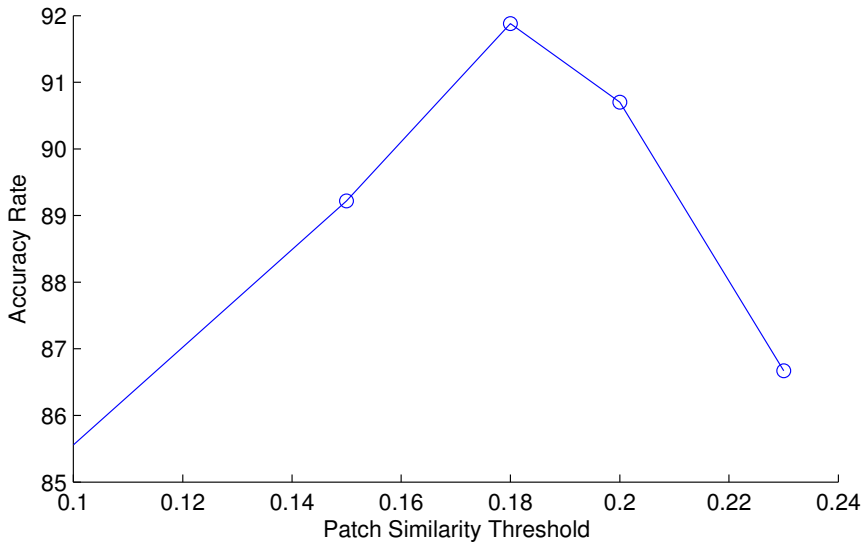

(a) Accuracy rates with patches of 9×9 pixels

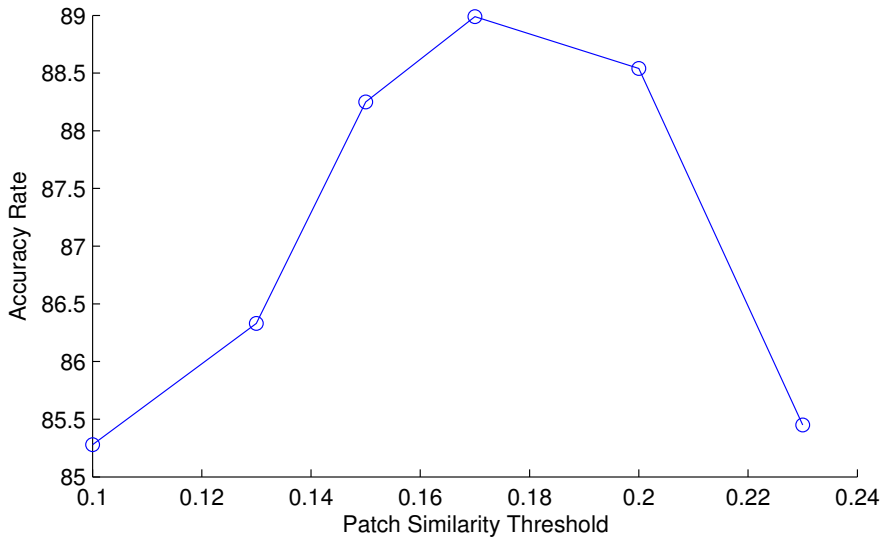

(b) Accuracy rates with patches of 10×10 pixels

Figure 4.8: Average accuracy rates of the 3-NN based on LPD model with patches of 9×9 pixels at the top and 10×10 pixels at the bottom. Experiment performed on the MNIST subset of 100 images.

Table 4.1: Results of the experiment performed on the MNIST subset of 300 images, using the 3-NN based on LPD model with patches ranging from 2×2 pixels to 9×9 pixels. Reported accuracy rates are averages of 10 runs.

Patch size	Patch similarity threshold	Accuracy
2×2	0.06	89.25%
3×3	0.07	90.68%
4×4	0.12	**92.50**%
5×5	0.17	91.53%
6×6	0.17	91.45%
7×7	0.15	91.44%
8×8	0.18	90.38%
9×9	0.18	89.89%

for the next experiments. Thus, LPD based on patches of 4×4 pixels will be used.

It is interesting to mention that the computational time of LPD is proportional to the patch similarity threshold. More precisely, a higher similarity threshold will give a higher probability of finding similar patches sooner, thus reducing the number of steps of the spatial search. However, the patch similarity threshold should be adjusted with respect to the accuracy of the LPD. Consequently, the rest of the experiments are conducted with a patch similarity threshold of 0.12 and 0.125, which are selected to obtain the highest accuracy with patches of 4×4 pixels. The similarity threshold of 0.125 is used for the heavy computational experiments to slightly speed up the computation without affecting the accuracy level.

Another parameter that needs to be tuned is the maximum offset radius. Several experiments were performed with various maximum offsets values such as 5, 10, 15, and 20 pixels. These experiments were performed by keeping the rest of the parameters unchanged. Patches of 4×4 pixels and a similarity threshold of 0.12 were used. The results with various maximum offsets are presented in Table 4.2. The maximum offset can be adjusted to optimize the trade-off between accuracy and time. Table 4.2 shows the average time needed to compute the dissimilarity between two images. The reported average times were measured on a computer with Intel Core i7 2.3 GHz processor and 8 GB of RAM memory

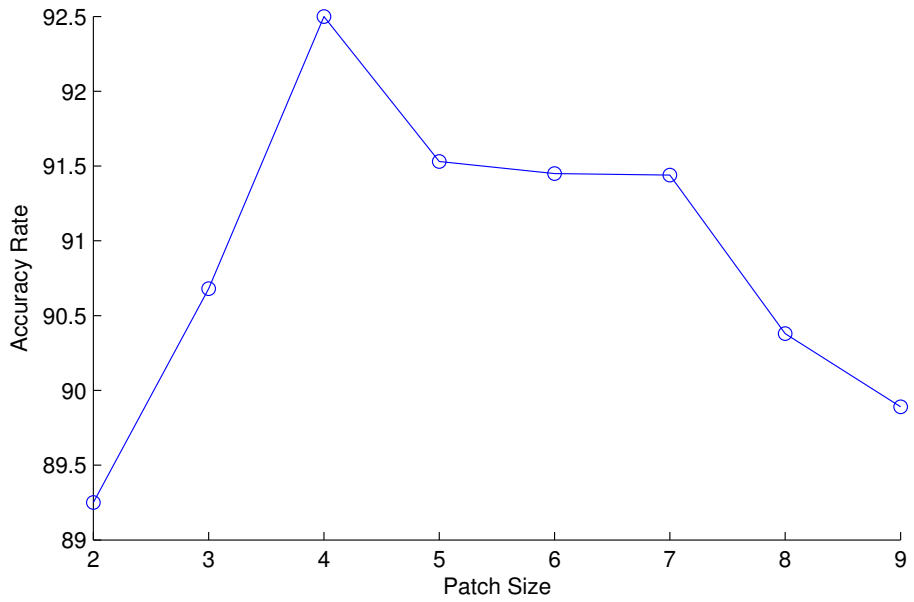

Figure 4.9: Average accuracy rates of the 3-NN based on LPD model with patches ranging from 2×2 pixels to 9×9 pixels. Experiment performed on the MNIST subset of 300 images.

using a single Core. The best time is obtained using a maximum offset of 5 pixels, while the best accuracy (92.50%) is obtained using a maximum offset of 15 pixels. Finally, the maximum offset chosen for the rest of the experiments is 15 pixels, which is close to half the height or width of the MNIST images.

Table 4.2: Results of the experiment performed on the MNIST subset of 300 images, using various maximum offsets, patches of 4×4 pixels, and a similarity threshold of 0.12. Reported accuracy rates are averages of 10 runs. The time needed to compute the pairwise dissimilarity is measured in seconds.

Maximum offset	Accuracy	Average time per pair
5	90.21%	0.11 seconds
10	92.11%	0.16 seconds
15	**92.50**%	0.19 seconds
20	91.98%	0.23 seconds

4.3.4 Baseline Experiment

The 3-NN classifier based on the LPD measure is compared with a baseline k-NN classifier. The 3-NN based on the euclidean distance measure (L_2-norm) between input images is the chosen baseline classifier. In [LeCun et al., 1998] an error rate of 5.00% on the regular test set with $k = 3$ for this classifier is reported. Other studies [Wilder, 1998] report an error rate of 3.09% on the same experiment. The experiment was recreated in this work, and an error rate of 3.09% was obtained.

The goal of this experiment is to prove that LPD can successfully be used as a distance measure for images and that it has good results. The two classifiers, that are distinct only by the metric used, are compared using the first 100, 300 and 1000 images extracted from the MNIST data set. These subsets contain randomly distributed digits from 0 to 9 produced by different writers. Since the number of samples in each subset is relatively small, the tests were performed using the 10-fold cross-validation procedure which is repeated 10 times, in order to obtain the final accuracy rates.

Table 4.3 compares the accuracy of the baseline 3-NN classifier with the accuracy of the 3-NN classifier based on LPD. Results are reported on all the MNIST subsets of 100, 300 and 1000 samples, respectively. For all these subsets, the accuracy of LPD was obtained with patches of 4×4 pixels and a similarity threshold of 0.12.

Table 4.3: Baseline 3-NN versus 3-NN based on LPD. Both the accuracy rate and standard deviation is reported for MNIST subsets of 100, 300 and 1000 images.

Number of samples	Baseline 3-NN	3-NN + LPD
100	$73.33\% \pm 9.68\%$	$\mathbf{87.53\%} \pm \mathbf{7.38\%}$
300	$83.19\% \pm 5.47\%$	$\mathbf{92.50\%} \pm \mathbf{4.23\%}$
1000	$87.12\% \pm 2.59\%$	$\mathbf{95.53\%} \pm \mathbf{1.78\%}$

The first test case requires only 100 images, but in order to obtain a more accurate result, the first 200 examples from the MNIST training set were extracted and divided into two subsets of 100 images each. The classification methods were applied on both subsets, and the reported accuracy rates were averaged on the two subsets of 100 samples. The baseline 3-NN classifier has an average accuracy

of 73.33%. The 3-NN classifier based on LPD has an average accuracy of 87.53%, which represents an improvement of 14.20% over the baseline. The next test case uses 300 images. This time, the baseline classifier has an accuracy of 83.19%. By using LPD, an accuracy of 92.11% is obtained, which is 9.31% over the baseline. The third test case uses 1000 images. The accuracy obtained with the baseline classifier in the third test case is 87.12%. Again, the 3-NN classifier based on LPD performs better than the baseline with an accuracy of 95.53%. This represents an improvement of 8.41%.

One can observe that both classifiers have an increased accuracy when the number of samples is larger. The baseline method has a 9.86% improvement from 100 images to 300 images, while the classifier based on LPD has an improvement of 4.97%. A similar improvement in accuracy, from 300 to 1000 images, can be observed. The baseline is 3.93% better and the classifier based on LPD is 3.03% better.

In all test cases the 3-NN classifier based on LPD outperforms the baseline 3-NN classifier. It is worth pointing out that the accuracy of the classifier based on LPD, that is trained and tested on 1000 images (95.53%), gets very close to the accuracy of the baseline classifier (96.91%) trained on the full MNIST data set with $60,000$ images and tested on other $10,000$ images.

Note that according to the standard deviations presented in Table 4.3, one can state with confidence that the results of the 3-NN based on LPD are better than the baseline classifier. A student test was performed on the results obtained on 1000 images by the 3-NN based on LPD classifier on one hand, and by the baseline classifier on the other hand. The null hypothesis, that obtained results are independent random samples from normal distributions with equal means and equal variances, was rejected with a 99% confidence interval.

The pairwise similarity matrix could reveal subtle characteristics of the similarity or dissimilarity function. To analyze the LPD measure in more depth, the pairwise similarity matrix produced by the LPD measure is compared with the pairwise euclidean distance matrix. Figure 4.10 shows the similarity matrix obtained with LPD, and Figure 4.11 shows the euclidean distance matrix. The two matrices are obtained on the same MNIST subset of 1000 images. For the visual analysis of the similarity matrices, the samples are sorted by class labels in

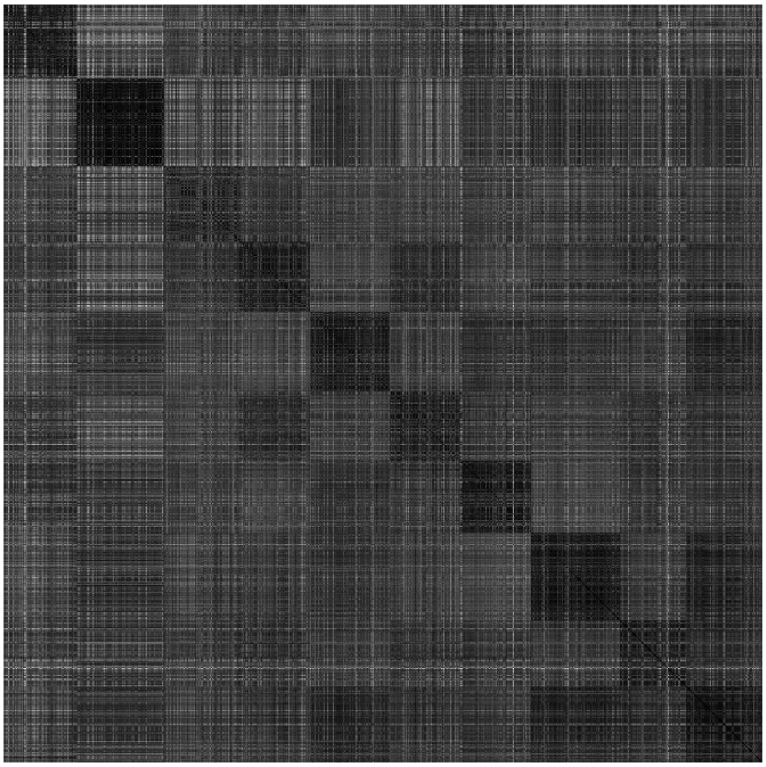

Figure 4.10: Similarity matrix based on LPD with patches of 4×4 pixels and a similarity threshold of 0.12, obtained by computing pairwise dissimilarities between the samples of the MNIST subset of 1000 images.

ascending order, starting with digit 0 and finishing with digit 9. Darker regions indicate higher similarity, and lighter regions indicate lower similarity. In both matrices, darker squares that indicate higher within-class similarities on the principal diagonal can be observed. The samples that represent the digit 1 are the most distinct from the other samples, in both matrices. However, the similarity matrix based on LPD has other distinctive classes such as digit 4, digit 6, digit 7 and digit 9. On the other hand, in the euclidean distance matrix the classes represented by digits 4 and 6 are also distinctive, but there is a greater amount of confusion between the digit 7 and digit 9 classes. The two measures also seem to mix up the digit 3 and digit 5 classes. Overall, the similarity matrices are fairly similar with each other, but the matrix produced by LPD seems to be slightly better. This is confirmed by the experiments presented in Table 4.3.

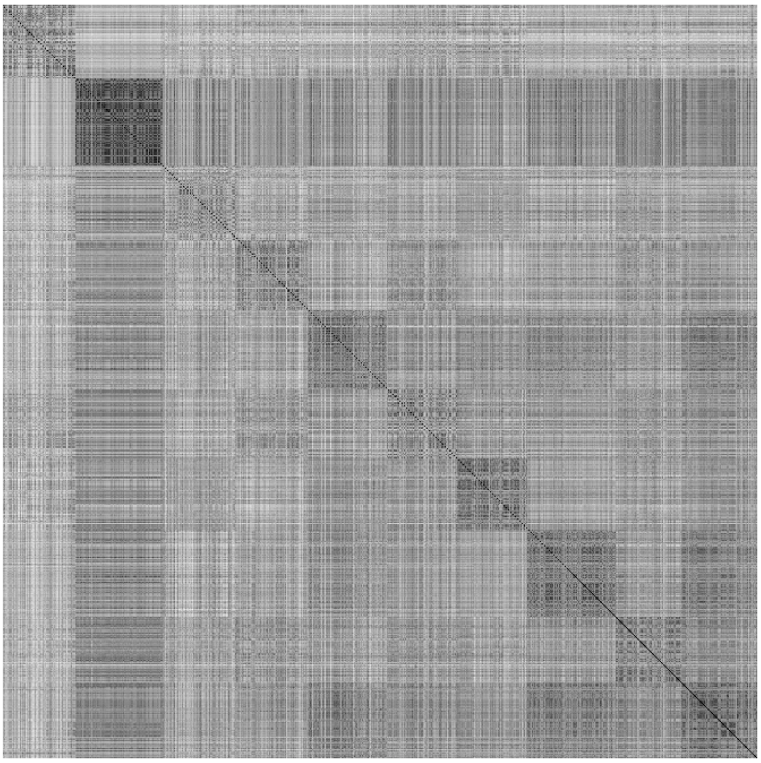

Figure 4.11: Euclidean distance matrix based on L_2-norm, obtained by computing pairwise distances between the samples of the MNIST subset of 1000 images.

4.3.5 Kernel Experiment

The goal of this experiment is to combine LPD with state of the art learning techniques (such as kernel methods) instead of the simple k-NN model, in order to improve the accuracy level. Therefore, the experiments on the MNIST subsets of 300 and 1000 images are repeated using SVM and Kernel Ridge Regression.

In Table 4.4 the accuracy rates of the 3-NN, SVM and KRR classifiers based on LPD are compared with the accuracy rates of the standard SVM and KRR methods. The kernel parameter σ is chosen to be equal 1000, since the square root of 1000 is close to the size of the images, which are 28×28 pixels. Results are reported on 300 and 1000 examples from the MNIST data set using 10-fold cross-validation. The last test case (identified as 300/700) divides the 1000 images into two sets: 300 images for training and 700 images for testing. The reported

results on this last test case are on the 700 images used for testing.

Table 4.4: Accuracy rates of several classifiers based on LPD versus the accuracy rates the standard SVM and KRR. Tests are performed on 300 and 1000 images using cross-validation (CV), respectively. Another test is performed using a 300/700 split.

Method	300 CV	1000 CV	300/700
SVM	86.33%	91.30%	81.71%
KRR	86.19%	91.58%	79.86%
3-NN+LPD	92.11%	95.53%	91.78%
SVM+LPD	**94.33**%	**96.90**%	**94.28**%
KRR+LPD	93.04%	96.16%	92.57%

As expected, the results slightly improve when a better learning method (such as SVM or KRR) is used rather than a simple 3-NN model. But what shows that LPD is very powerful, is that a simple 3-NN classifier based on LPD surpasses the standard SVM and KRR classifiers. The best results is obtained using the SVM combined with the LPD measure (96.90%).

The 300/700 test case shows that LPD is a robust dissimilarity measure because the results obtained on the test set of 700 images are very close to the results reported using 10-fold cross-validation. For example, the results of the SVM based on LPD drop from 94.33% on 300 images (using cross-validation) to only 94.28% on the other 700 images. On the other hand, the performance of the standard SVM and KRR classifiers reported on the 300/700 test case is much worse than the performance reported using 10-fold cross-validation.

4.3.6 Difficult Experiment

In [Vapnik & Vashist, 2009] the learning using privileged information paradigm is introduced. The problem of classifying images of digits 5 and 8 in the MNIST database is considered as an application. To make it more difficult, the authors have resized the digits from 28×28 pixel to 10×10 pixel images. The authors have used 100 samples of 10×10 pixel images as the training set, 4002 samples as the validation set (for tuning the parameters of SVM and SVM+) and the rest

of 1866 samples as the test set. The same split of the data set is used in this experiment.

The results of the standard SVM (based on euclidean distance) and the dSVM+ reported by [Vapnik & Vashist, 2009] are compared with three classifiers based on LPD. In Table 4.5 the accuracy rates of the SVM and dSVM+ classifiers are compared with the accuracy rates of the k-NN, SVM and KRR classifiers based on LPD. The number of neighbors of the k-NN model is 5, and it was chosen for best performance on the validation set. The parameters of the LPD are also tuned on the validation set. The best accuracy is obtained with patches of 3×3 pixels and a similarity threshold of 0.11. Since the images are smaller than in the previous experiments, it is natural to obtain better performance with smaller patches of 3×3 pixels instead of 4×4 pixels. The values of the kernel parameter σ is 100, because the images are 10×10 pixels in this case.

Table 4.5: Comparison of several classifiers (some based on LPD). Results for the difficult experiment on 1866 test images.

SVM	dSVM+	5-NN + LPD	SVM + LPD	KRR + LPD
92.50%	94.60%	91.32%	**95.10%**	95.00%

In this experiment one can observe that a simple 5-NN classifier based on LPD is very close to the standard SVM (the difference is only 1.18%), showing again that LPD is a very powerful dissimilarity.

The dSVM+ gains more than 2% in accuracy over the standard SVM by using privileged information in the training process. The dSVM+ classifier is surpassed by the SVM and KRR classifiers that are based on the LPD measure. Note that these classifiers (SVM + LPD and KRR + LPD) use no privileged information. This shows that using a better dissimilarity measure (such as LPD) is sometimes more important than using privileged information to improve accuracy.

4.3.7 Filter-based Nearest Neighbor Experiment

The results presented in Section 4.3.4 look promising, but LPD should be tested on the entire MNIST data set for a strong conclusion of its performance level.

The problem of the k-NN classifier based on LPD is that it is not feasible for very large data sets, since it takes too much time to compute all the pairwise dissimilarities. To avoid this problem, local learning methods that speed-up the learning algorithm can be used. Therefore, LPD is plugged into different local learning methods and used for image classification.

In this experiment, the local learning classifier employed for tests on the entire MNIST data set is the filter-based k-NN model. This classifier was chosen because it reflects the characteristics of the LPD measure. For the filter-based k-NN approach, the idea is to filter the nearest K neighbors using the standard euclidean distance measure (that is much faster to compute). Next, it selects the nearest k neighbors from those K images using LPD. The two-step selection process is much faster to compute on a large data set (such as the MNIST data set) than a standard k-NN based entirely on LPD. Results show that this method can improve accuracy and is among the top 4 k-NN models that reported results on the MNIST data set.

The k-NN based on LPD with filtering is compared with two other k-NN classifiers. One is the k-NN based on the euclidean distance measure (L_2-norm) between input images. This is the baseline classifier. In [LeCun et al., 1998], an error rate of 5.00% was reported on the regular test set with $k = 3$ for this classifier, while other studies [Wilder, 1998] report an error rate of 3.09% on the same experiment. The results obtained in this work also show an error rate of 3.09% on this baseline experiment. The second classifier is the k-NN based on Tangent Distance [Simard et al., 1996]. Tangent distance is insensitive to small distortions and translations of the input image. The error rate of this classifier reported in [LeCun et al., 1998] is 1.1%, but it was necessary to additionally process the images by subsampling to 16×16 pixels in order to obtain the reported error rate.

The accuracy of the k-NN based on LPD depends very much on the filtering. Take into account that the nearest K images are selected using the euclidean distance in the filtering phase. If K is close to k, a very fast classifier is obtained, but its accuracy will be near the baseline k-NN. As K increases the accuracy improves, but the method also becomes slower (since it has to compute LPD between more images than it was before). If K is equal to the number of training

examples, there is no filtering at all and the highest accuracy is obtained. However, the time to compute k-NN based on LPD with no filtering is too high to be considered. The idea is to choose an optimal K in order to obtain a trade-off between accuracy and time. Table 4.6 shows the error rate and the execution time of the 3-NN classifier based on LPD with filtering for several K values. The time was measured on a computer with Intel Core Duo 2.26 GHz processor and 4 GB of RAM memory using a single Core. Empirical results show that an optimal K would be somewhere between 100 and 500. When K is 100, approximately 8 seconds are needed to assign a label to a test image. This is reasonable for a real-time application, since computing LPD on GPU and adding parallel processing into assigning a label can improve the time even further.

Table 4.6: Error and time of 3-NN classifier based on LPD with filtering.

K	Error	Average time per test image	Overall time
3	2.73%	2.2 seconds	6 hours
10	1.78%	2.6 seconds	7 hours
30	1.45%	3.7 seconds	10 hours
50	1.38%	4.8 seconds	13 hours
100	1.26%	7.6 seconds	21 hours
200	1.15%	13.2 seconds	36 hours
500	1.09%	30.5 seconds	84 hours
1000	1.05%	58.8 seconds	162 hours

Looking at how the error gets lower as K increases, one can observe that the error tends to stabilize at some point. In other words, the error rate will not drop anymore after a certain K value. That error rate represents the actual error rate of a 3-NN classifier based on LPD (without filtering). The limitation of LPD induces this error, but what exactly is this error rate? Figure 4.12 gives an overview of this phenomenon and a hint about the point where the error stabilizes for both 3-NN and 6-NN classifiers. In order to make a prediction about the stabilization point of the error, the stability of the k-NN with filtering needs to be studied as K varies. It is clear from Figure 4.12 that the error drops with no variation when K increases. But increasing K may induce a misclassification on some test images (even if, overall, more images are classified correctly). For

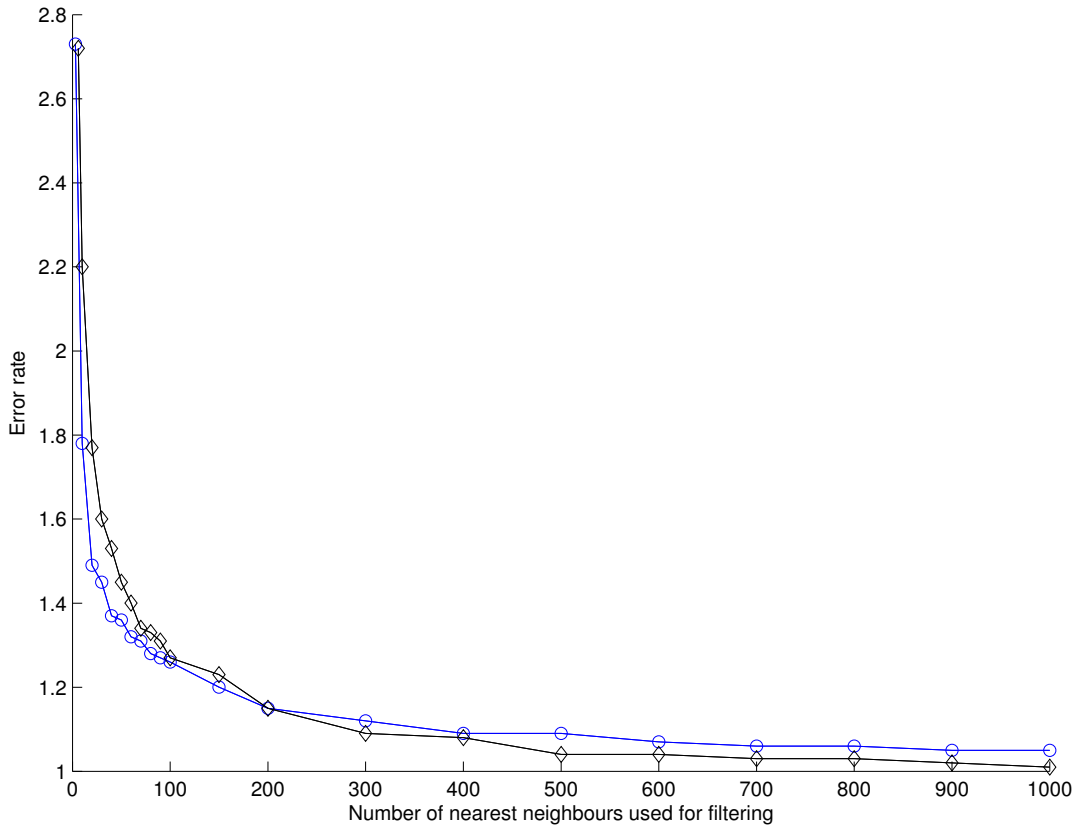

Figure 4.12: Error rate drops as K increases for 3-NN (∘) and 6-NN (⋄) classifiers based on LPD with filtering.

$K = 100, 200, ..., 1000$, the set of misclassified images for a certain value of K always includes the set of misclassified images for a greater value of K. Thus, the method has very stable behavior as K varies. In these circumstances, the error rates of the 3-NN and 6-NN classifiers based on LPD (without filtering) can be obtained by testing the classifiers only on the previously misclassified images. By doing so, an error rate of 1.03% is obtained for the 3-NN classifier and an error rate of 0.98% is obtained for the 6-NN classifier. These error rates are based only on a statistical proof. But as stated before, the real proof (that of testing the 3-NN and 6-NN classifiers with no filtering on all test images) is not practical

from the time perspective. The obtained error rates only give a good indication of the actual ones, and they are not compared with the error rates of the other k-NN classifiers based on euclidean and tangent distance, respectively.

The confusion matrix of the 3-NN based on LPD with filtering using $K = 50$ is presented in Table 4.7. The confusion matrix shows that most of the digits are fairly well distinguished by LPD, but some confusions stand out from the rest. The greatest confusions are between digits 4 and 9, between digits 3 and 5, and between digits 2 and 7, respectively. From the total amount of 138 misclassified images, there are 11 samples of digit 7 classified as digit 1, 10 samples of digit 2 classified as digit 7, and 10 samples of digit 4 classified as digit 9. The best per class accuracy of the 3-NN model is on digit 1 (99.65%) and digit 0 (99.49%). On the other hand, the worst accuracy is on digit 9 (97.82%) and digit 8 (97.95%). Thus, LPD is better on recognizing digits 1 and 0 and slightly worse at recognizing digits 9 and 8, despite the fact that there are not significant differences between the per digit classification accuracy rates. Overall, the confusion matrix shows that LPD is able to equally classify all the digits with only a few mistakes. Actually, there are only 138 misclassified images from the total of $10,000$ samples.

Table 4.7: Confusion matrix of the 3-NN based on LPD with filtering using $K = 50$.

Digits	0	1	2	3	4	5	6	7	8	9
0	975	1	1	0	0	1	1	1	0	0
1	0	1131	2	0	0	0	1	1	0	0
2	6	2	1013	0	0	0	1	10	0	0
3	0	0	1	994	1	6	0	5	1	2
4	0	4	0	0	963	0	4	0	1	10
5	1	0	0	4	1	883	1	0	1	1
6	2	3	0	0	2	1	950	0	0	0
7	0	11	3	1	0	0	0	1009	0	4
8	2	0	0	3	3	2	2	3	954	5
9	0	3	1	2	6	3	1	4	2	987

Table 4.8 compares error rates of the three k-NN classification methods (distinct only by the metric used) using the MNIST test set of $10,000$ samples. For the k-NN classifier based on LPD with filtering, $k = 3$ and $k = 6$ are used.

The error rates of the k-NN models based on LPD are obtained using the nearest $K = 1000$ images filtered by the euclidean distance. The LPD is based on patches of 4×4 pixels and a similarity threshold of 0.125. The LPD parameter tuning procedure is described in Section 4.3.3. The k-NN based on LPD with filtering model has a better accuracy than the other k-NN models. In fact, it is among the top 4 k-NN models that reported results on the MNIST data set. The 6-NN classifier based on LPD with filtering has an error rate of only 1.01%. Note that unlike the k-NN with filtering based on LPD, the other three methods from top 4 need additional preprocessing steps.

Table 4.8: Error rates on the entire MNIST data set for baseline 3-NN, k-NN based on tangent distance and k-NN based on LPD with filtering.

Method	Error
baseline 3-NN	3.09%
k-NN + tangent distance	1.1%
3-NN + LPD + filter	1.05%
6-NN + LPD + filter	**1.01**%

4.3.8 Local Learning Experiment

Because LPD is computationally heavy, it is not feasible to compute a kernel matrix with high dimensions. Even with a fast similarity measure, computing and storing a large kernel matrix could pose a serious problem for the design and implementation of a kernel classifier. Therefore, the use of kernel classifiers, such as SVM and KRR based on LPD, on the entire MNIST data set should be avoided as much as possible. Instead, kernel methods can be integrated into a local learning algorithm. The proposed approach for this experiment is very similar to the filter-based k-NN model. The filtering step remains unchanged. Thus, the first step is to filter the nearest K neighbors using the standard euclidean distance. The second step is to train a kernel classifier using only the filtered K neighbors. A new classifier is trained for each test image. The classifier will be used to predict only the label of the test image that was built for.

Before training the classifier, it is necessary to build a kernel matrix using LPD. It is not feasible for a real-time application to build a $K \times K$ kernel matrix for each test image, when K is larger than 100, especially if no GPU or parallel processing is done. But, a large number of K neighbors is needed in order to improve the accuracy of the kernel method. A feasible solution is to train a kernel classifier only when a majority of images with the same label greater than 60% among the filtered K neighbors is not available, and use a k-NN model when such a majority exists. There are two reasons for this approach. First, if such a majority exists, the kernel method will be biased towards choosing the majority class. Second, it is likely that a simple k-NN would also choose this majority class that is probably the right one.

This local learning algorithm was tested on the MNIST data set. Using $K = 200$, it gives an error rate of 1.07%. From the $10,000$ test samples, 983 of them had a majority class of less than 60% of the total 200 neighbors. For each of these 983 samples, a KRR classifier based on LPD was trained. The other test labels were predicted using the 3-NN based on LPD. Note that the 3-NN with filtering approach has an error rate of 1.15% for $K = 200$ and the local learning algorithm is able to improve it to 1.07%. Another local learning algorithm, that uses SVM instead of KRR, was tested without being able to improve the accuracy.

In conclusion, using kernel methods in a local learning context does not bring a significant improvement in accuracy to the k-NN with filtering approach. However, the local learning algorithm proposed here can successfully be used for handwritten digit recognition. It also benefits from a much faster computational time compared to standard kernel methods based on LPD.

4.3.9 Birds Experiment

In this experiment, LPD is used to classify a more general type of images available in the Birds data set. Several k-NN models based on different distance measures are compared. The first k-NN model uses the Bhattacharyya coefficient to compare spatiograms of HSV values extracted from images. This improved measure of comparing spatiograms is proposed in [Conaire et al., 2007]. The second k-NN model is based on the mean euclidean distance measure (L_1-norm) between input

images. Another two k-NN classifiers based on LPD are tested. One of them uses a slightly modified version of the LPD algorithm, in that it determines similar patches using the mean euclidean distance corresponding to the L_1-norm, which seems to work better than the L_2-norm on this experiment. The other one uses a fast version of the LPD algorithm that skips half of the comparisons between patches.

For both the euclidean distance measure and the LPD measure, images from the Birds data set need to be brought to the same size in order to be compared. Thus, images are resampled to 100×100 pixels. To observe the difference between original and resized images, the k-NN model based on the Bhattacharyya coefficient is tested on both types of images. The other k-NN models are tested only on the resampled images, that are also converted to gray-scale. While the method proposed by [Conaire et al., 2007] works on color images, the euclidean distance and LPD are naturally computed on gray-scale images. Table 4.9 compares the error rates of all these k-NN models. The empirical results show that skipping overlapping patches does not affect the accuracy of LPD.

Table 4.9: Error rates of different k-NN models on Birds data set.

Method	Preprocessing	Error
5-NN + Bhattacharyya	none	57.33%
5-NN + Bhattacharyya	resize	54.67%
3-NN + euclidean	resize, gray-scale	51.00%
3-NN + LPD	resize, gray-scale	**30.33**%
3-NN + LPD + skip	resize, gray-scale	**30.33**%

Next, three kernel methods based on the fast version of LPD (that skips half of the comparisons between patches) are compared with the state of the art texton learning methods from [Lazebnik et al., 2005a]. The proposed kernel methods based on LPD are the SVM, the KRR and the KDA classifiers. Table 4.10 compares error rates of kernel methods based on LPD and texton learning methods. The kernel methods based on LPD have an accuracy similar to some of the state of the art methods. However, the proposed kernel methods are more time efficient. In [Lazebnik et al., 2005a], a time of about 7 days for a single experiment is reported, while the kernel methods based on LPD need about 4 days for the

Table 4.10: Error on Birds data set for texton learning methods of [Lazebnik et al., 2005a] and kernel methods based on LPD.

Method	Error
Naive Bayes	21.33%
Exp. parts	**7.67**%
Exp. relations	24.67%
Exp. parts + relations	8.33%
SVM + LPD + skip	27.33%
KRR + LPD + skip	26.00%
KDA + LPD + skip	24.33%

same experiment on an Intel Core Duo 2.26 GHz processor and 4 GB of RAM memory. Note that error rates of all models based on LPD, used in this experiment, are obtained with patches of 4×4 pixels and a similarity threshold of 0.15. The parameters were obtained by cross-validation on the training set. In conclusion, the fast version of LPD can successfully be used as a kernel for image classification.

4.4 Local Texton Dissimilarity

This section presents a novel texture dissimilarity measure based on textons, termed Local Texton Dissimilarity (LTD). It represents a development adapted to textures of the more general LPD measure. Instead of patches, LTD works with textons, which are represented as a set of features extracted from image patches. It is reasonable to work with textons rather than patches, since many state of the art texture classification methods are based on textons. Some of these state of the art methods are presented in Section 4.4.1.

The algorithm proposed in [Dinu et al., 2012] and presented in Section 4.1.1 compares image patches by using the mean euclidean distance. LTD differs in the way it compares these patches. First, texture specific features are extracted from each patch. A patch can then be represented by a feature vector. Similar patches are represented through similar features. Thus, image patches are implicitly quantized into textons. Textons are compared using the Bhattacharyya coefficient

between their feature vectors. Section 4.4.2 describes the features extracted from image patches, while the LTD algorithm [Ionescu et al., 2014] is presented in Section 4.4.3.

4.4.1 Texton-based Methods

The work of [Lazebnik et al., 2005b] presents a texture representation that is invariant to geometric transformations based on descriptors defined on affine invariant regions. A probabilistic part-based approach for texture and object recognition is presented in [Lazebnik et al., 2005a]. Textures are represented using a part dictionary obtained by quantizing the appearance of salient image regions.

In [Leung & Malik, 2001], texture images are classified by using 3D textons, which are cluster centers of filter response vectors corresponding to different lighting and viewing directions of images. The work of [Varma & Zisserman, 2005] models textures by the joint distribution of filter responses. This distribution is represented by the frequency histogram of textons. For most texton based techniques, the textons are usually learned by k-means clustering. In [Xie et al., 2010], a novel texture classification method via patch-based sparse texton learning is proposed. The dictionary of textons is learned by applying sparse representation to image patches in the training data set.

4.4.2 Texture Features

Before computing LTD between texture images, a set of several image features is extracted from each patch to obtain the texton representation. There are 9 features extracted from patches, that are described next. An interesting remark is that the more features are added to the texton representation, the better the accuracy of the LTD method gets. However, a lighter representation, such as the one based on 9 features, results in a faster and more efficient algorithm. One may choose to add or remove features in order to obtain the desired trade-off between accuracy and speed. The texton representation based on the 9 features that are about to be presented next gives state of the art accuracy levels in several experiments presented in Section 4.5.

The first two statistical features extracted are the mean and the standard deviation. These two basic features can be computed indirectly, in terms of the image histogram. The shape of an image histogram provides many clues to characterize the image, but the features obtained from an image histogram are not always adequate to discriminate textures, since they are unable to indicate local intensity differences.

One of the most powerful statistical methods for textured image analysis is based on features extracted from the Gray-Level Co-Occurrence Matrix (GLCM), proposed in [Haralick et al., 1973]. The GLCM is a second order statistical measure of image variation and it gives the joint probability of occurrence of gray levels of two pixels, separated spatially by a fixed vector distance. Smooth texture gives a co-occurrence matrix with high values along diagonals for small distances. The range of gray level values within a given image determines the dimensions of a co-occurrence matrix. Thus, 4 bits gray level images give 16×16 co-occurrence matrices. Relevant statistical features for texture classification can be computed from a GLCM. The features proposed by [Haralick et al., 1973], which show a good discriminatory power, are the contrast, the energy, the entropy, the homogeneity, the variance and the correlation. Among these features that show a good discriminatory power, LTD uses only four of them, namely the contrast, the energy, the homogeneity, and the correlation.

Another feature that is relevant for texture analysis is the fractal dimension. It provides a statistical index of complexity comparing how detail in a fractal pattern changes with the scale at which it is measured. The fractal dimension is usually approximated. The most popular method of approximation is box counting [Falconer, 2003]. The idea behind the box counting dimension is to consider grids at different scale factors over the fractal image, and count how many boxes are filled over each grid. The box counting dimension is computed by estimating how this number changes as the grid gets finer, by applying a box counting algorithm. An efficient box counting algorithm for estimating the fractal dimension was proposed in [Popescu et al., 2013b]. The idea of the algorithm is to skip the computation for coarse grids, and count how many boxes are filled only for finer grids. LTD includes this efficient variant of box counting in the texton representation.

The work of [Daugman, 1985] found that cells in the visual cortex of mammalian brains can be modeled by Gabor functions. Thus, image analysis by the Gabor functions is similar to perception in the human visual system. A set of Gabor filters with different frequencies and orientations may be helpful for extracting useful features from an image.

The local isotropic phase symmetry measure (LIPSyM) presented in [Kuse et al., 2011] takes the discrete time Fourier transform of the input image, and filters this frequency information through a bank of Gabor filters. The work of [Kuse et al., 2011] also notes that local responses of each Gabor filter can be represented in terms of energy and amplitude. Thus, Gabor features, such as the mean-squared energy and the mean amplitude, can be computed through the phase symmetry measure for a bank of Gabor filters with various scales and rotations. These features are relevant because Gabor filters have been found to be particularly appropriate for texture representation and discrimination.

Finally, textons are represented by the mean and the standard deviation of the patch, the contrast, the energy, the homogeneity, and the correlation extracted from the GLCM, the (efficient) box counting dimension, and the mean-squared energy and the mean amplitude extracted by using Gabor filters. These texton features can be extracted from all images before comparing them with LTD. Thus, the LTD computation can be divided into two main steps, one for texton feature extraction, and one for dissimilarity computation. After the feature extraction step, features should be normalized. In practice, the described features work best on squared image patches of a power of two size.

4.4.3 Local Texton Dissimilarity Algorithm

To compute LTD between two gray-scale texture images, the idea is to sum up all the offsets of similar textons between the two images. The LTD algorithm is briefly described next. For every texton in one image, the algorithm searches for a similar texton in the other image. First, it looks for similar textons in the same position in both textures. If those textons are similar, it sums up 0 since there is no spatial offset between textons. If the textons are not similar, the algorithm starts exploring the vicinity of the initial texton position in the second image to

find a texton similar to the one in the first image. If a similar texton is found during this process, it sums up the offset between the two textons. The spatial search goes on until a similar texton is found or until a maximum offset is reached. The maximum texton offset must be set a priori. The computation of LTD is similar the algorithm presented in Section 4.1.2. In practice, the computation described above is too heavy for a large set of images. To speed up the algorithm, textons are extracted and compared using a dense grid over the image. This is similar to the idea of skipping overlapping patches to optimize LPD.

Algorithm 2 computes the LTD between gray-scale texture images img_1 and img_2, using the underlying Bhattacharyya coefficient to compute the similarity between texton feature vectors.

Algorithm 2 *Local Texton Dissimilarity*

***Input**:*

img_1 – *a gray-scale texture image of* $h_1 \times w_1$ *pixels;*

img_2 – *another gray-scale texture image of* $h_2 \times w_2$ *pixels;*

n – *the number of features that represent a texton;*

gridStep – the skip step that generates a dense grid over the image;

offsetStep – the skip step used for comparing patches at different offsets;

w – *a vector of feature weights (some features can be more important than others);*

th – *the texton similarity threshold.*

***Initialization**:*

$dist = 0$

$h = \min\{h_1, h_2\} - p + 1$

$w = \min\{w_1, w_2\} - p + 1$

***Computation**:*

for $x = 1$*:gridStep:*h

  for $y = 1$*:gridStep:*w

    get $texton^{left}$ *at position* (x, y) *in* img_1

    $d = 0$

    while did not find texton at offset d *similar to* $texton^{left}$

      get $texton^{right}$ *at offset* d *from position* (x, y) *in* img_2

$s_1 = \frac{1}{n}\sum_{i=1}^{n}\left(w_i \cdot \sqrt{texton_i^{left}} - w_i \cdot \sqrt{texton_i^{right}}\right)^2$
if $s_1 < th$
$dist = dist + d$
break
endif
if all textons at offset d were tested
$d = d+$ *offsetStep*
endif
endwhile
get $texton^{right}$ *at position* (x, y) *in* img_2
$d = 0$
while did not find texton at offset d similar to $texton^{right}$
get $texton^{left}$ *at offset d from position* (x, y) *in* img_1
$s_2 = \frac{1}{n}\sum_{i=1}^{n}\left(w_i \cdot \sqrt{texton_i^{right}} - w_i \cdot \sqrt{texton_i^{left}}\right)^2$
if $s_2 < th$
$dist = dist + d$
break
endif
if all textons at offset d were tested
$d = d+$ *offsetStep*
endif
endwhile
endfor
endfor

Output:

dist – the dissimilarity between textures img_1 *and* img_2.

Algorithm 2 needs a few input parameters besides the two images. The number of features gives the size of the feature vector. In this work, the 9 features described in Section 4.4.2 were used. In the algorithm, $texton_i$ represents the i-th

feature of the texton representation, and w_i represents the weight associated to the i-th feature.

The results of the LTD algorithm can further be improved by adding more features or probably by using completely different features. The parameter that generates a dense grid over the image, and the skip step used for comparing patches at different offsets are used to speed up the LTD algorithm without losing too much accuracy. These parameters induce a sparse representation of the images. Using a sparse representation is indeed necessary, since patch-based algorithms are heavy to compute with current computers because they usually manipulate millions of patches [Barnes et al., 2011]. The texton similarity threshold is a value in the $[0, 1]$ interval, that determines when two textons are considered to be similar. All these parameters need to be adjusted with regard to the data set size and to the image dimensions, in order to obtain a good trade-off between accuracy and speed.

4.5 Texture Experiments and Results

In the experiments, LTD is evaluated with different kernel methods to show that good performance levels are due to the use of LTD. Two data sets of texture images are used to assess the performance of several kernel methods based on LTD, namely the Brodatz data set and the UIUCTex data set. All the experiments presented in this work aim at showing that LTD has general applications for texture classification, and that LTD is indeed a robust dissimilarity measure.

A potential application of LTD discussed in this work is biomass type identification. A method to determine the biomass type has practical motivations for the biomass industry. Such methods are of great importance when one in the biomass industry needs to produce another energy product, such as biofuel or bioenergy, for example. Is the type of biomass appropriate to efficiently obtain the bioproduct? Is the biomass conversion method the right one for this type of biomass? Answering such questions can help reduce the operating costs of biomass power plants. But, these questions can be answered with the help of a biomass type identification method, such as the one presented in this chapter. Indeed, LTD can be used in combination with several machine learning methods

for biomass texture classification. Therefore, another classification experiment is conducted on a data set of biomass texture images.

It is important to mention that, in a general sense, *biomass* refers to the biological material from living, or recently living organisms. In this work, the term *biomass* refers to a renewable energy source, that can be directly converted into another type of energy product. The Biomass Texture data set used in this thesis is a collection of close-up photos of different samples of three types of biomass: municipal solid waste, corn, and wheat. The goal is to build a classifier that is able to distinguish between these three types of biomass. This is a totally different approach and understanding of the biomass classification problem, compared to other researches. Usually, biomass classification refers to land cover type or forest biomass classification. Land cover classification [Dash et al., 2007] and forest biomass estimation [Wulder et al., 2008] are active research topics in the area of remote sensing. The work of [Hoekman & Quinnones, 2000] shows that remotely sensed image classification systems may be designed to accurately monitor processes of deforestation, land and forest degradation and secondary forest regrowth.

4.5.1 Data Sets Description

The first data set used for testing the dissimilarity presented in this paper is the Brodatz data set [Brodatz, 1966]. This data set is probably the best known benchmark used for texture classification, but also one of the most difficult, since it contains 111 classes with only 9 samples per class. Samples of 213×213 pixels are cut using a 3 by 3 grid from larger images of 640×640 pixels. Figure 4.13 presents three sample images per class of three classes randomly selected from the Brodatz data set.

The second experiment is conducted on the UIUCTex data set of [Lazebnik et al., 2005b]. It contains 1000 texture images of 640×480 pixels representing different types of textures such as bark, wood, floor, water, and more. There are 25 classes of 40 texture images per class. Textures are viewed under significant scale, viewpoint and illumination changes. Images also include non-rigid deformations. This data set is available for download at `http://www-cvr.ai.uiuc.`

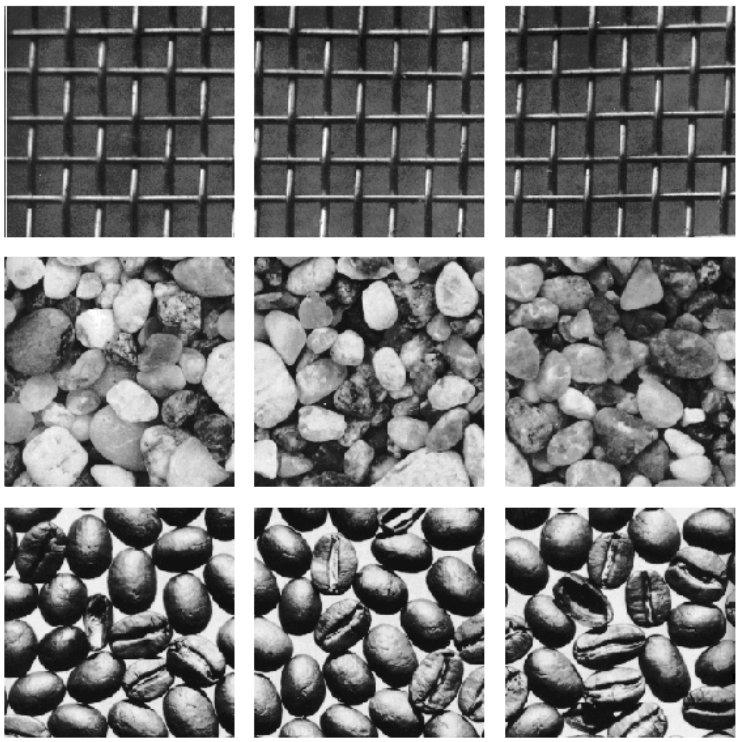

Figure 4.13: Sample images from three classes of the Brodatz data set.

edu/ponce_grp. Figure 4.14 presents four sample images per class of four classes representing bark, brick, pebbles, and plaid.

The third experiment is conducted on a data set of biomass texture images available at http://biomass.herokuapp.com. It contains 270 images of 512×512 pixels representing close up photos of three types of biomass resulted after the processing of wheat, municipal waste and corn, respectively. Photos where taken at different zoom levels, under various lighting conditions. Figure 4.15 shows a few random samples of biomass images from this data set. There are 90 images per class. The goal is to build a classifier that is able to identify the three types of biomass: wheat, waste, and corn, respectively.

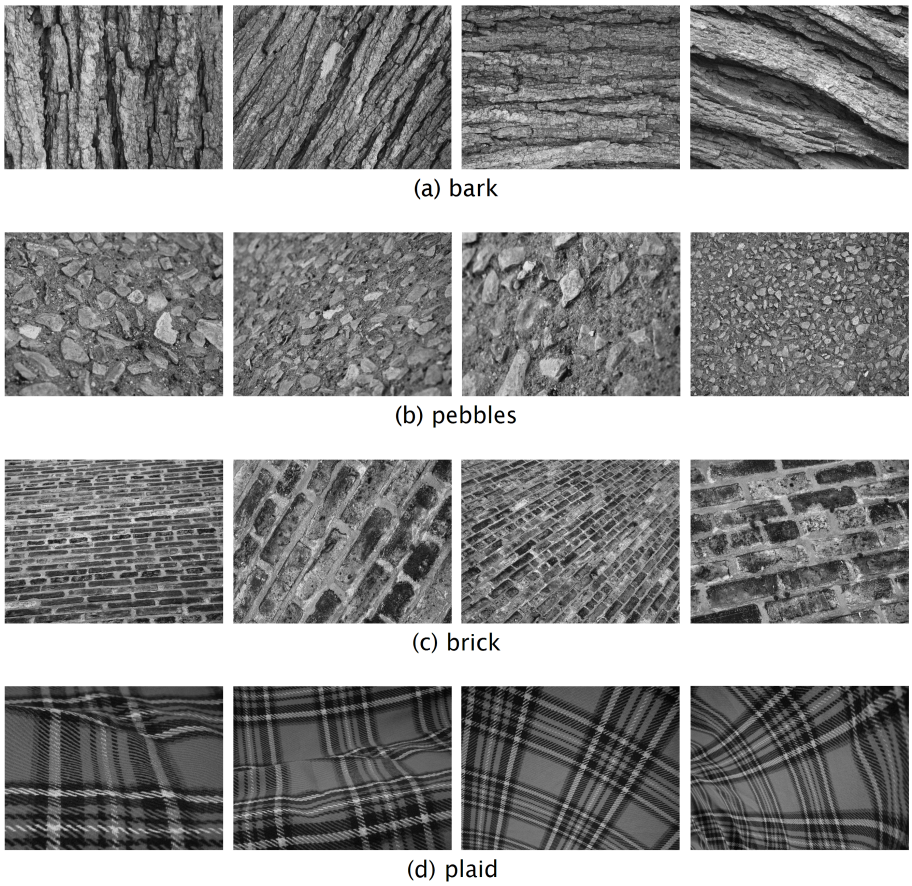

Figure 4.14: Sample images from four classes of the UIUCTex data set. Each image is showing a textured surface viewed under different poses.

4.5.2 Learning Methods

To use LTD for texture classification, it should be plugged into a similarity-based learning method. Several similarity-based classifiers are proposed. The first classifier used in the experiments is the k-NN. It was chosen because it directly reflects the discriminatory power of the dissimilarity measure. Several state of the art kernel methods are also used, namely the KRR, the SVM, the KDA, and the KPLS. LTD can be transformed into a similarity measure by using

Figure 4.15: Sample images from the Biomass Texture data set.

the Gaussian-like kernel, in a similar fashion to LPD:

$$k(img_1, img_2) = \exp\left(-\frac{LTD(img_1, img_2)}{2\sigma^2}\right),$$

where img_1 and img_2 are two gray-scale texture images. The parameter σ is usually chosen to match the number of features so that values of $k(img_1, img_2)$ are well scaled.

4.5.3 Brodatz Experiment

The baseline method proposed for this experiment is a 1-NN model that is based on the Bhattacharyya coefficient computed on the 9 texture features described in Section 4.4.2. The features are extracted from entire images. The second proposed model is a 1-NN classifier based on LTD. The baseline is useful to assess the performance gained by the use of LTD. The other proposed classifiers

are the KRR, the KPLS, the SVM and the KDA, all based on LTD. The KDA method is particularly suitable for problems with many classes, such as Brodatz.

In [Lazebnik et al., 2005b], the accuracy rate reported on the Brodatz data set using 3 training samples per class is 88.15%. Table 4.11 compares accuracy rates of the proposed classifiers with the accuracy rate of the state of the art method described in [Lazebnik et al., 2005b], using the same setup with 3 random samples per class for training. The accuracy rates presented in Table 4.11 are actually averages of accuracy rates obtained over 20 runs for each method. The 1-NN based on LTD model has a far better accuracy than the baseline, proving that LTD helps the learning method to achieve better results. All the kernel methods based on LTD are above the state of the art classifier. The best classifier among them is KDA, which has an accuracy of 90.87%. It is 5.46% better than the 1-NN based on LTD, and 2.72% better that the state of the art method. Therefore, it seems that LTD is a good dissimilarity measure for texture classification. Combined with suitable learning methods, LTD gives results comparable to state of the art method. Despite better texture classification methods exist [Zhang et al., 2007], the classifiers based on LTD can also be improved by adding more features to the texton representation.

Table 4.11: Accuracy rates on the entire Brodatz data set using 3 random samples per class for training. Learning methods based on LTD are compared with the state of the art method.

Method	Accuracy
baseline 1-NN	77.68%
Best of [Lazebnik et al., 2005b]	88.15%
1-NN + LTD	85.41%
KRR + LTD	89.43%
SVM + LTD	89.48%
KPLS + LTD	89.57%
KDA + LTD	**90.87%**

In this experiment, LTD was computed on patches of 32×32 pixels, using a similarity threshold of 0.02 and a maximum offset of 80 pixels. Patches were extracted on a dense grid with a gap of 32 pixels. Feature weighting can improve

accuracy by almost 1%. Thus, adjusting feature weights is not very important, but it helps the classifier. However, the feature weights were manually adjusted to increase the importance of Gabor features and fractal dimension by a factor of two, and to decrease the importance of the mean and the standard deviation by a factor of two. The weights were tuned on the baseline 1-NN model, which also uses feature weighting in the reported results. The parameter σ of the LTD kernel was chosen to be 10^{-3}. All the parameters were chosen by cross-validation on a subset of the Brodatz data set. An interesting remark is that these parameters do not change by too much on the other data sets.

Using these parameters, it takes less than 1 second to compute LTD between two images on a computer with Intel Core Duo 2.26 GHz processor and 4 GB of RAM memory using a single Core. Reported accuracy rates can be improved by a few percents using a more dense grid and a greater maximum offset, but the LTD computation will also take more time. However, with the current parameters, LTD is much faster than LPD, which takes about 5 minutes to compare two images from the Brodatz data set with similar parameters, without skipping overlapping patches.

The pairwise similarity matrix of LTD between Brodatz samples, shown in Figure 4.16, is analyzed next. It reveals that the LTD measure is able to discriminate most of the classes from the Brodatz data set. This fact is indicated in Figure 4.16 by the tiny darker squares along the diagonal of the similarity matrix. These squares represent a higher within class similarity. The fact that LTD discriminates most of the classes by itself is also suggested by the good performance of the 1-NN model based on LTD, compared to the 7.73% lower performance of the baseline 1-NN.

4.5.4 UIUCTex Experiment

In this experiment, the same classifiers evaluated on the Brodatz data set are also evaluated on the UIUCTex data set. More precisely, the evaluated classifiers are the baseline 1-NN model based on the Bhattacharyya coefficient, the 1-NN classifier based on LTD, and the kernel classifiers based on LTD, namely the KRR, the KPLS, the SVM, and the KDA. These classifiers are compared with

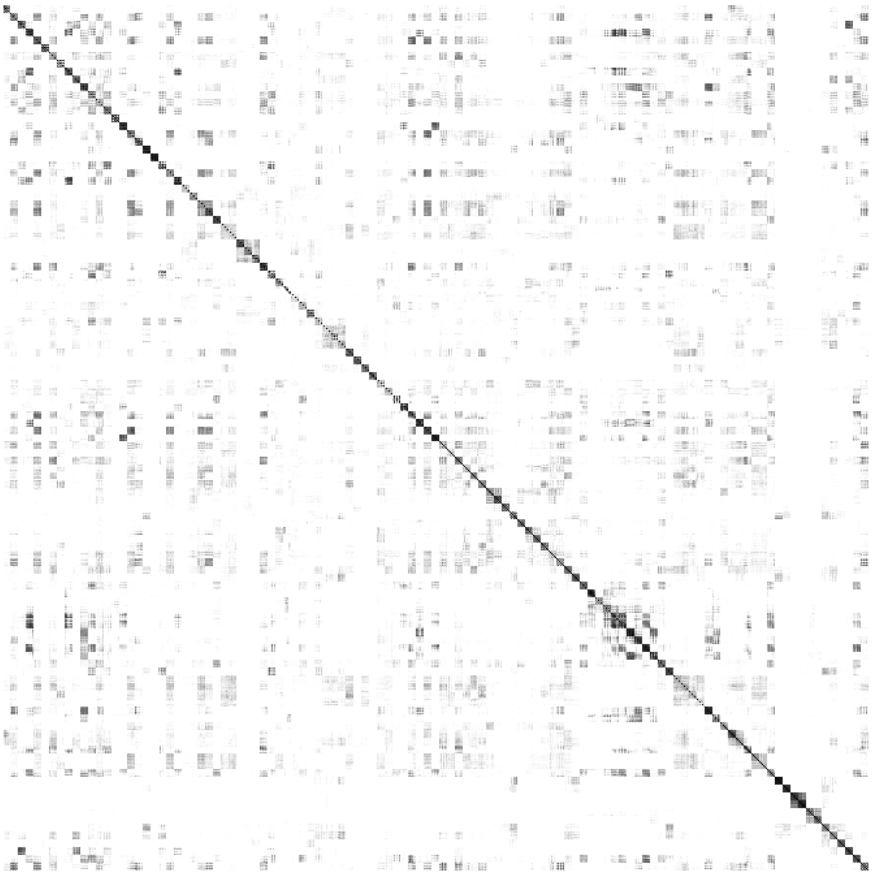

Figure 4.16: Similarity matrix based on LTD with patches of 32×32 pixels and a similarity threshold of 0.02, obtained by computing pairwise dissimilarities between the texture samples of the Brodatz data set.

the state of the art classifier of [Lazebnik et al., 2005b]. The best accuracy level of the state of the art classifier on the UIUCTex data set, reported in [Lazebnik et al., 2005b] using 20 training samples per class, is 97.41%.

Table 4.12 compares accuracy rates of the classifiers based on LTD with the accuracy rate of the state of the art classifier of [Lazebnik et al., 2005b], using the same setup with 20 random samples per class for training. The accuracy rates are averaged over 20 runs for each method. The accuracy of the 1-NN model based on LTD is 9.32% better than accuracy of the baseline 1-NN, proving again that LTD is able to achieve much better results. However, the accuracy of the 1-NN based on LTD is far behind the state of the art classifier. Even the

kernel methods have accuracy rates that are roughly 4% lower than the state of the art classifier. The best classifier based on LTD is the KPLS, with an accuracy of 93.79%, which is 3.62% lower than the state of the art method. The accuracy of these kernel methods depend on LTD, which depends in turn on the features extracted from images to obtain textons. Better features will result in a dissimilarity measure capable of making finer distinctions, and, consequently, in a better kernel classifier. But even with the 9 features proposed in Section 4.4.2, LTD seems to give results that are comparable to the state of the art method.

Table 4.12: Accuracy rates on the UIUCTex data set using 20 random samples per class for training. Learning methods based on LTD are compared with state of the art method.

Method	Accuracy
baseline 1-NN	79.34%
Best of [Lazebnik et al., 2005b]	**97.41**%
1-NN + LTD	88.66%
KRR + LTD	93.51%
SVM + LTD	93.62%
KPLS + LTD	93.79%
KDA + LTD	93.38%

In this experiment, LTD was computed on patches of 64×64 pixels, using a similarity threshold of 0.02 and a maximum offset of 240 pixels. Patches were extracted on a dense grid with a gap of 64 pixels. The same feature weights as in the Brodatz experiment were used. The parameter σ of the LTD kernel was chosen to be 10^{-3}. All the parameters were chosen by cross-validation on a subset of the UIUCTex data set.

The pairwise similarity matrix of LTD between UIUCTex samples, shown in Figure 4.17, seems to create confusions between many classes. Darker squares along the diagonal are not so visible as in the Brodatz case. One can observe that LTD is less capable of making fine distinctions between images from different classes. It may be that the 9 feature used for representing textons are less suitable for analyzing texture images with significant scale, viewpoint and illumination changes, such as those from the UIUCTex data set. Adding other features suitable

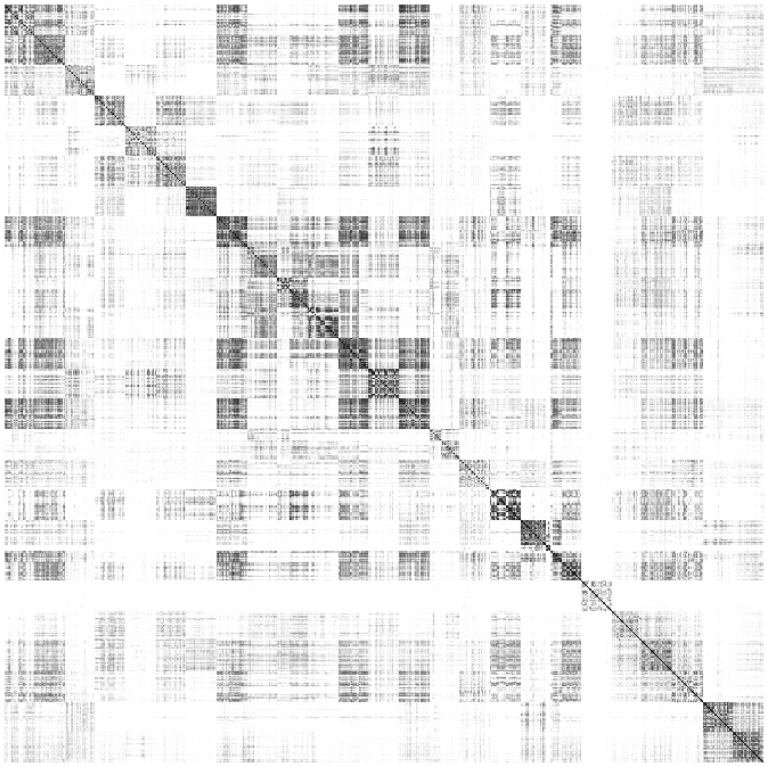

Figure 4.17: Similarity matrix based on LTD with patches of 64×64 pixels and a similarity threshold of 0.02, obtained by computing pairwise dissimilarities between the texture samples of the UIUCTex data set.

for this type of images could improve the accuracy.

4.5.5 Biomass Experiment

The classifiers evaluated in this experiment are the baseline 1-NN model based on the Bhattacharyya coefficient, the 1-NN classifier based on LTD, and the kernel classifiers based on LTD, namely the KRR, the KPLS, the SVM, and the KDA. These classifiers must identify the three classes of biomass from the Biomass Texture data set.

Table 4.13 presents accuracy rates of the proposed classifiers using three different setup procedures. The first setup is to use 20 random samples per class for training and the rest of 70 samples for testing. The second setup is to use 30

random samples per class for training and 60 samples for testing. The last setup is to use 40 random samples per class for training and 50 samples for testing. The accuracy rates are averaged over 50 runs for each method. As expected, the accuracy of each method improves when more training samples are used. For example, the accuracy of the baseline method grows by 6.83% from 20 training samples to 40 training samples. However, the classifiers based on LTD are more stable, since the accuracy of each classifier grows only by roughly $3 - 4\%$ from 20 training samples to 40 samples. The learning methods based on LTD show a significant improvement in accuracy over the baseline. The best classifier based on LTD is KPLS. In all the test cases, the KPLS based on LTD has an accuracy of at least 10% better than the accuracy of the baseline 1-NN. Overall, the kernel classifiers achieve roughly similar accuracy levels. The empirical results show again that LTD is a powerful dissimilarity measure for texture classification.

Table 4.13: Accuracy rates on Biomass Texture data set using 20, 30 and 40 random samples per class for training and 70, 60 and 50 for testing, respectively.

Method	20/70 Accuracy	30/60 Accuracy	40/50 Accuracy
baseline 1-NN	80.35%	84.72%	87.18%
1-NN + LTD	88.09%	90.20%	91.28%
KRR + LTD	93.72%	96.40%	97.64%
SVM + LTD	93.98%	96.58%	97.72%
KPLS + LTD	**94.48**%	**96.90**%	**97.97**%
KDA + LTD	94.08%	96.40%	97.67%

In this experiment, LTD was computed on patches of 64×64 pixels, using a similarity threshold of 0.02 and a maximum offset of 256 pixels. Patches were extracted on a dense grid with a gap of 64 pixels. Again, feature weights were adjusted to increase the importance of Gabor features and fractal dimension by a factor of two, and to decrease the importance of the mean and the standard deviation by a factor of two. The parameter σ of the LTD kernel was chosen to be 10^{-3}. All the parameters were chosen by cross-validation on a subset of the Biomass Texture data set.

4.6 Discussion and Future Work

In this chapter, a novel dissimilarity measure for images, which is based on patches was presented. Several methods of speeding it up were also discussed, such as, using a hash table to store already computed patch distances, and skipping the comparison step of some overlapping patches.

Empirical results showed that LPD can be used for real-time image classification, especially when local learning methods are preferred instead of standard machine learning algorithms. Local learning methods based on LPD were proposed and tested on the popular MNIST data set. The experiments show that local learning algorithms perform very well in terms of accuracy and time. The error rate achieved by the k-NN based on LPD with filtering approach is 1.01% on the MNIST data set, which makes it one of the top 4 k-NN models that report results on this data set.

There are other ways of avoiding the problem of high computational time that are not studied in this thesis. For example, another local learning method to solve this problem is to rescale images to a smaller size and compute LPD on those images. For the k-NN with filtering approach, the nearest K neighbors can be filtered using the smaller images, and then, the nearest k neighbors are selected from those remaining K, using the original images.

In future work, an even faster version of LPD based on image descriptors can be proposed. Instead of comparing the similarity between many patches, LPD can compare the similarity of a few SIFT descriptors, for example. This approach would bring a major improvement in terms of speed. Until further investigation, it remains uncertain if such an approach can have similar or more accurate results than the current formulation of LPD. A hint could be that LPD somehow measures the difference of spatial information between images. Can this difference still be measured using fewer image descriptors?

A step towards replacing raw patches with image descriptors or image features was already taken through the development of LTD. Instead of comparing patches, LTD compares textons, which are represented as a set of texture-specific features extracted from images. Texture experiments presented in this chapter showed that LTD is a robust dissimilarity measure, achieving state of the art

accuracy levels in several texture classification tasks. In future work, the LTD measure can further be improved by adding more features to the texton feature set, or by changing the features completely.

Chapter 5

Object Recognition with the Bag of Visual Words Model

The classical problem in computer vision is that of determining whether or not the image data contains some specific object, feature, or activity. Particular formulations of this problem are image classification, object recognition, object detection. Computer vision researchers have recently developed sophisticated methods for such image related tasks. Among the state of the art models are discriminative classifiers using the *bag of words* (BOW) representation [Sivic et al., 2005; Zhang et al., 2007] and spatial pyramid matching [Lazebnik et al., 2006], generative models [Fei-Fei et al., 2007] or part-based models [Lazebnik et al., 2005a]. The BOW model, which represents an image as a histogram of local features, has demonstrated impressive levels of performance for image categorization [Zhang et al., 2007], image retrieval [Philbin et al., 2007], or related tasks.

This chapter is focused on improving the BOW model in several ways. Usually, kernel methods are used to compare image histograms. Popular choices, besides the linear kernel, are the intersection, Hellinger's, χ^2 and Jensen-Shannon (JS) kernels. There is no reason to limit the choice of kernels to these options, when other kernels are available. The final goal, that is to improve the results for image related tasks, can be achieved by trying different kernels that could possibly work better. In this chapter, a kernel for histograms of visual words that was introduced in [Ionescu & Popescu, 2013b], namely the PQ kernel, is presented. The PQ

kernel is inspired from a class of similarity measures for ordinal variables, more precisely Goodman and Kruskal's gamma and Kendall's tau. The idea is to treat the visual words histograms as ordinal data, in which data is ordered but cannot be assumed to have equal distance between values. In this case, a histogram will be considered as a rank of visual words according to their frequencies in that histogram. Usage of the ranking of visual words instead of the actual values of the frequencies may seem as a loss of information, but the process of ranking can actually make PQ more robust, acting as a filter and eliminating the noise contained in the values of the frequencies. This work proves that PQ is a kernel and it also shows how to build its feature map.

Image categorization experiments are conducted in order to assess the performance of different kernels, including PQ, on two benchmark data sets of images, more precisely, the Pascal VOC data set and the Birds data set. The idea behind the evaluation is to use the same framework and variate only the feature maps computed with different kernels. The experiments show that the PQ kernel has the best mean average precision on both data sets.

In this chapter, an improved variant of the BOW model is also proposed for classifying human facial expression from low resolution images. The proposed model was also presented in [Ionescu et al., 2013] as an approach to the Facial Expression Recognition (FER) Challenge of the ICML 2013 Workshop in Challenges in Representation Learning (WREPL). The BOW model is a rather general approach for image categorization, because it does not use any particular characteristics of the image. More precisely, this approach treats images representing faces, objects, or textures in the same manner. The method developed for the FER Challenge stems from this generic approach. The model had to be adapted to the data set provided by the WREPL organizers. First, histograms of visual words are replaced with normalized presence vectors, to eliminate noise introduced by word frequencies. For facial expression recognition, the presence of a visual word is more important than its frequency. Second, local multiple kernel learning was used to predict class labels of test images, in order to reduce both the image variation and the labeling noise in the resulting training sets.

Preliminary experiments were performed to validate the BOW approach. Empirical results shown that presence vectors improve accuracy by roughly 1%, while

local learning improves performance by almost $2-3\%$. Several kernel methods were also evaluated in the experiments. The SVM classifier performs better than the KDA and the KRR. Experiments show that spatial information also helps to improve recognition performance by almost $2-3\%$. Presence vectors that record different spatial information are combined to improve accuracy even further. The improved BOW method was fairly successful, it ranked fourth in the FER Challenge, with an accuracy of 67.484% on the final (private) test, as the work of [Goodfellow et al., 2013] also reports.

The chapter is organized as follows. Section 5.1 presents the classical BOW framework used for image retrieval, image categorization and related tasks. The PQ kernel for histograms of visual words is discussed in Section 5.2. Object recognition experiments conducted on two benchmark data sets are presented in Section 5.3. Section 5.4 presents the BOW learning model adapted to facial expression recognition. The local learning approach is presented in Section 5.5. Experiments conducted on the Facial Expression Recognition Challenge data set are presented in section 5.6. Finally, a discussion about future developments is given in Section 5.7.

5.1 Bag of Visual Words Model

In computer vision, the BOW model can be applied to image classification and related tasks, by treating image descriptors as words. A bag of visual words is a sparse vector of occurrence counts of a vocabulary of local image features. This representation can also be described as a histogram of visual words. The vocabulary is usually obtained by vector quantizing image features into visual words.

The learning model (framework) has two different stages, one for training and one for testing. Each stage is divided into two major steps. The first step in both stages is for feature detection and representation. The second step is to train a kernel method (in the training stage) in order to predict the class label of new images (in the testing stage). The entire process, that involves both training and testing stages, is summarized in Figure 5.1.

The feature detection and representation step in the training stage works as

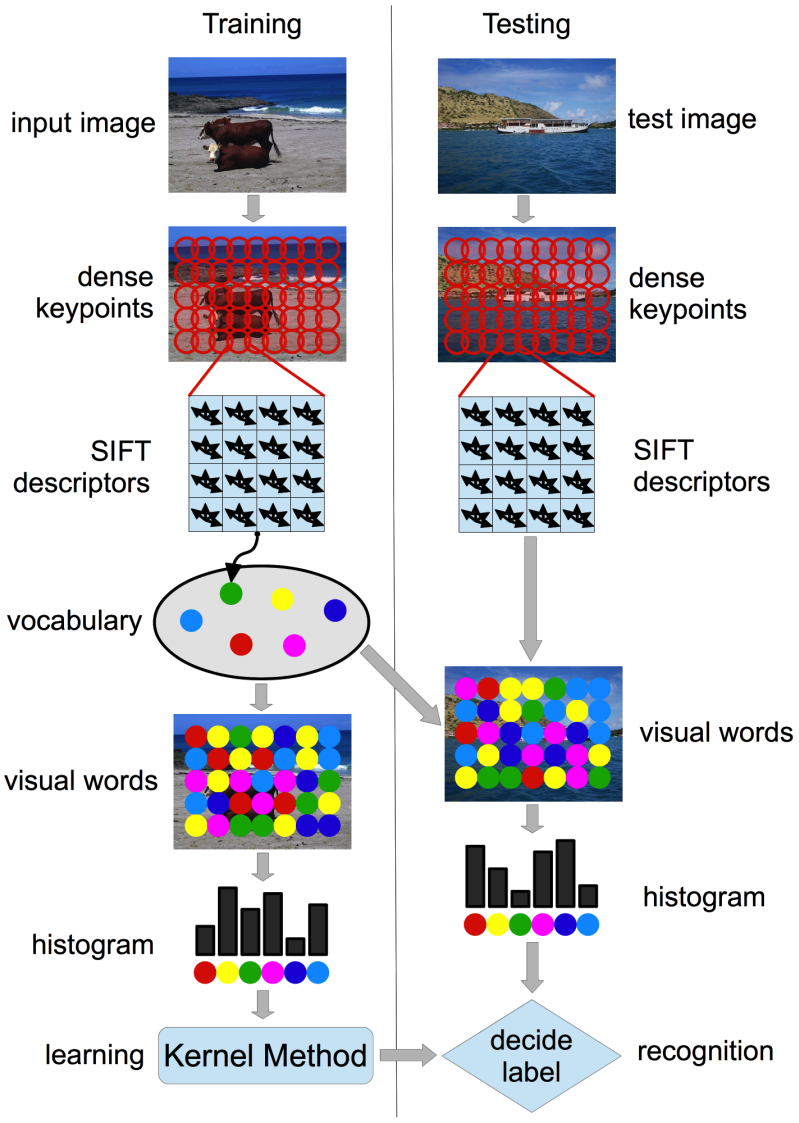

Figure 5.1: The BOW learning model for object class recognition. The feature vector consists of SIFT features computed on a regular grid across the image (dense SIFT) and vector quantized into visual words. The frequency of each visual word is then recorded in a histogram. The histograms enter the training stage. Learning is done by a kernel method.

follows. Features are detected using a regular grid across the input image. At each interest point, a SIFT feature [Lowe, 1999] is computed. This approach is known as dense SIFT [Bosch et al., 2007; Dalal & Triggs, 2005]. Next, SIFT descriptors are vector quantized into visual words and a vocabulary (or codebook) of visual words is obtained. The vector quantization process is done by k-means clustering [Leung & Malik, 2001], and visual words are stored in a randomized forest of k-d trees [Philbin et al., 2007] to reduce search cost. The frequency of each visual word is then recorded in a histogram which represents the final feature vector for the image. The histograms of visual words enter the training step. A kernel method is used for training. Several kernels can be used, such as the linear kernel, the intersection kernel, the Hellinger's kernel, the χ^2 kernel or the Jensen-Shannon kernel. In this chapter, a novel approach is proposed, that of using the PQ kernel described in Section 5.2.

Feature detection and representation is similar during the testing stage. The only difference is that of using the same vocabulary that was already obtained in the training stage by vector quantization. The histogram of visual words that represents the test image is compared with the histograms learned in the training stage. The system can return either a label (or a score) for the test image or a ranked list of images similar to the test image, depending on the application. For image categorization a label (or a score) is enough, while for image retrieval a ranked list of images is more appropriate.

As expected for an image retrieval system, the training stage can be done offline. For this reason, the time that is necessary for vector quantization and learning is not of great importance. What matters most is to return the result for a new (test) image as quick as possible.

Performance level of the described model depends on the number of training images, but also on the number of visual words. The number of visual words must be set a priori. The accuracy gets better as the number of visual words is greater.

An interesting remark is that the described model ignores spatial relationships between image features. A good way to improve performance is to include spatial information [Lazebnik et al., 2006]. This can be done by dividing the image into spatial bins. The frequency of each visual word is then recorded in a histogram

for each bin. The final feature vector for the image is a concatenation of these histograms. The first aim of this work is to improve the performance of the learning model by trying a different kernel method, namely the PQ kernel. Therefore, other methods of improving the performance level are disregarded, since they are beyond the purpose of this goal. However, one should be aware of all the possibilities of improving the described model for a real application, where the level of performance is of great importance. For example, spatial information is used for the BOW model for facial expression recognition proposed in Section 5.4.

5.2 PQ Kernel for Visual Words Histograms

All common kernels used in computer vision treat histograms of visual words either as finite probability distributions, for example, the Jensen-Shannon kernel, either as random variables whose values are the frequencies of different visual words in the respective images, for example, the Hellinger's kernel (Bhattacharyya's coefficient) and the χ^2 kernel. Even the linear kernel can be seen as the Pearson's correlation coefficient if the two histograms are standardized.

But the histograms of visual words can also be treated as ordinal data, in which data is ordered but cannot be assumed to have equal distance between values. In this case, the values of histograms will be the ranks of visual words according to their frequencies in the image, rather than of the actual values of these frequencies.

An entire set of correlation statistics for ordinal data are based on the number of concordant and discordant pairs among two variables. The number of concordant pairs among two variables (or histograms) $X, Y \in \mathbb{R}^n$ is:

$$P = |\{(i,j) \ : \ 1 \leq i < j \leq n, \, (x_i - x_j)(y_i - y_j) > 0\}|.$$

In the same manner, the number of discordant pairs is:

$$Q = |\{(i,j) \ : \ 1 \leq i < j \leq n, \, (x_i - x_j)(y_i - y_j) < 0\}|.$$

Goodman and Kruskal's gamma [Upton & Cook, 2004] is defined as:

$$\gamma = \frac{P - Q}{P + Q}.$$

Kendall developed several slightly different types of ordinal correlation as alternatives to gamma. *Kendall's tau-a* [Upton & Cook, 2004] is based on the number of concordant versus discordant pairs, divided by a measure based on the total number of pairs (n is the sample size):

$$\tau_a = \frac{P - Q}{\frac{n(n-1)}{2}}.$$

Kendall's tau-b [Upton & Cook, 2004] is a similar measure of association based on concordant and discordant pairs, adjusted for the number of ties in ranks. It is calculated as $(P - Q)$ divided by the geometric mean of the number of pairs not tied on X and the number of pairs not tied on Y, denoted by X_0 and Y_0, respectively:

$$\tau_b = \frac{P - Q}{\sqrt{(P + Q + X_0)(P + Q + Y_0)}}.$$

All the above three correlation statistics are very related. If n is fixed and X and Y have no ties, then P, X_0 and Y_0 are completely determined by n and Q. Actually, all are based on the difference between P and Q, normalized differently.

The PQ kernel between two histograms X and Y is defined as:

$$k_{PQ}(X, Y) = 2(P - Q).$$

Theorem 2 *The function denoted by k_{PQ} is a kernel function.*

Proof: To prove that k_{PQ} is indeed a kernel, the explicit feature map induced by k_{PQ} is provided next.

Let $X, Y \in \mathbb{R}^n$ be two histograms of visual words. Let Ψ be defined as follows:

$$\Psi : \mathbb{R}^n \to \boldsymbol{M}_{n,n} \quad \Psi(X) = (\Psi(X)_{i,j})_{1 \leq i \leq n, 1 \leq j \leq n},$$

with

$$\Psi(X)_{i,j} = \begin{cases} 1 & \text{if } x_i > x_j \\ -1 & \text{if } x_i < x_j \\ 0 & \text{if } x_i = x_j \end{cases}, \forall 1 \leq i, j \leq n.$$

Note that Ψ associates to each histogram a matrix that describes the order of its elements.

If matrices are treated as vectors, then the following equality is true:

$$k_{PQ}(X, Y) = 2(P - Q) = \langle \Psi(X), \Psi(Y) \rangle ,$$

where $\langle \cdot, \cdot \rangle$ denotes the scalar product. This proves that k_{PQ} is a kernel and provides the explicit feature map induced by k_{PQ}. □

Another approach inspired from rank correlation measures is the WTA hash proposed in [Yagnik et al., 2011]. For $K = 2$, the WTA hash is closely related to the PQ kernel. However, there are two important differences. The first one is that WTA hash works with a random selection of pairs from the feature set. The second one is that, unlike PQ kernel, the WTA hash ignores equal pairs. In terms of feature representation, the PQ kernel represents a histogram with a feature vector containing $\{-1, 0, 1\}$ (0 for equal pairs), while the WTA hash with $K = 2$ uses only $\{1, 0\}$. In the experiments, one can observe that these differences have direct consequences to the performance level, creating an even greater gap between the two methods.

According to the authors of [Vedaldi & Zisserman, 2010], the feature vectors of γ-homogeneous kernels should be L_γ-normalized. Being linear in the feature space, PQ is a 2-homogeneous kernel and the feature vectors should be L_2-normalized. Therefore, in the experiments, the PQ kernel is based on the L_2-norm. An important advantage of PQ being linear is that it can be used with linear SVM classifiers, such as the PEGASOS algorithm [Shalev-Shwartz et al., 2007], that are much faster to learn and evaluate than the original non-linear SVM.

Treating visual words frequencies as ordinal variables means that in the calculation of the distance (or similarity) measure, the ranks of visual words according

to their frequencies in the image will be used, rather than the actual values of these frequencies. Usage of the ranking of visual words in the calculation of the distance (or similarity) measure, instead of the actual values of the frequencies, may seem as a loss of information, but the process of ranking can actually make the measure more robust, acting as a filter and eliminating the *noise* contained in the values of the frequencies. For example, the fact that a specific visual word has the rank 2 (is the second most frequent feature) in one image, and the rank 4 (is the fourth most frequent feature) in another image can be more relevant than the fact that the respective feature appears 34 times in the first image, and only 29 times in the second.

It is important to note that for big vocabularies (with more than 1000 words), the kernel trick should be employed to obtain the kernel representation of PQ instead of computing its feature map, since there is a quadratic dependence between the feature map and the number of visual words.

5.3 Object Recognition Experiments

Object recognition experiments presented in this section compare the PQ kernel with state of the art kernels on two benchmark data sets. First, a brief description of the data sets is given. Details about the implementation of the learning model and the evaluation procedure are given next. Finally, the results for the two experiments are separately discussed.

5.3.1 Data Sets Description

The Pascal Visual Object Classes (VOC) challenge [Everingham et al., 2010] is a benchmark in visual object category recognition and detection, providing the vision and machine learning communities with a standard data set of images and annotation, and standard evaluation procedures. In the experiments of this work, the Pascal VOC 2007 data set is used. The reason for this choice is that this is the latest data set for which testing labels are available for download, and the experiments can be done offline. There are roughly 10 thousand images in this data set, that are divided into 20 classes. As Figure 5.2 shows, some

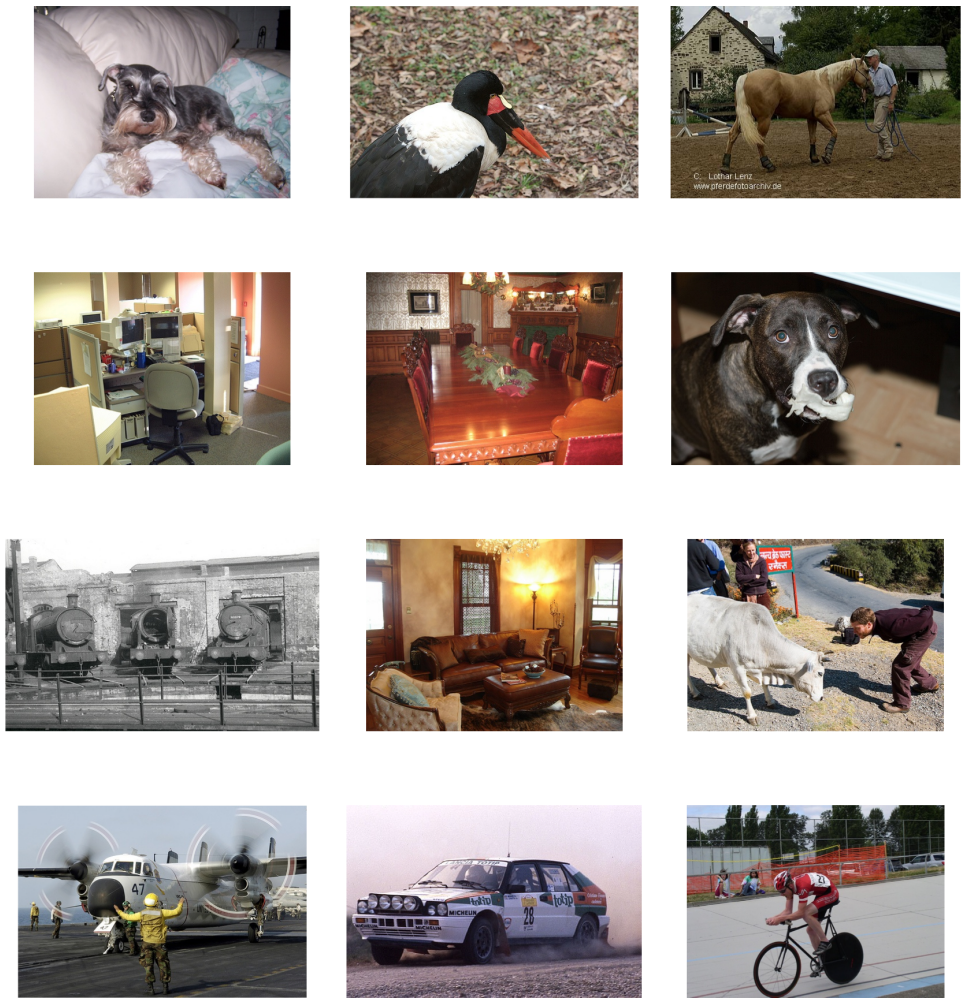

Figure 5.2: A random sample of 12 images from the Pascal VOC data set. Some of the images contain objects of more than one class. For example, the image at the top left shows a dog sitting on a couch, and the image at the top right shows a person and a horse. Dog, couch, person and horse are among the 20 classes of this data set.

images may contain objects from several classes. Thus, the class labels are not mutually exclusive. For each class the data set provides a training set, a validation set and a test set. The training and validation sets have roughly 2500 images each, while the test set has about 5000 images. This data set is available at http://pascallin.ecs.soton.ac.uk/challenges/VOC/voc2007/.

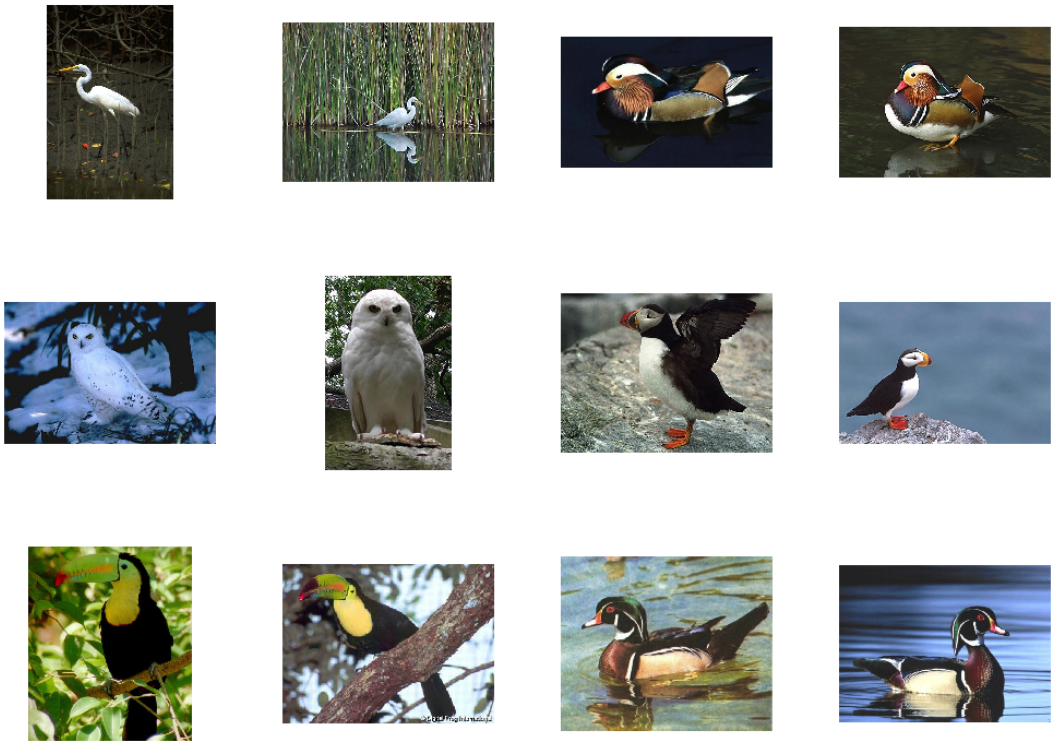

Figure 5.3: A random sample of 12 images from the Birds data set. There are two images per class. Images from the same class sit next to each other in this figure.

The second data set was collected from the Web by the authors of [Lazebnik et al., 2005a] and consists of 100 images each of 6 different classes of birds: egrets, mandarin ducks, snowy owls, puffins, toucans, and wood ducks. The training set consists of 300 images and the test set consists of another 300 images. For each class, the data set contains 50 positive train images and 50 positive test images. This data set of 600 images is used in order to assess kernels behavior when less training data is available. Figure 5.3 shows two images from each class of the Birds data set. The data set is available at `http://www-cvr.ai.uiuc.edu/ponce_grp/data/`.

5.3.2 Implementation and Evaluation Procedure

The framework described in Section 5.1 is used for object class recognition. Details about the implementation of the model are given next. In the feature detection and representation step, a variant of dense SIFT descriptors extracted at multiple scales is used [Bosch et al., 2007]. The number of visual words used in the experiments is 500. For better accuracy, up to $10,000$ or more visual words can be used.

Several state of the art kernel methods are compared with the PQ kernel in both experiments. The baseline method is the linear kernel, for which the histograms are L_2-normalized. One of the state of the art methods is based on the Hellinger's kernel. Two variants with different norms of this kernel are used. The first one is based on L_1-normalized feature vectors, and the second one is based on L_2-normalized feature vectors. Another state of the art kernel is Jensen-Shannon, which is L_1-normalized. Finally, these kernels are to be compared with the PQ kernel described in this chapter. The PQ kernel is L_2-normalized. For all kernel methods, feature maps are computed from the visual words histograms. The training is always done using a linear SVM on the computed feature maps. The linear SVM is based on an implementation of the PEGASOS algorithm described in [Shalev-Shwartz et al., 2007]. The feature map of the JS kernel cannot be computed directly. In order to use the same learning setting, its feature map has to be approximated using the method proposed in [Vedaldi & Zisserman, 2010]. To approximate the JS kernel, $10,500$ features are used. The idea behind the evaluation is to use the same framework and variate only the feature maps computed with different kernels, since the final goal of the experiments is to evaluate the difference between these kernels, in terms of performance. The implementation of both the feature detection and representation step, and the learning step, is mostly based on the VLFeat library [Vedaldi & Fulkerson, 2008].

The evaluation procedure for both experiments follows the Pascal VOC benchmark. The qualitative performance of the learning model is measured by using the classifier score to rank all the test images. Next, the retrieval performance is measured by computing a precision-recall curve. Note that the precision is given by the proportion of returned images that are positive, while the recall is given

by the proportion of positive images that are returned. In order to represent the retrieval performance by a single number (rather than a curve), the mean average precision (mAP) is often computed. The average precision as defined by TREC is used in the experiments. This is the average of the precision observed each time a new positive sample is recalled.

5.3.3 Pascal VOC Experiment

The first experiment is on the Pascal VOC 2007 data set. The validation set was used to validate the parameter C of the linear SVM algorithm. For the linear kernel and Hellinger's kernels, the values of parameter C range exponentially from 0.1 to 1000. For the JS and PQ kernels, the values of parameter C can be either 0.5 or 1.

Table 5.1 presents the mean AP of the linear kernel, the Hellinger's kernel, the JS kernel, the WTA hash (with $K = 2$ and $10,000$ random pairs) and the PQ kernel, on the Pascal VOC data set. Looking at the results obtained by the JS kernel on one hand, and the PQ kernel on the other, one can observe that these methods are somehow complementary in terms of performance. This gives the idea of combing the two kernels to possibly obtain better results. Indeed, in this experiment another kernel based on the sum of JS and PQ kernels is presented. In order to obtain the feature map of this kernel combination, the feature maps of JS and PQ kernels are simply concatenated.

The accuracy of the state of the art kernels is well above the accuracy of the baseline linear SVM. In terms of AP, the state of the art kernels are about 10% better than the baseline method. The PQ kernel improves the accuracy of the learning model, when compared to the state of the art methods. The mAP of the PQ kernel is 3.3% above the mAP of the Hellinger's kernels, 1.4% above the mAP of the WTA hash, and 1.2% above the mAP of the JS kernel. The combination of JS and PQ kernels improves the performance even further. The mAP of the JS+PQ kernel is 3.6% above the mAP of the Hellinger's kernels, 1.7% above the mAP of the WTA hash, and 1.5% above the mean AP of the JS kernel. PQ kernel improves results over WTA hash by 1.4%, showing that the two methods are distinct.

Table 5.1: Mean AP on Pascal VOC 2007 data set for machine learning methods based on visual words histograms with different kernels. The best AP on each class is highlighted with bold.

Class	Lin. L_2	Hel. L_1	Hel. L_2	WTA L_2	JS L_1	PQ L_2	JS+PQ
Airplane	0.395	0.555	0.558	0.534	0.564	0.526	**0.574**
Bicycle	0.189	0.339	0.337	0.398	0.367	**0.409**	0.386
Bird	0.178	0.248	0.247	0.274	0.284	0.281	**0.305**
Boat	0.334	0.540	0.551	0.476	0.549	0.505	**0.553**
Bottle	0.122	**0.143**	0.139	0.139	0.127	0.140	0.129
Bus	0.239	0.334	0.336	0.404	0.379	**0.419**	0.406
Car	0.518	0.599	0.602	0.659	0.644	**0.670**	0.659
Cat	0.281	0.349	0.351	0.382	0.378	**0.402**	0.393
Chair	0.308	0.399	0.399	0.398	**0.414**	0.405	**0.414**
Cow	0.117	0.174	0.172	**0.209**	0.169	**0.209**	0.198
Dining Table	0.205	0.238	0.227	0.237	0.242	0.253	**0.255**
Dog	0.212	0.271	0.266	0.263	0.293	0.287	**0.299**
Horse	0.484	0.518	0.530	0.601	0.595	0.609	**0.614**
Motorbike	0.213	0.398	0.389	0.427	0.413	**0.451**	0.450
Person	0.639	0.715	0.717	0.756	0.759	0.773	**0.774**
Potted Plant	0.099	**0.125**	0.110	0.110	0.112	0.111	0.115
Sheep	0.220	0.217	0.237	0.219	0.222	**0.259**	0.243
Sofa	0.184	0.304	0.320	0.310	0.325	0.322	**0.333**
Train	0.363	0.534	0.528	0.547	0.554	0.570	**0.574**
TV Monitor	0.196	0.309	0.295	0.345	0.336	**0.351**	0.342
Overall	0.275	0.365	0.365	0.384	0.386	0.398	**0.401**

If the best AP per class is considered, the PQ kernel and the JS+PQ kernel win most of the classes (18 out of 20). The results presented in Table 5.1 come to support this statement. The Hellinger's kernel based on the L_1-norm wins 2 classes, more precisely the *Bottle* and the *Potted Plant* classes. The L_1-normalized Hellinger's kernel seems to work best when classes are very difficult for all kernel methods. The best AP on the *Chair* class is shared by the JS kernel and the JS+PQ kernel, while the best AP on the *Cow* class is shared by the WTA hash and the PQ kernel. This is also the only class that the WTA hash is able to win. The PQ kernel has the best AP on 8 classes. The JS+PQ kernel wins 10 classes, also counting in the *Chair* class. Note that the linear kernel and the L_2-normalized Hellinger's kernel are not able to take any class.

The feature detection and representation phase, that builds a vocabulary of visual words and obtains histograms, takes a few hours on this data set. The time for the second phase of the learning framework, that includes computing feature maps, training and testing, depends on the number of features in the feature space for each kernel. The time for the second phase and the number of features for each kernel are reported in Table 5.2. The time was measured on a computer with Intel Core i7 2.3 GHz processor and 8 GB of RAM memory using a single Core. While the feature maps can be computed only once for the entire experiment along with the feature detection and representation stage, training and testing has to be repeated for each class. Despite the fact that the time for the PQ kernel ($14 - 15$ minutes) is higher than the time for other kernels ($2 - 15$ seconds), it does not add an overhead to the overall time of the learning framework, since the overall time is about $4 - 6$ hours.

Table 5.2: The time for the second stage of the learning model and the number of features for each kernel. The time is measured in seconds.

Kernel	Time	Features
Linear L_2	$1 - 2$	500
Hellinger's L_1	$2 - 3$	500
Hellinger's L_2	$2 - 3$	500
WTA L_2	$15 - 16$	$10,000$
JS L_1	$15 - 16$	$10,500$
PQ L_2	$830 - 860$	$250,000$
JS L_1 + PQ L_2	$850 - 880$	$260,500$

The PQ kernel and the JS+PQ kernel are constantly better than the other methods. In conclusion, the PQ kernel, used either alone or in combination with the JS kernel, has the best performance on this experiment.

5.3.4 Birds Experiment

The second experiment is on the Birds data set. Since there is no validation set this time, the parameter C of the linear SVM algorithm is cross-validated on the training set. Table 5.3 presents the mAP of the linear kernel, the Hellinger's kernel, the JS kernel, the WTA hash (with $K = 2$ and $10,000$ random pairs) and

the PQ kernel, on the Birds data set. A variant of the PQ kernel that ignores equal pairs (PQ iq), which is more similar to the WTA hash, is also added to the experiment to emphasize the difference between PQ kernel and WTA hash. This variant of PQ is also based on the L_2-norm.

Table 5.3: Mean AP on Birds data set for machine learning methods based on visual words histograms with different methods. The best AP on each class is highlighted with bold.

Class	Lin. L_2	Hel. L_1	Hel. L_2	JS L_1	WTA L_2	PQ iq	PQ L_2
Egret	0.552	**0.760**	0.747	0.416	0.735	0.738	0.753
Mandarin Duck	0.446	0.585	0.607	0.375	0.784	0.791	**0.835**
Owl	0.815	0.895	0.887	0.490	0.879	0.889	**0.915**
Puffin	0.427	0.696	0.730	0.369	0.708	0.703	**0.764**
Toucan	0.572	0.715	0.747	0.558	0.776	0.787	**0.845**
Wood Duck	0.608	0.795	0.816	0.361	0.767	0.769	**0.849**
Overall	0.570	0.741	0.756	0.428	0.775	0.779	**0.827**

The performance of the Hellinger's kernels is above the baseline linear SVM, as in the previous experiment. Both Hellinger's kernels are about 18% better than the baseline method. Unlike the previous experiment, the JS kernel has the worst accuracy on this data set, when compared to the rest of the methods. The mAP of the JS kernel is 14.2% below the baseline AP. The bad performance of the JS kernel on this data set can be explained by the fact that it is based on an informational measure that uses an estimation of the distribution of the data. The number of training samples may not be enough for a good estimation.

The results of the PQ kernel on this experiment are consistent with the previous experiment. The PQ kernel improves the performance of the learning model, when compared to the state of the art kernels. The mean AP of the PQ kernel is 8.6% above the mAP of the L_1-normalized Hellinger's kernel, 7.2% above the mAP of the L_2-normalized Hellinger's kernel, and 5.2% above the mAP of the WTA hash. Table 5.3 also shows that by ignoring equal pairs the mAP of the PQ kernel drops by 4.8%. By taking into account equal pairs and by considering the entire feature set, PQ has a significant improvement in terms of accuracy over WTA hash. There is no question that the two methods are distinct.

If the best AP per class is considered, the PQ kernel wins most of the classes, again. The Hellinger's kernel based on the L_1-norm wins the *Egret* class. The PQ kernel wins the rest 5 classes. Note that the linear kernel, the L_2-normalized Hellinger's kernel and the JS kernel are not able to win any class. The PQ kernel is constantly better than the other methods. In conclusion, the PQ kernel has the best performance on the Birds data set experiment.

It is worth mentioning that, for this experiment, there is no considerable difference in terms of speed between kernel methods, since the time to obtain results for each kernel is almost instant. Therefore, times are not reported for this experiment.

5.4 Bag of Visual Words for Facial Expression Recognition

In this section, several ways of improving the BOW model for facial expression recognition are discussed. The improved BOW model is evaluated in the FER Challenge of ICML 2013 WREPL Workshop. The experiments and results on the data set of the FER Challenge are presented in Section 5.6.

The bag of visual words model builds a vocabulary by vector quantizing local image features into visual words. For a particular image, the frequency of each visual word contained in the image is usually recorded in a histogram of visual words. For facial expression recognition, it seems that the presence of a visual word is more important than its frequency. For example, it should be enough to detect the presence of a cheek dimple to recognize a smiling face. Thus, instead of recording occurrence counts in a histogram, it is enough to record visual words presence in a presence vector. An important remark is that the presence vector should be normalized not to favor faces with more visual words.

The BOW model proposed for facial expression recognition has two stages, one for training and one for testing. Each stage is divided into two major steps. The first step in both stages is for feature detection and representation. The second step is to train a kernel method (in the training stage) in order to predict the class label of a new image (in the testing stage). For each test image, a

local classification problem is constructed by selecting only the nearest neighbors from the kernel feature space. The local learning part of the framework is further described in Section 5.5. The entire process, that involves both training and testing stages, is summarized in Figure 5.4. It is interesting to notice the different steps from the model presented in Figure 5.1.

The feature detection and representation step in the training stage is a slightly modified version of the approach described in Section 5.1, which uses k-means clustering [Leung & Malik, 2001] to quantize dense SIFT descriptors [Bosch et al., 2007; Dalal & Triggs, 2005] into visual words that are stored in a randomized forest of k-d trees [Philbin et al., 2007], to reduce search cost. The novelty consists of a semi-supervised approach, in the sense that it can leverage the SIFT descriptors from the unlabeled test set by including them in the k-means clustering process as well, together with those from the training data set. For increased test sets this has led to a better representation of the faces manifold and to increased classification performance. The presence of each visual word is recorded in a presence vector which represents the final feature vector for the image. Normalized presence vectors of visual words can now enter the learning step. Figure 5.5 presents a sample of 30 SIFT descriptors extracted from two images of the FER data set.

Feature detection and representation is similar during the testing stage. The presence vector of visual words that represents the test image is compared with the training presence vectors, through the implicit distance defined by the kernel, to select a number of nearest neighbors. For a certain test image, only its nearest neighbors actually enter the learning step. In other words, a local recognition problem is built for each test image. A kernel method is employed to learn the local recognition problem and finally predict a class label for the test image. Classifiers such as the SVM, the KDA or the KRR are good choices to perform the local learning task.

The model described so far ignores spatial relationships between image features. Despite ignoring spatial information, visual words showed a high discriminatory power and have been used for region or image level classification [Csurka et al., 2004; Fei-Fei & Perona, 2005; Zhang et al., 2007]. The performance improves when spatial information is included. This can be achieved by dividing

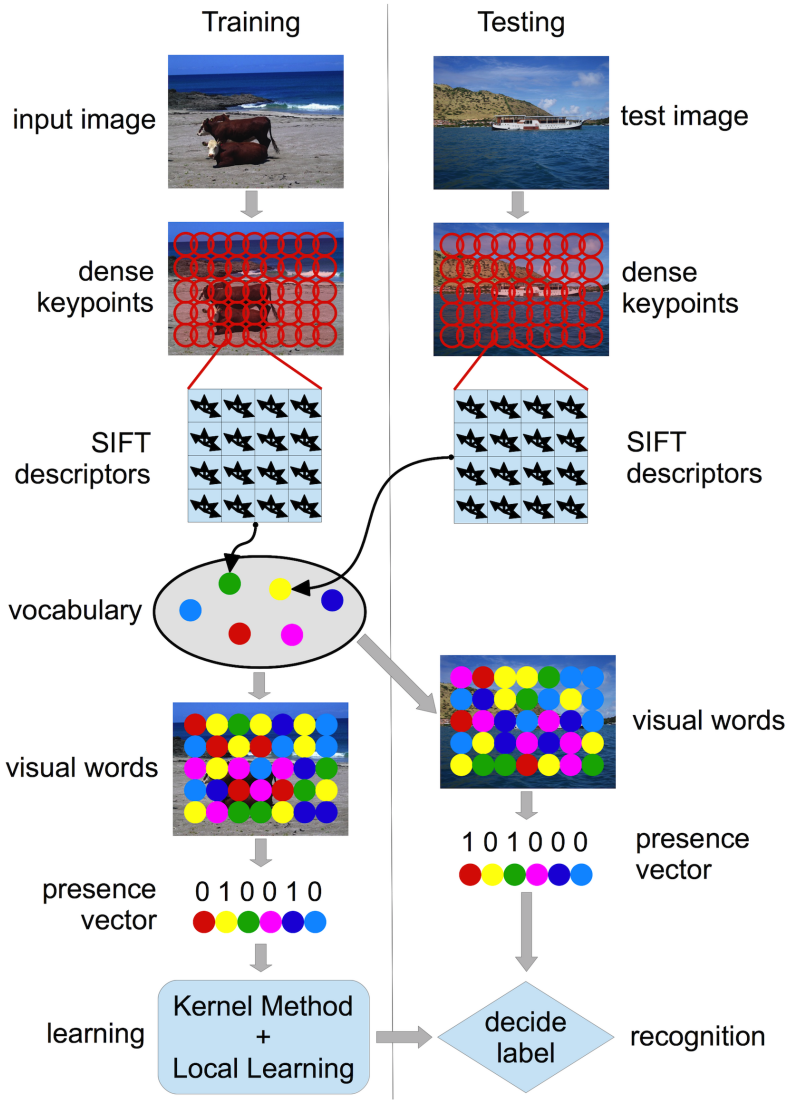

Figure 5.4: The BOW learning model for facial expression recognition. The feature vector consists of SIFT features computed on a regular grid across the image (dense SIFT) and vector quantized into visual words. The presence of each visual word is then recorded in a presence vector. Normalized presence vectors enter the training stage. Learning is done by a local kernel method.

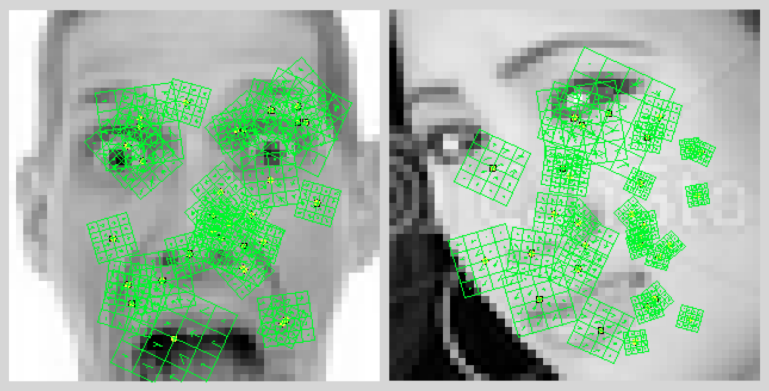

Figure 5.5: An example of SIFT features extracted from two images representing distinct emotions: fear (left) and disgust (right).

the image into spatial bins. The presence of each visual word is then recorded in a presence vector for each bin. The final feature vector for the image is a concatenation of these presence vectors. A more robust approach is to use a spatial pyramid, as the work of [Lazebnik et al., 2006] suggests. The spatial pyramid is usually obtained by dividing the image into increasingly fine sub-regions (bins) and computing histograms of visual words found inside each bin. It is worth mentioning that a similar approach for texture classification was recently proposed in [Popescu et al., 2013a]. The spatial pyramid representation presented in [Popescu et al., 2013a] is designed to capture the fractal structure in texture images. It can improve the accuracy by as much as 5% over the standard feature representation, showing that the pyramid structure is indeed useful for texture classification.

The framework proposed in this section makes use of the spatial information by computing a spatial pyramid from presence vectors. It is reasonable to think that dividing an image representing a face into bins is a good choice, since most features, such as the contraction of the muscles at the corner of the eyes, are only visible in a certain region of the face. In other words, one does not expect to find raised eyebrows on the cheek, or cheek dimples on the forehead.

5.5 Local Learning

Local learning methods attempt to locally adjust the performance of the training system to the properties of the training set in each area of the input space. A simple local learning algorithm works as follows: for each testing example, select a few training examples located in the vicinity of the testing example, train a classifier with only these few examples and apply the resulting classifier to the testing example.

The learning step of the BOW framework adapted to facial expression recognition is based on a local learning algorithm that uses the presence kernel to select nearest neighbors in the vicinity of a test image. Local learning has a few advantages over standard learning methods. First, it divides a hard classification problem into more simple sub-problems. Second, it reduces the variety of images in the training set, by selecting images that are most similar to the test one. Third, it improves accuracy for data sets affected by labeling noise. Considering all these advantages, a local learning algorithm is indeed suitable for the FER data set.

Figure 5.6 shows that the nearest neighbors selected from the vicinity of a particular test image are visually more relevant than a random selection of training images. It also gives a hint that local learning should perform better than a standard learning formulation.

5.6 Facial Expression Recognition Experiments

5.6.1 Data Set Description

The data set of the FER Challenge consists of 48×48 pixel gray-scale images of faces representing 7 categories of facial expressions: anger, disgust, fear, happiness, sadness, surprise, and neutral. There are 28709 examples for training, 3589 examples for testing, and another 3589 examples for private testing. The task is to categorize each face based on the emotion shown in the facial expression in to one of 7 categories. Images were collected from the web using a semi-automatic procedure. Therefore, the data set may contain images that do not represent

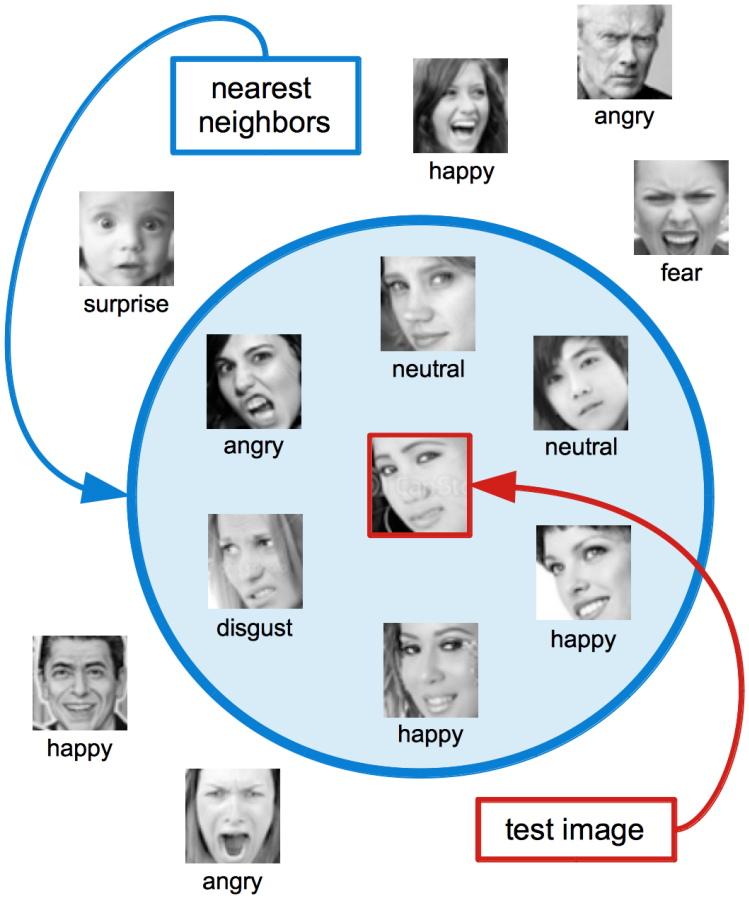

Figure 5.6: The six nearest neighbors selected with the presence kernel from the vicinity of the test image are visually more similar than the other six images randomly selected from the training set. Despite this fact, the nearest neighbors do not adequately indicate the test label. Thus, a learning method needs to be trained on the selected neighbors to accurately predict the label of the test image.

faces. Another issue is that the training data may also contain labeling noise, meaning that the labels of some faces do not indicate the right facial expression.

5.6.2 Implementation

The framework described in Section 5.4 is used for facial expression recognition. Details about the implementation of the model are given next. In the feature detection and representation step, a variant of dense SIFT descriptors extracted at multiple scales is used [Bosch et al., 2007]. The dense SIFT features were extracted using a grid step of 1 pixel at scales ranging from 2 to 8 pixels. These features are extracted from the entire FER data set. A random sample of $240,000$ features is selected to compute the vocabulary. The number of visual words used in the experiments ranges from $5,000$ to $20,000$. A slight improvement in accuracy can be observed when the vocabulary dimension grows. Both histograms of visual words and presence vectors were tested. Empirical results show that presence vectors are able to improve accuracy, by eliminating some of the noise encoded by the histogram representation.

Different spatial presence vectors were combined to obtain several spatial pyramid versions. Images were divided into 2×2 bins, 3×3 bins, and 4×4 bins to obtain spatial presence vectors. The basic presence vectors are also used in the computation of spatial pyramids.

The kernel trick is implied to obtain spatial pyramids. Kernel matrices are computed for each (spatial) presence vector representation. Then, kernel matrices are summed up to obtain the kernel matrix of a certain spatial pyramid. Some of the proposed models are based on a weighted sum of kernel matrices, with weights adjusted to match the accuracy level of each (spatial) presence vector. Summing up kernel matrices is equivalent to presence vector concatenation. But presence vectors are actually high-dimensional sparse vectors, and the concatenation of such vectors is not a viable solution in terms of space and time.

Several state of the art kernel methods are used to perform the local learning tasks, namely the SVM, the KDA and the KRR. Empirical results showed that the SVM performs slightly better than the KDA, and much better than the KRR. The number of nearest neighbors selected to enter the local learning phase for each

test image is 1000. However, an experiment is conducted to show the accuracy level as the number of nearest neighbors varies. The regularization parameter C of the SVM was set to 1000. This choice is motivated by the fact that the data set is separable since there is a small number of training examples (1000 neighbors), in a high-dimensional feature space. Thus, the best working SVM is a hard margin SVM that can be obtained by setting the C parameter of the SVM to a high value [Shawe-Taylor & Cristianini, 2004].

5.6.3 Parameter Tuning and Results

For parameter tuning and validation, the training set was randomly split in two thirds kept for training and one third for validation. Preliminary experiments using different models were performed on the validation set to assess the performance levels of the kernel methods. Obtained results point that the SVM is about $1-2\%$ better than the KRR, and about 0.5% better than KDA. They also indicate that presence vectors are $0.5-1\%$ better than histograms. In the experiments presented in Table 5.4 only results obtained with various SVM models based on presence vectors are included.

Several kernels based on different vocabularies and various ways of encoding spatial information were proposed. The model names of the form "8000 3×3" specify the size of the vocabulary, followed by the size of the grid used to partition the image into spatial bins. The kernel of "8000 SUM" is the mean of the kernels based on 8000 visual words computed on spatial bins ranging from 1×1 bins to 4×4 bins. In other words, the 8000 SUM model is based on spatial pyramids. It has performed on the validation set better than each of its terms. The kernel identified by "MIX3" is the mean of 17000 1×1, 14000 2×2, 11000 3×3, and 8000 4×4. Again, it has performed better than each of its terms. The kernel identified by "20K" is a variant of "MIX3" built on even larger vocabularies, as is the mean of 20000 1×1, 20000 2×2, 12000 3×3, and 8000 4×4. It did not perform better than MIX3, neither on the validation data set nor on the actual test set. The kernel identified as "MIX1" is the weighted mean of 7000 1×1, 7000 2×2, 7000 3×3, and 5000 4×4, with the weights 0.1, 0.2, 0.4, 0.3, respectively. Finally, the last proposed model is the kernel identified as "MIX2", which is the weighted

mean of 11000 1×1, 9000 2×2, 7000 3×3, and 5000 4×4, with the weights 0.2, 0.3, 0.3, 0.2, respectively. The vector quantization process of these models initially included the descriptors extracted from the 28709 examples for training and the 3589 examples for preliminary testing. Some of the models were re-built to add the 3589 examples from the private testing set in the vector quantization process.

In Table 5.4 one can observe that the performance of the global one-versus-all SVM is at least 2% lower than that obtained with the local learning based on one-versus-all SVM with the same parameters. Another interesting behavior that can be observed in this table is the effect on accuracy of dividing the image area into spatial bins: the accuracy increases as the image is divided into finer sub-regions. This table also shows the effect of the number of neighbors, another parameter that must be adjusted.

No model with more than 1500 neighbors was submitted to the FER Challenge, it may well be that using 3000 neighbors could have led to somewhat higher scores. The parameter tuning was limited both by the amount of RAM available in the machines (24 GB for the largest one) used to train the models, and by the speed of the CPUs (4-core Xeon E5540 at 2.53 GHz in the fastest one). Test cycles took therefore up to 9 hours. The best accuracy on the final test set is 67.484%. An interesting remark is that the proposed model has roughly achieved human-level performance on this data set.

5.7 Discussion and Further Work

This chapter discussed several improvements of the BOW model either for object recognition or for facial expression recognition. First, the work presented in this chapter showed that the results for image classification, image retrieval or related tasks, can be improved by using the PQ kernel. The PQ kernel comes from the idea of treating feature vectors of visual words as ordinal variables.

Object recognition experiments compared the PQ kernel with other state of the art kernels on two benchmark data sets. The PQ kernel, used either alone or in combination with the JS kernel, has the best accuracy on the Pascal VOC 2007 experiment. On the Birds experiment, the PQ kernel improved the perfor-

Table 5.4: Accuracy levels for several models obtained on the validation, test, and private test sets.

Model	Neighbors	Validation	Global SVM	Test	Private
8000 1×1	1000	59.07%			
8000 2×2	1000	62.22%			
8000 3×3	1000	62.27%			
8000 4×4	1000	62.93%			
8000 SUM	1000	63.27%		65.73%	66.73%
17000 1×1	1000	60.86%			
14000 2×2	1000	62.69%			
11000 3×3	1000	62.36%			
MIX1	1000	63.03%		65.89%	
MIX2	1000	63.74%		66.42%	
MIX3	1000	63.61%		66.65%	
Re-built Models					
MIX1	1000	62.91%	59.35%	66.59%	66.73%
MIX2	1000	63.99%	60.95%	67.01%	67.31%
MIX3	1000	64.30%	62.27%	67.32%	67.48%
MIX3	3000	64.23%	62.27%		
20K	500	63.59%	61.82%		
20K	1000	63.90%	61.82%		
20K	1500	64.10%	61.82%	66.53%	66.98%
20K	3000	64.45%	61.82%		
20K	5000	64.35%	61.82%		

mance again. The PQ kernel is constantly better than the other methods. The accuracy can be improved even further by increasing the number of visual words used for building the vocabulary. Because the feature map of the PQ kernel has a quadratic dependence of the size of the vocabulary, one should adjust the vocabulary size by taking into consideration the trade-off between accuracy and speed. Despite the fact that the kernel trick can be employed to use the PQ kernel with larger vocabularies, a greater importance should be given to the idea of selecting good visual words. A possible way of improving the results for the PQ kernel may be that of using a TF-IDF measure for visual words as in [Philbin et al., 2007]. Indeed, eliminating visual words that have a low TF-IDF score can lead to an approximation of the PQ kernel that works faster and possibly better.

Another way is to extract descriptors only from the interesting image regions. In the recent work of [Alexe et al., 2012], a measure that quantifies how likely it is for an image window to contain an object of any class is proposed. This measure is termed *objectness*. It is interesting to mention that objectness does not aim at identifying the type of object contained in the image, but rather the image region that potentially contains any kind of object. A vocabulary of visual words that is built only from the image regions with a high objectness score should improve the classification accuracy.

In future work, other methods inspired from ordinal measures can be investigated. For example, the most common correlation statistic for ordinal data, namely the Spearman rank-order coefficient [Upton & Cook, 2004], or its L_1 version, namely the Spearman footrule, are successfully used in text processing [Dinu & Popescu, 2009b]. It is perfectly reasonable to use them for image processing in the BOW model context, since the BOW model is also inspired from text processing. Methods to transform these measures into kernels would also have to be developed.

Other improvements of the bag of visual words were proposed to adapted it to the FER Challenge data set of faces. Histograms of visual words were replaced with normalized presence vectors, then local learning was used to predict class labels of test images. The proposed model also includes spatial information in the form of spatial pyramids computed from presence vectors. Experiments were performed to validate the proposed model. By reserving one third of the training data set as validation set, the method's parameters were tuned without overfitting, as can be seen in Table 5.4. Empirical results showed that the proposed model has an almost 5% improvement in accuracy over a classical BOW model. Also, using multiple kernel learning (with sum or weighted sum kernels) led to accuracy levels higher than that of the individual kernels involved. Finally, the proposed model ranked fourth in the FER Challenge, with an accuracy of 67.484% on the final test. A different approach to local learning, that of clustering train images to divide the learning task on each cluster separately, can be studied in future work.

Part II

Machine Learning in String Processing

Chapter 6

State of the Art

Researchers have developed a wide variety of methods for string data, that can be applied with success in different fields such as computational biology, natural language processing, information retrieval and so on. Such methods range from clustering techniques used to analyze the phylogenetic trees of different organisms, to kernel methods used to identify authorship or native language from text. This chapter gives an overview of the state of the art methods used in two major fields of study, namely computational biology and natural language processing.

Two intensively studied problems in computational biology are DNA sequencing and phylogenetic analysis. A state of the art of the methods used for sequencing and comparing DNA is given in Section 6.1.1. Phylogenetic analysis, one of the first problems in computational biology, is discussed in Section 6.1.2. Several methods that provide solutions to these computational biology problems are presented in Chapters 7 and 8, respectively.

Natural language processing (NLP) is a vast domain that studies machine translation, text summarization, document classification by topic, authorship identification, sentiment analysis, among others. An overview of the state of the art approaches in NLP is given in Section 6.2. Special consideration is given to an approach based on string kernels, that works at character level. The string kernel method has various applications that are discussed in Section 6.2.1. One of the recently studied problems in NLP is native language identification [Brooke & Hirst, 2012; Jarvis & Crossley, 2012; Tetreault et al., 2012]. A machine learning solution for native language identification based on string kernels is presented in

Chapter 9.

6.1 Computational Biology

6.1.1 Sequencing and Comparing DNA

In many important problems in computational biology a common task is to compare a new DNA sequence with sequences that are already well studied and annotated. DNA sequence comparison was ranked in the top of two lists with major open problems in bioinformatics [Koonin, 1999; Wooley, 1999] over a decade ago, but it is still receives the attention of researchers nowadays. Sequences that are similar would probably have the same function, or, if two sequences from different organisms are similar, there may be a common ancestor sequence [Liew et al., 2005]. Another important problem with practical motivations for biologists is related to the finding of motifs or common patterns in a set of given DNA sequences. A typical case where the last mentioned problem occurs is, for example, when one needs to design genetic drugs with structure similar to a set of existing sequences of RNA [Lanctot et al., 2003]. Other applications in computational biology which involve this task are (from a rich literature): PCR primer design [Gramm et al., 2002; Lanctot et al., 2003], genetic probe design [Lanctot et al., 2003], antisense drug design [Deng et al., 2003], finding unbiased consensus of a protein family [Ben-Dor et al., 1997], motif finding [Li et al., 2002; Wang & Dong, 2005] and many others.

The standard method used in computational biology for sequence comparison is by *sequence alignment*. Sequence alignment is a procedure of comparing DNA sequences, that aims at identifying regions of similarity that may be a consequence of functional, structural, or evolutionary relationships between the sequences. Algorithmically, the standard pairwise alignment method is based on dynamic programming [Smith & Waterman, 1981]. The method compares every pair of characters of the two sequences and generates an alignment and a score, which is dependent on the scoring scheme used, for example, a scoring matrix for the different base pair combinations, match and mismatch scores, or a scheme for insertion or deletion (gap) penalties. Although dynamic programming for

sequence alignment is mathematically optimal, in practice, it is far too slow for comparing a large number of bases, and too slow to be performed in a reasonable time.

Recently, many tools designed to align short reads have been proposed [Li & Homer, 2010]. The main efforts in the design of such tools are on improving speed and correctness. Fast tools are needed to keep the pace with data production, while the number of correctly placed reads is maximized. Usually, tools sacrifice correctness over speed, allowing only few mismatches between the reads and the reference genome. Tools that maximize such trade-off are BOWTIE [Langmead et al., 2009] and BWA [Li & Durbin, 2009]. They make use of the seed-and-extend heuristic: in order to align a read r, an almost exact match of the first $l < |r|$ bases of the read is a necessary condition. The BFAST [Homer et al., 2009] tool moves towards favoring correctness over speed, allowing alignments with a high number of mismatches and indels.

Another highly accurate tool able to align reads in the presence of extensive polymorphisms, high error rates and small indels, is rNA [Vezzi et al., 2012]. It achieves an accuracy greater than other tools in a feasible amount of time.

Most of the techniques for comparing and aligning DNA need to compare DNA strings based on a distance measure. Thus, several distance measures for strings have been proposed and developed. Since most variations between organisms of the same species consist of point mutations like single nucleotide polymorphisms, or small insertions or deletions, edit distance is the standard string measure in many biomedical analyses, such as the detection of genomic variation, genome assembly [Zerbino & Birney, 2008], identification and quantification of RNA transcripts [Tomescu et al., 2013; Trapnell et al., 2009, 2010], identification of transcription factor binding sites [Levy & Hannenhalli, 2002], or methylation patterns [Prezza et al., 2012].

In the case of genomic sequences coming from different related species other mutations are present, such as reversals [Bader et al., 2001], transpositions [Bafna & Pevzner, 1998], translocations [Hannenhalli, 1996], fissions and fusions [Hannenhalli & Pevzner, 1995]. For this reasons, there have been a series of different proposals of similarity between entire genomes, including rearrangement distance [Belda et al., 2005], k-break rearrangements [Alekseyev & Pevzner, 2008],

edit distance with block operations [Shapira & Storer, 2003]. The study of genome rearrangement [Palmer & Herbon, 1988] was also investigated under Kendall tau distance. Other choices of distance metrics in recent techniques are the Hamming distance [Chimani et al., 2011; Vezzi et al., 2012], Kendall tau distance [Popov, 2007], and many others [Felsenstein, 2004].

Rank distance [Dinu, 2003] is another such measure of similarity, having low computational complexity, but high significance in phylogenetic analysis [Dinu & Ionescu, 2012a; Dinu & Sgarro, 2006].

6.1.2 Phylogenetic Analysis

Biologists have spent many years creating a taxonomy (hierarchical classification) of all living things: kingdom, phylum, class, order, family, genus, and species. Thus, it is perhaps not surprising that much of the early work in cluster analysis sought to create a discipline of mathematical taxonomy that could automatically find such classification structures. More recently, biologists have applied clustering to analyze the large amounts of genetic information that are now available. For example, clustering has been used to find groups of genes that have similar functions.

The phylogenetic analysis of organisms remains one of the most important problems in biology. When a new organism is discovered, it needs to be placed in a phylogenetic tree in order to determine its class, order, family and species. But, the phylogenetic trees of already known organisms, obtained with different methods, are still disputed by researchers. For example, there is no definitive agreement on either the correct branching order or differential rates of evolution among the higher primates, despite the research in this area. Joining human with chimpanzee and the gorilla with the orangutan is currently favored, but the alternatives that group humans with either gorillas or the orangutan rather than with chimpanzees also have support [Holmquist et al., 1988]. Others have tried to find the right place of an entire order of organisms in the evolutionary tree of species. One such example is the work of [Reyes et al., 2000], which finds that the position of Rodents in the mammalian tree remains an open question.

While distance methods are commonly utilized (for example, the neighbor-

joining method due to [Saitou & Nei, 1987] uses only distances), the standard method of phylogenetic analysis is probably the maximum likelihood for the evolution of the strings under a biologically motivated model of evolution, for example the Markov model (also known as General Time Reversible Model) [Saccone et al., 1990] with various supplements such as some invariant states. Similarly, the now commonly used Bayesian methods [Munch et al., 2008; Yang & Rannala, 1997] are based on the aligned strings themselves, not on some distances between the strings. Many trees are also found using parsimony methods. Some researchers have also proposed to examine the phylogenetic evolution using only proteins encoded by mitochondrial DNA [Cao et al., 1998], instead of entire mtDNA sequences.

There are many standard methods of phylogenetic inference from distances, such as the Unweighted Pair Group Method with Arithmetic Mean (UPGMA) of [Sneath & Sokal, 1973], least square methods [Bryant & Waddell, 1998; Fitch & Margoliash, 1967], minimum evolution methods [Rzhetsky & Nei, 1992], or neighbor-joining [Saitou & Nei, 1987]. These have been studied considerably in the literature. Broad overviews may be found in [Nei & Kumar, 2000] and in [Felsenstein, 2004]. The phylogenetic analysis methods proposed in Chapters 7 and 8 are also distance based. More precisely, Chapter 7 presents several clustering methods based on rank distance [Dinu, 2003], while Chapter 8 discusses a new distance measure for strings with applications in phylogeny [Ionescu, 2013a].

6.2 Natural Language Processing

There are two main directions in the study of NLP problems. One direction is to develop methods based on linguistic knowledge, that comes from the study of grammar, morphology, syntax, semantics, and so on. The other direction is based on finding machine learning methods that can be used as good approximate solutions for certain problems such as machine translation, text summarization, or document classification, to name only a few of them. The two directions are a result of the conjunction of researchers with different backgrounds. While some of them dedicated their time to the study of language, the others developed machine learning methods that can be applied with success in several domains, including

NLP. This thesis falls in the second category, as it studies a machine learning approach for the task of native language identification. Therefore, this state of the art section is only focused on the machine learning approach.

In the recent years, massive amounts of unstructured and semi-structured data, including text documents, have become available with the help of the Internet. Data mining and machine learning techniques can be employed to find patterns in this data, but they rely on other methods for structuring text. Indeed, machine learning methods usually work with features or pairwise similarities, that must be obtained from the unstructured data. In order to treat text as a set of features, researchers have proposed several representations that also keep the relevant information from text. One of the most popular representations is the bag of words model. In this model, text is represented as an unordered collection of words, disregarding grammar and even word order. Other popular representations are based on word n-grams. An n-gram is defined as a contiguous sequence of n items from a given sequence of text. An n-gram of size 1 is referred to as *unigram*, one of size 2 is referred to as *bigram*, and one of size 3 is referred to as *trigram*. While the use of word n-grams seems natural for text analysis, another approach is to use character n-grams. String kernels based on character n-grams have achieved state of the art performance in text categorization (by topic), authorship identification, plagiarism detection. A recent application of string kernels, that of identifying the native language from text, is presented in Chapter 9.

Other tasks, such as machine translation, need to understand the syntactical and semantic structure of text. Some researchers have developed part-of-speech tagging techniques to identify the part of speech of words in a given text. Others have studied word sens disambiguation (WSD) techniques that try to resolve the ambiguity of words in a given context. All these techniques, that try to automatically extract syntactic or semantic information from text, have applications beyond machine translation. For example, unsupervised WSD has been used to improve the precision of an information retrieval (IR) system for difficult queries [Chifu & Ionescu, 2012]. The approach is not concerned with performing a straightforward WSD, but rather with discriminating among the meanings of a polysemous word by identifying clusters of similar contexts, where each clus-

ter shows the polysemous word being used in a particular meaning. This type of approach (sense discrimination) is quite distinct from the traditional task of WSD, which classifies words relative to existing senses. The unsupervised WSD method is employed to cluster the documents initially retrieved by the IR system. Documents are assigned to the most probable group given the context as defined by the Naïve Bayes model, where the parameter estimates are formulated via unsupervised techniques. Feature selection based on the WordNet lexical database, which has provided good disambiguation results for all parts of speech [Hristea et al., 2008], was used.

Natural language processing is an active area of research with many applications. Researchers have developed a broad variety of techniques that aim at solving different NLP tasks. Extensive overviews of such techniques may be found in [Jurafsky & Martin, 2000; Manning & Schütze, 1999; Manning et al., 2008].

6.2.1 String Kernels

Using words is natural in text analysis tasks like text categorization (by topic), authorship identification and plagiarism detection. Perhaps surprisingly, recent results have proved that methods handling the text at character level can also be very effective in text analysis tasks [Grozea et al., 2009; Lodhi et al., 2002; Popescu, 2011; Popescu & Dinu, 2007; Popescu & Grozea, 2012; Sanderson & Guenter, 2006].

In [Lodhi et al., 2002] string kernels were used for document categorization with very good results. Trying to explain why treating documents as symbol sequences and why using string kernels led to such good results, the authors suppose that: "the [string] kernel is performing something similar to stemming, hence providing semantic links between words that the word kernel must view as distinct".

String kernels were also successfully used in authorship identification [Popescu & Dinu, 2007; Popescu & Grozea, 2012; Sanderson & Guenter, 2006]. For example, the system described in [Popescu & Grozea, 2012] ranked first in most problems and overall in the PAN 2012 Traditional Authorship Attribution tasks. A possible reason for the success of string kernels in authorship identification is

given in [Popescu & Dinu, 2007]: "the similarity of two strings as it is measured by string kernels reflects the similarity of the two texts as it is given by the short words (2-5 characters) which usually are function words, but also takes into account other morphemes like suffixes ('ing' for example) which also can be good indicators of the author's style".

Even more interesting is the fact that two methods, that are essentially the same, obtained very good results for text categorization (by topic) [Lodhi et al., 2002] and authorship identification [Popescu & Dinu, 2007]. Both are based on SVM and a string kernel of length 5. Traditionally, the two tasks, text categorization by topic and authorship identification are viewed as opposite. How is it possible to obtain good results with the same technique? When words are considered as features, for text categorization the (stemmed) content words are used (the stop words being eliminated), while for authorship identification the function words (stop words) are used as features, the other words (content words) being eliminated. Then, why did the same string kernel (of length 5) work well in both cases? It seems that the key factor is the kernel-based learning algorithm. The string kernel implicitly embeds the texts in a high dimensional feature space, in this case the space of all (sub)strings of length 5. The kernel-based learning algorithm (SVM or any other kernel method), aided by regularization, implicitly assigns a weight to each feature, thus selecting the features that are important for the discrimination task. In this way, in the case of text categorization the learning algorithm enhances the features (substrings) representing stems of content words, while in the case of authorship identification the same learning algorithm enhances the features representing function words.

Using string kernels will make the corresponding learning method completely language independent, because the texts will be treated as sequences of symbols (strings). Methods working at the word level or above very often restrict their feature space according to theoretical or empirical principles. For example, they select only features that reflect various types of spelling errors or only some type of words, such as function words, for example. These features prove to be very effective for specific tasks, but other, possibly good features, depending on the particular task, may exist. String kernels embed the texts in a very large feature space, given by all the substrings of length k, and leave it to the learning algo-

rithm to select important features for the specific task, by highly weighting these features. It is important to note that this approach is also language theory neutral, since it disregards any features of natural language such as words, phrases, or meaning.

Chapter 7

Clustering based on Rank Distance

Clustering has long played an important role in a wide variety of fields: biology, statistics, pattern recognition, information retrieval, machine learning, data mining, psychology and other social sciences. There are various clustering algorithms that differ significantly in their notion of what constitutes a cluster. The appropriate clustering algorithm and parameter settings depend on the individual data set. But not all clustering algorithms can be applied on a particular data set. For example, clustering methods that depend on a standard distance function (such as k-means) cannot be applied on a data set of objects (such as strings) for which a standard distance function cannot be computed.

The primary goal of this chapter is to exhibit several clustering algorithms for strings, or more precisely, that are based on a distance measure for strings. Many distance measures for strings can be considered, but this work is focused on using a single distance that has very good results in terms of accuracy and time for many important problems. The considered distance is termed *rank distance* [Dinu, 2003] and it has applications in biology [Dinu & Ionescu, 2012b; Dinu & Sgarro, 2006], natural language processing [Dinu & Dinu, 2005], authorship attribution [Dinu et al., 2008], and many other fields. The first type of clustering algorithms presented in this chapter can be described as a centroid model that represents each cluster either by a single median string or by a single closest

string. The second type can be described as a connectivity model that builds a hierarchy of clusters based on distance connectivity. Clusters are connected by considering either the median string, the closest string, or the consensus string of each cluster. All the clustering methods described in this chapter were introduced in previous work [Dinu & Ionescu, 2012a,c, 2013a,b].

The secondary goal of this chapter is to investigate the consensus string in the rank distance paradigm, which is extremely interesting and has many applications. Indeed, in various research fields a common task is to summarize the information shared by a collection of objects and to find a consensus of them. In many scenarios, the object items for which a consensus needs to be determined are rankings, and the process is called *rank aggregation*. Common applications of rank aggregation schemes are electoral processes, meta-search engines, document classification, selecting documents based on multiple criteria, and many others. This chapter presents a particular application of such aggregation schemes, that of finding motifs or common patterns in a set of given DNA sequences. Among the conditions that a string should satisfy to be accepted as consensus, are the median string and closest string. These approaches have been intensively studied separately, but only recently, the work of [Amir et al., 2009] tries to combine both problems: to solve the consensus string problem by minimizing both distance sum and radius, in the Hamming distance paradigm.

Theoretical results show that it is not possible to identify a consensus string via rank distance for three or more strings. Thus, an efficient genetic algorithm is proposed to find the optimal consensus string, by adapting the approach proposed in [Dinu & Ionescu, 2012b]. The genetic algorithm is used in the hierarchical clustering algorithm based on consensus string.

Phylogenetic experiments using mitochondrial DNA sequences extracted from several mammals demonstrate the clustering performance and the utility of the two algorithms. The goal of these experiments is to compare the proposed methods by their ability to determine the evolutionary relationships among species. Experiments on DNA comparison are also presented to show the efficiency of the proposed genetic algorithm for consensus string.

The chapter is organized as follows. Section 7.1 introduces notation and mathematical preliminaries. Section 7.2 gives on overview of related work regarding

the closest string, the median string and the consensus string, studied under different distance metrics. Section 7.3 discusses the approach on consensus string problem via rank distance. The genetic algorithm to find and optimal consensus string is given in Section 7.4. The clustering algorithms are described in Section 7.5. The experiments using mitochondrial DNA sequences from mammals are presented in Section 7.6. Finally, a discussion is given in Section 7.7.

7.1 Preliminaries

A ranking is an ordered list that represents the result of applying an ordering criterion to a set of objects. A formal definition is given next.

Definition 9 *Let $\mathcal{U} = \{1, 2, ..., \#\mathcal{U}\}$ be a finite set of objects, named universe, where $\#\mathcal{U}$ denotes the cardinality of $\mathcal{U}$. A* ranking *over $\mathcal{U}$ is an ordered list: $\tau = (x_1 > x_2 > ... > x_d)$, where $x_i \in \mathcal{U}$ for all $1 \leq i \leq d$, $x_i \neq x_j$ for all $1 \leq i \neq j \leq d$, and $>$ is a strict ordering relation on the set $\{x_1, x_2, ..., x_d\}$.*

A ranking defines a partial function on $\mathcal{U}$, where for each object $i \in \mathcal{U}$, $\tau(i)$ represents the position of the object i in the ranking τ.

The rankings that contain all the objects of an universe $\mathcal{U}$ are termed *full rankings*, while the others are *partial rankings*. The order of an object $x \in \mathcal{U}$ in a ranking σ of length d is defined by $ord(\sigma, x) = |d + 1 - \sigma(x)|$. By convention, if $x \in \mathcal{U} \setminus \sigma$, then $ord(\sigma, x) = 0$.

Definition 10 *Given two partial rankings σ and τ over the same universe $\mathcal{U}$, the rank distance between them is defined as:*

$$\Delta(\sigma, \tau) = \sum_{x \in \sigma \cup \tau} |ord(\sigma, x) - ord(\tau, x)|.$$

Rank distance is an extension to partial rankings of the Spearman footrule distance [Diaconis & Graham, 1977], defined below.

Definition 11 *If σ and τ are two permutations of the same length, then $\Delta(\sigma, \tau)$ is named the Spearman footrule distance.*

The rank distance is naturally extended to strings. The following observation is immediate: if a string does not contain identical symbols, it can be transformed directly into a ranking (the rank of each symbol is its position in the string). Conversely, each ranking can be viewed as a string, over an alphabet equal to the universe of the objects in the ranking. The next definition formalizes the transformation of strings, that can have multiple occurrences of identical symbols, into rankings.

Definition 12 *Let n be an integer and let $w = a_1 \dots a_n$ be a finite word of length n over an alphabet Σ. The extension to rankings of w, is defined as $\bar{w} = a_{1,i(1)} \dots a_{n,i(n)}$, where $i(j) = |a_1 \dots a_j|_{a_j}$ for all $j = 1, \dots, n$ (i.e. the number of occurrences of a_j in the string $a_1 a_2 \dots a_j$).*

Observe that given $\bar{w}$, the string w can be obtained by simply removing all the index annotations. Rank distance can be extended to arbitrary strings as follows.

Definition 13 *Given $w_1, w_2 \in \Sigma^*$:*

$$\Delta(w_1, w_2) = \Delta(\bar{w}_1, \bar{w}_2).$$

Example 2 *Given two strings $x = abcaa$ and $y = baacc$, the annotated versions of x and y are $\bar{x} = a_1 b_1 c_1 a_2 a_3$ and $\bar{y} = b_1 a_1 a_2 c_1 c_2$, respectively. Thus, the rank distance between x and y is the sum of the absolute differences between the orders of the characters in $\bar{x}$ and $\bar{y}$ (for missing characters, the maximum possible offset is considered):*

$$\Delta(x, y) = |1 - 2| + |4 - 3| + 5 + |2 - 1| + |3 - 4| + 5 = 14.$$

It is important to note that throughout this chapter, the notion of string and the notion of ranking may be used interchangeably. The transformation of a string into a ranking can be done in linear time, by memorizing for each symbol, in an array, how many times it appears in the string. The computation of the rank distance between two rankings can also be done in linear time in the cardinality of the universe [Dinu & Sgarro, 2006].

Let χ_n be the space of all strings of size n over an alphabet Σ and let $P = \{p_1, p_2, \ldots, p_k\}$ be k strings from χ_n. The closest (or centre) string problem (CSP) is to find the center of the sphere of minimum radius that includes all the k strings. An alternative formulation of the problem is to find a string from χ_n which minimizes the distance to all the input strings.

Problem 1 *The* closest string problem via rank distance (CSRD) *is to find a minimal integer d (and a corresponding string t of length n) such that the maximum rank distance from t to any string in P is at most d. Let t denote the closest string to P, and d denote the radius. Formally, the goal is to compute:*

$$\min_{x \in \chi_n} \max_{i=1..k} \Delta(x, p_i). \tag{7.1}$$

The median string problem (MSP) is similar to the closest string problem, only that the goal is to minimize the average distance to all the input strings, or equivalently, the sum of distances to all the input strings.

Problem 2 *The* median string problem via rank distance (MSRD) *is to find a minimal integer d (and a corresponding string t of length n) such that the average rank distance from t to any string in P is at most d. Let t denote the median string of P. Formally, the goal is to compute:*

$$\min_{x \in \chi_n} \operatorname*{avg}_{i=1..k} \Delta(x, p_i). \tag{7.2}$$

Finally, the consensus string problem is to minimize both the maximum and the average distance to all the input strings.

Problem 3 *The* consensus string problem via rank distance *is to find a minimal integer d (and a corresponding string t of length n) such that the sum of the maximum and the average rank distance from t to any string in P is at most d. Let t denote the consensus string of P. Formally, the goal is to compute:*

$$\min_{x \in \chi_n} \left(\max_{i=1..k} \Delta(x, p_i) + \operatorname*{avg}_{i=1..k} \Delta(x, p_i) \right). \tag{7.3}$$

7.2 Related Work

The closest and the median string problems use a particular distance, and various distance metrics usually conduct to different results. The most studied approach was the one based on edit distance. In [Nicolas & Rivals, 2005], it is shown that closest string and median string via edit distance are NP-hard for finite and even binary alphabets. The existence of fast exact algorithms, when the number of input strings is fixed, is investigated in [Nicolas & Rivals, 2003]. The first distance measure used for the CSP was the Hamming distance and emerged from a coding theory application [Frances & Litman, 1997]. The CSP via Hamming distance is known to be NP-hard [Frances & Litman, 1997]. There are recent studies that investigate CSP under Hamming distance with advanced programming techniques such as integer linear programming (ILP) [Chimani et al., 2011]. In recent years, alternative distance measures were also studied. The work of [Popov, 2007] shows that the CSP via swap distance (or Kendall distance) and element duplication distance are also NP-hard.

However, the consensus string problem was only studied recently. The work of [Amir et al., 2009] presents a first algorithm which tries to combine both problems: to solve the consensus string problem by minimizing both distance sum and radius in the same time. The problem was solved only for the set of three strings in the case of the Hamming distance measure, and, as authors state, the problem is still open for the edit distance or for more than three strings. The consensus problem was also studied in the case of circular strings in [Lee et al., 2013]. The work presents algorithms to find a consensus and an optimal alignment for circular strings by the Hamming distance. This chapter investigates the consensus string problem under rank distance. Furthermore, several clustering methods that involve computing either the median string, the closest string, or the consensus string from strings within clusters, using the underlying rank distance, are proposed.

Rank distance (RD) was introduced in [Dinu, 2003] and has applications in biology [Dinu & Ionescu, 2012b; Dinu & Sgarro, 2006], natural language processing [Dinu & Dinu, 2005; Dinu et al., 2008], computer science and many other fields. Rank distance can be computed fast and benefits from some features of

the edit distance.

The distance between two strings can be measured with rank distance by scanning (from left to right) both strings. Letters need to be annotated in order to eliminate duplicates. For each annotated letter, rank distance measures the offset between its position in the first string and its position in the second string. Finally, all these offsets are summed up to obtain the rank distance. Intuitively, the rank distance gives us the total non-alignment score between two sequences. Rank distance is formally defined in Section 7.1.

Clearly, rank distance gives a score zero only to letters which are in the same position in both strings, as Hamming distance does. Note that Hamming distance is given by the number of positions where two strings of the same length differ. On the other hand, an important aspect is the reduced sensitivity of rank distance with respect to deletions and insertions. Reduced sensitivity is of paramount importance, since it allows the ad hoc extension to arbitrary strings, without affecting the low computational complexity. In contrast, the extensions of Hamming distance are mathematically optimal but computationally too heavy, and lead to the edit distance [Levenshtein, 1966], which is the base of the standard alignment principle.

Theoretically, rank distance works on strings from any alphabet, finite or infinite. But, in many practical situations the alphabet is of fixed constant size. For example, in computational biology, the DNA and protein alphabets are respectively of size 4 and 20. For some applications, one needs to encode the DNA or protein sequences on a binary alphabet that expresses only a binary property of the molecule, for instance the hydrophoby, which is used in some protocols that identify similar DNA sequences [States & Agarwal, 1996].

In [Dinu & Popa, 2012], it is shown that the CSRD is NP-hard. On the other hand, the median string problem is tractable [Dinu & Manea, 2006] in the rank distance case. In [Dinu & Ionescu, 2011], an approximation for CSRD based on genetic algorithms was proposed, which was further developed in [Dinu & Ionescu, 2012b]. In the clustering algorithms that are about to be presented in this chapter, CSRD and MSRD are important because steps in the presented algorithms involve finding the closest or median string for a cluster (subset) of strings.

7.3 Consensus String under Rank Distance

There are a few things to consider for solving the consensus string problem in the case of rank distance. Before going into details, it is important to note that the CSRD and MSRD problems do not have unique solutions. In other words, there are more strings that may satisfy one of the conditions imposed by the two problems. There are three possible directions to follow that could lead to finding the consensus string. The first direction is to obtain all the closest strings, and then search for a median string among the closest strings. The second approach is to obtain all the median strings at first, and then search for a closest string among the median strings. The third and last approach is to directly minimize equation (7.3). It has been shown that there is at least one string that satisfies both conditions (7.1) and (7.2) in the same time, for a set of two strings [Dinu & Sgarro, 2011]. However, the consensus problem was not discussed in the case of three or more strings. Theorem 3 shows that it is not always possible to minimize both the radius and the median distance, in the case of three or more strings.

Theorem 3 *A string that minimizes both equations* (7.1) *and* (7.2) *does not always exist, in the case of three or more strings.*

Proof: Let $x = 4321$, $y = 4312$ and $z = 2143$ be three strings with letters from $\Sigma = \{1, 2, 3, 4\}$. The closest strings of x, y and z are $CS = \{4213, 4123\}$ at a radius of 4. The median strings are $MS = \{4312, 4312\}$ at a median distance of 10. Observe that $CS \cap MS = \emptyset$. Thus, there is no solution that minimizes both the radius and the median distance. Despite this fact, a consensus string exists. The consensus string that minimizes equation (7.3) is $c = 4213$. □

The proof of Theorem 3 points to the fact that a solution for Problem 3 can be found, despite it is sometimes impossible to minimize conditions (7.1) and (7.2) in the same time. This leads to the fact that trying to search either for a closest string among median strings, or for a median string among closest strings, might not lead to a solution of Problem 3. The only remaining approach is to find an algorithm to directly minimize equation (7.3).

Theorem 4 *The consensus problem via rank distance (defined in Problem 3) is NP-hard.*

Proof: Since the closest string problem via rank distance is NP-hard [Dinu & Popa, 2012], it follows that Problem 3 is also NP-hard. □

Because Problem 3 is NP-hard, an efficient genetic algorithm is employed to find a close-to-optimal solution for the consensus string problem via rank distance.

7.4 Genetic Algorithm for Rank Distance Consensus

Genetic algorithms simulate the biological process of natural selection. The algorithm proposed in this chapter applies this biological process to find a consensus string. It applies a set of operations on a population of chromosomes over a number of generations. The population is a set of individual elements (also known as chromosomes) represented as strings. The set of operations used are the ones inspired from nature, namely the crossover, the mutation, and the selection.

Algorithm 3 *Genetic algorithm for consensus string*
***Input**: A set of strings from an alphabet Σ.*
***Initialization**: Generate a random population that represents the first generation.*
***Loop**: For a number of generations apply the next operations:*

1. *Apply the crossover according to the probability of having a crossover.*
2. *Apply mutations according to the probability of having a mutation.*
3. *Sort the chromosomes based on equation (7.3).*
4. *Select the best candidates for the next generation using a density of probability.*

***Output**: Choose the best individual from the last generation as the optimal consensus string.*

All chromosomes are strings from an alphabet Σ. Each chromosome is a possible candidate for the consensus string. At first, chromosomes are randomly generated. In the case of DNA, chromosomes are actually DNA sequences, with characters from the alphabet $\Sigma = \{A, C, G, T\}$.

The crossover operation between two chromosomes is straightforward. First, a random cutting point is generated. The prefixes of the two chromosomes remain

in place, while the suffixes of the two chromosomes are swapped. This is the standard crossover operation inspired directly from nature.

To apply a mutation to a certain chromosome, one position is randomly chosen. The character found at that position will be changed with another character from the alphabet Σ. Multiple mutations may appear in the same chromosome, although this is very unlikely. This is the classic mutation operation that can also be found in nature.

To select the individuals for the next generation from the current one, a density of probability function is used. The new generation is involved in the next iteration of the algorithm. The first step is to sort the individuals using equation (7.3) so that chromosomes at the top minimize the sum of the maximum and the average rank distance. Then, indexes are generated according to the density of probability function from the top to the bottom of the list of candidates. The indexes close to the top have a greater probability of making it into the next generation. Thus, good candidates for the consensus string will occur more often in the next generation, while bad candidates will occur less often.

To speed up the selection process, an efficient sorting algorithm proposed in [Ionescu, 2013b] was used. The *Unisort* algorithm has two main stages, one for partitioning the numbers into bins, and another one to build sub-arrays and combine them with merge sort. Given a uniformly distributed array of numbers, the algorithm places the numbers in bins to obtain sorted sub-arrays in the first stage. The second stage of the algorithm is straight forward. The sorted sub-arrays are merged two by two, until a single array is obtained. A simple strategy of merging is used to improve efficiency. At each step, the shortest two arrays are merged. The Unisort algorithm obtains the final sorted array in $O(n)$ time, assuming that the numbers are uniformly distributed.

The density probability function used to select the candidates for the next generation of the genetic algorithm is the normal distribution of mean 0 and variance 0.081 on the interval $[0, 1]$:

$$f(x) = \frac{1}{\sqrt{2 \cdot \pi \cdot 0.0816}} e^{\frac{-x^2}{2 \cdot 0.0816}}.$$

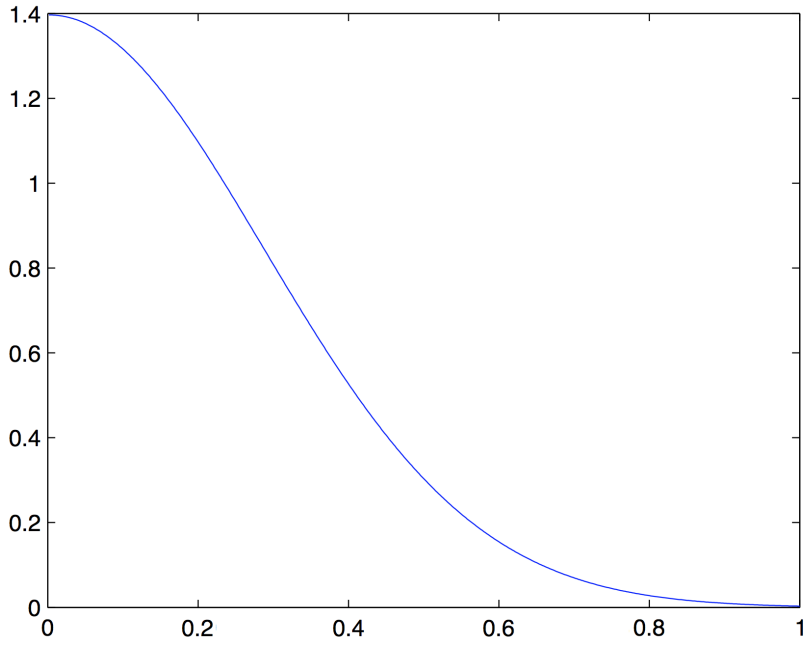

Figure 7.1: The graph of the density probability function.

The graph of the function used to select the candidates is represented in Figure 7.1. In the implementation of the algorithm the fitness function was statistically approximated.

The motivation for using this fitness function is based on test results. This fitness function reduces the number of generations that are required to obtain a close-to-optimal solution. Helped by the crossover and mutation operations, the fitness function has a good generalization capacity: it does not favor certain chromosomes which could narrow the solution space and lead to local minima solutions.

An interesting remark is that the proposed genetic algorithm can also be used to find a consensus substring. This is an important advantage of the algorithm if one wants to a find consensus between strings of different lengths, such as DNA sequences.

7.5 Clustering Methods based on Rank Distance

This section describes several clustering algorithms that are based on rank distance. These algorithms are to be applied on data sets that contain objects represented as strings, such as text, DNA sequences, etc.

Despite using rank distance, the five proposed algorithms are different in other aspects. Two of the algorithms are centroid based models similar to k-means, but each of them minimizes a different objective function, with regard to the median string and the closest string problems, respectively.

The other three algorithms build hierarchical trees without using a linkage criterion as standard hierarchical clustering methods do. Instead, they compute the centroid for each newly formed cluster and join clusters based on the rank distance between their centroids. Centroids are obtained by minimizing the radius (closest string), the average distance (median string), or both (consensus string).

The proposed algorithms are linked by the fact that they are designed to work only for strings (with and without repetitions), since cluster centroids are computed directly from strings, and the obtained centroids are also strings. This is possible with the use of a distance metric, in this case rank distance, to solve the median string, the closest string, or the consensus string problems, respectively.

7.5.1 K-means-type Algorithms based on Rank Distance

The k-means clustering technique is a simple method of cluster analysis which aims to partition a set of objects into K clusters, in which each object belongs to the cluster with the nearest mean. If string objects are considered for clustering, then a way to determine the centroid string for a certain cluster of strings is needed. The use of the median string computed with rank distance has been proposed in [Dinu & Ionescu, 2012a], while the use of the closest string has been proposed in [Dinu & Ionescu, 2012c]. Rank distance is also used to assign strings to the nearest median or closest string. Thus, the described algorithms are entirely based on rank distance.

Algorithm 4 partitions a set of strings into K clusters using rank distance and

median string. It aims at minimizing an objective function, given by

$$J = \sum_{j=1}^{k} \sum_{i=1}^{n} \Delta(x_i^{(j)}, c_j),$$

where $\Delta(x_i^{(j)}, c_j)$ is the rank distance between a string $x_i^{(j)}$ in cluster j and the cluster centroid c_j. The objective function is simply an indicator of the distance of the input strings from their respective cluster centers.

Algorithm 4 *K-means based on rank distance and median string*
1. ***Initialization****: Randomly select K strings as initial centroids.*
2. ***Loop****: Repeat until centroids do not change or until a maximum number of iterations is reached*
a. Form K clusters by assigning each string to its nearest median string.
b. Recompute the centroid (median string) of each cluster using rank distance.

Theorem 5 *Algorithm 4 converges to a solution in a finite number of iterations for any K strings as initial centroids.*

Proof: The demonstration of the finite convergence of k-means algorithm for any metric is given in [Selim & Ismail, 1984]. The rank distance is a metric function [Dinu, 2003]. □

Algorithm 5 partitions a set of strings into K clusters using rank distance and closest (centre) string. It aims at minimizing a different objective function, in this case given by

$$J = \sum_{j=1}^{k} \max_{i=1..n} \Delta(x_i^{(j)}, c_j).$$

Algorithm 5 *K-means-type algorithm based on rank distance and centre string*
1. ***Initialization****: Randomly select K strings as initial centroids.*
2. ***Loop****: Repeat until centroids do not change or until a maximum number of iterations is reached*
a. Form K clusters by assigning each string to its nearest centre string.

b. Recompute the centroid (centre string) of each cluster using rank distance.

Notice that Algorithm 5 is only similar to a k-means clustering approach since the choice of clusters centroids is fundamentally different from a standard k-means. Thus, on should refer to Algorithm 5 as a k-means-type algorithm.

Although the two algorithms will always terminate, they do not necessarily find the most optimal configuration, corresponding to the global objective function minimum. The algorithms are also significantly sensitive to the initial randomly selected centroids. However, they can be run multiple times to reduce this effect. Despite Algorithm 4 uses the method described in [Dinu & Manea, 2006] to compute the median string, and Algorithm 5 uses the genetic algorithm presented in [Dinu & Ionescu, 2012b], the computational complexity of both algorithms is $O(m \times K \times n^3)$, where n is the string length, K is the desired number of clusters, and m is the maximum number of iterations.

7.5.2 Hierarchical Clustering based on Rank Distance

Many hierarchical clustering techniques are variations on a single algorithm: starting with individual objects as clusters, successively join the two nearest clusters until only one cluster remains. These techniques connect objects to form clusters based on their distance. Apart from the choice of a distance function, another decision is needed for the linkage criterion to be used. Popular choices are single-linkage, complete-linkage, or average-linkage.

A standard method of hierarchical clustering that uses rank distance is presented in [Dinu & Sgarro, 2006]. It presents a phylogenetic tree of several mammals comparable to the structure of phylogenetic trees reported by other studies [Li et al., 2004; Reyes et al., 2000]. But, a hierarchical clustering method designed to deeply integrate rank distance might perform better.

The three hierarchical clustering methods presented here work only on string objects. Both use rank distance, but instead of a linkage criterion they use a different approach, that is to determine a centroid string for each cluster and join clusters based on the rank distance between their centroid strings. Algorithm 6 uses the median string as cluster centroid, while Algorithm 7 uses the closest

(or centre) string. Finally, Algorithm 8 employs the consensus string as cluster centroid.

Algorithm 6 *Hierarchical clustering based on rank distance and median string*

1. ***Initialization**: Compute rank distances between all initial strings.*
2. ***Loop**: Repeat until only one cluster remains*
    a. *Join the nearest two clusters to form a new cluster.*
    b. *Determine the median string of the newly formed cluster.*
    c. *Compute rank distances from this new median string to existing median strings.*

Algorithm 7 *Hierarchical clustering based on rank distance and closest string*

1. ***Initialization**: Compute rank distances between all initial strings.*
2. ***Loop**: Repeat until only one cluster remains*
    a. *Join the nearest two clusters to form a new cluster.*
    b. *Determine the closest string of the newly formed cluster.*
    c. *Compute rank distances from this new closest string to existing closest strings.*

Algorithm 8 *Hierarchical clustering based on consensus rank distance*

***Initialization**: Compute rank distances between all initial strings.*

***Loop**: Repeat until only one cluster remains*

1. *Join the nearest two clusters to form a new cluster.*
2. *Determine the consensus string of the newly formed cluster.*
3. *Compute rank distances from this new consensus string to existing consensus strings.*

The analysis of the computational complexity of the proposed hierarchical algorithms is straightforward. Let m be the number of the input strings. The time required to compute rank distances between the input strings is $O(m^2)$. Each algorithm builds a binary tree structure where the leaves are the initial m strings. Thus, each algorithm creates $m - 1$ intermediate clusters until only one cluster remains. While the closest string in Algorithm 7 is computed with the genetic algorithm presented in [Dinu & Ionescu, 2012b], the consesus string in Algorithm 8 is computed with the genetic approach described in Section 7.4. The

most heavy computational step is to determine the centroid of a cluster using one of the genetic algorithms, which takes $O(n^3)$ time, where n is the string length. Usually n is much greater than m and the algorithm complexity in this case is $O(m \times n^3)$.

7.6 Experiments

7.6.1 Data Set Description

The clustering methods are tested on a classical problem in bioinformatics: the phylogenetic analysis of the mammals. In the phylogenetic experiments presented in this chapter, mitochondrial DNA sequence genome of 22 mammals is used. The genomes are available for download in the EMBL database (http://www.ebi.ac.uk/ena/) using the accession numbers given in Table 7.1. The mammals selected for the experiments belong to one of the following 7 orders: Carnivora, Cetartiodactylae, Metatheria, Monotremata, Perissodactylae, Primates, and Rodentia. Additionally, the fat dormouse (*Myoxus glis*, AJ001562) genome is only considered in the DNA comparison experiment.

Mitochondrial DNA (mtDNA) is the DNA located in organelles called mitochondria. The DNA sequence of mtDNA has been determined from a large number of organisms and individuals, and the comparison of those DNA sequences represents a mainstay of phylogenetics, in that it allows biologists to elucidate the evolutionary relationships among species. In mammals, each double-stranded circular mtDNA molecule consists of $15,000 - 17,000$ base pairs. DNA from two individuals of the same species differs by only 0.1%. This means, for example, that mtDNA from two different humans differs by less than 20 base pairs. Because this small difference cannot affect the study, the experiments are conducted using a single mtDNA sequence for each mammal.

7.6.2 DNA Comparison

In this section an experiment is performed to show that finding the consensus string for a set of DNA strings is relevant from a biological point of view, thus

Table 7.1: The 22 mammals from the EMBL database used in the phylogenetic experiments. The accession number is given on the last column.

Mammal	Latin Name	Accession
human	*Homo sapiens*	V00662
common chimpanzee	*Pan troglodytes*	D38116
pigmy chimpanzee	*Pan paniscus*	D38113
gorilla	*Gorilla gorilla*	D38114
orangutan	*Pongo pygmaeus*	D38115
Sumatran orangutan	*Pongo pygmaeus abelii*	X97707
gibbon	*Hylobates lar*	X99256
horse	*Equus caballus*	X79547
donkey	*Equus asinus*	X97337
Indian rhinoceros	*Rhinoceros unicornis*	X97336
white rhinoceros	*Ceratotherium simum*	Y07726
harbor seal	*Phoca vitulina*	X63726
gray seal	*Halichoerus grypus*	X72004
cat	*Felis catus*	U20753
fin whale	*Balaenoptera physalus*	X61145
blue whale	*Balaenoptera musculus*	X72204
cow	*Bos taurus*	V00654
sheep	*Ovis aries*	AF010406
rat	*Rattus norvegicus*	X14848
mouse	*Mus musculus*	V00711
North American opossum	*Didelphis virginiana*	Z29573
platypus	*Ornithorhynchus anatinus*	X83427

being an interesting problem for biologists. The genetic algorithm described in Section 7.4 is employed to find the consensus string. Only the rat, the house mouse, the fat dormouse, and the cow genomes are used in the experiment. The task is to find the consensus string between the rat and house mouse DNAs, between the rat and fat dormouse DNAs, and between the rat and cow DNAs. The goal of this experiment is to compare the distances associated to the three consensus strings. The cow belongs to the Cetartiodactylae order, while the rat, the house mouse, and the fat dormouse belong to the Rodentia order. Expected results should show that the rat-house mouse distance and the rat-fat dormouse distance are smaller than the rat-cow distance. The same experiment was also conducted in [Dinu & Ionescu, 2012b] by using three genetic algorithms based

on closest string via Hamming distance, edit distance, and rank distance, respectively. To compare the results of these algorithms with the results obtained by the genetic algorithm proposed in this work, the same experiment setting is used. The genetic algorithm parameters used to obtain the presented results are given next. The population size is 1800 chromosomes, the crossover probability is 0.36, and the mutation probability is 0.1, while the size of each DNA sequence is 150 nucleotides. The chromosomes are let to evolve for 300 generations.

The results based on consensus string are presented in Table 7.2. The obtained results show that the proposed genetic algorithm can efficiently find consensus strings. The reported times are computed by measuring the average time of 10 runs of the genetic algorithm on a computer with Intel Core i7 2.3 GHz processor and 8 GB of RAM memory using a single Core.

Table 7.2: Consensus string results obtained with the genetic algorithm.

Consensus Results	rat-house mouse	rat-fat dormouse	rat-cow
Distance	1542	3493	8807
Average time	2.5 seconds	2.6 seconds	2.6 seconds

Figure 7.2 shows the distance evolution of the best chromosome at each generation for consensus string via rank distance versus the closest string via rank distance, Hamming distance, and Levenshtein distance, respectively. The consensus strings obtained by the genetic algorithm are biologically relevant in that they show a greater similarity between the rat DNA and house mouse DNA and a lesser similarity between the rat DNA and cow DNA. In terms of speed, the proposed method is similar to the other algorithms based on closest string via low-complexity distances (Hamming and rank distance).

7.6.3 K-means Experiment

The first experiment is to cluster the 22 mammalian DNA sequences using k-means clustering into 7 clusters. The clustering is relevant if the produced clusters match the 7 orders of mammals available in the data set. In the experiment, only the first 1000 nucleotides extracted from each DNA sequence are used. The

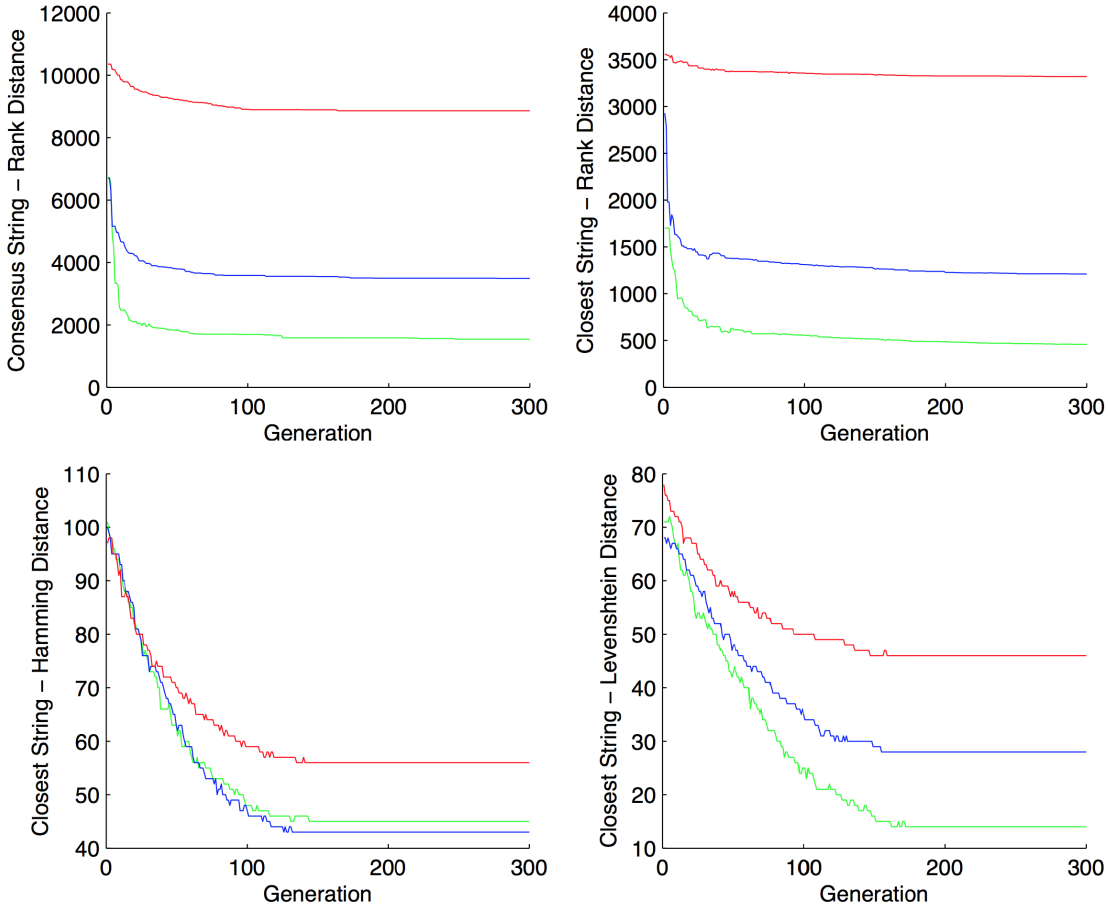

Figure 7.2: The distance evolution of the best chromosome at each generation for the Rat-Mouse-Cow experiment. GREEN = rat-house mouse distance, BLUE = rat-fat dormouse, RED = rat-cow distance.

clustering results of the two k-means methods are shown on columns in Table 7.3. The number of correctly clustered mammals per class is represented in terms of accuracy.

Both algorithms are able to separate the Metatheria, Monotremata, and Rodentia orders. The k-means algorithm based on closest string is also able to clearly distinguish the Perissodactylae order. On the other hand, the k-means algorithm based on the median string is able to clearly distinguish the Carnivora and Primates orders. Both algorithms leave the sheep out of the Cetartiodactylae order. Overall, the evaluated algorithms give comparable results. The algorithm based

Table 7.3: Comparative results of the k-means based on median string (k-median) versus the k-means based on closest string (k-closest). Clustering results for 22 DNA sequences using rank distance.

Order	k-median	k-closest
Cetartiodactylae	75%	75%
Carnivora	100%	0%
Metatheria	100%	100%
Monotremata	100%	100%
Rodentia	100%	100%
Primates	100%	85%
Perissodactylae	50%	100%
Overall	86%(19/22)	77%(17/22)

on the median string seems to perform slightly better, but the two techniques should be compared on more data sets in future work before a strong conclusion can be drawn.

7.6.4 Hierarchical Clustering Experiment

The second experiment is to apply the three hierarchical clustering methods based on rank distance on the 22 DNA sequences. The resulted phylogenetic trees are compared with phylogenetic trees obtained with standard hierarchical clustering methods, such as the one presented in [Dinu & Sgarro, 2006]. In this experiments, the mammals are represented only by the first 3000 nucleotides of each mtDNA sequence.

The phylogenetic tree obtained with Algorithm 6 is presented in Figure 7.3, the tree obtained with Algorithm 7 is presented in Figure 7.4, and the tree obtained with Algorithm 8 is given in Figure 7.5. Analyzing the phylogenetic trees, one can observe that all the proposed clustering methods are able to separate the Primates, Perissodactylae and Carnivora orders. The only confusion of the phylogenetic tree obtained with median string is that the rat is clustered with the sheep instead of the house mouse. The phylogenetic tree based on closest string is slightly worse, since it is also unable to cluster the platypus, besides the rat and the sheep. There are also two mistakes in the tree obtained with consensus

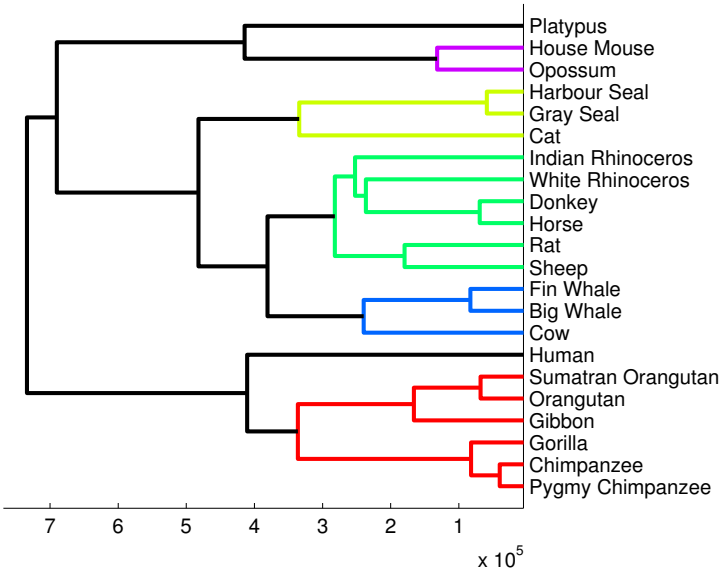

Figure 7.3: Phylogenetic tree obtained for 22 mammalian mtDNA sequences using median string via rank distance.

string. First, the rat is clustered with the sheep instead of the house mouse. Second, the platypus should also be in the same cluster with the opossum and the house mouse. Overall, the phylogenetic trees are relevant from a biological point of view.

By comparing all the resulted trees, one can observe that the clusters near the root are influenced by the use of the median, the closest, or the consensus string, respectively. The clusters near the leaves are more similar for the three methods, since the formation of these clusters is influenced by the distance itself (in this case, rank distance). Thus, good results are in part an aftermath of rank distance.

By considering the Primates cluster, one can observe a really interesting fact: the human is very different from the other Primates, in all three methods. For example, by choosing a cutting point that would separate the dendrogram obtained with Algorithm 6 in 7 clusters, the human falls in a separate cluster. In other words, there will be a cluster that contain a single representative DNA sequence, that of the human's.

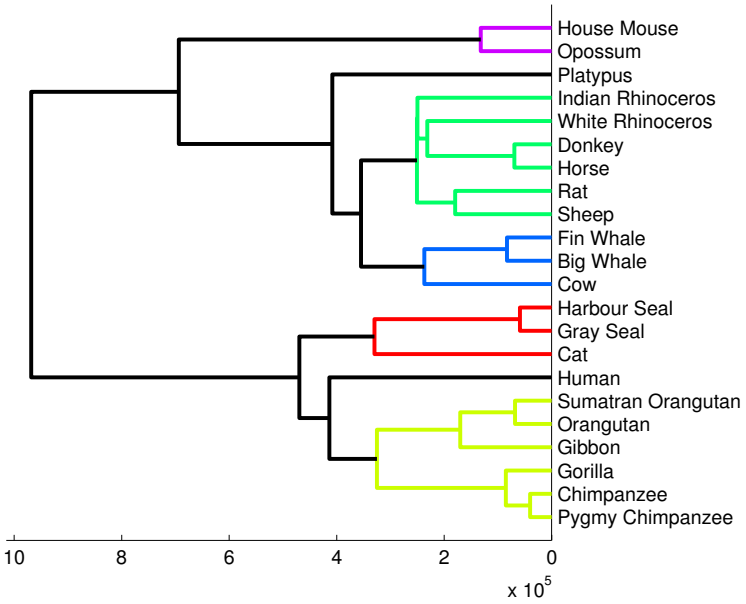

Figure 7.4: Phylogenetic tree obtained for 22 mammalian mtDNA sequences using closest string via rank distance.

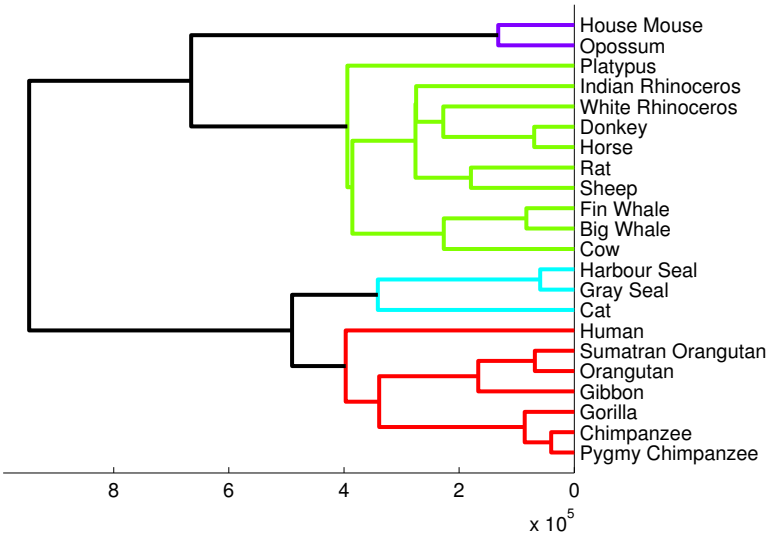

Figure 7.5: Phylogenetic tree obtained for 22 mammalian mtDNA sequences using consensus string via rank distance.

By contrast to the results obtained here, in the phylogenetic tree presented in [Dinu & Sgarro, 2006] the Perissodactylae and Carnivora orders are mixed together. The standard hierarchical clustering method used in [Dinu & Sgarro, 2006] is also unable to join the rat with the house mouse. The phylogenetic trees presented in this work are also comparable to those obtained in other studies [Li et al., 2004; Reyes et al., 2000]. Therefore, the hierarchical clustering methods presented in this chapter perform better or at least comparable to the state of the art clustering methods.

7.7 Discussion and Further Work

The experiments demonstrate the utility of the algorithms described in this chapter. Empirical results show that the proposed algorithms produce relevant clusters, being good alternative approaches for the phylogenetic analysis of mammals. Indeed, the results are similar or sometimes better to those reported in the literature [Dinu & Sgarro, 2006; Reyes et al., 2000]. Good results are in part an aftermath of rank distance. The work of [Dinu & Ionescu, 2012b] shows that rank distance can achieve better results than Hamming distance or edit distance, when it comes to DNA sequence comparison. However, for other applications and different kind of strings, the use of another distance metric may be more appropriate.

One should also consider the computational time when there are many strings to be clustered. Hamming distance should work faster than rank distance, and it might be more suitable for use in a particular application. But, for the phylogenetic analysis problem, where there are usually not many individuals to be clustered, rank distance works fine in terms of time efficiency and it also gives more accurate clusters. For example, the results for the k-means experiment can be obtained in less than half an hour on a machine with 2.3 GHz Intel Core i7 processor and 8GB of RAM. The most costly step in the algorithm is to solve either the median string, the closest string, or the consensus string problems to obtain cluster centroids. However, the parameters of the genetic algorithm presented in [Dinu & Ionescu, 2012b], that can be used to solve these three problems, can easily be adjusted to speed up clustering. The trade-off between accuracy

and time must not be disregarded when setting up the parameters.

This chapter also investigated the consensus string problem under the rank distance metric, and an efficient genetic algorithm was proposed. The genetic approach has the advantage of finding the consensus for any number of strings, being suitable for computational biology applications. The DNA comparison experiment shows that the results of the genetic algorithm are indeed relevant from a biological point of view. From the phylogenetic experiments, it seems that the median string would be a better choice for the proposed clustering techniques. Other applications of the proposed clustering methods, beyond computational biology, might reveal that the median string is not always the best choice. In future work, other distance measures, such as Hamming or edit distance, can also be used for clustering instead of rank distance.

Chapter 8

Local Rank Distance

Computer science researchers have developed a wide variety of methods that can be applied with success in computational biology. Such methods range from clustering techniques used to analyze the phylogenetic trees of different organisms, to genetic algorithms used to find motifs or common patterns in a set of given DNA sequences. The results of many state of the art techniques for phylogenetic analysis or DNA sequence comparison are inaccurate from a biological point of view, and can always be improved. Some of these methods are based on a distance measure for strings. Popular choices for recent techniques are the Hamming distance [Chimani et al., 2011; Vezzi et al., 2012], edit distance [Shapira & Storer, 2003], Kendall-tau distance [Popov, 2007], rank distance [Dinu & Ionescu, 2012a,b], and many others [Felsenstein, 2004].

In this context, the chapter aims to introduce a new distance measure, termed Local Rank Distance (LRD) [Ionescu, 2013a], inspired from the recently introduced Local Patch Dissimilarity for images [Dinu et al., 2012]. Designed to conform to more general principles and adapted to DNA strings, LRD is more suitable to be used instead of other distances, from a biological point of view. Phylogenetic analysis and DNA comparison experiments show that the use of LRD enables significant improvements over several state of the art methods.

Theoretical properties of LRD are also investigated in this thesis. First, some restrictions are imposed to LRD in order to prove that LRD can be a distance function. A theoretical result about the expected distance between two random strings is given next. Finally, the lower and the upper bounds of LRD with

respect to the Hamming distance are given.

The chapter is organized as follows. LRD and its principles are described in Section 8.1. Section 8.2 presents the LRD definition. An algorithm to compute LRD is presented in Section 8.3. Theoretical properties of LRD and a proof that LRD can be a distance function are given in Section 8.4. Experiments conducted on two important problems in computational biology are presented in Section 8.5. The final remarks are given in Section 8.6.

8.1 Approach

The development of Local Rank Distance [Ionescu, 2013a] is based on Local Patch Dissimilarity [Dinu et al., 2012], which is a generalization of rank distance for two-dimensional input (digital images). Rank distance [Dinu, 2003] has applications in biology [Dinu & Ionescu, 2012b; Dinu & Sgarro, 2006], natural language processing [Dinu & Dinu, 2005; Dinu et al., 2008], computer science and many other fields. Despite of having such broad applications, rank distance is not always adequate for specific data types. Local Rank Distance comes from the idea of adapting rank distance to string data, in order to capture a better similarity (or dissimilarity) between string objects, such as DNA sequences or text.

The distance between two strings can be measured with rank distance by scanning (from left to right) both strings. First, characters need to be annotated with indexes in order to eliminate duplicates. For each annotated letter, rank distance measures the offset between its position in the first string and its position in the second string. Finally, all these offsets are summed up to obtain the rank distance. In other words, the rank distance measures the offset between the positions of a letter in the two given strings, and then sums up these values. Intuitively, the rank distance computes the total non-alignment score between two sequences.

Rank distance is based on mathematical principles that are not suited for specific input data, such as images or DNA sequences. The reason is that rank distance was designed to work with rankings (ordered sets of objects). It is useful to consider the following example to understand how rank distance works on text and how it can be adapted to specific input data. For two strings s_1 and s_2,

the characters are first annotated. The annotation step is necessary to transform the strings into (full or partial) rankings. Now, rank distance can be computed between annotated strings $\bar{s_1}$ and $\bar{s_2}$.

Example 3 *If* $s_1 = CCGAATACG$ *and* $s_2 = TGACTCA$*, the annotated strings are* $\bar{s_1} = C_1C_2G_1A_1A_2T_1A_3C_3G_2$ *and* $\bar{s_2} = T_1G_1A_1C_1T_2C_2A_2$*. The rank distance between* s_1 *and* s_2 *is*

$$\begin{aligned}\Delta_{RD}(s_1, s_2) = \Delta_{RD}(\bar{s_1}, \bar{s_2}) = |1-4| + |2-6| + |3-2| + |4-3| \\ + |5-7| + |6-1| + x + x + x + x,\end{aligned}$$

where x *represents the offset of characters that cannot be matched (because they are missing in the other string), such as* A_3 *or* C_3*.*

In order to compute rank distance on strings, a global order is introduced by the annotation step. Notice that there are annotated characters in $\bar{s_1}$ (such as A_3 or C_3) that have no matching characters in $\bar{s_2}$. In practice, conventions are made to replace x (the offset of unmatched characters) with the maximum possible offset between two characters, or the average offset. To reduce the effect of missing characters, strings can be annotated both from left to right and from right to left. Some of these approaches are studied in [Dinu & Sgarro, 2006]. Another idea with results similar to previous approaches is to consider circular DNA sequences [Dinu & Ghetu, 2011]. However, these mathematical tricks are not natural from a biological point of view. Thus, one may ask whether this global order is really necessary or whether the global order is defined in the right way (for example, should strings be annotated from right to left instead of left to right). One can argue that strings can be annotated from left to right and from right to left, and the two distances obtained after annotation can be summed up. But, in order to define rank distance for specific input data (digital images, for example), answering such questions becomes difficult. One would have to ask which is the first pixel of the image, then which is the second one? There is a very large number of possibilities to define a global order on the pixels of an image. Local Patch Dissimilarity solves this problem by simply dropping the annotation step and by replicating only the local phenomenon and how rank

distance is computed on strings. Therefore, pixels or patches have no global order to conform to. This will also be the case of Local Rank Distance, where the annotation step is dropped, and characters in one string are simply matched with the nearest similar characters in the other string. The advantage of using no annotation immediately becomes clear. In Example 3, A_3 remains unmatched in the case of rank distance, while in the case of LRD, A_3 from $\bar{s_1}$ will be matched with A_2 from $\bar{s_2}$, as in Example 4, since there are no annotations.

If long DNA strings (as found in nature) are considered, that contain only characters in the alphabet $\Sigma = \{A, C, G, T\}$, one can observe that measuring the non-alignment score between characters that might be randomly distributed (with a uniformly distributed frequency) is not too relevant, because scores between different strings will almost be the same. Therefore, important information encoded in the DNA strings might be lost or not completely captured by a distance measure that works at character level (this is the case of Hamming or rank distance, for example). There is a similar situation in image processing. Instead of analyzing images at the pixel level, computer vision researchers have developed techniques that work with patches [Barnes et al., 2011; Cho et al., 2010]. To extract meaning from image, computer vision techniques, including Local Patch Dissimilarity, look at certain features such as contour, contrast or shape. It is clear that these features cannot be captured in single pixels, but rather in small, overlapping rectangles of fixed size (e.g., 10×10 pixels), called patches. A similar idea was introduced in the early years of bioinformatics, where k-mers (also known as n-grams or substrings) are used instead of single characters. There are recent studies that use k-mers for the phylogenetic analysis of organisms [Li et al., 2004], or for sequence alignment [Melsted & Pritchard, 2011]. Analyzing DNA at substring level is also more suited from a biological point of view, because DNA substrings may contain meaningful information. For example, genes are encoded by a number close to 100 base pairs, or codons that encode the twenty standard amino acids are formed of 3-mers. LRD should also be designed to compare DNA strings based on k-mers and not on single characters.

It is interesting to note that LRD does not require an alignment of the strings by the addition of insertions and deletions, unlike other commonly used phylogenetic analysis methods. The most common methods in phylogeny deal with

aligned strings, and the alignment process is itself complicated. Removing this step greatly speeds up the calculation of the distance between two strings.

Both rank distance [Dinu, 2003] and LRD [Ionescu, 2013a] are related to the rearrangement distance [Amir et al., 2006]. The rearrangement distance works with indexed k-mers and is based on a process of converting a string into another, while LRD does not impose such global rules. LRD focuses only on the local phenomenon present in DNA: strings may contain similar k-mers that are not perfectly aligned.

8.2 Local Rank Distance Definition

To compute the LRD between two DNA strings, the idea is to sum up all the offsets of similar k-mers between the two strings. For every k-mer in one string, the LRD approach is to search for a similar k-mer in the other string. First, LRD looks for similar k-mers in the same position in both DNA strings. If those k-mers are similar, it sums up 0 since there is no offset between them. If the k-mers are not similar, it starts looking around the initial k-mer position in the second string to find a k-mer similar to the one in the first DNA string. If a similar k-mer is found during this process, the offset between the two k-mers is summed up to the total distance. The search goes on until a similar k-mer is found or until a maximum offset is reached. Note that the maximum k-mer offset must be set a priori and should be proportional to the size of the alphabet and to the lengths of the DNA strings. Using the maximum offset parameter ensures that the search is limited by a fixed window centered on the initial k-mer position. Finding similar matches beyond this window is costly and it may also bring unwanted noise in the process. A similar search limitation brought improvements in terms of accuracy and speed for Local Patch Dissimilarity [Dinu et al., 2012; Ionescu & Popescu, 2013a]. LRD is formally defined next.

Definition 14 *Let $S_1, S_2 \in \Sigma^*$ be two strings with symbols (k-mers) from the*

alphabet Σ. *Local Rank Distance between* S_1 *and* S_2 *is defined as:*

$$\begin{aligned}\Delta_{LRD}(S_1, S_2) &= \Delta_{left} + \Delta_{right} \\ &= \sum_{x_s \in S_1} \min_{x_s \in S_2} \{|pos_{S_1}(x_s) - pos_{S_2}(x_s)|, m\} \\ &+ \sum_{y_s \in S_2} \min_{y_s \in S_1} \{|pos_{S_1}(y_s) - pos_{S_2}(y_s)|, m\},\end{aligned} \tag{8.1}$$

where x_s *and* y_s *are occurrences of symbol* $s \in \Sigma$ *in strings* S_1 *and* S_2, $pos_S(x_s)$ *represents the position (or the index) of the occurrence* x_s *of symbol* $s \in \Sigma$ *in string* S, *and* $m \geq 1$ *is the maximum offset.*

A string may contain multiple occurrences of a symbol $s \in \Sigma$. LRD matches each occurrence x_s of symbol $s \in \Sigma$ from a string, with the nearest occurrence of symbol s in the other string. A symbol can be defined either as a single character, or as a sequence of characters (k-mer). Overlapping k-mers are also permitted in the computation of LRD, since there is no restriction that tells where k-mers should start or end in a DNA string. Notice that in order to be a symmetric distance measure, LRD must consider every k-mer in both strings. Offsets between matched k-mers are computed with the euclidean distance based on the L_1-norm. Thus, offsets are always non-negative integer values.

To understand how LRD actually works, it is useful to consider Example 4 where LRD is computed between strings s_1 and s_2 from Example 3 using 1-mers (single characters).

Example 4 *Let* s_1 *and* s_2 *be defined as in Example 3, and* $m = 10$ *be the maximum offset. The LRD between* s_1 *and* s_2 *is given by:*

$$\Delta_{LRD}(s_1, s_2) = \Delta_{left} + \Delta_{right},$$

where the two sums Δ_{left} *and* Δ_{right} *are computed as follows:*

$$\begin{aligned}\Delta_{left} &= \sum_{x_s \in s_1} \min_{x_s \in s_2} \{|pos_{s_1}(x_s) - pos_{s_2}(x_s)|, 10\} \\ &= |1-4| + |2-4| + |3-2| + |4-3| + |5-3| \\ &+ |6-5| + |7-7| + |8-6| + |9-2| = 19,\end{aligned}$$

$$\Delta_{right} = \sum_{y_s \in s_2} \min_{y_s \in s_1} \{|pos_{s_1}(y_s) - pos_{s_2}(y_s)|, 10\}$$
$$= |1-6| + |2-3| + |3-4| + |4-2| + |5-6|$$
$$+ |6-8| + |7-7| = 12.$$

In other words, Δ_{left} considers every 1-mer from s_1, while Δ_{right} considers every 1-mer from s_2. It is easy to observe that $\Delta_{LRD}(s_1, s_2) = \Delta_{LRD}(s_2, s_1)$.

An interesting fact to mention in favor of LRD is that it has successfully been used for native language identification [Popescu & Ionescu, 2013], achieving an accuracy of 75.8% in the closed NLI Shared Task [Tetreault et al., 2013]. This shows that LRD can be used as a general approach to measure string similarity, despite of being designed for DNA. The application of LRD on text data for native language identification is further discussed in Chapter 9.

8.3 Local Rank Distance Algorithm

Algorithm 9 computes the LRD between DNA strings seq_1 and seq_2 using k-mers. In this algorithm, k-mers are paired when they match exactly. Another solution that is more flexible, is to compute the similarity between k-mers using the Hamming distance. In this case, a threshold should be used to determine which k-mers are similar and which are not. This will allow LRD to pair k-mers even in the presence of different mutations in DNA. Using Hamming distance between k-mers also implies a more computationally heavy algorithm.

Algorithm 9 *Local Rank Distance*
***Input**:*
seq_1 – *a DNA sequence of* l_1 *bases;*
seq_2 – *another DNA sequence of* l_2 *bases;*
k – *the size of the* k*-mers to be compared;*
m – *the maximum offset.*
***Initialization**:*
$dist = 0$
***Computation**:*

```
for i = 1 to l_1 − k + 1 // compute Δ_left
    get k-mer_i at position i in seq_1
    j = 0
    found = false
    while j < m and found == false
        get k-mer_left at position i − j in seq_2
        get k-mer_right at position i + j in seq_2
        if k-mer_i == k-mer_left or k-mer_i == k-mer_right
            dist = dist + j
            found = true
        endif
        j = j + 1
    endwhile
    if found == false
        dist = dist + m
    endif
endfor
for i = 1 to l_2 − k + 1 // compute Δ_right
    get k-mer_i at position i in seq_2
    j = 0
    found = false
    while j < m and found == false
        get k-mer_left at position i − j in seq_1
        get k-mer_right at position i + j in seq_1
        if k-mer_i == k-mer_left or k-mer_i == k-mer_right
            dist = dist + j
            found = true
        endif
        j = j + 1
    endwhile
    if found == false
        dist = dist + m
    endif
```

endfor

***Output**:*

dist – the Local Rank Distance between seq_1 and seq_2.

Algorithm 9 needs two input parameters besides the two DNA strings. The k-mer size parameter represents the number of characters (bases) for the substrings involved in the computation of LRD. The maximum offset parameter determines the size of the search window. These parameters need to be adjusted with regard to the length of the DNA strings. For example, using 10-mers for DNA strings of 100 or 200 bases is not reasonable, since finding similar 10-mers in such short DNA strings is rare, if not almost impossible. But 10-mers are suited for mitochondrial DNA strings of $15.000 - 17.000$ bases. Notice that the maximum offset parameter should be adjusted accordingly. Using 10-mers and a maximum offset that is too small, such as 50, will result in finding almost no similar 10-mers in the search window. This happens because there are $|\Sigma|^k$ possible k-mers, where $|\Sigma|$ is the size of the alphabet $\Sigma = \{A, C, G, T\}$. In the case of 10-mers, it means that there are $4^{10} = 1.048.576$ combinations.

The analysis of the computational complexity of Algorithm 9 is straightforward. Let $l = \max\{l_1, l_2\}$ be the maximum length of the two strings. The complexity of the Algorithm 9 is $O(l \times m \times k)$, when using brute (linear) search to find similar k-mers. Using advanced string searching algorithms [Knuth et al., 1977] the complexity can be reduced to $O(l \times m)$. If only 1-mers are considered, the computational complexity of LRD becomes linear as Hamming distance or rank distance. If approximate matches are allowed between k-mers, by using Hamming distance to compare k-mers for example, the time complexity remains $O(l \times m \times k)$, since computing the Hamming distance between two strings (or k-mers) cannot be done faster than linear time.

8.4 Properties of Local Rank Distance

LRD replicates how Local Patch Dissimilarity works on images. As Local Patch Dissimilarity is adapted to images, LRD is based on principles that make it more

suited to DNA sequences. LRD essentially measures the non-alignment score between k-mers. Both LRD and Local Patch Dissimilarity can be considered as extended versions of rank distance [Dinu, 2003], which are adapted to specific input data. Despite the fact that LRD is more adapted to DNA strings, LRD remains a distance function. A proof that LRD is a distance function is first given. More theoretical properties of LRD are studied next. The expected distance between two random strings is also discussed in this section. Finally, the lower and and the upper bounds of LRD with respect to the Hamming distance are given.

The definition of a distance function is considered next, as the first concern of this section is to prove that LRD is a distance measure.

Definition 15 *A metric on a set X is a function (called the distance function or simply distance) $d : X \times X \to \mathbb{R}$. For all $x, y, z \in X$, this function is required to satisfy the following conditions:*

$$
\begin{aligned}
&(i)\ d(x,y) \geqslant 0 \ \textit{(non-negativity, or separation axiom);}\\
&(ii)\ d(x,y) = 0 \ \textit{if and only if } x = y \ \textit{(coincidence axiom);}\\
&(iii)\ d(x,y) = d(y,x) \ \textit{(symmetry);}\\
&(iv)\ d(x,z) \leqslant d(x,y) + d(y,z) \ \textit{(triangle inequality).}
\end{aligned}
$$

One can observe that axioms (i) and (ii) from Definition 15 produce positive definiteness. It can be easily observed that LRD is not a distance function if a k-mer from one string is associated with two or more identical k-mers from the other string. However, it can be demonstrated that LRD is a distance function for a given $k \geq 1$, such that all the k-mers occur only a single time in each of the two strings.

Theorem 6 *For all $k \geq 1$, such that all the k-mers of length k occur only a single time in each of the compared strings, Local Rank Distance is a distance function.*

Proof: The proof is based on showing that Δ_{LRD} given by Definition 14 satisfies the conditions in Definition 15.

Let $S_1, S_2 \in \Sigma^*$.

(i) **Proof of non-negativity**

$\Delta_{LRD}(S_1, S_2)$ is a sum of positive or 0 values that represent offsets between symbols in S_1 and S_2. This sum can only be greater or equal to 0. This ensures the non-negativity condition in Definition 15.

(ii) **Proof of coincidence axiom**

($\Rightarrow$): Let $\Delta_{LRD}(S_1, S_2) \neq 0$. There is at least one occurrence $x_s \in S_1$ for which $\min_{x_s \in S_2}\{|pos_{S_1}(x_s) - pos_{S_2}(x_s)|, m\} > 0$, or at least one occurrence $y_s \in S_2$ for which $\min_{y_s \in S_1}\{|pos_{S_1}(y_s) - pos_{S_2}(y_s)|, m\} > 0$, otherwise $\Delta_{LRD}(S_1, S_2)$ would be 0.

Case 1: If $\min_{x_s \in S_2}\{|pos_{S_1}(x_s) - pos_{S_2}(x_s)|, m\} > 0$, then the symbol s corresponding to $x_s \in S_1$ does not occur in the same position in S_2 as in S_1. It means S_2 contains a symbol different from s at the position given by $pos_{S_1}(x_s)$. $S1$ and $S2$ have at least one different symbol, therefore $S_1 \neq S_2$.

Case 2: If $\min_{y_s \in S_1}\{|pos_{S_1}(y_s) - pos_{S_2}(y_s)|, m\} > 0$, the proof is analogous to Case 1. The implication is proven.

($\Leftarrow$): Let $S_1 \neq S_2$. There is at least one position i in S_1, or j in S_2 with different symbols.

Case 1: The occurrence x_s of symbol s at position $i = pos_{S_1}(x_s)$ in S_1 is considered. Since S_2 does not contain the same symbol s at position i, $\min_{x_s \in S_2}\{|pos_{S_1}(x_s) - pos_{S_2}(x_s)|, m\} > 0$. In other words, there is at least one term in the sum Δ_{left} that is positive. Consequently, $\Delta_{LRD}(S_1, S_2) \neq 0$.

Case 2: The proof for occurrence y_s of symbol s at position $j = pos_{S_2}(y_s)$ in S_2 is analogous to Case 1. The coincidence axiom is proven.

(iii) **Proof of symmetry**

Using the commutative property of the + operation and that of the euclidean

distance, the proof of symmetry for Δ_{LRD} is immediate:

$$\begin{aligned}\Delta_{LRD}(S_1, S_2) = &\sum_{x_s \in S_1} \min_{x_s \in S_2} \{|pos_{S_1}(x_s) - pos_{S_2}(x_s)|, m\} + \\ &+ \sum_{y_s \in S_2} \min_{y_s \in S_1} \{|pos_{S_1}(y_s) - pos_{S_2}(y_s)|, m\} \\ &= \sum_{y_s \in S_2} \min_{y_s \in S_1} \{|pos_{S_2}(y_s) - pos_{S_1}(y_s)|, m\} + \\ &+ \sum_{x_s \in S_1} \min_{x_s \in S_2} \{|pos_{S_2}(x_s) - pos_{S_1}(x_s)|, m\} = \Delta_{LRD}(S_2, S_1).\end{aligned} \tag{8.2}$$

(iv) **Proof of triangle inequality**

Let $A, B, C \in \Sigma^*$. To show that

$$\Delta_{LRD}(A, B) + \Delta_{LRD}(B, C) \geq \Delta_{LRD}(A, C), \tag{8.3}$$

the Δ_{left} and Δ_{right} sums are treated as separate inequalities, as follows:

$$\Delta_{left}(A, B) + \Delta_{left}(B, C) \geq \Delta_{left}(A, C), \tag{8.4}$$

$$\Delta_{right}(A, B) + \Delta_{right}(B, C) \geq \Delta_{right}(A, C). \tag{8.5}$$

Obviously, summing inequalities given by equations 8.4 and 8.5, the triangle inequality (equation 8.3) for LRD is obtained. Regarding equation 8.4, for each occurrence x_s in A, B and C, there are three possible cases for the positions of x_s in the respective strings. Let $i = pos_A(x_s)$ be a fixed position of x_s in A. Let j and k denote the nearest positions of x_s in B and C, respectively. Positions j and k are formally defined as:

$$\begin{aligned}j &= \operatorname*{argmin}_{p = pos_B(x_s)} \{|i - p|, m\}, \\ k &= \operatorname*{argmin}_{q = pos_C(x_s)} \{|i - q|, m\}.\end{aligned} \tag{8.6}$$

There are six possible combinations of sorting positions i, j, k in ascending

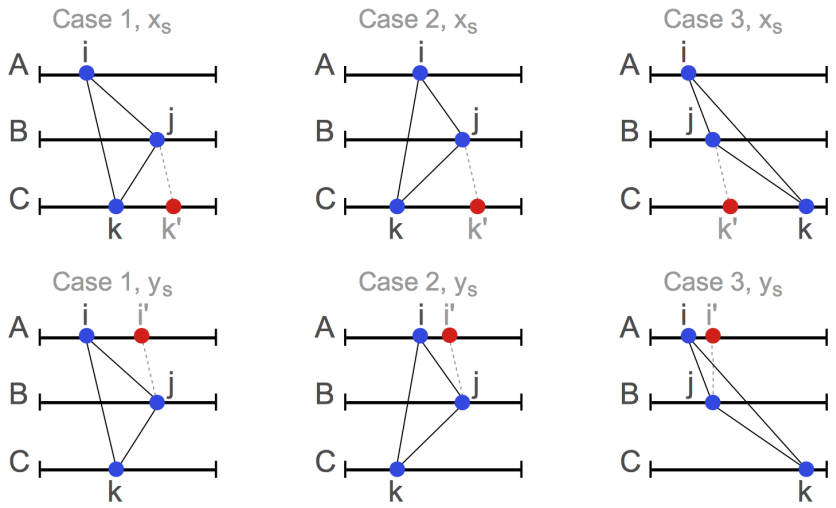

Figure 8.1: The intuition behind the proof of the triangle inequality for LRD. For each occurrence x_s, the three possible cases of sorting i, j and k are shown in the upper side of the figure. The nearest match position in C is denoted by k'. For each occurrence y_s, the three possible cases are shown in the lower side of the figure. The nearest match position in A is denoted by i'.

order. This brings three distinct situations (or cases) that are discussed next. Figure 8.1 shows the intuition behind the demonstration of the triangle inequality. Cases 1, 2 and 3 for occurrences x_s can be observed visually.

Case 1 ($i < k < j$ or $j < k < i$):

Since LRD works with absolute positive values and $i < k < j$ or $j < k < i$, the following inequality is true:

$$|i - j| \geq |i - k|. \tag{8.7}$$

Note that the occurrence of x_s in B may be matched with another closer occurrence of x_s in C rather than the occurrence at position k. Let k' denote the position of this nearest occurrence. Position k' is formally defined as:

$$k' = \underset{q=pos_C(x_s)}{\operatorname{argmin}} \{|j - q|, m\}. \tag{8.8}$$

If position k' exists, then:

$$|j - k| > |j - k'| \geq 0. \tag{8.9}$$

If a distinct k' does not exist, then $k' = k$. From equations 8.7 and 8.9, it results that the triangle inequality is satisfied for each x_s (even when $k' \neq k$):

$$|i - j| + |j - k'| \geq |i - k|. \tag{8.10}$$

Case 2 ($k < i < j$ or $j < i < k$):

Note that the euclidean distance based on the L_1-norm is used to compute differences between positions i, j and k. Since the euclidean distance satisfies the triangle inequality, the following equation is also satisfied:

$$|i - j| + |j - k| \geq |i - k|. \tag{8.11}$$

As in Case 1, the occurrence of x_s in B may be matched with another closer occurrence of x_s in C. Let k' defined as in equation 8.8 denote the position of this nearest occurrence. If $k' \neq k$ exists, then equation 8.9 also holds for Case 2. However, the equation 8.11 still holds if the condition in equation 8.7 is met. In other words, the triangle inequality is still satisfied if the offset (euclidean distance) between i and j is greater than the offset between i and k.

In the other case, when the condition in equation 8.7 is not met, the following equations are possible:

$$|i - j| + |j - k'| \leq |i - k|, \tag{8.12}$$

$$|i - j| + |j - k'| \geq |i - k'|. \tag{8.13}$$

Equations 8.12 and 8.13 imply that:

$$|i - k| \geq |i - k'|. \tag{8.14}$$

From the definition of LRD and equation 8.14, it results that $k' = k$. This

contradicts the assumption that $k' \neq k$. Therefore, equation 8.12 can never be true, and the triangle inequality holds for Case 2.

Case 3 ($i < j < k$ or $k < j < i$):

Case 3 is similar to Case 2. Since the euclidean distance satisfies the triangle inequality, equation 8.11 is also satisfied for this case. As in Case 1, the occurrence of x_s in B may be matched with another closer occurrence of x_s in C. Let k' defined as in equation 8.8 denote the position of this nearest occurrence. If $k' \neq k$ exists, then equation 8.9 also holds for Case 3.

However, the condition in equation 8.7 cannot be met since $i < j < k$ or $k < j < i$, and equations 8.12 and 8.13 become possible. Again, equations 8.12 and 8.13 imply equation 8.14. From the definition of LRD and equation 8.14, it results that $k' = k$, contradicting the assumption that $k' \neq k$.

For each occurrence x_s in A, B and C, the triangle inequality is satisfied. This implies that equation 8.4 is true, because Δ_{left} involves only x_s. The demonstration is similar for each occurrence y_s in A, B and C. The difference is made by the fact that the occurrence of y_s in B may be matched with another closer occurrence of y_s in A, also shown in Figure 8.1. Equation 8.5 is also true, because Δ_{right} involves only y_s. Finally, LRD satisfies the conditions in Definition 15. This ends the proof of Theorem 6. □

The coincidence axiom is not longer verified if approximate matches are allowed between k-mers. The use of Hamming distance to compare k-mers (and match them under a similarity threshold) may seem appropriate from a biological point of view, but from a mathematical point of view, LRD can no longer be considered a distance function. In practice, better results may be obtained by using approximate matches, but this subject is left for future study.

LRD measures the distance between two DNA strings. Knowing the maximum offset (used to stop similar k-mer searching), the maximum LRD value between two strings can be computed as the product between the maximum offset and the number of pairs of compared k-mers. Thus, LRD can be normalized to a value in the $[0, 1]$ interval. By normalizing, LRD can also be transformed into a similarity or dissimilarity measure.

The following theorem gives an approximation of LRD between two random strings.

Theorem 7 *Given $S_1, S_2 \in \Sigma^*$ and a maximum offset threshold m, where Σ is an alphabet of symbols (or k-mers), the expected Local Rank Distance between S_1 and S_2 can be approximated by:*

$$\Delta_{LRD}(S_1, S_2) \approx \left[\left(1 - \left(\frac{|\Sigma| - 1}{|\Sigma|} \right)^{2m+1} \right) \frac{m}{2} + \left(\frac{|\Sigma| - 1}{|\Sigma|} \right)^{2m+1} m \right] (|S_1| + |S_2|), \tag{8.15}$$

where $|\Sigma|$ gives the number of symbols in Σ, $|S_1|$ is the length of S_1, and $|S_2|$ is the length of S_2, respectively.

Proof: For every symbol that occurs in S_1, LRD adds the offset to the nearest occurrence in S_2. In the same manner, for every symbol that occurs in S_2, LRD adds the offset to the nearest occurrence in S_1. If the expected offset is defined by $x \in [0, m]$, then the following equation approximates LRD:

$$\Delta_{LRD}(S_1, S_2) \approx x(|S_1| + |S_2|). \tag{8.16}$$

To determine the expected offset x of a certain symbol, the following discussion is made. Let s be a symbol from Σ. LRD searches for symbol s in a window of $2m + 1$ symbols. But the symbol s may or may not occur in the search window. Let A be the event defined by "there is at least one occurrence of symbol s in a string of $2m + 1$ symbols". Let A^C denote the complementary event of A.

The probability of event A^C is given by:

$$P(A^C) = \left(\frac{|\Sigma| - 1}{|\Sigma|} \right)^{2m+1}. \tag{8.17}$$

The probability of event A can be determined using equation 8.17 as follows:

$$P(A) = 1 - P(A^C) = 1 - \left(\frac{|\Sigma| - 1}{|\Sigma|} \right)^{2m+1}. \tag{8.18}$$

When event A occurs, the average offset of symbol s is $m/2$, since each position in the search window is equally likely to be the occurrence of s. When the

complementary event A^C occurs, LRD adds the maximum offset, since symbol s is not found in the search window. Thus, the expected offset is given by:

$$x = \left(1 - \left(\frac{|\Sigma| - 1}{|\Sigma|}\right)^{2m+1}\right)\frac{m}{2} + \left(\frac{|\Sigma| - 1}{|\Sigma|}\right)^{2m+1} m \tag{8.19}$$

By replacing x in equation 8.16 with the value determined in equation 8.19, the equation 8.15 is obtained. This ends the proof. □

Theorem 7 approximates the expected distance between two strings. This approximation is useful in practice, especially when one wants to determine the similarity of two strings. If the obtained distance is lower than the value given in equation 8.15, then the strings can be considered as being similar. Otherwise, the strings can be considered as being dissimilar.

The following theorem shows the relationship between LRD and Hamming distance.

Theorem 8 *Given $S_1, S_2 \in \Sigma^*$ and a maximum offset threshold m, the following equation gives the lower and the upper bounds of the Local Rank Distance with respect to the Hamming distance:*

$$\Delta_H(S_1, S_2) \leq \Delta_{LRD}(S_1, S_2) \leq m \cdot \Delta_H(S_1, S_2). \tag{8.20}$$

Proof: Let X be the set of positions with matching symbols in S_1 and S_2. The Hamming distance is given by:

$$\Delta_H(S_1, S_2) = |S_1| - |X| + |S_2| - |X|, \tag{8.21}$$

where $|X|$ is the size of set X, $|S_1|$ is the length of S_1, and $|S_2|$ is the length of S_2, respectively. Basically, the Hamming distance counts the number of symbols that are not matched between S_1 and S_2. In the same manner, LRD adds an offset of 0 for the symbols in X. For the other symbols, LRD adds an offset in the interval $[1, m]$. The bounds are determined by considering the two extreme cases.

Supposing that LRD always adds an offset of 1 for unmatched symbols, the

following equation is true:

$$\Delta_{LRD}(S_1, S_2) = |S_1| - |X| + |S_2| - |X|. \tag{8.22}$$

Since 1 is the minimum offset that can be added, the lower bound is obtained from equations 8.21 and 8.22:

$$\Delta_H(S_1, S_2) \leq \Delta_{LRD}(S_1, S_2). \tag{8.23}$$

Supposing that LRD always adds an offset of m for unmatched symbols, the following equation is true:

$$\Delta_{LRD}(S_1, S_2) = m\left(|S_1| - |X|\right) + m\left(|S_2| - |X|\right). \tag{8.24}$$

Since m is the maximum offset that can be added, the upper bound is obtained from equations 8.21 and 8.24:

$$\Delta_{LRD}(S_1, S_2) \leq m \cdot \Delta_H(S_1, S_2). \tag{8.25}$$

□

Theorem 8 shows that LRD is a much more sensible distance than the Hamming distance. LRD is being able to capture not only the unmatched symbols, but also the offsets of such symbols. These offsets are recorded at a very fine scale, giving LRD the power to find subtle differences between the two strings.

8.5 Experiments and Results

8.5.1 Data Set Description

LRD is tested on two important problems in bioinformatics: the phylogenetic analysis of mammals and the finding of common substrings in a set of given DNA strings. In the experiments presented in this chapter, mitochondrial DNA sequence genome of the 27 mammals is used. The 27 mammals along with their associated accession numbers are given in Table 8.1. The mtDNA sequences are

available for download in the EMBL database (http://www.ebi.ac.uk/ena/). The mammals selected for the experiments belong to one of the following 8 orders: Carnivora, Cetartiodactylae, Chiroptera, Metatheria, Monotremata, Perissodactylae, Primates, and Rodentia.

Table 8.1: The 27 mammals from the EMBL database used in the phylogenetic experiments. The accession number is given on the last column.

Mammal	Latin Name	Accession
human	*Homo sapiens*	V00662
common chimpanzee	*Pan troglodytes*	D38116
pigmy chimpanzee	*Pan paniscus*	D38113
gorilla	*Gorilla gorilla*	D38114
orangutan	*Pongo pygmaeus*	D38115
Sumatran orangutan	*Pongo pygmaeus abelii*	X97707
gibbon	*Hylobates lar*	X99256
hamadryas baboon	*Papio hamadryas*	Y18001
horse	*Equus caballus*	X79547
donkey	*Equus asinus*	X97337
Indian rhinoceros	*Rhinoceros unicornis*	X97336
white rhinoceros	*Ceratotherium simum*	Y07726
harbor seal	*Phoca vitulina*	X63726
gray seal	*Halichoerus grypus*	X72004
cat	*Felis catus*	U20753
fin whale	*Balaenoptera physalus*	X61145
blue whale	*Balaenoptera musculus*	X72204
cow	*Bos taurus*	V00654
sheep	*Ovis aries*	AF010406
pig	*Sus scrofa*	AF034253
rat	*Rattus norvegicus*	X14848
mouse	*Mus musculus*	V00711
fat dormouse	*Myoxus glis*	AJ001562
Jamaican fruit-eating bat	*Artibeus jamaicensis*	AF061340
North American opossum	*Didelphis virginiana*	Z29573
wallaroo	*Macropus robustus*	Y10524
platypus	*Ornithorhynchus anatinus*	X83427

Some general aspects on mtDNA sequences are discussed in Section 7.6. It is worth mentioning that mtDNA from two individuals of the same species differs by only 0.1%. This means, for example, that mtDNA from two different humans

differs by less than 20 base pairs. Because this small difference cannot affect the study, the experiments are conducted using a single mtDNA sequence for each mammal, as in Chapter 7.

8.5.2 Phylogenetic Analysis

Two experiments are performed on the phylogenetic analysis of mammals. The first one includes mitochondrial DNA sequence genome of 22 mammals from the EMBL database. Results on this data set of 22 mammals are also reported by [Dinu & Ionescu, 2012a, 2013a; Dinu & Sgarro, 2006]. Similar studies were also performed by [Cao et al., 1998; Li et al., 2004; Reyes et al., 2000].

In this work, a hierarchical clustering technique based on LRD, using the average linkage criterion, is tested on the 22 mammals data set. Single or complete linkage criteria show similar results, but the average linkage seems to work best in combination with LRD. Figures 8.2, 8.3, 8.4, 8.5, 8.6 show the results obtained with the hierarchical clustering based on LRD using different k-mer sizes. As the size of the k-mers grows, the dendrograms look better and better. For LRD with 8-mers (Figure 8.5) and 10-mers (Figure 8.6), perfect phylogenetic trees are obtained. In other words, mammals are clustered according to their biological orders. The maximum offset of LRD ranges from 640 to 1000, and it is adjusted proportional to the size of k-mers used. Another dendrogram presented in Figure 8.7 is obtained by summing up the Local Rank Distances with 6-mers, 7-mers, 8-mers, 9-mers and 10-mers, respectively. Again, mammals are perfectly clustered according to their orders. The idea of summing up distances obtained with different k-mers makes the hierarchical clustering method more robust.

Table 8.2 shows the number of misclustered mammals of previously proposed techniques and that of the hierarchical clustering based on LRD with sum of k-mers. The best result with 100% accuracy is obtained by the hierarchical clustering based on LRD.

Since the hierarchical clustering based on LRD obtains perfect accuracy, another clustering experiment with more DNA sequences is performed. This second experiment includes mtDNA sequences from all the 27 mammals obtained from the EMBL database. If 8-mers are enough to obtain a perfect phylogenetic tree

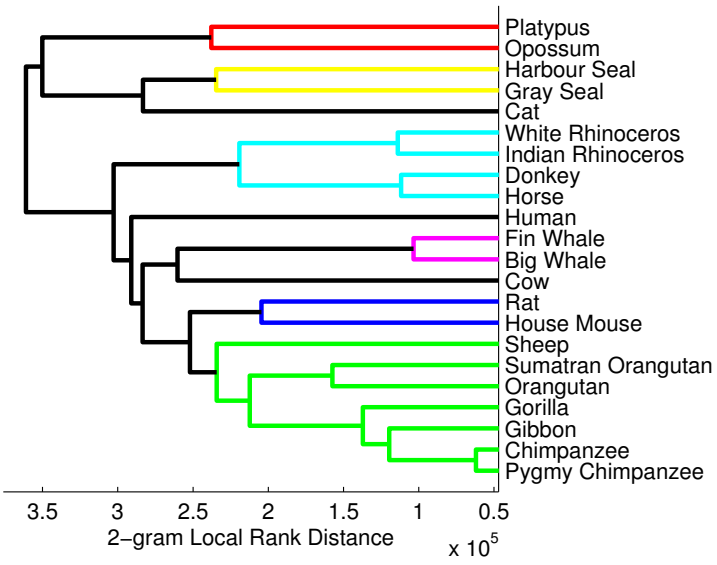

Figure 8.2: Phylogenetic tree obtained for 22 mammalian mtDNA sequences using LRD based on 2-mers.

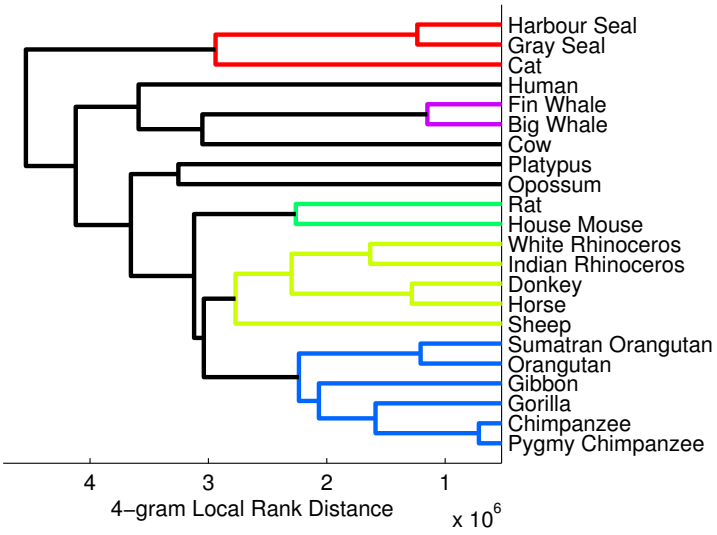

Figure 8.3: Phylogenetic tree obtained for 22 mammalian mtDNA sequences using LRD based on 4-mers.

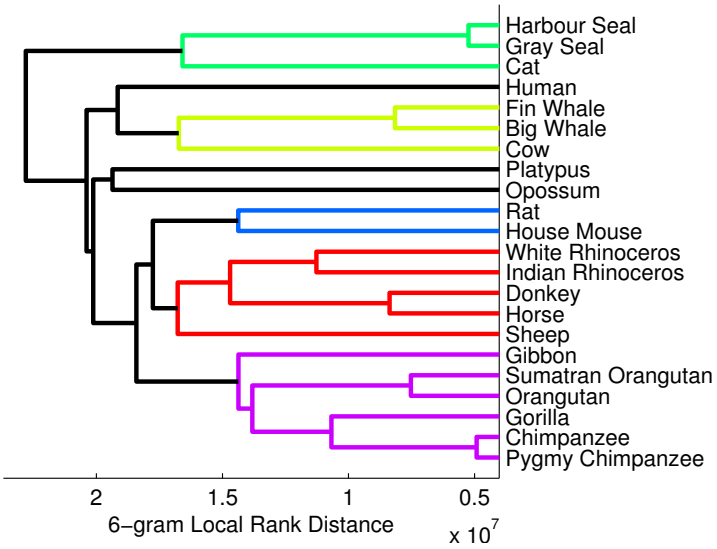

Figure 8.4: Phylogenetic tree obtained for 22 mammalian mtDNA sequences using LRD based on 6-mers.

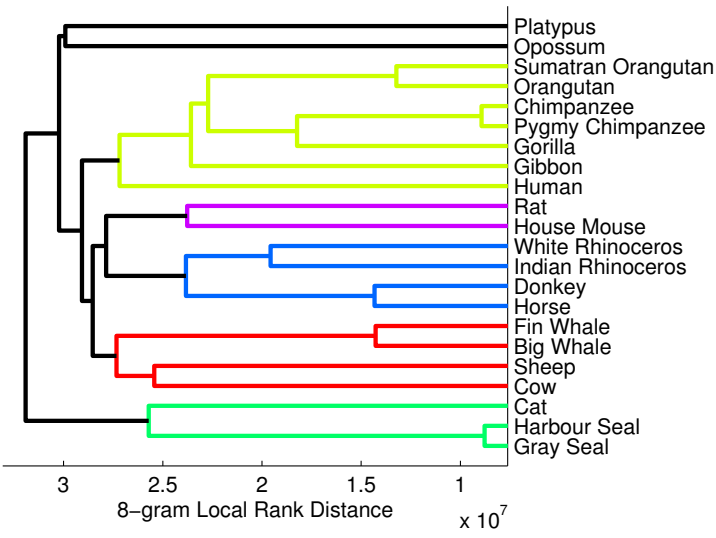

Figure 8.5: Phylogenetic tree obtained for 22 mammalian mtDNA sequences using LRD based on 8-mers.

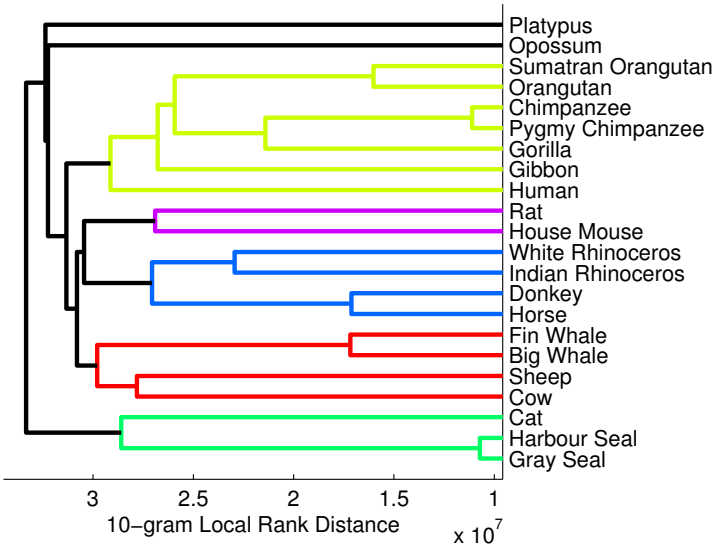

Figure 8.6: Phylogenetic tree obtained for 22 mammalian mtDNA sequences using LRD based on 10-mers.

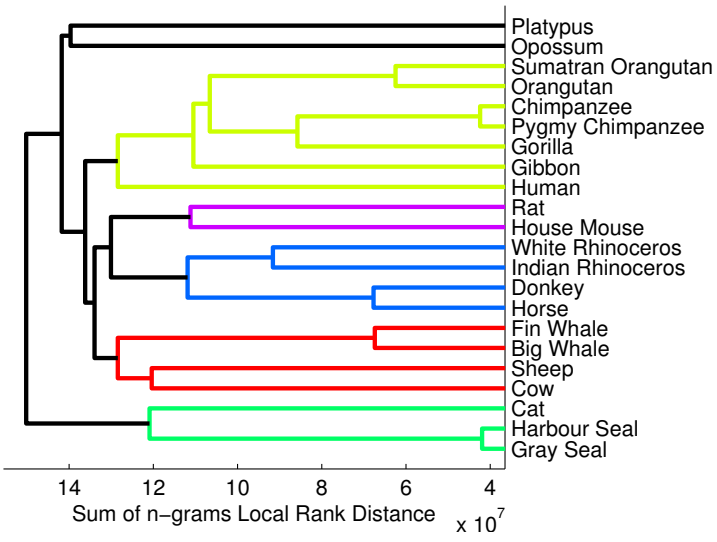

Figure 8.7: Phylogenetic tree obtained for 22 mammalian mtDNA sequences using LRD based on sum of k-mers.

Table 8.2: The number of misclustered mammals for different clustering techniques on the 22 mammals data set.

Method	Misclustered	Accuracy
Proposed by [Dinu & Sgarro, 2006]	3/22	86.36%
Proposed by [Dinu & Ionescu, 2012a]	3/22	86.36%
LRD + sum of k-mers	0/22	100.00%

in the first experiment, longer k-mers are considered for the second experiment. Figure 8.8 shows the dendrogram obtained by the hierarchical clustering based on LRD using 18-mers. Again the average linkage criterion gives the best results. The only mistake of the proposed method is that it clusters the pig together with members of the Carnivora order instead of the Cetartiodactylae order. Having 1 out of 27 misclustered mammals, the accuracy is 96.29% this time.

Overall, the accuracy level achieved by the clustering method based on LRD is better or at least comparable with state of the art methods proposed in similar studies [Cao et al., 1998; Dinu & Sgarro, 2006; Li et al., 2004; Reyes et al., 2000].

8.5.3 DNA Comparison

In this section an experiment is performed to show that LRD can also be used to find the closest string (or closest substring) for set of DNA strings, using a genetic algorithm based on LRD. Here, the genetic algorithm proposed in [Dinu & Ionescu, 2012b] is combined with LRD.

Only the rat, house mouse, fat dormouse and cow genomes are used in the experiment. The task is to find the closest string between the rat and house mouse DNAs, between the rat and fat dormouse DNAs, and between the rat and cow DNAs. The goal of this experiment is to compare the distances associated to the three closest strings. The cow belongs to the Cetartiodactylae order, while the rat, the house mouse, and the fat dormouse belong to the Rodentia order. Expected results should show that the rat-house mouse distance and the rat-fat dormouse distance are smaller than the rat-cow distance. The same experiment was also conducted in [Dinu & Ionescu, 2012b] by using three genetic algorithms based on Hamming distance, edit distance and rank distance, respectively. To compare

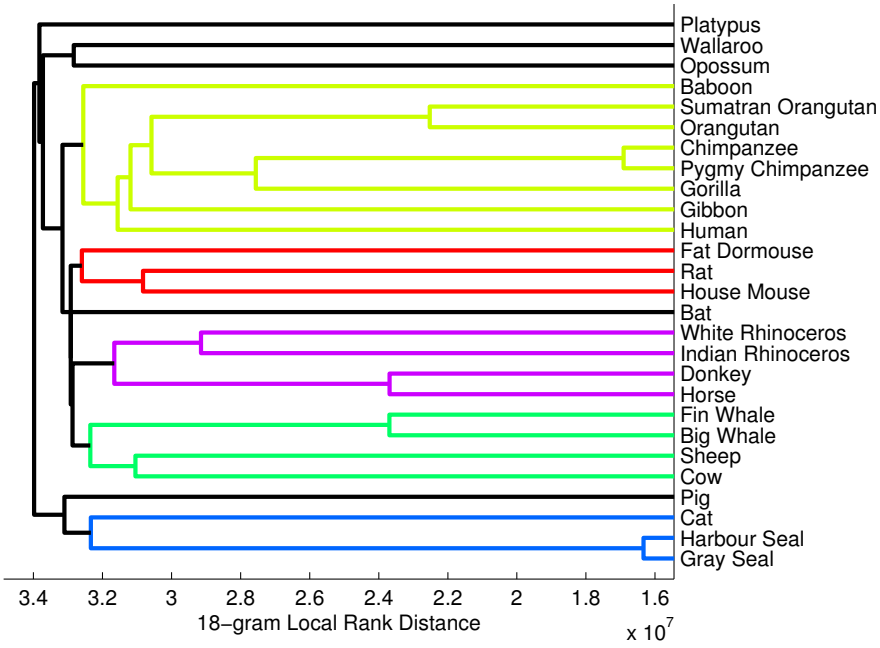

Figure 8.8: Phylogenetic tree obtained for 27 mammalian mtDNA sequences using LRD based on 18-mers

the results of these algorithms with the results obtained by the genetic algorithm based on LRD, the same experiment setting is used. The genetic algorithm parameters used to obtain the presented results are given next. The population size is 600 chromosomes, the number of generations is 200, the crossover probability is 0.36, the mutation probability is 0.005, and size of each DNA sequence is 150 bases. Details regarding experiment organization and parameters of the genetic algorithm can also be found in [Dinu & Ionescu, 2012b]. The results presented in Table 8.3 are obtained using LRD with 3-mers and a maximum offset of 48. The reported time is computed by measuring the average time of 10 runs of the genetic algorithm on a computer with Intel Core i7 2.3 GHz processor and 8 GB of RAM memory using a single Core.

Table 8.3: Closest string results for the genetic algorithm based on LRD with 3-mers.

LRD Results	rat-house mouse	rat-fat dormouse	rat-cow
Distance	1524	2379	4169
Average time	12 seconds	14 seconds	17 seconds

Figure 8.9 shows the distance evolution of the best chromosome at each generation for Local Rank Distance, rank distance, Hamming distance and edit (Levenshtein) distance. The use of LRD enables the genetic algorithm to achieve better results than previously studied genetic algorithms [Dinu & Ionescu, 2012b], but with a smaller population of chromosomes (600 instead of 1800) and a lower number of generations (200 instead of 300). In terms of speed, the proposed method is similar to the other algorithms based on low-complexity distances (Hamming and rank distance).

8.6 Discussion and Future Work

Designed to conform to more general principles and adapted to DNA strings, LRD comes to improve several state of the art methods for DNA sequence analysis. Phylogenetic experiments show that trees produced by LRD are better or at least comparable with those reported in the literature [Dinu & Ionescu, 2012a; Dinu

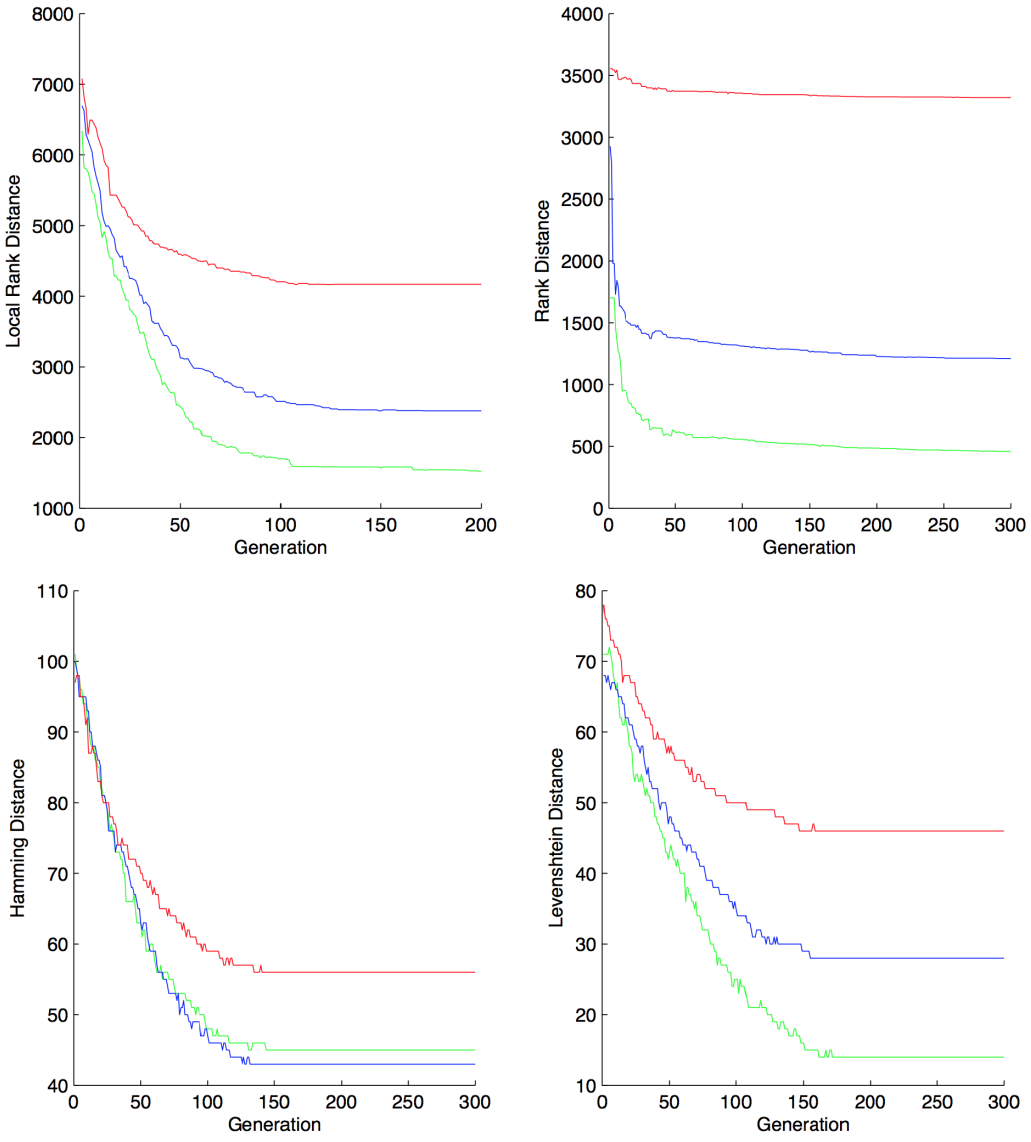

Figure 8.9: The distance evolution of the best chromosome at each generation for the Rat-Mouse-Cow experiment. GREEN = rat-house mouse distance, BLUE = rat-fat dormouse, RED = rat-cow distance.

& Sgarro, 2006; Li et al., 2004; Reyes et al., 2000]. The closest string experiment shows that the use of LRD enables genetic algorithms to achieve similar or better results than previously studied methods [Dinu & Ionescu, 2012b]. In conclusion, LRD can be used to improve the results of several methods for DNA sequence analysis or related tasks.

In future work, the Hamming distance could be used to compare k-mers in the computation of LRD. This seems to be more appropriate from a biological point of view, in that it allows the pairing of k-mers with mutations. A faster version of LRD, that considers only the significant or the most frequent k-mers, is also of great interest for sequence alignment or related tasks. Significant k-mers could be those that encode genes, for example.

An interesting fact to mention in favor of LRD is that it has successfully been used for native language identification [Popescu & Ionescu, 2013], achieving an accuracy of 75.8% in the closed NLI Shared Task [Tetreault et al., 2013]. This shows that LRD can be used as a general approach to measure string similarity, despite being designed for DNA. The native language identification results are discussed in Chapter 9.

Chapter 9

Native Language Identification with String Kernels

Using words is natural in text analysis tasks like text categorization, authorship identification and plagiarism detection, among others. Perhaps surprisingly, recent results have proved that methods handling the text at character level can also be very effective in text analysis tasks [Grozea et al., 2009; Lodhi et al., 2002; Popescu, 2011; Popescu & Dinu, 2007; Popescu & Grozea, 2012; Sanderson & Guenter, 2006]. This chapter follows this line of research and aims to investigate if the native language can be identified with machine learning methods that work at the character level. By disregarding features of natural language such as words, phrases, or meaning, an approach that works at the character level has an important advantage in that it is language independent.

This chapter describes an approach based on string kernels. In this approach, texts are treated just as sequences of symbols (strings). Different string kernels are combined with different kernel-based learning methods in a series of experiments to assess the best performance level that can be achieved on native language identification. It seems that the machine learning approach based on string kernels achieves state of the art performance in native language identification. Actually, the Unibuc team [Popescu & Ionescu, 2013] participated with the described method in the Native Language Identification (NLI) Shared Task 2013 and obtained the third place [Tetreault et al., 2013].

The chapter is organized as follows. A motivation in favor of using character level methods is given in Section 9.1. The string kernels are presented in Section 9.2. Section 9.3 explains how the LRD measure can be used for text analysis, and how to transform it into a kernel. Section 9.4 presents details about the experiments. It gives details about choosing the learning method, parameter tuning, combining kernels and results of submitted systems. Finally, the future work is discussed in Section 9.5.

9.1 Motivation and Discussion

The string kernel implicitly embeds the texts in a high dimensional feature space. Then, a kernel-based learning algorithm implicitly assigns a weight to each feature, thus selecting the features that are important for the discrimination task. For example, in the case of text categorization the learning algorithm enhances the features representing stems of content words [Lodhi et al., 2002], while in the case of authorship identification the same learning algorithm enhances the features representing function words [Popescu & Dinu, 2007].

Using string kernels will make the corresponding learning method completely language independent, because the texts will be treated as sequences of symbols (strings). Methods working at the word level or above very often restrict their feature space according to theoretical or empirical principles. Thus, a method that considers words as features can not be language independent. Even a method that uses only function words as features is not completely language independent because it needs a list of function words (specific to a language) and a way to segment a text into words which is not an easy task for some languages, like Chinese.

It is interesting to mention that character n-grams were already used in native language identification [Brooke & Hirst, 2012; Tetreault et al., 2012]. The reported performance when only character n-grams were used as features was modest compared with other type of features. But, in the above mentioned works, the authors investigated only the bigrams and trigrams, as they probably considered that longer n-grams would not improve the performance or that are too expensive to compute. Particularly, in a set of preliminary experiments of

this work, similar results with [Tetreault et al., 2012] were obtained when using character bigrams. However, the best performance has been achieved using a range of 5 to 8 n-grams. A similar approach was used with success for the related task of identifying translationese [Popescu, 2011]. Combining 5 to 8 n-grams would generate millions of features, which are indeed expensive to compute and represent. The key of avoiding to compute such a large number of features lies in using the dual representation provided by the string kernel. String kernel similarity matrices can be computed much faster and are extremely useful when the number of samples is much lower than the number of features.

The first application of string kernel ideas came in the field of text categorization, with the paper [Lodhi et al., 2002], followed by applications in bioinformatics [Leslie et al., 2002]. Computer science researchers have developed a wide variety of methods that can be applied with success in computational biology. Such methods range from clustering techniques used to analyze the phylogenetic trees of different organisms [Dinu & Ionescu, 2012a; Dinu & Sgarro, 2006], to genetic algorithms used to find motifs or common patterns in a set of given DNA sequences [Dinu & Ionescu, 2012b]. Some of these methods are based on distance measure for strings that work at the character level. Among these measures are the Hamming distance [Chimani et al., 2011; Vezzi et al., 2012], the edit distance [Shapira & Storer, 2003], the Kendall-tau distance [Popov, 2007], or the rank distance [Dinu, 2003]. A similar idea to character n-grams was introduced in the early years of bioinformatics, where k-mers are used instead of single characters [1]. There are recent studies that use k-mers for the phylogenetic analysis of organisms [Li et al., 2004], or for sequence alignment [Melsted & Pritchard, 2011]. Analyzing DNA at substring level is also more suited from a biological point of view, because DNA substrings may contain meaningful information. For example, genes are encoded by a number close to 100 base pairs, or codons that encode the twenty standard amino acids are formed of 3-mers.

The Local Rank Distance [Ionescu, 2013a] has been recently proposed as an extension of rank distance. LRD drops the annotation step of rank distance, and uses k-mers instead of single characters. Chapter 8 shows that LRD is a distance

[1] In biology, single DNA characters are also referred to as nucleotides or monomers. Polymers are also known as k-mers.

function and that it has very good results in phylogenetic analysis and DNA sequence comparison. But, LRD can be applied to any kind of string sequences, not only to DNA. Thus, LRD is transformed into a kernel and used for native language identification. Despite the fact it has no linguistic motivation, LRD gives surprisingly good results for this task. Its performance level is lower than string kernel, but LRD can contribute to the improvement of string kernel when the two methods are combined.

9.2 String Kernels

The kernel function offers to the kernel methods the power to naturally handle input data that is not in the form of numerical vectors, such as strings. The kernel function captures the intuitive notion of similarity between objects in a specific domain and can be any function defined on the respective domain that is symmetric and positive definite. For strings, many such kernel functions exist with various applications in computational biology and computational linguistics [Shawe-Taylor & Cristianini, 2004].

Perhaps one of the most natural ways to measure the similarity of two strings is to count how many substrings of length p the two strings have in common. This gives rise to the p-spectrum kernel. Formally, for two strings over an alphabet Σ, $s, t \in \Sigma^*$, the p-spectrum kernel is defined as:

$$k_p(s,t) = \sum_{v \in \Sigma^p} \text{num}_v(s) \cdot \text{num}_v(t),$$

where $\text{num}_v(s)$ is the number of occurrences of string v as a substring in s [1]. The feature map defined by this kernel associates to each string a vector of dimension $|\Sigma|^p$ containing the histogram of frequencies of all its substrings of length p (p-grams).

A variant of this kernel can be obtained if the embedding feature map is modified to associate to each string a vector of dimension $|\Sigma|^p$ containing the

[1] Note that the notion of substring requires contiguity. In [Shawe-Taylor & Cristianini, 2004], the authors discuss the ambiguity between the terms *substring* and *subsequence* across different domains: biology, computer science.

presence bits (instead of frequencies) of all its substrings of length p. Thus, the character p-grams presence bits kernel is obtained:

$$k_p^{0/1}(s,t) = \sum_{v \in \Sigma^p} \text{in}_v(s) \cdot \text{in}_v(t),$$

where $\text{in}_v(s)$ is 1 if string v occurs as a substring in s, and 0 otherwise.

Normalized versions of these kernels ensure a fair comparison of strings of different lengths:

$$\hat{k}_p(s,t) = \frac{k_p(s,t)}{\sqrt{k_p(s,s) \cdot k_p(t,t)}},$$
$$\hat{k}_p^{0/1}(s,t) = \frac{k_p^{0/1}(s,t)}{\sqrt{k_p^{0/1}(s,s) \cdot k_p^{0/1}(t,t)}}.$$

Taking into account p-grams of different length and summing up the corresponding kernels, new kernels, termed *blended spectrum kernels*, can be obtained.

9.3 Local Rank Distance

Local Rank Distance is an extension of rank distance that drops the annotation step and uses n-grams instead of single characters. Thus, characters in one string are simply matched with the nearest similar characters in the other string. To compute the LRD between two strings, the idea is to sum up all the offsets of similar n-grams between the two strings. For every n-gram in one string, the algorithm searches for a similar n-gram in the other string. First, it looks for similar n-grams in the same position in both strings. If those n-grams are similar, it sums up 0 since there is no offset between them. If the n-grams are not similar, the algorithm start looking around the initial n-gram position in the second string to find an n-gram similar to the one in the first string. If a similar n-gram is found during this process, it sums up the offset between the two n-grams. The search goes on until a similar n-gram is found or until a maximum offset is reached. LRD based on n-grams is formally defined next.

Definition 16 *Let $S_1, S_2 \in \Sigma^*$ be two strings with symbols (n-grams) from the alphabet Σ. Local Rank Distance between S_1 and S_2 is defined as:*

$$\begin{aligned}\Delta_{LRD}(S_1, S_2) &= \Delta_{left} + \Delta_{right} \\ &= \sum_{x_s \in S_1} \min_{x_s \in S_2} \{|pos_{S_1}(x_s) - pos_{S_2}(x_s)|, m\} + \\ &+ \sum_{y_s \in S_2} \min_{y_s \in S_1} \{|pos_{S_1}(y_s) - pos_{S_2}(y_s)|, m\},\end{aligned}$$

where x_s and y_s are occurrences of symbol $s \in \Sigma$ in strings S_1 and S_2, $pos_S(x_s)$ represents the position (or the index) of the occurrence x_s of symbol $s \in \Sigma$ in string S, and $m \geq 1$ is the maximum offset.

Notice that Definitions 14 and 16 are essentially the same. The only difference is terminology adopted for the substrings. While in biology, LRD compares DNA sequences using k-mers, in natural language processing, LRD compares texts using n-grams. In both cases, a string may contain multiple occurrences of a symbol $s \in \Sigma$. LRD matches each occurrence x_s of symbol $s \in \Sigma$ from a string, with the nearest occurrence of symbol s in the other string. A symbol can be defined either as a single character, or as a sequence of characters (n-grams). Overlapping n-grams are also permitted in the computation of LRD. Notice that in order to be a symmetric distance measure, LRD must consider every n-gram in both strings.

LRD measures the distance between two strings. Knowing the maximum offset (used to stop similar n-gram searching), the maximum LRD value between two strings can be computed as the product between the maximum offset and the number of pairs of compared n-grams. Thus, LRD can be normalized to a value in the $[0, 1]$ interval. By normalizing, LRD is transformed into a dissimilarity measure. LRD can be also used as a kernel, since kernel methods are based on similarity. The classical way to transform a distance or dissimilarity measure into a similarity measure is by using the Gaussian RBF kernel [Shawe-Taylor & Cristianini, 2004]:

$$k(s_1, s_2) = \exp\left(-\frac{\Delta_{LRD}(s_1, s_2)}{2\sigma^2}\right),$$

where s_1 and s_2 are two strings. The parameter σ is usually chosen to match the number of features (characters) so that values of $k(s_1, s_2)$ are well scaled.

9.4 Experiments

9.4.1 Data Set Description

The data set for the NLI shared task is the TOEFL11 corpus [Blanchard et al., 2013]. This corpus contains 9900 examples for training, 1100 examples for development (or validation) and another 1100 examples for testing. Each example is an essay written in English by a person that is a non-native English speaker. The people that produced the essays have one of the following native languages: German, French, Spanish, Italian, Chinese, Korean, Japanese, Turkish, Arabic, Telugu, Hindi. More details about the corpus are given in [Blanchard et al., 2013].

The approach described in this chapter participated only in the closed NLI shared task, where the goal of the task is to predict the native language of testing examples, only by using the training and the development data. In the string kernels approach proposed in this work, documents or essays from this corpus are treated as strings. Therefore, the notions of *string* or *document* is used interchangeably throughout this chapter. Because the approach works at the character level, there is no need to split the texts into words, or to do any NLP-specific preprocessing. The only editing done to the texts was the replacing of sequences of consecutive space characters (space, tab, new line, and so on) with a single space character. This normalization was needed in order to prevent the artificial increase or decrease of the similarity between texts, as a result of different spacing. All uppercase letters were converted to the corresponding lowercase ones. The additional information from *prompts* or the English language proficiency level were not used in the proposed approach.

9.4.2 Choosing the Learning Method

Kernel-based learning algorithms work by embedding the data into a Hilbert feature space, and searching for linear relations in that space. The embedding is

performed implicitly, that is by specifying the inner product between each pair of points rather than by giving their coordinates explicitly.

Various kernel methods differ in the way they learn to separate the samples. In the case of binary classification problems, kernel-based learning algorithms look for a discriminant function, a function that assigns $+1$ to examples belonging to one class and -1 to examples belonging to the other class. For the NLI experiments, two binary kernel classifiers are used, namely the SVM [Cortes & Vapnik, 1995], and the KRR. Support Vector Machines try to find the vector of weights that defines the hyperplane that maximally separates the images in the Hilbert space of the training examples belonging to the two classes. Kernel Ridge Regression selects the vector of weights that simultaneously has small empirical error and small norm in the Reproducing Kernel Hilbert Space generated by the kernel k. More details about SVM and KRR can be found in [Shawe-Taylor & Cristianini, 2004]. The important fact is that the above optimization problems are solved in such a way that the coordinates of the embedded points are not needed, only their pairwise inner products which in turn are given by the kernel function k.

SVM and KRR produce binary classifiers and native language identification is a multi-class classification problem. There are a lot of approaches for combining binary classifiers to solve multi-class problems. Typically, the multi-class problem is broken down into multiple binary classification problems using common decomposing schemes such as: one-versus-all (OVA) and one-versus-one (OVO). There are also kernel methods that directly take into account the multi-class nature of the problem, such as KPLS or KDA. Both the KPLS and the KDA classifiers are used in the experiments presented in this chapter, despite the fact that KDA was not initially considered for the NLI Shared Task. The KDA classifier is able to improve accuracy by avoiding the masking problem [Hastie & Tibshirani, 2003]. In the case of multi-class native language identification, the masking problem may appear when non-native English speakers have acquired, as the second language, a different language rather than English. For example, an essay written in English produced by a French native speaker that is also proficient in German, can be identified either as French or German.

A series of preliminary experiments were conducted in order to select the learn-

ing method. In these experiments the string kernel was fixed to the p-spectrum normalized kernel of length 5 ($\hat{k}_5$) and plugged it in the following learning methods: OVO SVM, OVA SVM, OVO KRR, OVA KRR and KPLS. At this stage, the concern is to select the best learning method, and not to find the right kernel. The preliminary tests were performed using $\hat{k}_5$ because it was reported to work well in the case of the related task of identifying translationese [Popescu, 2011].

A 10-fold cross-validation procedure was carried out on the training set and the obtained results (with the best parameters setting) are shown in Table 9.1.

Table 9.1: Accuracy rates using 10-fold cross-validation on the train set for different kernel methods with $\hat{k}_5$ kernel.

Method	Accuracy
OVO SVM	72.72%
OVA SVM	74.94%
OVO KRR	73.99%
OVA KRR	**77.74%**
KPLS	74.99%

The results show that for native language identification the one-vs-all scheme performs better than the one-versus-one scheme. The same fact was reported in [Brooke & Hirst, 2012]. Several arguments in favor of the one-vs-all scheme are given in [Rifkin & Klautau, 2004]. The best result was obtained by one-vs-all Kernel Ridge Regression and it was therefore selected as the learning method in the following experiments.

It is important to mention that KDA was not compared in the preliminary experiments with the other kernel methods. Actually, at the time of the competition, KDA was not considered at all. Consequently, no system based on KDA was submitted to compete in the NLI Shared Task. However, KDA was later found to work even better than KRR. Therefore, results of several systems based on KDA are also presented in Section 9.4.6, despite the fact that they were not submitted to the competition.

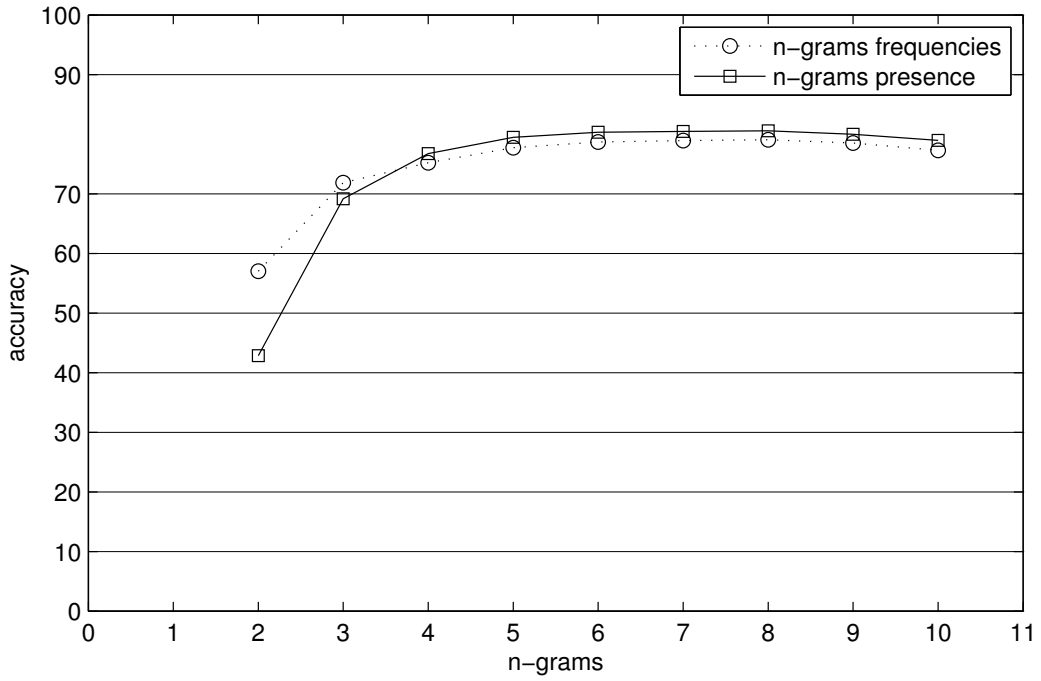

Figure 9.1: 10-fold cross-validation accuracy on the train set for different n-grams.

9.4.3 Parameter Tuning for String Kernel

To establish the type of kernel, (blended) p-spectrum kernel or (blended) p-grams presence bits kernel, and the length(s) of n-grams that must be used, another set of experiments was performed. For both p-spectrum normalized kernel and p-grams presence bits normalized kernel, and for each value of p from 2 to 10, a 10-fold cross-validation procedure was carried out on the train set. The results are summarized in Figure 9.1.

As can be seen, both curves have similar shapes, both achieve their maximum at 8, but the accuracy of the p-grams presence bits normalized kernel is generally better than the accuracy of the p-spectrum normalized kernel. It seem that in native language identification the information provided by the presence of an n-gram is more important than the the information provided by the occurrence frequency of the respective n-gram. This phenomenon was also noticed in the

context of sexual predator identification [Popescu & Grozea, 2012].

Experiments with different blended kernels were conducted to see whether combining n-grams of different lengths can improve the accuracy. The best result was obtained when all the n-grams with the length in the range 5-8 were used, that is the 5-8-grams presence bits normalized kernel ($\hat{k}^{0/1}_{5-8}$). The 10-fold cross-validation accuracy on the train set for this kernel was 80.94%. It was obtained for the KRR parameter λ set to 10^{-5}. The authors of [Bykh & Meurers, 2012] also obtained better results using n-grams with the length in a range, rather than using n-grams of a fixed length.

9.4.4 Parameter Tuning for LRD Kernel

Parameter tuning for LRD kernel (K_{LRD}) was also done by using 10-fold cross-validation on the training data. An interesting observation is that the KRR based on LRD works much better with the normalized version of LRD (K_{nLRD}). Another concern was to choose the right length of n-grams. Several n-grams that are around the mean English word length of 5-6 letters were evaluated. More precisely, LRD kernels of 4-grams, 6-grams, and 8-grams, were used. The tests show that the LRD kernels based on 6-grams (K_{nLRD_6}) and 8-grams (K_{nLRD_8}) give the best results. In the end, the LRD kernels based on 6-grams and 8-grams are combined to obtain even better results. The results of different kernel combinations, including the LRD kernel based on 6-grams and 8-grams, are given in Section 9.4.5.

Finally, the maximum offset parameter m involved in the computation of LRD was chosen so that it generates a search window size close to the average number of letters per document from the TOEFL 11 set. There are 1802 characters per document on average, and m was chosen to be 700. This parameter was also chosen with respect to the computational time of LRD, which is proportional to the parameter value. Table 9.2 shows the results of the LRD kernel with different parameters cross-validated on the training set. For K_{nLRD}, the σ parameter of the Gaussian-like kernel was set to 1. The reported accuracy rates were obtained with the KRR parameter λ set to 10^{-5}.

Regarding the length of strings, it seems that LRD is affected by the variation

Table 9.2: Accuracy rates, using 10-fold cross-validation on the training set, of LRD with different n-grams, with and without normalization. Normalized LRD is much better.

Method	Accuracy
KRR + K_{LRD_6}	42.1%
KRR + K_{nLRD_4}	70.8%
KRR + K_{nLRD_6}	74.4%
KRR + K_{nLRD_8}	**74.8**%

of string lengths. When comparing two documents with LRD, the idea of cutting the longer document to match the length of the shorter one was proposed and evaluated. This made the accuracy even worse. It seems that the parts cut out from longer documents contain valuable information for LRD. In the end, a decision was made to use the entire strings, despite the fact that the variation of string lengths brought a lot of noise. However, some of this noise is eliminated by normalizing the LRD kernel.

9.4.5 Combining Kernels

A good way to improve results with almost no extra effort is to combine the kernels in different ways. First, notice that the blended string kernels presented in Section 9.4.3 are essentially a sum of the string kernels with different n-grams. This combination improves the accuracy, being more stable and robust. In the same manner, the LRD kernels based on 6-grams and 8-grams, respectively, were summed up to obtain the kernel denoted by $K_{nLRD_{6+8}}$. Indeed, the $K_{nLRD_{6+8}}$ kernel presented in Table 9.3 works better than each of its components presented in Table 9.2.

There are other options to combine the string kernels with LRD kernels, besides summing them up. One option is by kernel alignment [Cristianini et al., 2001]. Instead of simply summing kernels, kernel alignment assigns weights for each of the two kernels based on how well they are aligned with the ideal kernel YY' obtained from labels. Thus, the 5-8-grams presence bits normalized kernel ($\hat{k}^{0/1}_{5-8}$) was combined with the LRD kernel based on sum of 6,8-grams ($K_{nLRD_{6+8}}$),

Table 9.3: Accuracy rates of different kernel combinations using 10-fold cross-validation on the training set.

Method	Accuracy
KRR + $K_{nLRD_{6+8}}$	75.4%
KRR + $\hat{k}^{0/1}_{5-8}$ + $K_{nLRD_{6+8}}$	**81.6**%
KRR + $(\hat{k}^{0/1} + K_{nLRD})_{6+8}$	80.9%

by kernel alignment. From our experiments, kernel alignment worked slightly better than the sum of the two kernels. This also suggests that kernels can be combined only by using kernel alignment. Therefore, the string kernel of length 6 was aligned with the LRD kernel based on 6-grams. In the same way, the string kernel of length 8 was aligned with the LRD kernel based on 8-grams. The two kernels obtained by alignment are combined together, again by kernel alignment, to obtain the kernel denoted by $(\hat{k}^{0/1} + K_{nLRD})_{6+8}$. The results of all kernel combinations are presented in Table 9.3. The reported accuracy rates were obtained with the KRR parameter λ set to 10^{-5}.

9.4.6 Results and Discussion

For the closed NLI Shared Task, two main systems were separately submitted, namely the 5-8-grams presence bits normalized kernel and the LRD kernel based on sum of 6,8-grams. Another two submissions are the kernel combinations discussed in Section 9.4.5. These four submitted systems were tested using several evaluation procedures, with results shown in Table 9.4. First, they were tested using 10-fold cross-validation on the training set. Next, the systems were tested on the development set. In this case, the systems were trained on the entire training corpus. Another 10-fold cross-validation procedure was done on the corpus obtained by combining the training and the development sets. This time, the folds were provided by the organizers. Finally, the results of our systems on the NLI Shared Task test set are given in the last column of Table 9.4. For testing, the systems were trained on the entire training and development set, with the KRR parameter λ set to $2 \cdot 10^{-5}$.

Table 9.4: Accuracy rates of submitted systems on different evaluation sets. The Unibuc team ranked third in the closed NLI Shared Task with the kernel combination improved by the heuristic to level the predicted class distribution.

Method	CV Tr.	Dev.	CV Tr.+Dev.	Test
KRR + $\hat{k}^{0/1}_{5-8}$	80.9%	85.4%	82.5%	82.0%
KRR + $K_{nLRD_{6+8}}$	75.4%	76.3%	75.7%	75.8%
KRR + $\hat{k}^{0/1}_{5-8}$ + $K_{nLRD_{6+8}}$	**81.6**%	**85.7**%	**82.6**%	82.5%
KRR + $(\hat{k}^{0/1} + K_{nLRD})_{6+8}$	80.9%	85.6%	82.0%	81.4%
KRR + $\hat{k}^{0/1}_{5-8}$ + $K_{nLRD_{6+8}}$ + heuristic	-	-	-	**82.7**%

The $K_{nLRD_{6+8}}$ kernel was not expected to perform better than the other systems on the test set. This system was submitted just to be compared with systems submitted by other participants. Considering that LRD was originally designed for biology applications, and that it has no ground in computational linguistics, it performed very well, by standing in the top half of the ranking of all submitted systems.

The kernel obtained by aligning the $\hat{k}^{0/1}_{5-8}$ and $K_{nLRD_{6+8}}$ kernels gives the best results, no matter the evaluation procedure. It is followed closely by the other two submitted systems.

A good idea to improve the accuracy on the test set was to exploit the distribution of the test set in the last submitted system. This idea emerged by learning that there should be exactly 100 examples per class for testing. The kernel expected to give the best accuracy among the submitted systems was chosen for an adjustment of its output, in order to level the predicted class distribution. The kernel obtained by combining the $\hat{k}^{0/1}_{5-8}$ and $K_{nLRD_{6+8}}$ kernels was considered for this adjustment, since it obtains the best accuracy in all the other experiments. The adjustment consists of taking all the classes with more than 100 examples, and rank the examples by their confidence score (returned by regression) to be part of the predicted class. The examples ranked below 100 were chosen to be redistributed to the classes that had less than 100 examples per class. Examples were redistributed only if their second most confident class had less than 100 examples. This heuristic improved the results on the test set by 0.2%, enough to

put the Unibuc team on third place in the closed NLI Shared Task.

The submitted systems achieve state of the art performance levels. But, it seems that better results can be obtained by replacing the KRR classifier with a classifier that is more suitable for the multi-class problem, such as KDA. Since it is able to handle the class masking problem, KDA was chosen as the preferred method of classification for the following experiments. Three systems based on KDA are evaluated next. The first two systems are the 5-8-grams presence bits normalized kernel and the LRD kernel based on sum of 6,8-grams. The best submitted system, obtained by combining the $\hat{k}^{0/1}_{5-8}$ and $K_{nLRD_{6+8}}$ kernels, is also used in conjunction with KDA. The results of these three KDA systems on different evaluation sets are presented in Table 9.5.

Table 9.5: Accuracy rates on different evaluation sets of systems based on the KDA classifier. These systems were not submitted to the closed NLI Shared Task.

Method	CV Tr.	Dev.	CV Tr.+Dev.	Test
KDA + $\hat{k}^{0/1}_{5-8}$	82.4%	86.2%	83.5%	84.0%
KDA + $K_{nLRD_{6+8}}$	76.3%	78.8%	77.3%	78.1%
KDA + $\hat{k}^{0/1}_{5-8}$ + $K_{nLRD_{6+8}}$	**82.8**%	**87.3**%	**84.0**%	**84.3**%

Compared to the submitted systems, the results are roughly 2% better when KDA is used. It is important to note that significant improvements are obtained for all the three systems, on all the evaluation sets. There is no doubt that KDA performs better than KRR on this task. It seems that KDA equally helps all the three kernels, in such a way that the ranking of the three systems is preserved. More precisely, the best system remains the kernel combination of $\hat{k}^{0/1}_{5-8}$ and $K_{nLRD_{6+8}}$ with an accuracy of 84.3% on the test set, followed closely by the standalone $\hat{k}^{0/1}_{5-8}$ kernel with an accuracy of 84.0%. The $K_{nLRD_{6+8}}$ kernel comes in last place among the three, with an accuracy of 78.1%. However, the kernel based on LRD shows an improvement of 2.3% on the test set, when KDA is used instead of KRR. This improvement in accuracy makes the LRD kernel a good standalone solution for native language identification. The overall results strongly suggest that approaching the task of native language identification with methods that work at the character level is probably the best solution at the

moment.

9.5 Discussion and Further Work

An approach for the 2013 NLI Shared Task was presented in this chapter. What makes this system stand out is that it works at the character level, making the approach completely language independent and linguistic theory neutral. The results obtained were very good. A standard approach based on string kernels, that proved to work well in many text analysis tasks, obtained an accuracy of 82% on test data with a difference of only 1.6% between it and the top performing system. A second system based on a new kernel K_{LRD}, inspired from biology with no ground in computational linguistics, performed also unexpectedly well, by standing in the top half of the ranking of all submitted systems. The combination of the two kernels obtained an accuracy of 82.5% making it to the top five, while an heuristic improvement of this combination ranked third with an accuracy of 82.7%. After the competition, the KDA classifier was also evaluated on this task, only to improve the accuracy to 84.3%. This final system is 0.7% above to top performing system of the NLI Shared Task.

Despite the fact that the approach based on string kernels performed so well, there is little information known about why does the system works so well and why is it better than the other systems that take into account words, lemmas, syntactic information, or even semantics. It seems that enough mistakes that are particular to certain non-native English speakers can be captured by n-grams of different lengths. An interesting remark is that using a range of n-grams generates a lot of features that include (but are not limited to) stop words, stems of content words, word terminations, entire words, and even n-grams of short words. Instead of doing feature selection before the training step, which is the usual NLP approach, the kernel classifier is the one that selects the most relevant features, during training. With enough training samples, the kernel classifier does a better job in selecting the right features from a very high feature space. This might give a good reason of why the string kernel approach works so well.

In future work, the proposed system can probably be improved by including spatial information, in a similar fashion to the spatial pyramid representa-

tion [Lazebnik et al., 2006] that improves the recognition performance of the bag of visual words model. The spatial pyramid approach divides the image into increasingly fine sub-regions, and records the frequency of each visual word in a histogram for each bin. In a similar way, the text document can be divided into increasingly fine chunks of text. Then, n-grams can be extracted from each chunk of text, and combined to obtain the final pyramid representation of the document. The pyramid representation adds some information about the location of the n-grams in the original text. It may be that this location information might be useful to obtain a better classification performance.

Chapter 10

Conclusions

Machine learning is currently a vast area of research with applications in a variety of fields, such as computer vision [Fei-Fei & Perona, 2005; Forsyth & Ponce, 2002; Zhang et al., 2007], computational biology [Dinu & Ionescu, 2013a; Inza et al., 2010; Leslie et al., 2002], information retrieval [Chifu & Ionescu, 2012; Manning et al., 2008], natural language processing [Lodhi et al., 2002; Popescu & Grozea, 2012], data mining [Enăchescu, 2004], and many others. This thesis has proposed several machine learning methods that are designed for specific tasks, ranging from handwritten digit recognition, texture classification, object recognition, or facial expression recognition, to phylogenetic analysis, DNA comparison, or native language identification. For this broad range of applications several similarity-based learning methods [Chen et al., 2009] have been employed. This thesis studied approaches such as Nearest Neighbor models, kernel methods [Shawe-Taylor & Cristianini, 2004], and clustering methods [Enăchescu, 2004]. The has studied methods exhibit state of the art performance levels in the approached tasks. To support this claim, it is important to mention the improved bag of visual words model [Ionescu et al., 2013] that has obtained the fourth place at the Facial Expression Recognition (FER) Challenge of the ICML 2013 Workshop in Challenges in Representation Learning (WREPL), and the system based on string kernels [Popescu & Ionescu, 2013] that has ranked on third place in the closed Native Language Identification Shared Task of the BEA-8 Workshop of NAACL 2013.

The applications approached in this thesis can be divided into two different ar-

eas: computer vision and string processing. Despite the fact that computer vision and string processing seem to be unrelated fields of study, recent results as the ones presented in this thesis suggest that image analysis and string processing are actually similar in several ways. The concept of treating image and text in a similar fashion has proven to be very fertile for particular applications in computer vision [Duygulu et al., 2002; Farhadi et al., 2010; Leung & Malik, 2001; Sadeghi & Farhadi, 2011; Sivic et al., 2005] and natural language processing [Barnard & Johnson, 2005; Barnard et al., 2003; Ionescu, 2013a]. The concept of treating image and text in a similar manner was also exploited in various ways in this thesis. First, a dissimilarity measure for images was presented in Chapter 4. The dissimilarity measure was inspired from the rank distance measure [Dinu, 2003]. The main concern was to extend rank distance from one-dimensional input (strings) to two-dimensional input (digital images). While rank distance is a highly accurate measure for strings, the experiments presented in Chapter 4 suggest that the proposed extension of rank distance to images is very accurate for handwritten digit recognition and texture analysis. Second, some improvements to the popular bag of visual words model were proposed in Chapter 5. This model is inspired by the bag of words model from natural language processing and information retrieval. Third, a new distance measure was introduced in Chapter 8. It was inspired from the image dissimilarity measure presented in Chapter 4. Designed to conform to more general principles and adapted to DNA strings, Local Rank Distance has shown that it can achieve better results than several state of the art methods for DNA sequence analysis. Furthermore, another application of this novel distance measure for strings was presented in Chapter 9. More precisely, a kernel based on this distance measure was used for native language identification. To summarize, all the contributions that were presented in this thesis come to support the concept of treating image and text in a similar manner.

Although a significant amount of research has been conducted using the idea of borrowing and adapting concepts from text processing to computer vision, or from computer vision to text processing, the concept of treating image and text in a similar fashion is far from saturated. The methods presented in this thesis exploit this concept, only to lay the ground for future exploration. One interesting approach that should be addressed in future work is mentioned here. Inspired

by the spatial pyramid representation [Lazebnik et al., 2006] that improves the recognition performance of the bag of visual words model in computer vision, an interesting future development would be to use a similar approach for text categorization. Text documents can be divided into increasingly fine chunks of text. Then, n-grams or any kind of features can be extracted from each chunk of text in order to obtain pyramid representations of the documents. This is just one of the directions that can be investigated in future work.

To conclude, this thesis represents a strong argument in favor of treating image and text in a similar fashion, a concept that is very promising and truly fertile for specific applications.

Bibliography

Achtert, Elke, Bohm, Christian, Kriegel, Hans P., Kroger, Peer, Muller-Gorman, Ina, and Zimek, Arthur. Finding hierarchies of subspace clusters. *Proceedings of PKDD*, pp. 446–453, 2006. 32

Achtert, Elke, Bohm, Christian, Kriegel, Hans P., Kroger, Peer, Muller-Gorman, Ina, and Zimek, Arthur. Detection and visualization of subspace cluster hierarchies. *Proceedings of DASFAA*, pp. 152–163, 2007. 32

Agarwal, Shivani and Roth, Dan. Learning a Sparse Representation for Object Detection. *Proceedings of ECCV*, pp. 113–127, June 2002. 3, 40

Agirre, Eneko and Edmonds, Philip Glenny. *Word Sense Disambiguation: Algorithms and Applications*. Springer, 2006. 4, 5, 32

Agrawal, Rakesh, Gehrke, Johannes, Gunopulos, Dimitrios, and Raghavan, Prabhakar. Automatic subspace clustering of high dimensional data for data mining applications. *SIGMOD Record*, 27(2):94–105, 1998. 32

Alekseyev, Max A. and Pevzner, Pavel A. Multi-break rearrangements and chromosomal evolution. *Theoretical Computer Science*, 395(2-3):193–202, 2008. 128

Alexe, Bogdan, Deselaers, Thomas, and Ferrari, Vittorio. Measuring the objectness of image windows. *IEEE Transactions on Pattern Analysis and Machine Intelligence*, 34(11):2189–2202, 2012. 124

Altschul, S. F., Gish, W., Miller, W., Myers, E. W., and Lipman, D. J. Basic local alignment search tool. *Journal of Molecular Biology*, 215(3):403–410, October 1990. ISSN 0022-2836. 14

Amir, Amihood, Aumann, Yonatan, Benson, Gary, Levy, Avivit, Lipsky, Ohad, Porat, Ely, Skiena, Steven, and Vishne, Uzi. Pattern matching with address errors: rearrangement distances. *Proceedings of SODA*, pp. 1221–1229, 2006. 163

Amir, Amihood, Landau, Gad M., Na, Joong Chae, Park, Heejin, Park, Kunsoo, and Sim, Jeong Seop. Consensus optimizing both distance sum and radius. *Proceedings of the 16th International Symposium on String Processing and Information Retrieval*, pp. 234–242, 2009. 136, 140

Bader, David A., Moret, Bernard M. E., and Yan, Mi. A Linear-Time Algorithm for Computing Inversion Distance between Signed Permutations with an Experimental Study. *Proceedings of the 7th International Workshop on Algorithms and Data Structures*, pp. 365–376, 2001. 128

Bafna, Vineet and Pevzner, Pavel A. Sorting by transpositions. *SIAM Journal on Discrete Mathematics*, 11(2):224–240, 1998. 128

Barnard, Kobus and Johnson, Matthew. Word sense disambiguation with pictures. *Artificial Intelligence*, 167(1-2):13–30, September 2005. ISSN 0004-3702. 7, 205

Barnard, Kobus, Duygulu, Pinar, Forsyth, David, de Freitas, Nando, Blei, David M., and Jordan, Michael I. Matching words and pictures. *Journal of Machine Learning Research*, 3:1107–1135, March 2003. ISSN 1532-4435. 7, 205

Barnes, Connelly, Goldman, Dan B., Shechtman, Eli, and Finkelstein, Adam. The PatchMatch Randomized Matching Algorithm for Image Manipulation. *Communications of the ACM*, 54(11):103–110, November 2011. 39, 40, 48, 52, 56, 85, 162

Bay, Herbert, Ess, Andreas, Tuytelaars, Tinne, and Gool, Luc Van. Speeded-Up Robust Features (SURF). *Computer Vision and Image Understanding*, 110(3): 346–359, June 2008. ISSN 1077-3142. 41

Belda, E., Moya, A., and Silva, F.J. Genome rearrangement distances and gene order phylogeny in gamma-proteobacteria. *Molecular Biology and Evolution*, 22(6):1456–1467, 2005. 128

Belongie, S., Malik, J., and Puzicha, J. Shape matching and object recognition using shape contexts. *IEEE Transactions on Pattern Analysis and Machine Intelligence*, 24(4):509–522, April 2002. 13, 17, 35, 39, 41

Ben-Dor, Amir, Lancia, Giuseppe, Perone, Jennifer, and Ravi, R. Banishing Bias from Consensus Sequences. *Proceedings of CPM*, (1264):247–261, 1997. 127

Bengio, Yoshua. Learning deep architectures for AI. *Foundations and Trends in Machine Learning*, 2(1):1–127, 2009. 4, 35

Bishop, Christopher M. *Neural Networks for Pattern Recognition*. Oxford University Press, Inc., New York, NY, USA, 1995. ISBN 0198538642. 2

Blanchard, Daniel, Tetreault, Joel, Higgins, Derrick, Cahill, Aoife, and Chodorow, Martin. TOEFL11: A Corpus of Non-Native English. Technical report, Educational Testing Service, 2013. 193

Bohm, Christian, Kailing, Karin, Kroger, Peer, and Zimek, Arthur. Computing clusters of correlation connected objects. *Proceedings of the 2004 ACM SIGMOD*, pp. 455–466, 2004. 32

Borg, I. and Groenen, P. J. F. *Modern multidimensional scaling: Theory and applications*. Springer Verlag, 2005. 20

Bosch, Anna, Zisserman, Andrew, and Munoz, Xavier. Image Classification using Random Forests and Ferns. *Proceedings of ICCV*, pp. 1–8, 2007. 42, 102, 109, 115, 120

Bottou, Leon and Vapnik, Vladimir. Local Learning Algorithms. *Neural Computation*, 4:888–900, 1992. 19

Breiman, Leo. Random forests. *Machine Learning*, 45(1):5–32, October 2001. ISSN 0885-6125. 2

Brodatz, Phil. *Textures: a photographic album for artists and designers*. Dover pictorial archives. Dover Publications, New York, USA, 1966. 86

Brooke, Julian and Hirst, Graeme. Robust, Lexicalized Native Language Identification. *Proceedings of COLING 2012*, pp. 391–408, December 2012. 126, 188, 195

Bryant, David and Waddell, Peter. Rapid evaluation of least squares and minimum evolution criteria on phylogenetic trees. *Molecular Biology and Evolution*, 15(10):1346–1359, 1998. 130

Bykh, Serhiy and Meurers, Detmar. Native Language Identification using Recurring n-grams – Investigating Abstraction and Domain Dependence. *Proceedings of COLING 2012*, pp. 425–440, December 2012. 197

Canny, John. A Computational Approach to Edge Detection. *IEEE Transactions on Pattern Analysis and Machine Intelligence*, 8(6):679–698, June 1986. 41

Cao, Y., Janke, A., Waddell, P. J., Westerman, M., Takenaka, O., Murata, S., Okada, N., Paabo, S., and Hasegawa, M. Conflict among individual mitochondrial proteins in resolving the phylogeny of Eutherian orders. *Journal of Molecular Evolution*, 47:307–322, 1998. 130, 178, 182

Caruana, Rich and Niculescu-Mizil, Alexandru. An empirical comparison of supervised learning algorithms. *Proceedings of ICML*, pp. 161–168, 2006. 2

Cazzanti, Luca and Gupta, Maya R. Local similarity discriminant analysis. *Proceedings of ICML*, pp. 137–144, 2007. 15

Cazzanti, Luca, Gupta, Maya R., and Koppal, Anjali J. Generative models for similarity-based classification. *Pattern Recognition*, 41(7):2289–2297, July 2008. ISSN 0031-3203. 15

Chen, Yihua, Garcia, Eric K., Gupta, Maya R., Rahimi, Ali, and Cazzanti, Luca. Similarity-based Classification: Concepts and Algorithms. *Journal of Machine Learning Research*, 10:747–776, June 2009. ISSN 1532-4435. 3, 14, 15, 204

Chifu, Adrian-Gabriel and Ionescu, Radu Tudor. Word sense disambiguation to improve precision for ambiguous queries. *Central European Journal of Computer Science*, 2(4):398–411, 2012. 3, 5, 11, 32, 131, 204

Chimani, M., Woste, M., and Bocker, S. A closer look at the closest string and closest substring problem. *Proceedings of ALENEX*, pp. 13–24, 2011. 14, 129, 140, 159, 189

Cho, Taeg Sang, Avidan, Shai, and Freeman, William T. The patch transform. *IEEE Transactions on Pattern Analysis and Machine Intelligence*, 32(8):1489–1501, 2010. 40, 162

Conaire, Ciarn O, O'Connor, Noel E., and Smeaton, Alan F. An Improved Spatiogram Similarity Measure for Robust Object Localisation. *Proceedings of ICASSP*, 1:1069–1072, 2007. 77, 78

Cortes, Corinna and Vapnik, Vladimir. Support-Vector Networks. *Machine Learning*, 20(3):273–297, 1995. 2, 25, 57, 194

Cortes, Corinna, Mohri, Mehryar, and Rostamizadeh, Afshin. Multi-Class Classification with Maximum Margin Multiple Kernel. *Journal of Machine Learning Research*, 28(3):46–54, June 2013. 28

Cover, T. and Hart, P. Nearest neighbor pattern classification. *IEEE Transactions on Information Theory*, 13(1):21–27, 1967. ISSN 0018-9448. 18

Cristianini, Nello, Shawe-Taylor, John, Elisseeff, André, and Kandola, Jaz S. On kernel-target alignment. *Proceedings of NIPS*, pp. 367–373, December 2001. 28, 199

Csurka, Gabriella, Dance, Christopher R., Fan, Lixin, Willamowski, Jutta, and Bray, Cdric. Visual categorization with bags of keypoints. *In Workshop on Statistical Learning in Computer Vision, ECCV*, pp. 1–22, 2004. 34, 42, 43, 115

Dalal, Navneet and Triggs, Bill. Histograms of Oriented Gradients for Human Detection. *Proceedings of CVPR*, 1:886–893, 2005. 41, 102, 115

Dasarathy, B. V. *Nearest neighbor (NN) norms: Pattern Classification Techniques*. IEEE Computer Society Press, Los Alamitos, CA, 1991. 18

Dash, J., Mathur, A., Foody, G. M., Curran, P. J., Chipman, J. W., and Lillesand, T. M. Land cover classification using multi-temporal MERIS vegetation indices. *International Journal of Remote Sensing*, 28(6):1137–1159, January 2007. 86

Daugman, John G. Uncertainty relation for resolution in space, spatial frequency, and orientation optimized by two-dimensional visual cortical filters. *Journal of the Optical Society of America A*, 2(7):1160–1169, 1985. 82

Deng, Xiaotie, Li, Guojun, Li, Zimao, Ma, Bin, and Wang, Lusheng. Genetic Design of Drugs Without Side-Effects. *SIAM Journal on Computing*, 32(4): 1073–1090, 2003. 127

Deselaers, Thomas, Keyser, Daniel, and Ney, Hermann. Discriminative Training for Object Recognition using Image Patches. *Proceedings of CVPR*, pp. 157–162, 2005. 40, 43

Devroye, L., Györfi, L., and Lugosi, G. *A Probabilistic Theory of Pattern Recognition*. Springer, 1996. 18

Deza, Elena and Deza, Michel-Marie. *Dictionary of Distances*. Elsevier, The Netherlands, 1998. 36

Diaconis, P. and Graham, R. L. Spearman footrule as a measure of disarray. *Journal of Royal Statistical Society. Series B (Methodological)*, 39(2):262–268, 1977. 137

Dinu, Anca and Dinu, Liviu P. On the syllabic similarities of romance languages. *Proceedings of CICLing*, 3406:785–788, 2005. 46, 135, 140, 160

Dinu, Liviu P. On the classification and aggregation of hierarchies with different constitutive elements. *Fundamenta Informaticae*, 55(1):39–50, 2003. 8, 46, 53, 129, 130, 135, 140, 147, 160, 163, 168, 189, 205

Dinu, Liviu P. and Ionescu, Radu Tudor. A genetic approximation for closest string via rank distance. *Proceedings of SYNASC*, pp. 207–215, 2011. 11, 141

Dinu, Liviu P. and Ionescu, Radu Tudor. Clustering Based on Rank Distance with Applications on DNA. *Proceedings of ICONIP*, 7667, 2012a. 3, 11, 14, 129, 136, 146, 159, 178, 182, 184, 189

Dinu, Liviu P. and Ionescu, Radu Tudor. An efficient rank based approach for closest string and closest substring. *PLoS ONE*, 7(6):e37576, 06 2012b. 3, 11, 14, 46, 135, 136, 140, 141, 148, 149, 151, 157, 159, 160, 182, 184, 186, 189

Dinu, Liviu P. and Ionescu, Radu Tudor. Clustering Methods Based on Closest String via Rank Distance. *Proceedings of SYNASC*, pp. 207–214, 2012c. 3, 11, 136, 146

Dinu, Liviu P. and Ionescu, Radu Tudor. A Rank-Based Approach of Cosine Similarity with Applications in Automatic Classification. *Proceedings of SYNASC*, pp. 260–264, 2012d.

Dinu, Liviu P. and Ionescu, Radu Tudor. Clustering based on Median and Closest String via Rank Distance with Applications on DNA. *Neural Computing and Applications*, 24(1):77–84, 2013a. 3, 11, 46, 136, 178, 204

Dinu, Liviu P. and Ionescu, Radu Tudor. An Efficient Algorithm for Rank Distance Consensus. *Proceedings of AI*IA*, 8249:505–516, 2013b. 3, 11, 136

Dinu, Liviu P. and Manea, Florin. An efficient approach for the rank aggregation problem. *Theoretical Computer Science*, 359(1–3):455–461, 2006. 141, 148

Dinu, Liviu P. and Popa, Alin. On the closest string via rank distance. *Proceedings of CPM*, 7354:413–426, 2012. 141, 143

Dinu, Liviu P. and Popescu, Marius. Language independent kernel method for classifying texts with disputed paternity. *Proceedings of ASMDA*, 2009a. 46

Dinu, Liviu P. and Popescu, Marius. Comparing Statistical Similarity Measures for Stylistic Multivariate Analysis. *Proceedings of RANLP*, 2009b. 124

Dinu, Liviu P. and Sgarro, Andrea. A Low-complexity Distance for DNA Strings. *Fundamenta Informaticae*, 73(3):361–372, 2006. 46, 129, 135, 138, 140, 148, 154, 157, 160, 161, 178, 182, 184, 189

Dinu, Liviu P. and Sgarro, Andrea. *Estimating Similarities in DNA Strings Using the Efficacious Rank Distance Approach, Systems and Computational Biology – Bioinformatics and Computational Modeling*. InTech, 2011. ISBN 978-953-307-875-5. 142

Dinu, Liviu P., Popescu, Marius, and Dinu, Anca. Authorship identification of romanian texts with controversial paternity. *Proceedings of LREC*, 2008. 135, 140, 160

Dinu, Liviu P., Ionescu, Radu Tudor, and Popescu, Marius. Local Patch Dissimilarity for Images. *Proceedings of ICONIP*, 7663:117–126, 2012. 3, 9, 44, 53, 79, 159, 160, 163

Dinu, Liviu Petrisor and Ghetu, Florin. Circular Rank Distance: A New Approach for Genomic Applications. *DEXA Workshops*, pp. 397–401, 2011. 161

Duygulu, P., Barnard, Kobus, Freitas, J. F. G. de, and Forsyth, David A. Object Recognition as Machine Translation: Learning a Lexicon for a Fixed Image Vocabulary. *Proceedings of ECCV*, pp. 97–112, 2002. 6, 7, 205

Efros, Alexei A. and Freeman, William T. Image quilting for texture synthesis and transfer. *Proceedings of SIGGRAPH '01*, pp. 341–346, 2001. 39, 48

Enăchescu, Denis. *Unsupervised Statistical Learning and Data Mining*. Cooperativa Libraria Editrice Universit di Padova, Padova, Italy, 2004. ISBN 88-7178-948-2. 3, 29, 30, 204

Everingham, Mark, van Gool, Luc, Williams, Christopher K., Winn, John, and Zisserman, Andrew. The Pascal Visual Object Classes (VOC) Challenge. *International Journal of Computer Vision*, 88(2):303–338, June 2010. 106

Falconer, Kenneth. *Fractal Geometry: Mathematical Foundations and Applications*. Wiley, 2 edition, November 2003. ISBN 0470848626. 81

Faragó, A., Linder, T., and Lugosi, G. Fast Nearest-Neighbor Search in Dissimilarity Spaces. *IEEE Transanctions on Pattern Analysis and Machine Intelligence*, 15(9):957–962, September 1993. ISSN 0162-8828. 18

Farhadi, Ali, Hejrati, Mohsen, Sadeghi, Mohammad Amin, Young, Peter, Rashtchian, Cyrus, Hockenmaier, Julia, and Forsyth, David. Every picture tells a story: generating sentences from images. *Proceedings of ECCV*, pp. 15–29, 2010. 6, 205

Fei-Fei, Li and Perona, Pietro. A Bayesian Hierarchical Model for Learning Natural Scene Categories. *Proceedings of CVPR*, 2:524–531, 2005. 2, 34, 42, 115, 204

Fei-Fei, Li, Fergus, Rob, and Perona, Pietro. Learning generative visual models from few training examples: An incremental Bayesian approach tested on 101 object categories. *Computer Vision and Image Understanding*, 106(1):59–70, April 2007. 98

Felsenstein, Joseph. *Inferring Phylogenies*. Sinauer Associates, Sunderland, Massachusetts, 2004. 129, 130, 159

Fisher, R. A. The Use of Multiple Measurements in Taxonomic Problems. *Annals of Eugenics*, 7(7):179–188, 1936. 25

Fitch, W. M. and Margoliash, E. Construction of phylogenetic trees. *Science*, 155(760):279–284, January 1967. ISSN 0036-8075. 130

Fix, E. and Hodges, J. Discriminatory analysis, non-parametric discrimination: consistency properties. Technical report, USAF School of Aviation and Medicine, Randolph Field, TX, 1951. Technical Report 4. 15

Forsyth, David A. and Ponce, Jean. *Computer Vision: A Modern Approach*. Prentice Hall Professional Technical Reference, 2002. ISBN 0130851981. 2, 204

Frances, M. and Litman, A. On covering problems of codes. *Theory of Computing Systems*, 30(2):113–119, 1997. 140

Frey, Brendan J. and Dueck, Delbert. Clustering by passing messages between data points. *Science*, 315:972–976, 2007. 32

Gonen, Mehmet and Alpaydin, Ethem. Multiple Kernel Learning Algorithms. *Journal of Machine Learning Research*, 12:2211–2268, July 2011. ISSN 1532-4435. 28

Goodfellow, Ian J., Erhan, Dumitru, Carrier, Pierre Luc, Courville, Aaron, Mirza, Mehdi, Hamner, Ben, Cukierski, Will, Tang, Yichuan, Thaler, David, Lee, Dong-Hyun, Zhou, Yingbo, Ramaiah, Chetan, Feng, Fangxiang, Li, Ruifan, Wang, Xiaojie, Athanasakis, Dimitris, Shawe-Taylor, John, Milakov, Maxim, Park, John, Ionescu, Radu Tudor, Popescu, Marius, Grozea, Cristian, Bergstra, James, Xie, Jingjing, Romaszko, Lukasz, Xu, Bing, Chuang, Zhang, and Bengio, Yoshua. Challenges in Representation Learning: A report on three machine learning contests. *Proceedings of ICONIP*, 8228:117–124, 2013. 10, 100

Graepel, T., Herbrich, R., Scholkopf, Bernhard, Smola, A., Bartlett, P., Muller, K., Obermayer, K., and Williamson, R. Classification on proximity data with LP-machines. *Proceedings of ICANN*, 1:304–309, 1999. ISSN 0537-9989. 14

Graepel, Thore, Herbrich, Ralf, Bollmann-Sdorra, Peter, and Obermayer, Klaus. Classification on pairwise proximity data. *Proceedings of NIPS*, pp. 438–444, 1998. 14

Gramm, Jens, Huffner, Falk, and Niedermeier, Rolf. Closest Strings, Primer Design, and Motif Search. *Presented at RECOMB 2002 poster session*, pp. 74–75, 2002. 127

Grozea, C., Gehl, C., and Popescu, M. ENCOPLOT: Pairwise Sequence Matching in Linear Time Applied to Plagiarism Detection. In *3rd PAN WORKSHOP. UNCOVERING PLAGIARISM, AUTHORSHIP AND SOCIAL SOFTWARE MISUSE*, pp. 10, 2009. 132, 187

Guo, Guodong and Dyer, Charles R. Patch-based Image Correlation with Rapid Filtering. *Proceedings of CVPR*, 2007. 40, 48

Hafner, James L., Sawhney, Harpreet S., Equitz, William, Flickner, Myron, and Niblack, Wayne. Efficient Color Histogram Indexing for Quadratic Form Distance Functions. *IEEE Transactions on Pattern Analysis and Machine Intelligence*, 17(7):729–736, 1995. 36

Hannenhalli, Sridhar. Polynomial-time algorithm for computing translocation distance between genomes. *Discrete Applied Mathematics*, 71(1-3):137–151, 1996. 128

Hannenhalli, Sridhar and Pevzner, Pavel A. Transforming men into mice (polynomial algorithm for genomic distance problem. *Proceedings of 36th Annual IEEE Symposium on Foundations of Computer Science*, pp. 581–592, 1995. 128

Haralick, Robert M., Shanmugam, K., and Dinstein, Its'Hak. Textural Features for Image Classification. *IEEE Transactions on Systems, Man and Cybernetics*, 3(6):610–621, November 1973. ISSN 0018-9472. 81

Harris, C. and Stephens, M. A combined corner and edge detector. *Proceedings of the 4th Alvey Vision Conference*, pp. 147–151, 1988. 41

Hastie, Trevor and Tibshirani, Robert. *The Elements of Statistical Learning*. Springer, corrected edition, July 2003. ISBN 0387952845. 26, 30, 194

Hoekman, Dirk H. and Quinnones, Marcela J. Land cover type and biomass classification using AirSAR data fro evaluation of monitoring scenarios in the Colombian Amazon. *IEEE Transactions on Geoscience and Remote Sensing*, 38:685–696, 2000. 86

Holmquist, Richard, Miyamoto, Michael M., and Goodman, Morris. Higher-Primate Phylogeny - Why Can't We Decide? *Molecular Biology and Evolution*, 3(5):201–216, 1988. 129

Homer, Nils, Merriman, Barry, and Nelson, Stanley F. BFAST: An Alignment Tool for Large Scale Genome Resequencing. *PLoS ONE*, 4(11):e7767+, November 2009. 128

Hristea, Florentina, Popescu, Marius, and Dumitrescu, Monica. Performing word sense disambiguation at the border between unsupervised and knowledge-based techniques. *Artificial Intelligence Review*, 30(1-4):67–86, 2008. ISSN 0269-2821. 132

Huang, Zhexue. Extensions to the k-means algorithm for clustering large data sets with categorical values. *Data Mining and Knowledge Discovery*, 2(3):283–304, 1998. 31

Indow, Tarow. A Critical Review of Luneburg's Model With Regard to Global Structure of Visual Space. *Psychological Review*, 98(3):430–453, 1991. 36

Inza, Iñaki, Calvo, Borja, Armañanzas, Rubén, Bengoetxea, Endika, Larrañaga, Pedro, and Lozano, José A. Machine learning: an indispensable tool in bioinformatics. *Methods in Molecular Biology (Clifton, N.J.)*, 593:25–48, 2010. ISSN 1940-6029. 3, 204

Ionescu, Radu Tudor. Local Rank Distance. *Proceedings of SYNASC*, pp. 221–228, 2013a. 3, 12, 130, 159, 160, 163, 189, 205

Ionescu, Radu Tudor. Unisort: An algorithm to sort uniformly distributed numbers in O(n). *International Journal on Information Technology (IREIT)*, 1(3): 171–188, May 2013b. 11, 144

Ionescu, Radu Tudor and Popescu, Marius. Speeding Up Local Patch Dissimilarity. *Proceedings of ICIAP*, 8156:1–10, 2013a. 3, 9, 44, 163

Ionescu, Radu Tudor and Popescu, Marius. Kernels for Visual Words Histograms. *Proceedings of ICIAP*, 8156:81–90, 2013b. 3, 10, 14, 98

Ionescu, Radu Tudor, Popescu, Marius, and Grozea, Cristian. Local Learning to Improve Bag of Visual Words Model for Facial Expression Recognition. *Workshop on Challenges in Representation Learning, ICML*, 2013. 3, 10, 99, 204

Ionescu, Radu Tudor, Popescu, Andreea Lavinia, Popescu, Dan, and Popescu, Marius. Local Texton Dissimilarity with Applications on Biomass Classification. *Proceedings of VISAPP*, January 2014. 3, 9, 45, 80

Jarvis, Scott and Crossley, Scott (eds.). *Approaching Language Transfer Through Text Classification: Explorations in the Detection-based Approach*, volume 64. Multilingual Matters Limited, Bristol, UK, 2012. 126

Jurafsky, Daniel and Martin, James H. *Speech and Language Processing: An Introduction to Natural Language Processing, Computational Linguistics, and Speech Recognition*. Prentice Hall PTR, Upper Saddle River, NJ, USA, 1st edition, 2000. ISBN 0130950696. 6, 132

Jurie, Frederic and Schmid, Cordelia. Scale-invariant shape features for recognition of object categories. *Proceedings of CVPR*, 2:90–96, 2004. 41

Kadir, Timor and Brady, Michael. Saliency, Scale and Image Description. *International Journal of Computer Vision*, 45(2):83–105, November 2001. 41

Kailing, Karin, Kriegel, Hans P., and Kroger, Peer. Density-connected subspace clustering for high-dimensional data. *Proceedings of the 4th SIAM International Conference on Data Mining*, 2004. 29, 32

Ke, Yan and Sukthankar, Rahul. PCA-SIFT: a more distinctive representation for local image descriptors. *Proceedings of CVPR*, pp. 506–513, 2004. 41

Knuth, Donald E., Morris, J. H., and Pratt, Vaughan R. Fast pattern matching in strings. *SIAM Journal of Computing*, 6(2):323–350, 1977. 167

Koonin, E. V. The emerging paradigm and open problems in comparative genomics. *Bioinformatics*, 15:265–266, 1999. 127

Kriegel, Hans P., Kroger, Peer, and Zimek, Arthur. Clustering high-dimensional data: A survey on subspace clustering, pattern-based clustering, and correlation clustering. *ACM Transactions on Knowledge Discovery from Data*, 3(1): 1:1–1:58, 2009. 32

Krizhevsky, Alex, Sutskever, Ilya, and Hinton, Geoffrey E. ImageNet Classification with Deep Convolutional Neural Networks. *Proceedings of NIPS*, pp. 1106–1114, 2012. 35

Kuse, Manohar, Wang, Yi-Fang, Kalasannavar, Vinay, Khan, Michael, and Rajpoot, Nasir. Local isotropic phase symmetry measure for detection of beta cells and lymphocytes. *Journal of Pathology Informatics*, 2(2):2, 2011. 82

Lanctot, Kevin J., Li, Ming, Ma, Bin, Wang, Shaojiu, and Zhang, Louxin. Distinguishing string selection problems. *Information and Computation*, 185(1): 41–55, August 2003. ISSN 0890-5401. 127

Langmead, Ben, Trapnell, Cole, Pop, Mihai, and Salzberg, Steven. Ultrafast and memory-efficient alignment of short DNA sequences to the human genome. *Genome Biology*, 10(3):R25–10, March 2009. ISSN 1465-6906. 128

Lazebnik, Svetlana, Schmid, Cordelia, and Ponce, Jean. A Maximum Entropy Framework for Part-Based Texture and Object Recognition. *Proceedings of ICCV*, 1:832–838, 2005a. xxii, 55, 78, 79, 80, 98, 108

Lazebnik, Svetlana, Schmid, Cordelia, and Ponce, Jean. A Sparse Texture Representation Using Local Affine Regions. *IEEE Transactions on Pattern Analysis and Machine Intelligence*, 27(8):1265–1278, August 2005b. 4, 80, 86, 90, 92, 93

Lazebnik, Svetlana, Schmid, Cordelia, and Ponce, Jean. Beyond Bags of Features: Spatial Pyramid Matching for Recognizing Natural Scene Categories. *Proceedings of CVPR*, 2:2169–2178, 2006. 4, 14, 24, 98, 102, 117, 202, 206

LeCun, Yann, Jackel, Lawrence D., Boser, Bernhard, Denker, John S., Graf, Hans P., Guyon, Isabelle, Henderson, Donnie, Howard, R. E., and Hubbard, Wayne. Handwritten digit recognition: Applications of neural net chips and automatic learning. *IEEE Communications*, pp. 41–46, November 1989. 54

LeCun, Yann, Bottou, Leon, Bengio, Yoshua, and Haffner, Patrick. Gradient-based learning applied to document recognition. *Proceedings of the IEEE*, 86 (11):2278–2324, November 1998. 54, 55, 66, 72

Lee, Taehyung, Na, Joong Chae, Park, Heejin, Park, Kunsoo, and Sim, Jeong Seop. Finding consensus and optimal alignment of circular strings. *Theoretical Computer Science*, 468:92–101, 2013. 140

Leslie, Christina S., Eskin, Eleazar, and Noble, William Stafford. The spectrum kernel: A string kernel for svm protein classification. *Proceedings of Pacific Symposium on Biocomputing*, pp. 566–575, 2002. 3, 189, 204

Leung, Thomas and Malik, Jitendra. Representing and Recognizing the Visual Appearance of Materials using Three-dimensional Textons. *International Journal of Computer Vision*, 43(1):29–44, June 2001. ISSN 0920-5691. 4, 5, 32, 34, 42, 80, 102, 115, 205

Levenshtein, V. I. Binary codes capable of correcting deletions, insertions and reverseals. *Cybernetics and Control Theory*, 10(8):707–710, 1966. 46, 141

Levy, Samuel and Hannenhalli, Sridhar. Identification of transcription factor binding sites in the human genome sequence. *Mammalian Genome*, 13(9): 510–514, September 2002. ISSN 0938-8990. 128

Li, Heng and Durbin, Richard. Fast and accurate short read alignment with Burrows-Wheeler transform. *Bioinformatics*, 25(14):1754–1760, July 2009. ISSN 1367-4803. 128

Li, Heng and Homer, Nils. A survey of sequence alignment algorithms for next-generation sequencing. *Briefings in bioinformatics*, 11(5):473–483, September 2010. ISSN 1477-4054. 128

Li, Ming, Ma, Bin, and Wang, Lusheng. Finding Similar Regions in Many Sequences. *Journal of Computer and System Sciences*, 65(1):73–96, August 2002. 127

Li, Ming, Chen, Xin, Li, Xin, Ma, Bin, and Vitanyi, Paul M. B. The similarity metric. *IEEE Transactions on Information Theory*, 50(12):3250–3264, 2004. 148, 157, 162, 178, 182, 186, 189

Liao, Li and Noble, William S. Combining Pairwise Sequence Similarity and Support Vector Machines for Detecting Remote Protein Evolutionary and Structural Relationships. *Journal of Computational Biology*, 10(6):857–868, December 2003. ISSN 1066-5277. 14

Liew, Alan W., Yan, Hong, and Yang, Mengsu. Pattern recognition techniques for the emerging field of bioinformatics: A review. *Pattern Recognition*, 38(11): 2055–2073, November 2005. 127

Lindeberg, Tony. Feature detection with automatic scale selection. *International Journal of Computer Vision*, 30:79–116, 1998. 41

Lipman, D. J. and Pearson, W. R. Rapid and sensitive protein similarity searches. *Science*, 227:1435–1441, 1985. 14

Lodhi, Huma, Saunders, Craig, Shawe-Taylor, John, Cristianini, Nello, and Watkins, Christopher J. C. H. Text classification using string kernels. *Journal of Machine Learning Research*, 2:419–444, 2002. 3, 14, 132, 133, 187, 188, 189, 204

Lowe, David G. Object Recognition from Local Scale-Invariant Features. *Proceedings of ICCV*, 2:1150–1157, 1999. 5, 41, 102

Manning, Christopher D. and Schütze, Hinrich. *Foundations of Statistical Natural Language Processing*. MIT Press, Cambridge, MA, USA, 1999. ISBN 0-262-13360-1. 5, 6, 132

Manning, Christopher D., Raghavan, Prabhakar, and Schütze, Hinrich. *Introduction to Information Retrieval*. Cambridge University Press, New York, NY, USA, 2008. ISBN 0521865719, 9780521865715. 2, 3, 4, 5, 14, 132, 204

McCallum, Andrew, Nigam, Kamal, and Ungar, Lyle H. Efficient clustering of high-dimensional data sets with application to reference matching. *Proceedings of ACM SIGKDD*, pp. 169–178, 2000. 29, 31

Meila, Marina. Comparing clusterings by the variation of information. *Proceedings of COLT*, 2777:173–187, 2003. 32

Melsted, Pall and Pritchard, Jonathan. Efficient counting of k-mers in DNA sequences using a bloom filter. *BMC Bioinformatics*, 12(1):333, 2011. 162, 189

Mikolajczyk, Krystian and Schmid, Cordelia. Indexing Based on Scale Invariant Interest Points. *Proceedings of ICCV*, 1:525–531, 2001. 41

Mikolajczyk, Krystian and Schmid, Cordelia. A Performance Evaluation of Local Descriptors. *IEEE Transactions on Pattern Analysis and Machine Intelligence*, 27(10):1615–1630, October 2005. 41, 42

Montavon, Grégoire, Orr, Geneviève B., and Müller, Klaus-Robert (eds.). *Neural Networks: Tricks of the Trade*, volume 7700 of *Lecture Notes in Computer Science (LNCS)*. Springer, 2nd edition, 2012. 4, 35

Munch, Kasper, Boomsma, Wouter, Huelsenbeck, John P., Willerslev, Eske, and Nielsen, Rasmus. Statistical Assignment of DNA Sequences Using Bayesian Phylogenetics. *Systematic Biology*, 57(5):750–757, October 2008. ISSN 1076-836X. 130

Nadaraya, E A. On estimating regression. *Theory of Probability and its Applications*, 9:141–142, 1964. 19

Nei, Masatoshi and Kumar, Sudhir. *Molecular Evolution and Phylogenetics*. Oxford University Press, USA, 1 edition, August 2000. ISBN 0195135857. 130

Ng, Raymond T. and Han, Jiawei. Clarans: A method for clustering objects for spatial data mining. *IEEE Transactions on Knowledge and Data Engineering*, 14(5):1003–1016, 2002. 31

Nicolas, F. and Rivals, E. Complexities of centre and median string. *Proceedings of CPM*, 2676:315–327, 2003. 140

Nicolas, F. and Rivals, E. Hardness results for the center and median string problems under the weighted and unweighted edit distances. *Journal of Discrete Algorithms*, 3:390–415, 2005. 140

Nilsson, Nils J. The quest for artificial intelligence: A history of ideas and achievements. 2010. 2

Nister, David and Stewenius, Henrik. Scalable Recognition with a Vocabulary Tree. *Proceedings of CVPR*, 2:2161–2168, 2006. 42

Palmer, J. and Herbon, L. Plant mitochondrial DNA evolves rapidly in structure, but slowly in sequence. *Journal of Molecular Evolution*, 28:87–89, 1988. 129

Paredes, Roberto, Prez-Cortes, Juan, Juan, Alfons, and Vidal, Enrique. Local Representations and a Direct Voting Scheme for Face Recognition. *Proceedings*

of Workshop on Pattern Recognition in Information Systems, pp. 71–79, July 2001. 40

Passino, Giuseppe and Izquierdo, Ebroul. Patch-based image classification through conditional random field model. *Proceedings of the International Conference on Mobile Multimedia Communications*, pp. 6:1–6:6, 2007. 40

Pekalska, Elzbieta and Duin, Robert P. W. Dissimilarity representations allow for building good classifiers. *Pattern Recognition Letters*, 23(8):943–956, June 2002. ISSN 0167-8655. 14

Philbin, James, Chum, Ondrej, Isard, Michael, Sivic, Josef, and Zisserman, Andrew. Object retrieval with large vocabularies and fast spatial matching. *Proceedings of CVPR*, pp. 1–8, 2007. 6, 35, 42, 98, 102, 115, 123

Popescu, Andreea Lavinia, Ionescu, Radu Tudor, and Popescu, Dan. A Spatial Pyramid Approach for Texture Classification. *Proceedings of ISEEE*, October 2013a. 117

Popescu, Andreea Lavinia, Popescu, Dan, Ionescu, Radu Tudor, Angelescu, Nicoleta, and Cojocaru, Romeo. Efficient Fractal Method for Texture Classification. *Proceedings of ICSCS*, August 2013b. 10, 45, 81

Popescu, Marius. Studying translationese at the character level. *Proceedings of RANLP*, pp. 634–639, September 2011. 132, 187, 189, 195

Popescu, Marius and Dinu, Liviu P. Kernel methods and string kernels for authorship identification: The federalist papers case. *Proceedings of RANLP*, September 2007. 14, 132, 133, 187, 188

Popescu, Marius and Grozea, Cristian. Kernel methods and string kernels for authorship analysis. *CLEF (Online Working Notes/Labs/Workshop)*, September 2012. 3, 14, 132, 187, 196, 204

Popescu, Marius and Ionescu, Radu Tudor. The Story of the Characters, the DNA and the Native Language. *Proceedings of the Eighth Workshop on Innovative Use of NLP for Building Educational Applications*, pp. 270–278, June 2013. 3, 12, 14, 165, 186, 187, 204

Popov, Y. V. Multiple genome rearrangement by swaps and by element duplications. *Theoretical Computer Science*, 385(1-3):115–126, 2007. 14, 129, 140, 159, 189

Prezza, Nicola, Fabbro, Cristian Del, Vezzi, Francesco, Paoli, Emanuale De, and Policriti, Alberto. ERNE-BS5: aligning BS-treated sequences by multiple hits on a 5-letters alphabet. *Proceedings of BCB*, pp. 12–19, 2012. 128

Reyes, A., Gissi, C., Pesole, G., Catzeflis, F. M., and Saccone, C. Where Do Rodents Fit? Evidence from the Complete Mitochondrial Genome of Sciurus vulgaris. *Molecular Biology and Evolution*, 17(6):979–983, 2000. 129, 148, 157, 178, 182, 186

Rifkin, Ryan and Klautau, Aldebaro. In defense of one-vs-all classification. *Journal of Machine Learning Research*, 5(January):101–141, 2004. 195

Rubner, Yossi, Tomasi, Carlo, and Guibas, Leonidas J. The Earth Mover's Distance as a Metric for Image Retrieval. *International Journal of Computer Vision*, 40(2):99–121, 2000. 13, 35, 38

Rzhetsky, Andrey and Nei, Masatoshi. A Simple Method for Estimating and Testing Minimum–Evolution Trees. *Molecular Biology and Evolution*, 9(5): 945–967, 1992. 130

Saccone, Cecilia, Lanave, Cecilia, Pesole, Graziano, and Preperata, Giuliano. In Doolittle, Russsell F. (ed.), *Molecular evolution: computer analysis of protein and nucleic acid sequences*, volume 183 of *Methods In Enzymology*, chapter 35, pp. 570–583. Academic Press, New York, 1990. 130

Sadeghi, M. A. and Farhadi, A. Recognition using visual phrases. *Proceedings of CVPR*, pp. 1745–1752, 2011. 7, 205

Saitou, N. and Nei, M. The neighbor-joining method: a new method for reconstructing phylogenetic trees. *Molecular Biology and Evolution*, 4(4):406–425, July 1987. ISSN 1537-1719. 130

Sanderson, Conrad and Guenter, Simon. Short text authorship attribution via sequence kernels, markov chains and author unmasking: An investigation. *Proceedings of the 2006 Conference on Empirical Methods in Natural Language Processing*, pp. 482–491, July 2006. 14, 132, 187

Selim, Shokri Z. and Ismail, M. A. K-means-type algorithms: A generalized convergence theorem and characterization of local optimality. *IEEE Transactions on Pattern Analysis and Machine Intelligence*, PAMI-6(1):81–87, 1984. ISSN 0162-8828. 147

Shalev-Shwartz, Shai, Singer, Yoram, and Srebro, Nathan. Pegasos: Primal Estimated sub-GrAdient SOlver for SVM. *Proceedings of ICML*, pp. 807–814, 2007. 105, 109

Shapira, Dana and Storer, James A. Large Edit Distance with Multiple Block Operations. *Proceedings of SPIRE*, 2857:369–377, 2003. 14, 129, 159, 189

Shawe-Taylor, John and Cristianini, Nello. *Kernel Methods for Pattern Analysis*. Cambridge University Press, 2004. ISBN 978-0-521-81397-6. 3, 14, 20, 24, 26, 57, 121, 190, 192, 194, 204

Simard, Patrice, LeCun, Yann, Denker, John S., and Victorri, Bernard. Transformation Invariance in Pattern Recognition, Tangent Distance and Tangent Propagation. *Neural Networks: Tricks of the Trade*, 1996. 13, 17, 35, 38, 72

Sivic, Josef and Zisserman, Andrew. Video Google: A Text Retrieval Approach to Object Matching in Videos. *Proceedings of ICCV*, 2:1470–1477, 2003. 41

Sivic, Josef, Russell, Bryan C., Efros, Alexei A., Zisserman, Andrew, and Freeman, William T. Discovering Objects and their Localization in Images. *Proceedings of ICCV*, pp. 370–377, 2005. 4, 6, 34, 42, 98, 205

Smith, T. and Waterman, M. Comparison of biosequences. *Advances in Applied Mathematics*, 2(4):482–489, December 1981. ISSN 01968858. 127

Sneath, P. and Sokal, R. Numerical taxonomy. 1973. 130

Socher, Richard, Huval, Brody, Bath, Bharath, Manning, Christopher, and Ng, Andrew. Convolutional-Recursive Deep Learning for 3D Object Classification. *Proceedings of NIPS*, pp. 665–673, 2012. 35

Srihari, Sargur N. High-performance reading machines. *Proceedings of the IEEE (Special issue on Optical Character Recognition)*, 80(7):1120–1132, July 1992. 54

States, D. J. and Agarwal, P. Compact encoding strategies for dna sequence similarity search. *Proceedings of the 4th International Conference on Intelligent Systems for Molecular Biology*, pp. 211–217, 1996. 141

Suen, Ching Y., Nadal, Christine, Legault, Raymond, Mai, T. A., and Lam, Louisa. Computer recognition of unconstrained handwritten numerals. *Proceedings of the IEEE (Special issue on Optical Character Recognition)*, 80(7): 1162–1180, July 1992. 54

Tetreault, Joel, Blanchard, Daniel, Cahill, Aoife, and Chodorow, Martin. Native Tongues, Lost and Found: Resources and Empirical Evaluations in Native Language Identification. *Proceedings of COLING 2012*, pp. 2585–2602, December 2012. 126, 188, 189

Tetreault, Joel, Blanchard, Daniel, and Cahill, Aoife. A report on the first native language identification shared task. *Proceedings of the Eighth Workshop on Innovative Use of NLP for Building Educational Applications*, pp. 48–57, June 2013. 165, 186, 187

Tomescu, Alexandru I., Kuosmanen, Anna, Rizzi, Romeo, and Mäkinen, Veli. A Novel Min-Cost Flow Method for Estimating Transcript Expression with RNA-Seq. 14(Suppl 5):S15, 2013. presented at RECOMB-Seq 2013. 128

Trapnell, Cole, Pachter, Lior, and Salzberg, Steven L. TopHat: discovering splice junctions with RNA-Seq. *Bioinformatics*, 25(9):1105–1111, 2009. 128

Trapnell, Cole, Williams, B.A., Pertea, G., Mortazavi, A., Kwan, G., van Baren, M.J., Salzberg, S.L., Wold, B.J., and Pachter, Lior. Transcript assembly and

quantification by RNA-Seq reveals unannotated transcripts and isoform switching during cell differentiation. *Nature Biotechnology*, 28:511–515, 2010. 128

Upton, Graham and Cook, Ian. *A Dictionary of Statistics*. Oxford University Press, Oxford, 2004. 104, 124

Vapnik, Vladimir. Estimation of dependencies based on empirical data (Information Science and Statistics). *Springer-Verlag*, 2nd edition, 2006. 18

Vapnik, Vladimir and Chervonenkis, Alexey. On the Uniform Convergence of Relative Frequencies of Events to Their Probabilities. *Theory of Probability and its Applications*, 16(2):264–280, 1971. 18, 19

Vapnik, Vladimir and Vashist, Akshay. A new learning paradigm: Learning using privileged information. *Neural Networks*, 22(56):544 – 557, 2009. ISSN 0893-6080. 57, 70, 71

Varma, Manik and Zisserman, Andrew. A Statistical Approach to Texture Classification from Single Images. *International Journal of Computer Vision*, 62 (1-2):61–81, April 2005. 80

Vedaldi, Andrea and Fulkerson, B. VLFeat: An Open and Portable Library of Computer Vision Algorithms. http://www.vlfeat.org/, 2008. 109

Vedaldi, Andrea and Zisserman, Andrew. Efficient additive kernels via explicit feature maps. *Proceedings of CVPR*, pp. 3539–3546, 2010. 27, 105, 109

Vezzi, Francesco, Fabbro, Cristian Del, Tomescu, Alexandru I., and Policriti, Alberto. rNA: a fast and accurate short reads numerical aligner. *Bioinformatics*, 28(1):123–124, 2012. 14, 128, 129, 159, 189

Wang, Lusheng and Dong, Liang. Randomized Algorithms for Motif Detection. *Journal of Bioinformatics and Computational Biology*, 3(5):1039–1052, 2005. 127

Wilder, Kenneth J. *Decision tree algorithms for handwritten digit recognition*. Electronic Doctoral Dissertations for UMass Amherst, January 1998. URL http://scholarworks.umass.edu/dissertations/AAI9823791. 66, 72

Winn, J., Criminisi, A., and Minka, T. Object Categorization by Learned Universal Visual Dictionary. *Proceedings of ICCV*, 2:1800–1807, 2005. 42, 43

Wooley, J. C. Trends in computational biology: a summary based on a RECOMB plenary lecture. *Journal of Computational Biology*, 6:459–474, 1999. 127

Wulder, Michael A., White, Joanne C., Fournier, Richard A., Luther, Joan E., and Magnussen, Steen. Spatially Explicit Large Area Biomass Estimation: Three Approaches Using Forest Inventory and Remotely Sensed Imagery in a GIS. *Sensors*, 8(1):529–560, 2008. 86

Xie, Jin, Zhang, Lei, You, Jane, and Zhang, David. Texture classification via patch-based sparse texton learning. *Proceedings of ICIP*, pp. 2737–2740, 2010. 43, 80

Yagnik, Jay, Strelow, Dennis, Ross, David A., and Lin, Ruei-Sung. The power of comparative reasoning. *Proceedings of ICCV*, pp. 2431–2438, 2011. 105

Yang, Z. and Rannala, B. Bayesian phylogenetic inference using DNA sequences: a Markov Chain Monte Carlo Method. *Molecular Biology and Evolution*, 14 (7):717–724, July 1997. ISSN 1537-1719. 130

Yin, Chuanhuan, Zhao, Xiang, Mu, Shaomin, and Tian, Shengfeng. A fast multi-class classification algorithm based on cooperative clustering. *Neural Processing Letters*, pp. 1–14, 2013. 32

Zerbino, Daniel R. and Birney, Ewan. Velvet: Algorithms for de novo short read assembly using de bruijn graphs. *Genome Research*, 18(5):821–829, 2008. 128

Zhang, Bin and Srihari, Sargur N. Fast k-nearest neighbor classification using cluster-based trees. *IEEE Transactions on Pattern Analysis and Machine Intelligence*, 26(4):525–528, 2004. ISSN 0162-8828. 18

Zhang, Jian, Marszalek, Marcin, Lazebnik, Svetlana, and Schmid, Cordelia. Local Features and Kernels for Classification of Texture and Object Categories: A Comprehensive Study. *International Journal of Computer Vision*, 73(2):213–238, June 2007. 3, 6, 34, 35, 42, 90, 98, 115, 204

Zhang, Tian, Ramakrishnan, Raghu, and Livny, Miron. Birch: an efficient data clustering method for very large databases. *SIGMOD Record*, 25(2):103–114, 1996. ISSN 0163-5808. 31